Glucocorticoid Excess, the NAD^+ Metabolome and Energy Metabolism

by

Samuel Richard Heaselgrave

A thesis submitted to The University of Birmingham

for the degree of

DOCTOR OF PHILOSOPHY

Institute of Metabolism and Systems Research

College of Medical and Dental Sciences

University of Birmingham

March 2023

Abstract

Glucocorticoids are crucial for healthy metabolic function and regulation of homeostasis. They can also be used as exogenous medical treatments to treat a plethora of conditions. However, sustained glucocorticoid excess is extremely detrimental to metabolic health and function, ultimately resulting in the condition, Cushing's syndrome. These consequences are often dependent upon the presence of the enzyme 11β-hydroxysteroid dehydrogenase type 1 (11β-HSD1). Whether global markers of energy metabolism or the metabolically vital molecule nicotinamide adenine dinucleotide (NAD^+) are also affected by glucocorticoid excess, and whether 11β-HSD1 is required to mediate them, remains unclear. Additionally, it is unknown if NAD^+ metabolome augmentation, through nicotinamide riboside (NR), is a viable therapeutic strategy to combat sustained glucocorticoid excess. Through *in vivo* investigation with male and female C57BL/6J (wild type, WT) and 11β-HSD1 knock out mice, this thesis identifies the existence of a 11β-HSD1 dependent mechanism by which glucocorticoid excess elevates markers of energy metabolism whilst also altering parts of the NAD^+ metabolome, in a tissue specific and/or sex specific manner. However, NR treatment does not attenuate any of these effects. These findings show energy metabolism and NAD^+ disruption are consequences of sustained glucocorticoid excess, however whether they contribute to other effects of glucocorticoid excess and the exact genomic or non-genomic mechanisms involved remains undetermined. Findings also provide further evidence supporting 11β-HSD1 inhibition to prevent the consequence of glucocorticoid excess whilst also questioning the viability of NAD^+ metabolome augmentation as a treatment strategy.

Acknowledgements

I would first like to thank my supervisor Professor Gareth Lavery for his continued support, knowledge, and friendship throughout my entire PhD. His guidance and encouragement has helped me become the scientist I am today and for that I am incredibly grateful. I couldn't have asked for a better supervisor. I would also like to thank my second supervisor Professor Kostas Tsintzas for his valuable inputs throughout.

I would also like to acknowledge my colleagues within the Lavery group (Dave, Silke, Dean, Stuart, Lucy, Rachel, Pete, Yasir, Ali and Olivia). All of whom I have loved working with and am indebted to. Firstly, I would like to thank the vital contributes of Dave, Silke, Dean and Stuart who all helped with my work, shared their invaluable knowledge, and taught me many of the techniques I will use throughout my career. I would also like to thank Pete, Yasir, Lucy, and Rachel for the same reason. Whilst we only worked together for a relatively short time the techniques and general approach to science, they taught me will always be invaluable. I would also like to thank Ali and Olivia for their support and friendship. I have enjoyed starting and undertaking a PhD alongside them and I am confident they will both gone onto further success post PhD. I am grateful to have met and worked alongside such capable people and made such fantastic friends. I will always treasure my time in the Lavery group for this reason.

Additionally, I would also like to draw attention to those within the IMSR who have helped me, and those outside of the IMSR I have been fortunate enough to collaborate with along the way. I am grateful to Dr Rowan Hardy, Dr Christian Ludwig, Dr Jennie Roberts, Dr Gabriela Da Silva Xavier and Professor Nicholas Morton for sharing their expertise, facilitating my research and supporting my professional development.

Finally, I would like to thank my family, especially my parents, and my girlfriend Vish. My parents have always supported my academic career and encouraged me to follow the path I choose. I know I would not be where I am today without them, and I could not ask for more. I am grateful to Vish for her never ending support and enduring me throughout. She has made the years of my PhD far more enjoyable and driven me to achieve all I can.

Table of Contents

Table of Figures

Table of Tables

Abbreviations

µg	Microgram
µl	Microlitre
µM	Micromolar
11β-HSD1	11β-hydroxysteroid dehydrogenase 1
11β-HSD2	11β-hydroxysteroid dehydrogenase 2
4E-BP1	eIF4E-binding protein 1
AA	Amino acids
Ac	Acetyl group
ACMS	α-amino-β-carboxymuconate-ε-semialdehyde
ACTH	Adrenocorticotropic hormone
ADP	Adenosine diphosphate
ADPr	Adenosine diphosphate ribose
AFM	Kynurenine formamidase
AgRP	Agouti-related protein
AK	Adenosine kinase
AKT	Protein kinase B
ANCOVA	Analysis of covariance
ANGPTL4	Angiopoietin-like 4
ANOVA	Analysis of variance
ATGL	Adipose triglyceride lipase
ATP	Adenosine triphosphate
BAT	Brown adipose tissue
BIOPS	Biopsy preservation medium
BM	Bone mass
BMAL1	Brain and muscle Arnt-like protein-1
C1	Complex 1, NADH dehydrogenase
C2	Complex 2, succinate dehydrogenase
C3	Complex 3, ubiquinol-cytochrome c reductase
C4	Complex 4, cytochrome c oxidase
CA	Co-activator

Ca^{2+}	Calcium
cADPR	cADP-ribose
CBG	Corticosteroid binding globulin
cDNA	Complementary deoxyribonucleic acid
CF	Co-factor
cGR	Cytosolic glucocorticoid receptor
CO_2	Carbon dioxide
CORT	Corticosterone
CRH	Corticotrophin-releasing hormone
Ct	Cycle threshold
DBD	DNA binding domain
dCt	Delta cycle threshold
DEX	Dexamethasone
DNA	Deoxyribonucleic acid
EE	Energy expenditure
eNAMPT	Extracellular nicotinamide phosphoribosyltranferase
ETC	Electron transport chain
FBF	Free bodily fluid
FCCP	Carbonyl cyanide-4-(trifluoromethoxy)phenylhydrazone
FFA	Free fatty acids
FM	Fat mass
G3P	Glyceraldhyde-3-phosphate
GAPDH	Glyceraldhyde-3-phosphate dehydrogenase
GPCR	G-protein coupled receptor
GR	Glucocorticoid receptor
GRE	Glucocorticoid response element
H&E	Haematoxylin and eosin
H6PDH	Hexose-6-phospate dehydrogenase
HAO	3-HAA 3,4-dioxygenase
HC	Hydrocortisone
HFD	High fat diet

HPA	Hypothalamus-pituitary-adrenal
HSL	Hormone sensitive lipase
HSP	Heat shock proteins
IDO	Indoleamine 2,3-dioxygenase
IGF1	Insulin growth factor 1
iNAMPT	Intracellular nicotinamide phosphoribosyltranferase
IP	Intraperitoneal
KMO	Kynurenine 3-monooxygenase
KO	Knockout
KYU	Kynureninase
LBM	Lean body mass
LCMS	Liquid chromatography–mass spectrometry analysis
LPL	Lipoprotein lipase
MA	Malate-aspartate
MAFbx	Muscle atrophy F-box
MAMN	Nicotinic acid mononucleotide
MAPKs	Mitogen-activated protein kinases
MeNAM	Methylated nicotinamide
mg	Milligram
mGR	Membrane bound glucocorticoid receptor
min	Minute
MIR05	Mitochondrial respiration buffer
ml	Millilitre
mM	Millimole
MPC	Multi-protein complex
MR	Mineralocorticoid receptor
mRNA	Messenger ribonucleic acid
mTOR	Mechanistic target or rapamycin
MuRF1	Muscle RING finger 1
NA	Nicotinic acid
NAAD	Nucleic acid dinucleotide

NAD^+	Nicotinamide adenine dinucleotide
NADH	Reduced nicotinamide adenine dinucleotide
NADK	NADK kinase
$NADP^+$	Nicotinamide adenine dinucleotide phosphate
NADPH	Reduced nicotinamide adenine dinucleotide phosphate
NADSYN	Nicotinamide adenine dinucleotide synthetase
NAFLD	Non-alcoholic fatty liver disease
NAM	Nicotinamide
NAMPT	Nicotinamide phosphoribosyltranferase
NAPRT	Nicotinic acid phosphoribosyltransferase
NFW	Nuclease free water
nGRE	Negative glucocorticoid response element
nM	Nanomole
NMN	Nicotinamide mononucleotide
NMNAT	Nicotinamide adenylyl tranferase
NMNH	Reduced nicotinamide mononucleotide
NNMT	Nicotinamide N-methyltransferase
NR	Nicotinamide riboside
NRH	Reduced nicotinamide riboside
NRK	Nicotinamide riboside kinase
NTD	N-terminal transactivation terminal
O_2	Oxygen
O2K	Oxygraph-2k
PAI-1	Plasminogen activator inhibitor-1
PARPs	Poly-ADP ribose polymerases
PDH	Pyruvate dehydrogenase
Pi	Phosphate
PKA	Protein kinase A
PKC	Protein kinase C
PNP	Purine nucleoside phosphorylase
POMC	Pro-opiomelancortin

PPARα	Peroxisome proliferator-activated receptor alpha
PRED	Prednisone
QA	Quinolinc acid
QAPRT	Quinolinate phosphoribosyltransferase
qPCR	Real-time PCR
RER	Respiratory exchange ratio
RNA	Ribonucleic acid
ROS	Reactive oxygen species
RT	Reverse transcription
S6K1	S6 kinase 1
SIRT	Sirtuin
StAR	Steroidogenic acute regulatory protein
TAG	Triglyceride
TCA	Tricarboxylic acid
TDO	Tryptophan 2,3-dioxygenase
TF	Transcription factor
Trp	Tryptophan
UCP1	Uncoupling protein 1
VLDL	Very-low-density lipoprotein
WAT	White adipose tissue
WT	Wild type

CHAPTER 1 - INTRODUCTION

Endocrine regulation of metabolism is a cornerstone feature of physiology that influences homeostatic norms and adaptive responses to endogenous or exogenous stimuli (Hiller-Sturmhofel and Bartke, 1998). Whether it be global or tissue specific effects, evidence for the regulation of metabolism by an array of hormones is continually being discovered. Steroid hormones are one such class of hormones that are vital for metabolic control and homeostasis across just about all domains of life (Cole et al., 2019). Within this classification of hormones are the 'glucocorticoids' which influence an exhaustive number of metabolic and physiological processes (Magomedova and Cummins, 2016). However, our appreciation of the complexity of glucocorticoid regulation of metabolism remains incomplete, particularly when we consider the consequences of hormone excess as it relates to glucocorticoids. Whilst glucocorticoid excess is known to result in severe metabolic disfunction and florid disease, the full impact on homeostasis, energy metabolism, metabolic processes and key metabolic molecules and the mechanisms of action are yet to be determined. This is of great importance given the burden of glucocorticoid excess in the general population that require new therapies. It is therefore critical to determine the impact of glucocorticoid disruption on the molecule is nicotinamide adenine dinucleotide (NAD^+), as well as its wider metabolome. Crucial for an abundance of metabolic processes, homeostatic control and potential therapeutic intervention (Xie et al., 2020a), it is not clear if or how the NAD^+ metabolome is affected by glucocorticoid excess and whether it is implicated in the metabolic disfunction associated with it. As both glucocorticoids and NAD^+ are considered vital parts of the global metabolic system it remains plausible that they might be closely involved with one another and that perturbation to one will feedback into changes to the other and/or its effects.

This introduction will therefore give an overview of the functions and importance to metabolism of both glucocorticoids and the NAD^+ metabolome. It will also discuss the known consequences of glucocorticoid excess as well as alteration to the NAD^+ metabolome. In addition, it will also outline what is known, or theorised, about their interactions and outline why an improved understanding is required. This includes a better understanding of the affect altering one has on the other, their shared impact on energy metabolism and potential mechanisms linking the two.

1.1 Glucocorticoids

Glucocorticoids are a class of steroid hormones that are critical for energy metabolism and homeostasis (Tomlinson and Stewart, 2001). Serving permissive regulators, and as closely regulated stress response hormones, they drive transcriptional regulation, in response to external or internal stimuli, to alter metabolic processes (Nicolaides et al., 2015). This function is vital for metabolism, cardiovascular function, skeletal muscle health and growth, as well as many more (Ramamoorthy and Cidlowski, 2016). Complete loss of glucocorticoid sensitivity through tissue wide glucocorticoid receptor (GR) knockout (KO) has therefore been reported to cause metabolic complications or even death in mice (Heitzer et al., 2007). Glucocorticoid deficiency in humans (Addision's disease) is equally deleterious to health, metabolic function and homeostasis (Betterle et al., 2019). Likewise glucocorticoid excess (Cushing's syndrome/disease), resulting from endogenous or exogenous factors, is causative of severe metabolic complications and increased mortality (Lacroix et al., 2015). Therefore, dysregulated glucocorticoid concentrations, especially excessive levels, are known to contribute to the pathologies of obesity, diabetes, hypertension, glaucoma, osteoporosis,

skeletal muscle atrophy and many more (Oray et al., 2016, Ramamoorthy and Cidlowski, 2016).

1.2 Glucocorticoid synthesis

In humans, glucocorticoids are found in an inactive form (cortisone) and an active form (cortisol) (11 dehydro-corticosterone and corticosterone respectively in rodents) (Breuner and Orchinik, 2002, Ramamoorthy and Cidlowski, 2016) (Fig. 1.1). Glucocorticoids are usually secreted in a diurnal pattern with levels remaining low during sleep and peaking prior to waking to meet changing metabolic demands and maintain homeostasis (Krieger et al., 1971, Weitzman et al., 1971, Ramamoorthy and Cidlowski, 2016). Plasma concentrations of glucocorticoids in humans normally remain below 250nM, but can reach 700nM during stressful stimuli (Krieger et al., 1971).

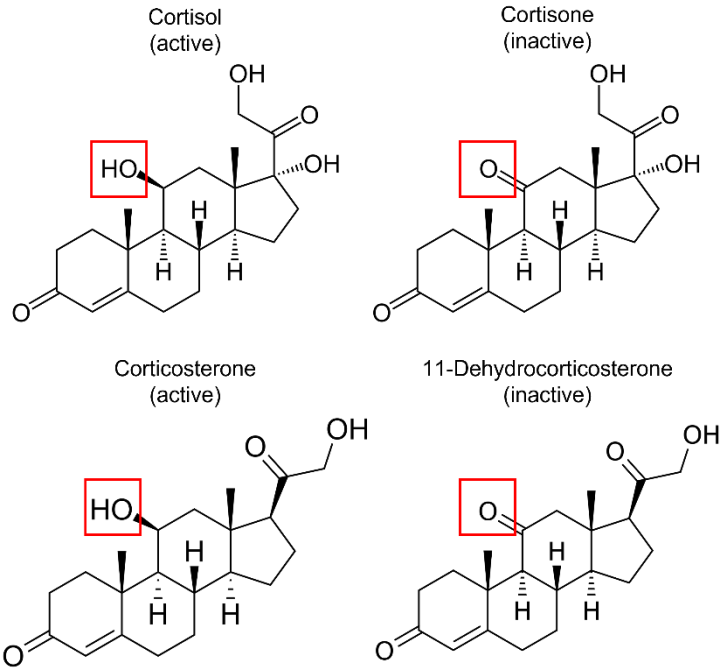

Figure 1.1: Chemical and structural difference the primary human and rodent glucocorticoids. Human glucocorticoids are cortisol (active) and cortisone (inactive). Rodent glucocorticoids are corticosterone (active) and 11-dehydrocorticosterone (inactive).

Glucocorticoids (predominantly cortisol/cortisone in humans) are synthesised from cholesterol within the adrenal glands, in a process called steroidogenesis (Payne and Hales, 2004, Miller and Auchus, 2011). This process is regulated by the hypothalamus-pituitary-adrenal (HPA) axis which stimulates synthesis and release in accordance with circadian rhythm and changes in metabolic demands (Ramamoorthy and Cidlowski, 2016) (Fig. 1.2). These changes in metabolic demands, which present themselves as endogenous or exogenous stressors, cause activation of the suprachiasmatic nucleus and the para-ventricular nucleus within the hypothalamus, causing the release of corticotrophin-releasing hormone (CRH) (Ramamoorthy and Cidlowski, 2016). The released CRH activates corticotroph cells of the anterior pituitary and pituitary pro-opiomelancortin (POMC) gene transcription leading to the release of adrenocorticotropic hormone (ACTH) (de Guia et al., 2014, Ramamoorthy and Cidlowski, 2016). This then stimulates glucocorticoid production in the adrenal glands and release from the adrenal cortex (Newton, 2000, Rose and Herzig, 2013, de Guia et al., 2014, Ramamoorthy and Cidlowski, 2016). Due to the nature of glucocorticoids, all the glucocorticoids released from the adrenal glands need to be promptly synthesised following ACTH action as none can be stored in anticipation (Walker et al., 2015, Ramamoorthy and Cidlowski, 2016). ACTH action activates protein kinase A (PKA) leading to the phosphorylation of hormone sensitive lipases (HSL), increasing translocation of cholesterol into the cell (Ramamoorthy and Cidlowski, 2016). Further phosphorylation of steroidogenic acute regulatory protein (StAR) causes this accumulated cellular cholesterol to be transported into the mitochondria (Ramamoorthy and Cidlowski, 2016). First converted to pregnenolone in the mitochondria before the remainder of the steroidogenesis process is carried out between the mitochondria and endoplasmic reticulum of the adrenal cortex, zona fasciculata and glomerulosa resulting in synthesised glucocorticoids (Newton, 2000, Rose and Herzig, 2013,

de Guia et al., 2014, Ramamoorthy and Cidlowski, 2016). It is important to note that rodents cannot produce cortisol as they do not express the enzyme CYP17A1 in the adrenals, making corticosterone their primary glucocorticoid (Missaghian et al., 2009). Once synthesised glucocorticoids enter the circulation where the majority bind with high affinity to corticosteroid binding globulin (CBG). This is true of both cortisol in humans and corticosterone in rodents. Additionally, both can also bind to albumin. Only a small fraction of circulating glucocorticoids are found unbound (Breuner and Orchinik, 2002, Ramamoorthy and Cidlowski, 2016). Approximately 80-90% are found bound to CBG, 5-10% bound to albumin and 3-10% circulates freely (Perogamvros et al., 2012). Excessive production of glucocorticoids is rapidly prevented by the GR, as well as the mineralocorticoid receptor (MR), which provide an inhibitory signal to the hypothalamus and anterior pituitary, preventing secretion of CRH and ACTH respectively (Newton, 2000, Walker et al., 2015, Ramamoorthy and Cidlowski, 2016, Gjerstad et al., 2018).

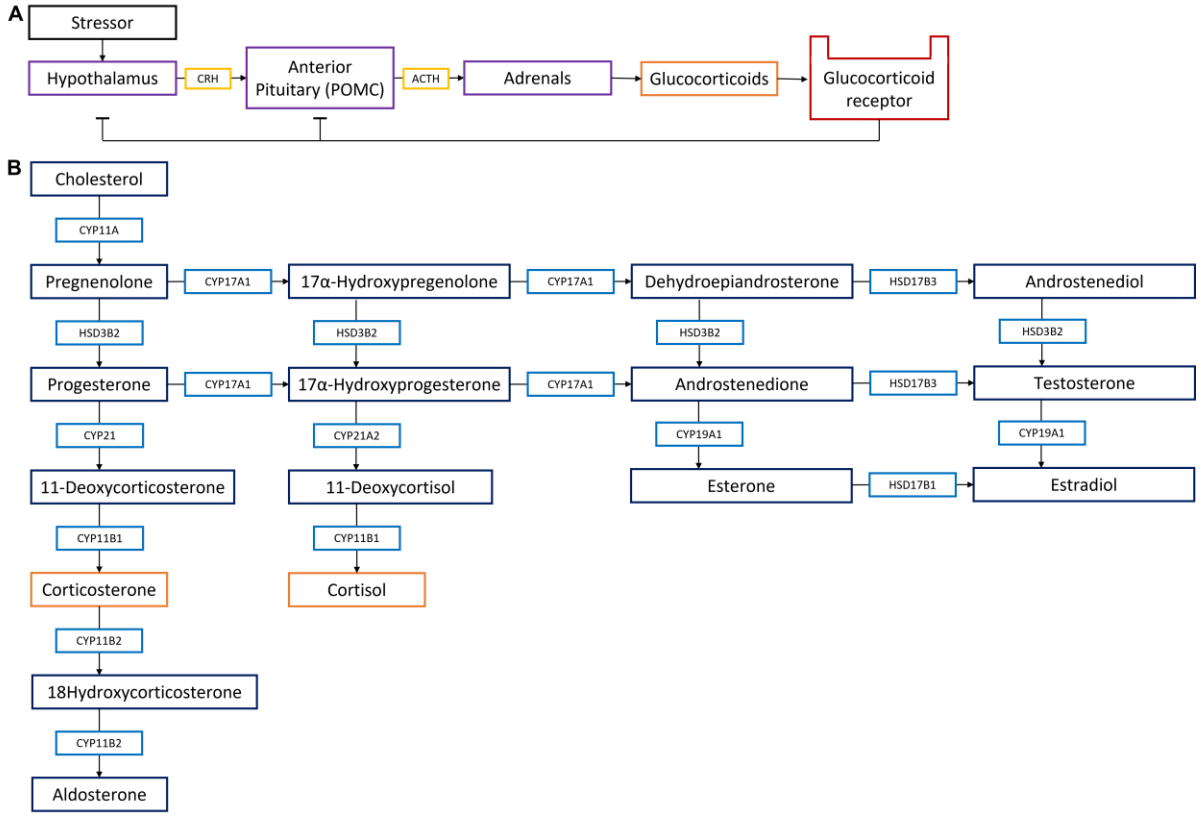

Figure 1.2: Cortisol synthesis from cholesterol (steroidogenesis) within the adrenal cortex and regulated by the hypothalamus-pituitary-adrenal axis. A. Hypothalamus-pituitary adrenal axis. B. Glucocorticoid sysnthesis within the steroidogenesis pathway. Purple, HPA; yellow, hormones released by the HPA; dark blue, intermediates of steroidogenesis; light blue, enzymatic steps of steroidogenesis; orange, glucocorticoids; red, glucocorticoid receptor. Abbreviations: CRH, corticotrophin-releasing hormone; ACTH, adrenocorticotrophic hormone.

1.3 Glucocorticoid activation and inactivation

After traveling in the circulation to the target tissue glucocorticoids are activated, and inactivated, primarily by the enzymes 11β-hydroxysteroid dehydrogenase 1 and 2 (11β-HSD1/2) (Seckl, 2004, Tomlinson et al., 2004) (Fig. 1.3). These enzymes require NAD^+ in a reduced, oxidised or phosphorylated form for use as redox cofactors that drive the reaction (Agarwal and Auchus, 2005). 11β-HSD1 is dependent on phosphorylated NAD^+ ($NADP^+$), requiring the reduced from (NADPH) to act as a reductase that converts inactive cortisone to

active cortisol, converting NADPH to $NADP^+$ (Lakshmi et al., 1993, Burton et al., 1998, Agarwal and Auchus, 2005). Alternatively, and to a lesser extent, 11β-HSD1 can act as a dehydrogenase to drive the reaction in the other direction, using $NADP^+$ as the cofactor, converting it to NADPH (Lakshmi et al., 1993, Burton et al., 1998, Agarwal and Auchus, 2005). Similarly, 11β-HSD2 also acts as a dehydrogenase to convert active cortisol to inactive cortisone but instead using NAD^+ as a redox cofactor, converting it to NADH (Agarwal and Auchus, 2005, Rusvai and Naray-Fejes-Toth, 1993). These reactions are highly dependent on the cofactor availability, gradient, and redox ratio, which can all act as rate limiting factors (Agarwal and Auchus, 2005). For example, sufficient resupply of NADPH, by the enzyme hexose-6-phospate dehydrogenase (H6PDH) enhances 11β-HSD1 activity, resulting in almost complete conversion of cortisone to cortisol (Agarwal and Auchus, 2005) (Fig. 1.4). Separate to 11β-HSD1/2, cortisol can also be deactivated by 5α-reductase and 5β-reducatase, in a reversible reaction, which converts it to 5α-dihydrocortisol and 5β-dihydrocortisol respectively (Russell and Wilson, 1994, Westerbacka et al., 2003, Gambineri et al., 2009, Hazlehurst et al., 2016).

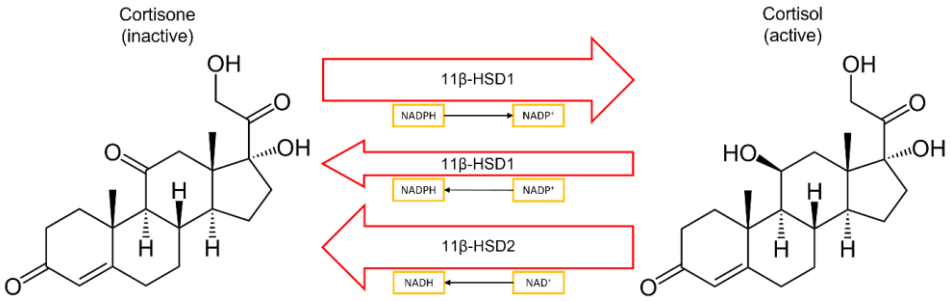

Figure 1.3: Glucocorticoid activation and inactivation by 11β-hydroxysteroid dehydrogenase 1 and 2. Abbreviations: 11β-HSD1, 11β-hydroxysteroid dehydrogenase 1; 11β-HSD2, 11β-hydroxysteroid dehydrogenase 2; NAD^+, nicotinamide adenice dinucleotide; NADH, reduced NAD^+; $NADP^+$, reduced phosphorylated NAD^+; NADPH, phosphorylated NAD^+.

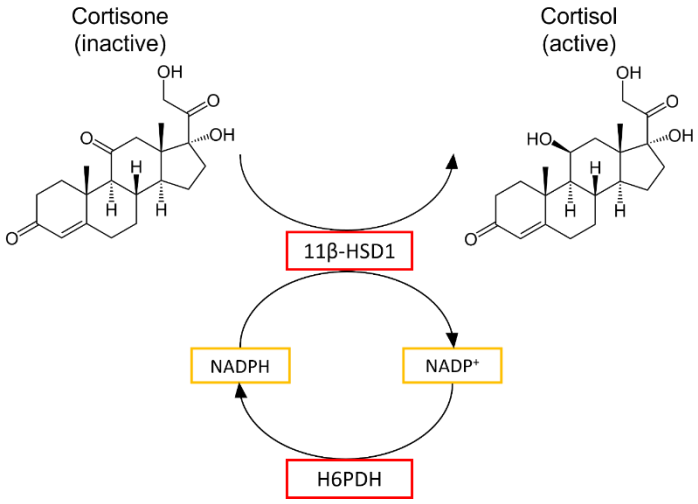

Figure 1.4: Hexose-6-phospate dehydrogenase maintenance of NADPH level to facilitate 11β-hydroxysteroid dehydrogenase 1 activity. Abbreviations: 11β-HSD1, 11β-hydroxysteroid dehydrogenase 1; H6PDH, hexose-6-phospate dehydrogenase; $NADP^+$, reduced phosphorylated NAD^+; NADPH, phosphorylated NAD^+.

1.4 Glucocorticoid mechanisms of action

Once activated glucocorticoids elicit effects through two primary mechanisms, genomic and non-genomic (Groeneweg et al., 2012, Ramamoorthy and Cidlowski, 2016) (Fig. 1.5). Genomic mechanisms are the primary, or at least better understood, or the two, but are slower acting taking anywhere from 15 minutes to several hours to take effect (Haller et al., 2008, Groeneweg et al., 2012). Non-genomic mechanisms on the other hand are fast acting and range from a few seconds to a several minutes (Liu et al., 2007, Xiao et al., 2010, Groeneweg et al., 2012, Ramamoorthy and Cidlowski, 2016). The effects elicited from these mechanisms are not universal and are often cell and tissue dependent (Lamberts et al., 1996, Ramamoorthy and Cidlowski, 2016).

1.4.1 Genomic mechanisms

Genomic mechanisms are well known to occur through the glucocorticoid receptor (GR) (Newton, 2000, Almawi and Melemedjian, 2002, Stahn et al., 2007, Groeneweg et al., 2012,

Ramamoorthy and Cidlowski, 2016). This receptor consists of three main parts; the N-terminal transactivation terminal (NTD) which modulates post translational modification, the DNA binding domain (DBD) which binds to a section of DNA known as the glucocorticoid response element (GRE), and finally the C-terminal ligand binding domain, which binds to glucocorticoids (Kumar and Thompson, 2005). It its inactive state the GR is found in the cytoplasm (cytosolic GR (cGR)) of the cell bound to multiple multi-protein complexes which keep the GR in a state of high affinity for glucocorticoid binding (Pratt and Toft, 1997, Grad and Picard, 2007, Stahn et al., 2007). When glucocorticoids, which can easily pass through the plasma membrane of the cell (Stahn et al., 2007), bind to the cGR at the ligand binding domain a conformational change occurs causing the multi-protein complexes to dissociate (Newton, 2000, Stahn et al., 2007, Ramamoorthy and Cidlowski, 2016). The cGR then undergoes dimerization combining two individual GR monomers into a single dimer (Bledsoe et al., 2002, Timmermans et al., 2022). The cGR, along with the bound glucocorticoid, subsequently translocate into the nucleus of the cell where it binds to the GRE along the DNA via the DBD of each monomer, completing the dimerization process (Savory et al., 1999, Newton, 2000, Bledsoe et al., 2002, Stahn et al., 2007, Ramamoorthy and Cidlowski, 2016, Timmermans et al., 2022). This promotes the transcription of new genes in a process known as transactivation (Fig. 1.5 I), or alternatively if the GR binds to a negative GRE (nGRE) it inhibits transcription in a process known as transrepression (Fig. 1.5 III) (Savory et al., 1999, Newton, 2000, Stahn et al., 2007, Ramamoorthy and Cidlowski, 2016). In addition to this the GR can also bind with cofactors, as well as the GRE, which further facilitates transactivation/repression (Fig. 1.5 II) (Ronacher et al., 2009, Ramamoorthy and Cidlowski, 2016). Other genomic mechanisms however do not require GR binding to the GRE and instead bind with just transcription factors (Fig. 1.5.IV), or the co-activators of transcription factors (Fig. 1.5 V) to prevent transcription

factor and DNA binding, therefore inhibiting transcription (Newton, 2000, Almawi and Melemedjian, 2002, Stahn et al., 2007). Membrane bound GR (mGR), which can exist at or translocate to the membrane surface, where glucocorticoids can bind, in response to a stress stimulus (Bartholome et al., 2004) are now also thought to have a genomic role. Glucocorticoid and mGR binding results in the nuclear translocation of an unliganded cGR within the cytoplasm, by a yet unidentified signalling cascade, resulting in gene transcription different to that induced by GR and glucocorticoid binding within the cell (Ritter and Mueller, 2014, Rainville et al., 2019). The genomic mechanisms of glucocorticoids can also be driven by the mineralocorticoid receptor (MR). Like the GR, the MR, which has a high affinity for glucocorticoids (Joels et al., 2008, Groeneweg et al., 2012), is also found both the cytoplasm (Beato et al., 1996, Groeneweg et al., 2012) and along the cell membrane (Karst et al., 2005, Olijslagers et al., 2008, Groeneweg et al., 2012), functioning in a similar manner (Groeneweg et al., 2012). Other hormones, specifically the sex hormones (androgens and estrogens) modulate the transcriptional activity of the GR, resulting in sexual dimorphism (further discussed in section 1.5.5) in the metabolic response to glucocorticoids. Through direct binding with the GR or the activity of their own receptors (androgen receptor (AR) or estrogen receptor (ER)), androgens are thought to act as agonists to increase GR transcriptional activity in response to glucocorticoid binding, whilst estrogens are thought to have the opposite, antagonistic effect (Dakin et al., 2015, Spaanderman et al., 2018, Kroon et al., 2020).

1.4.2 Non-genomic mechanisms

Non-genomic mechanisms allow for faster glucocorticoid effects, however unlike the genomic mechanisms, these can be caused by or independent of GR interaction in the cytoplasm or along the membrane (Stahn et al., 2007, Groeneweg et al., 2012, Ramamoorthy

and Cidlowski, 2016) (Fig. 1.5). Upon cGR and glucocorticoid binding in the cytoplasm, the dissociated multi-protein complexes then elicit non-genomic effects (Croxtall et al., 2000, Stahn et al., 2007). These complexes contain several heat shock proteins (HSP), immunophilins and several kinases including mitogen-activated protein kinases (MAPKs) and protein kinase B (AKT), that once dissociated activate signalling pathways in which they are involved (Buttgereit and Scheffold, 2002, Stahn et al., 2007, Boncompagni et al., 2015, Ramamoorthy and Cidlowski, 2016, Rainville et al., 2019). Alongside this, increased activation of protein kinase A (PKA) (Han et al., 2005) and C (PKC) activity (Qi et al., 2005) have also been reported as non-genomic mechanisms. Membrane-bound GR also activate signalling through these pathways (Boncompagni et al., 2015, Rainville et al., 2019), as do both cytosolic and membrane-bound MR (Groeneweg et al., 2012). Asides from the proteins contained in these multi-protein complexes, non-genomic effects have also been linked with G-protein coupled receptors (Groeneweg et al., 2012) which are found in the cellular membrane (Rosenbaum et al., 2009) and have been reported to have high affinity for glucocorticoids in rats (Guo et al., 1995). Once activated by glucocorticoids, these G-protein coupled receptors have been shown to promote endocannabinoid and nitric oxide production (Di et al., 2003, Di et al., 2005, Di et al., 2009). Finally fluctuating glucocorticoid concentrations can alter cell sodium and calcium channels, membrane potential, mitochondrial proton leak and even adenosine triphosphate (ATP) production without any direct binding (Buttgereit and Scheffold, 2002, Stahn et al., 2007).

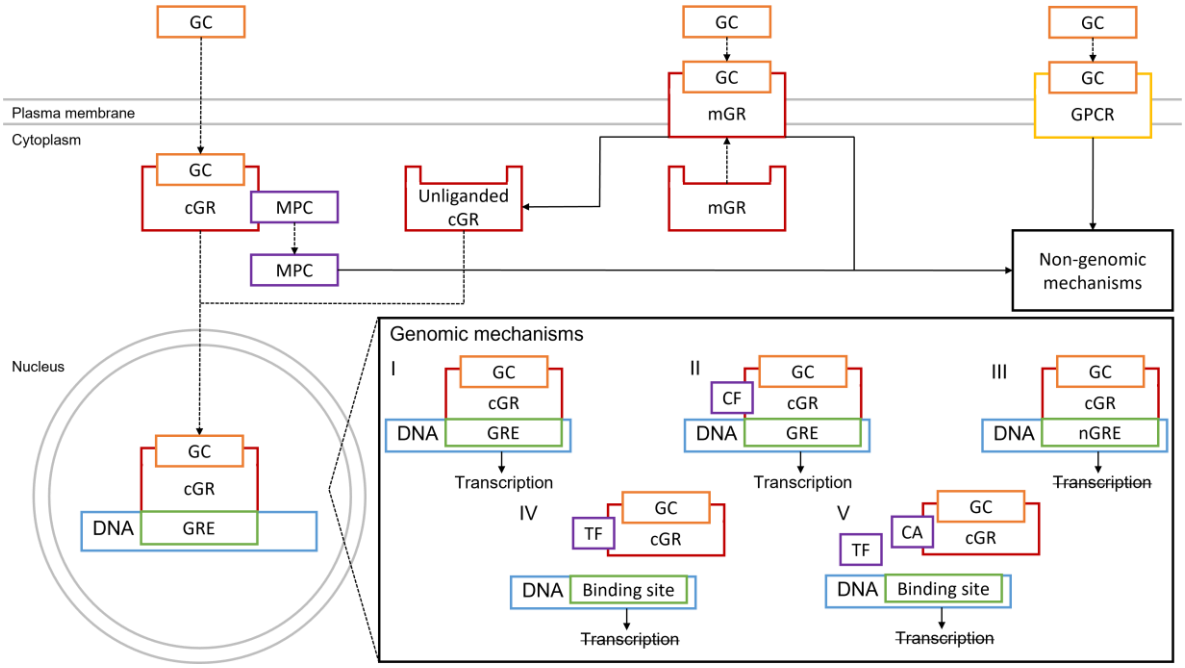

Figure 1.5: Glucocorticoid genomic and non-genomic mechanisms of action. Abbreviations: GC, glucocorticoid; GR, glucocorticoid receptor; cGR, cytosolic GR; mGR, membrane bound GR; GRE, glucocorticoid response element; nGRE, negative GRE; GPCR, G-protein coupled receptor; MPC, multi-protein complex; CF, co-factor; TF, transcription factor; CA, co-activator.

1.5 Metabolic functions of glucocorticoids

As previously stated, glucocorticoids are essential for metabolic function and homeostasis (Tomlinson and Stewart, 2001). Unsurprisingly, given their name, glucocorticoids are key regulators of glucose, but they also help regulate lipid and protein metabolism in all tissues of the body. However, the extent of glucocorticoid effects, and whether they are regulatory and facilitative, or disruptive and inhibitory depends on factors such as concentration and duration. At basal concentrations (values considered to be within healthy circulating fluctuations) glucocorticoids often perform the former role, whilst glucocorticoid excess (concentrations greater than basal circulating levels) often drive the latter.

1.5.1 Glucocorticoid regulation of tissue glucose homeostasis

At basal concentrations glucocorticoids regulate glucose metabolism in the liver, adipose tissue, and skeletal muscle (Kuo et al., 2015, Magomedova and Cummins, 2016) (Fig. 1.6). Through their stress response role glucocorticoids ultimately regulate whole body glucose metabolism to ensure sufficient glucose supply to the brain (Magomedova and Cummins, 2016).

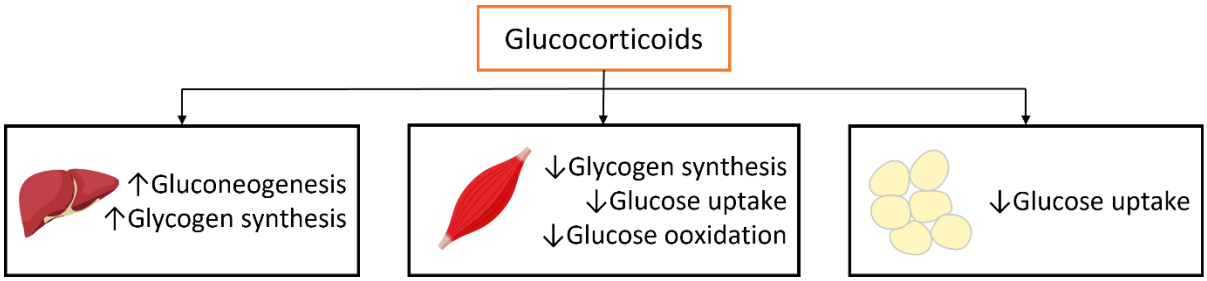

Figure 1.6: Glucocorticoid effects on glucose metabolism in the liver, skeletal muscle, and adipose tissue. Adapted from Magomedova and Cummins (2016).

1.5.1.1 Liver

One of the most important tissues for maintaining the circulating glucose supply is the liver, especially in a fasted state (Kuo et al., 2015, Magomedova and Cummins, 2016), in fact in the absence of the hepatic GR, fasted circulating glucose levels are not maintained, resulting in hypoglycaemia (Opherk et al., 2004). Glucocorticoids therefore help to maintain circulating glucose supply by increasing hepatic gluconeogenesis (Magomedova and Cummins, 2016). They have been shown to drive the transcription of key glycolytic enzymes (Pilkis and Granner, 1992, Barthel and Schmoll, 2003), such as phosphoenolpyruvate carboxykinase (Imai et al., 1990) and glucose-6-phosphatase (Lange et al., 1994), facilitating glucose release into the circulation. In studies where the GR has been knocked out the transcription of these enzymes is attenuated (Cole et al., 1995, Opherk et al., 2004). Interestingly, glucocorticoids also have another effect in the liver, promoting glycogen synthesis, increasing hepatic glucose storage. This is done through inhibition of glycogen phosphorylase activity whilst simultaneously

increasing glycogen synthase activity (Coderre et al., 1992, Dimitriadis et al., 1997, Buren et al., 2008, Magomedova and Cummins, 2016). However excessive glucocorticoid concentrations can compromise these processes. Specifically glucocorticoid excess can over stimulate hepatic gluconeogenesis and glucose release into the circulation causing hyperglycaemia (Lenzen and Bailey, 1984). Glucocorticoid excess can also cause hepatic insulin resistance by preventing AKT phosphorylation (Du et al., 2003, Magomedova and Cummins, 2016).

1.5.1.2 Skeletal muscle

Within skeletal muscle glucocorticoids have three main effects, reducing glucose uptake, glycogen synthesis and glucose oxidation (Kuo et al., 2015, Magomedova and Cummins, 2016). Much of this is caused by glucocorticoid induced of insulin resistance, which much like the liver, is caused by preventing AKT phosphorylation (Long et al., 2003). Glucocorticoids decrease cellular glucose uptake by reducing sensitivity to insulin, thus inhibiting GLUT4 translocation to the cellular membrane and subsequent glucose uptake (Weinstein et al., 1995, Weinstein et al., 1998). Glucocorticoid regulation of insulin also inhibits skeletal muscle glycogen synthesis through inhibition of glycogen synthase (Ruzzin et al., 2005), the opposite effect of glucocorticoids in the liver. Finally, glucocorticoids regulate glucose oxidation, and therefore the use of glucose for fuel, by inhibiting the activity of pyruvate dehydrogenase, thus preventing the continuation of glucose-derived energy production (Sugden and Holness, 2003, Patel et al., 2014, Magomedova and Cummins, 2016). Therefore, in skeletal muscle glucocorticoid concentrations are closely regulated to optimise glucose metabolism. However much like in the liver excessive glucocorticoid concentrations disrupts their regulatory nature

and causes negative side effects including excessive skeletal muscle insulin resistance, as well as hyperglycaemia (McMahon et al., 1988, de Guia et al., 2014, Burke et al., 2017).

1.5.1.3 Adipose tissue

The role of glucocorticoids in regulating glucose metabolism in adipose tissue is regulating glucose uptake (Magomedova and Cummins, 2016). Much like skeletal muscle the effect of glucocorticoids on insulin reduces glucose uptake through decreased GLUT4 translocation, which in turn reduces glucose utilisation (Sakoda et al., 2000, Lundgren et al., 2004, Kuo et al., 2015, Magomedova and Cummins, 2016). Glucocorticoids can instead promote lipolysis in adipose tissue which liberates glycerol, making it available for gluconeogenesis within the liver (Kuo et al., 2015). Enhanced lipolysis also generates the energy needed for gluconeogenesis (Kuo et al., 2015). Within adipose tissue glucocorticoids also regulate adipokine expression, which can then influence glucose metabolism in other tissues (Kuo et al., 2015). Two of these adipokines, plasminogen activator inhibitor-1 (PAI-1) and angiopoietin like 4 (ANGPTL4) are both increased by glucocorticoids and have been shown to attenuate insulin sensitivity, and therefore glucose uptake in the liver (Kuo et al., 2015, Tamura et al., 2015, Chen et al., 2017, Lee et al., 2018b). However, these adipokines, specifically PAI-1 have been shown to subsequently increases gluconeogenic enzymes within the liver (Tamura et al., 2015, Lee et al., 2018b).

1.5.1.4 Beta cells

As mentioned with the liver, skeletal muscle and adipose tissue, glucocorticoids regulate insulin sensitivity and the effects of insulin in these tissues. Glucocorticoids also regulate insulin secretion from beta cells (Rafacho et al., 2008, Magomedova and Cummins, 2016)

making them even more important for glucose metabolism. It has been shown that excess glucocorticoid levels can inhibit insulin secretion and dysregulate beta cell function (Lambillotte et al., 1997, Blondeau et al., 2012) by inhibition of GLUT2 availability (Gremlich et al., 1997). Additionally glucocorticoid excess can also drive beta cell death, further reducing insulin production (Reich et al., 2012). Therefore, glucocorticoid excess causes both reduced insulin secretion from beta cells, whilst also causing increased insulin resistance and the tissue level which inhibits glucose metabolism, leading to hyperglycaemia and even diabetes mellitus (McMahon et al., 1988, Rafacho et al., 2008, Di Dalmazi et al., 2012, Magomedova and Cummins, 2016, Burke et al., 2017).

1.5.2 Glucocorticoid regulation of tissue lipid homeostasis

Lipid metabolism in the liver and adipose tissue is closely regulated by glucocorticoids and can also be dysregulated by glucocorticoid excess, much like glucose metabolism (Fig. 1.7). If left untreated glucocorticoid excess increases central adiposity, dyslipidaemia, hypertension, and hepatic steatosis (Peckett et al., 2011, Magomedova and Cummins, 2016).

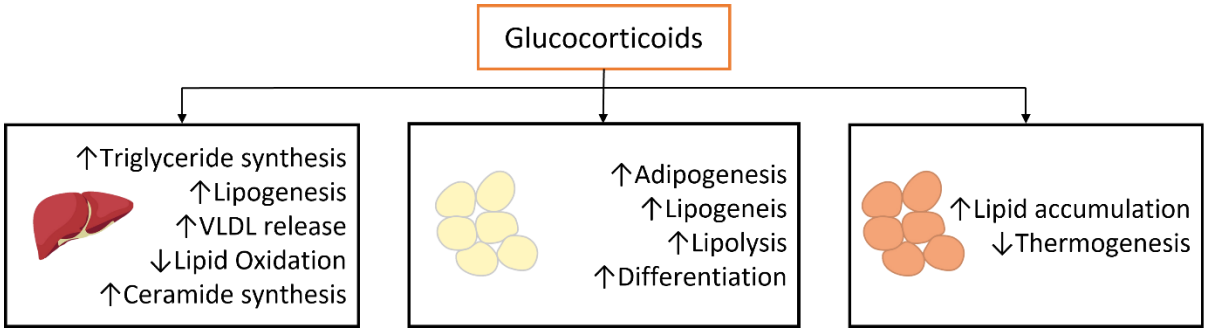

Figure 1.7: Glucocorticoid effects on lipid metabolism in the liver, white adipose tissue, and brown adipose tissue. Adapted from Magomedova and Cummins (2016). Abbreviations: VLDL, very-low-density lipoprotein.

1.5.2.1 Liver

Glucocorticoids are reported to primarily increase hepatic triglyceride content by regulating multiple lipid synthesising and breakdown pathways (Peckett et al., 2011, de Guia et al., 2014, Magomedova and Cummins, 2016). Firstly, glucocorticoids are known to increase fatty acid synthesis, or de novo lipogenesis, producing free fatty acids (FFA) (Diamant and Shafrir, 1975, Berdanier, 1989, Peckett et al., 2011, Magomedova and Cummins, 2016). These FFA are then utilised by the liver as glucocorticoids increase the expression of genes involved in triglyceride synthesis, which incorporates FFA into triglycerides for storage (Dolinsky et al., 2004). Glucocorticoids support this process further by simultaneously increasing FFA uptake into the liver (Rahimi et al., 2020). The synthesis and storage of triglycerides is exacerbated by a concurrent reduction in lipid oxidation (Letteron et al., 1997, Magomedova and Cummins, 2016). The process of beta oxidation, which is the use of lipids for energy production, has been shown to be inhibited within the liver by glucocorticoids. Key acyl-CoA dehydrogenase enzymes are downregulated, inhibiting the process (Letteron et al., 1997). Additionally, the expression of the lipolytic gene, Hes1, is reported to be downregulated by glucocorticoids (Lemke et al., 2008). Therefore, the net effect is one of hepatic triglyceride accumulation, which can lead to the condition hepatic steatosis seen following glucocorticoid excess or in Cushing's syndrome (Peckett et al., 2011, de Guia et al., 2014, Magomedova and Cummins, 2016). The accumulation of hepatic triglycerides, especially increased synthesis, is also thought to contribute to increased very low-density lipoprotein (VLDL) release from the liver (Cole et al., 1982, Taskinen et al., 1983, Peckett et al., 2011), increasing circulating triglyceride concentrations and even causing dyslipidaemia and hypertension when broken down to FFA by circulating lipoprotein lipase (LPL), especially following glucocorticoid excess (Arnaldi et al., 2010, Goodwin and Geller, 2012). However, the release of VLDL is debated and may not be elevated by glucocorticoid excess (Dolinsky et al., 2004, Tiryakioglu et al., 2010). Finally,

glucocorticoids stimulate the production of the fatty acid composed ceramides in the liver (Hannun, 1994) which have been shown to contribute to glucocorticoid induced insulin resistance, which is exacerbated by glucocorticoid excess (Holland et al., 2007, Magomedova and Cummins, 2016).

1.5.2.2 Adipose tissue

As the primary location of lipids within the body it is unsurprising that glucocorticoids also affect adipose tissue lipid metabolism (Peckett et al., 2011, Magomedova and Cummins, 2016). During fasting, glucocorticoids stimulate lipolysis to breakdown triglyceride, liberating FFA for fat oxidation across the body. Glucocorticoids do this by increasing the expression of the lipolytic enzymes adipose triglyceride lipase (ATGL) and hormone sensitive lipase (HSL) (Slavin et al., 1994, Yu et al., 2010, Campbell et al., 2011). Concurrently, glucocorticoids inhibit FFA liberation from circulating triglycerides and subsequent uptake into adipose tissue by increasing angiopoietin-like 4 (ANGPTL4) expression which inhibits circulating LPL activity (Shan et al., 2009). Instead ANGPLT4 expression increases circulating triglyceride concentration by promoting lipolysis within adipose tissue (Gray et al., 2012). Therefore, at fasting basal concentrations glucocorticoids enable lipid utilisation as fuel by prioritising lipolysis within adipose tissue. However, in a fed state glucocorticoids drive a shift in focus to one of de novo lipogenesis and fatty acid synthesis (Peckett et al., 2011, de Guia et al., 2014, Magomedova and Cummins, 2016), by increasing both fatty acid synthase and acyl-CoA carboxylase expression (Diamant and Shafrir, 1975, Volpe and Marasa, 1975, Peckett et al., 2011, Wang et al., 2012), promoting adipose tissue lipid accumulation. Anti-lipolytic effects of glucocorticoids have also been report during glucocorticoid excess (Campbell et al., 2011, Peckett et al., 2011) or disrupted diurnal glucocorticoid oscillations (Tholen et al., 2022), so

much so that severe abdominal adiposity, obesity, and metabolic syndrome can develop (Peckett et al., 2011, Magomedova and Cummins, 2016). However, the anti-lipolytic or lipogenic effects induced by glucocorticoid excess are focused abdominally (Rebuffe-Scrive et al., 1988, Yu et al., 2010, Chimin et al., 2014) with genes expressed that promote triglyceride synthesis and storage (Yu et al., 2010). In peripheral adipose tissue, found in the limbs, glucocorticoid excess has the opposite effect, driving lipolysis through increased HSL and AGTL expression (Slavin et al., 1994, Yu et al., 2010, Campbell et al., 2011), as well as the expression of other genes associated with lipolysis and lipid transport (Yu et al., 2010). However, the net effect of the two pleiotropic processes is lipid redistribution to the abdominal region and increased circulating triglycerides, resulting in overall lipid accumulation and dyslipidaemia (Magomedova and Cummins, 2016). Developmentally glucocorticoids enhance adipose tissue growth as they have been shown both *in vitro* and *in vivo* to increase pre-adipocyte and adipocyte differentiation of both white adipose tissue (WAT) and brown adipose tissue (BAT) (Shima et al., 1994, Steger et al., 2010, Campbell et al., 2011). In BAT exclusively, glucocorticoid excess has been shown to inhibit one of its primary functions, thermogenesis, whilst also increasing lipid content (Strack et al., 1995), as has been previously discussed in WAT.

1.5.3 Glucocorticoid regulation of tissue protein metabolism

Much like glucose and lipids, protein metabolism is all affected by glucocorticoids. As the storage location for amino acids (AA) most of these effects are witnessed within skeletal muscle. Under stress glucocorticoids work to liberate AA to meet changes in metabolic demand, however glucocorticoid excess can lead to serve skeletal muscle atrophy (Magomedova and Cummins, 2016, Sato et al., 2018).

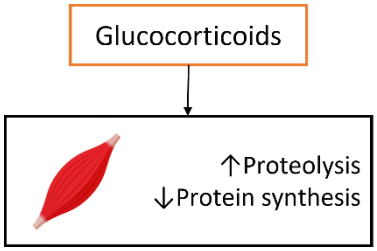

Figure 1.8: Glucocorticoid effects on protein metabolism in skeletal muscle.

1.5.3.1 Skeletal muscle

Glucocorticoids primarily impact protein metabolism in skeletal muscle by regulating two key processes. Glucocorticoids both enhance catabolic, proteolytic pathways (Hasselgren, 1999, Bodine et al., 2001, Schakman et al., 2013, Fry et al., 2016, Morgan et al., 2016a, Wang et al., 2017) and attenuate anabolic mechanisms that enhance muscle protein synthesis (Kostyo and Redmond, 1966, Liu et al., 2001, Schakman et al., 2013), decreasing muscle mass overall (Magomedova and Cummins, 2016, Sato et al., 2018). Multiple proteolytic mechanisms are upregulated by glucocorticoids, one of which being the ubiquitin proteasome system (Bodine et al., 2001). This involves an upregulation of the enzymes muscle RING finger 1 (MuRF1) and muscle atrophy F-box (MAFbx) (Bodine et al., 2001, Clarke et al., 2007, Fry et al., 2016, Katsuki et al., 2019, Hsieh et al., 2020). Glucocorticoids have also been shown to increase the expression of other catabolic enzymes or markers of skeletal muscle atrophy, including REDD1, KLF15 (Schiaffino et al., 2013), FOXO (Cho et al., 2010) and myostatin (Ma et al., 2003) as well as increase the activity of the calcium dependent and lysosomal systems catabolic pathways (Hasselgren, 1999). A glucocorticoid induced decrease in muscle protein synthesis is also caused by multiple factors (Magomedova and Cummins, 2016). Glucocorticoids have been shown to decrease amino acid delivery to skeletal muscle (Kostyo and Redmond, 1966), restricting the building blocks of protein synthesis. Additionally, glucocorticoids downregulate the activity and transcription of key anabolic enzymes. Through inhibition of mechanistic

target or rapamycin (mTOR) (Morgan et al., 2016a, Wang et al., 2017, Hsieh et al., 2020) and AKT (Hsieh et al., 2020) phosphorylation of eIF4E-binding protein 1 (4E-BP1), S6 kinase 1 (S6K1) (Liu et al., 2001) is attenuated, reducing muscle protein synthesis. Finally, insulin resistance and reduced insulin growth factor 1 (IGF1) concentrations induced by glucocorticoids, further attenuate muscle protein synthesis (Hu et al., 2009, Inder et al., 2010, Dhindsa et al., 2019) whilst also enabling apoptosis and proteolysis (Inder et al., 2010). Therefore, it is unsurprising that a sustained overexpression of glucocorticoids leads to reduced muscle size (Morgan et al., 2016a, Gokulakrishnan et al., 2017, Alev et al., 2018, Hsieh et al., 2020, Katsuki et al., 2019) with a preference for type II muscle fibres (Dekhuijzen et al., 1995, Schakman et al., 2013). This is accompanied by reduced muscle force (Shin et al., 2000), increased stiffness (Alev et al., 2018) and myopathy (Schakman et al., 2008, Sato et al., 2018), all of which can be implicated in multiple disease states (Abad et al., 2001, Gokulakrishnan et al., 2017).

1.5.4 Other metabolic functions of glucocorticoids

Beyond just glucose, lipid and protein metabolism glucocorticoids also influence other metabolic functions and parts of the body. An example of this is bone tissue as glucocorticoids regulate osteoblast proliferation and differentiation (Hardy et al., 2018). However, once again glucocorticoid excess can inhibit these processes leading to bone loss or osteoporosis (Hardy et al., 2018). Other evidence suggests that glucocorticoids partly regulate the central nervous system, specifically the paraventricular and arcuate nuclei in the brain (Magomedova and Cummins, 2016). Through these nuclei glucocorticoids regulate energy intake and even insulin resistance in the previously mentioned tissues (Yi et al., 2012). Mitochondrial function and content can also be increased by glucocorticoids however only up to a point (Yoon et al., 2001,

Weber et al., 2002, Puigserver and Spiegelman, 2003, Suzuki et al., 2018). In fact, corticosterone has been shown to increase mitochondrial oxidation, in a dose and time dependent manner in rats, with lower doses potentiating and higher doses attenuating (Du et al., 2009). In fact, Tang et al. (2013) found that greater concentrations of corticosterone increased protein carbonylation (protein oxidation caused by reactive oxygen species (ROS)) and reduced complex 1 activity within the electron transport chain, mitochondrial function. Glucocorticoid excess also inhibits the antioxidant enzymes required to combat the increase in ROS (Tang et al., 2013, Spiers et al., 2014).

1.5.5 Sexual and species-specific dimorphism in the metabolic effects of glucocorticoids

Whilst the overall metabolic impact of glucocorticoids is similar between males and females, some instances of sexual dimorphism have been identified. Within the liver alone of rodents, synthetic glucocorticoid treatment has been show to alter the transcription of 2388 transcripts exclusively in males, whilst also exclusively altering the transcription of 4293 transcripts in females (Quinn and Cidlowski, 2016, Kroon et al., 2020). For examples, transcription of apoptosis genes were more greatly effected within males, whilst genes effecting circadian rhythm and hypoxia were more effected within females (Quinn and Cidlowski, 2016, Kroon et al., 2020). Within rodent models of glucocorticoid excess male mice have been reported more susceptible to hyperglycaemia and insulin resistance whilst females appear more susceptible to hyperlipidaemia, adipose accumulation, and weight gain (Gasparini et al., 2019, Kaikaew et al., 2019, Kroon et al., 2020). Additionally, within humans, it appears that males are more susceptible to glucocorticoid induced osteoporosis and skeletal muscle atrophy (Kroon et al., 2020). However, also in humans exposed to increased synthetic glucocorticoid excess females are more susceptible to hyperglycaemia, whilst also

being more susceptible to obesity and hyperlipemia (Kroon et al., 2020), indicating species specific dimorphism. Additional species-specific dimorphism between rodents and humans have also been identified. For example, within BAT glucocorticoid are thought to suppress thermogenesis in rodents, whilst evidence in humans indicates the opposite effect (Ramage et al., 2016). Likewise, the impact of glucocorticoids on some inflammatory regulation genes has also been reported to differ between humans and rodents (Tchen et al., 2010).

1.6 Metabolic issues caused by glucocorticoid excess

As mentioned throughout section 1.5 glucocorticoid excess can compromise numerous metabolic functions and cause numerous metabolic conditions. These include hyperglycaemia (Lenzen and Bailey, 1984, Burke et al., 2017), insulin resistance (Du et al., 2003, Holland et al., 2007, Burke et al., 2017), reduced insulin secretion (Lambillotte et al., 1997, Blondeau et al., 2012), diabetes mellitus (Di Dalmazi et al., 2012, Rafacho et al., 2008), apoptosis (Reich et al., 2012), dyslipidaemia (Arnaldi et al., 2010), hypertension (Goodwin and Geller, 2012), hepatic steatosis (Peckett et al., 2011, Woods et al., 2015), abdominal obesity (Abraham et al., 2013), skeletal muscle atrophy (Morgan et al., 2016a, Schakman et al., 2013), reduced skeletal muscle force output (Shin et al., 2000), increased stiffness (Alev et al., 2018) myopathy (Schakman et al., 2008), osteoporosis (Hardy et al., 2018) and impaired mitochondrial function (Du et al., 2009, Tang et al., 2013, Spiers et al., 2014). However, there are other metabolic conditions, in other parts of the body, not mentioned in section 1.5 that are also caused by glucocorticoid excess. These can include cardiovascular issues such as coronary heart disease or heart failure (Fardet and Feve, 2014). Dermatologically issues such as skin atrophy, impaired wound healing and bruising are all common (Oray et al., 2016). Gastrointestinal issues such as gastritis (Gabriel et al., 1991) can occur, as can

ophthalmological issues such as cataracts and glaucoma (Tripathi et al., 1999, James, 2007). Finally immune response complications can arise both making people more susceptible and less able to combat certain conditions (Stuck et al., 1989, Oray et al., 2016). The most prominent condition, and the one that is most synonymous with glucocorticoid excess is Cushing's syndrome or disease (Lacroix et al., 2015, Chaudhry and Singh, 2022, Cushing, 1994). Termed as Cushing's syndrome, if linked directly to excess endogenous or exogenous cortisol (corticosterone in rodents) within the blood, or Cushing's disease if linked to excessive ACTH production caused by a pituitary adenoma (EndocrineSociety, 2022). Incorporating many of the previously mentioned conditions, Cushing's syndrome and disease both result in a classic phenotype first identified by Harvey Williams Cushing in 1912 and shown in Fig. 1.9 (Cushing, 1994, Lonser et al., 2017). Cushing's disease remains a rare condition affecting between 10 and 15 people per million annually (EndocrineSociety, 2022). Endogenous Cushing's syndrome also remains rare and affects between 1.8 and 3.2 people per million globally (Hakami et al., 2021). Exogenous Cushing's syndrome on the other hand is far more prevalent accounting for up to 80% of all cases of syndrome or disease (EndocrineSociety, 2022). It is also continually growing in prevalence, with up 2% of the United Kingdom and United States populations now prescribed exogenous glucocorticoid treatment (Morgan et al., 2016b). However, unlike the other two conditions the epidemiological data for the number of cases per million is lacking. Regardless of cause, with insufficient treatment Cushing's syndrome and disease remain potentially life-threatening conditions (Barbot et al., 2020, Hakami et al., 2021). Even with successful treatment mortality risk remains elevated due to the number of lasting metabolic complications Cushing's syndrome and disease present (Hakami et al., 2021).

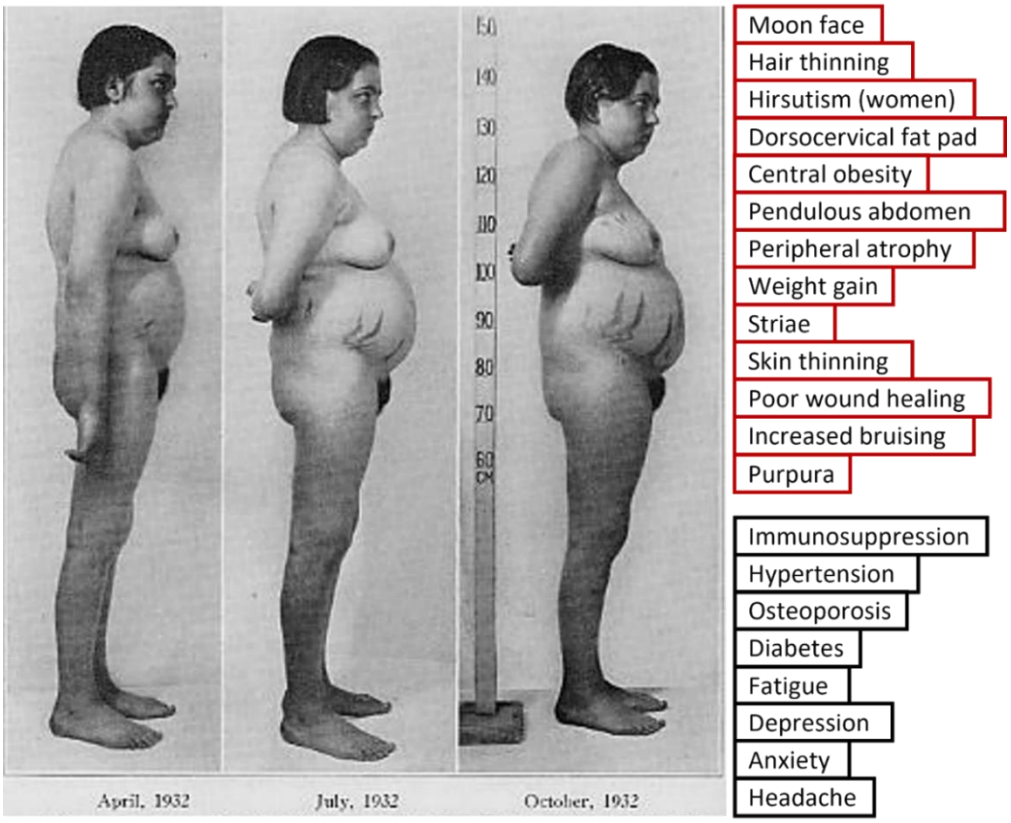

Figure 1.9: Cushing's syndrome phenotype and symptoms. Red, visible; black, non-visible. Adapted from Cushing (2016) - The basophil adenomas of the pituitary body and their clinical manifestations (pituitary basophilism). 1932

1.7 Sources of excess endogenous glucocorticoids

As previously mentioned, endogenous glucocorticoids are synthesised from cholesterol within the adrenal glands (Payne and Hales, 2004, Miller and Auchus, 2011). A process that is regulated by the HPA axis (Ramamoorthy and Cidlowski, 2016). However, dysfunction of the axis can promote glucocorticoid excess (Raff and Carroll, 2015). The source of this dysfunction is often excess ACTH production, likely from an ACTH secreting adenomas or tumours which are most often found on the pituitaries but can occur on other tissues (Isidori and Lenzi, 2007, Raff et al., 2014, Raff and Carroll, 2015). These cause subsequent stimulation of the adrenals and increased glucocorticoid synthesis. Additionally, adrenal adenomas can stimulate glucocorticoid synthesis without the need for ACTH (Raff and Carroll, 2015). Finally, there is

some evidence that the ageing process contributes to dysfunction of the HPA axis feedback loop (Sapolsky et al., 1986, Mizoguchi et al., 2009) resulting in greater circulating glucocorticoid concentrations (Gupta and Morley, 2014). However, endogenous glucocorticoid excess, and therefore endogenous Cushing's syndrome and Cushing's disease, remain relatively rare (Lindholm et al., 2001).

1.8 Sources of excess exogenous glucocorticoids

A prominent function of glucocorticoids and a major reason for exogenous glucocorticoid treatment is their use as anti-inflammatory drugs. Through previously mentioned mechanisms (section 1.4) iatrogenic glucocorticoids can combat inflammation related conditions (Barnes, 1998, Rhen and Cidlowski, 2005) such as tendinopathy, arthritis, asthma and more (Barnes, 1998, Ducharme et al., 2009, Coombes et al., 2010). Synthetic glucocorticoids, which are often more potent than endogenous glucocorticoids, are prescribed for this purpose. These include prednisolone, prednisone, methylprednisolone, dexamethasone, betamethasone and hydrocortisone which can be administered multiple ways (Overman et al., 2013, Raff and Carroll, 2015). Whilst they are effective drugs, prolonged or excessive use of often supraphysiological doses greatly increase circulating glucocorticoid concentrations (Raff and Carroll, 2015). Iatrogenic glucocorticoids are therefore the most common cause of Cushing's syndrome (Barbot et al., 2020, Chaudhry and Singh, 2022).

1.9 Treatments for glucocorticoid excess

The treatments and efficacy of treatment for Cushing's syndrome/disease are determined by its cause. Several treatment options are available if the cause is endogenous in nature (Nieman et al., 2015, Lacroix et al., 2015). Drug treatments aimed at inhibiting

steroidogenesis, or the glucocorticoid receptor are popular non-invasive options (Lacroix et al., 2015). Additionally, drugs that target specific receptors within an adenoma, in either an agonistic or antagonistic role can be used (Lacroix et al., 2015). However, drug treatments are often accompanied with side effects such as hyperglycaemia, hypogonadism, and gastrointestinal issues (Lacroix et al., 2015). Surgical interventions are another option for treating endogenous Cushing's syndrome. In the case of an ACTH secreting tumour or adenoma, surgery to remove it is often used (Nieman et al., 2015, Lacroix et al., 2015). Another, more extreme, option is a unilateral or bilateral adrenalectomy (Nieman et al., 2015, Lacroix et al., 2015). Whilst effective these surgical interventions might not provide a definitive solution. Tumours can reform post-surgery in up to 25% of patients (Lacroix et al., 2015). Additional post surgery exogenous glucocorticoid treatment is needed until HPA axis function recovers or indefinitely if it does not (Lacroix et al., 2015). Care must be taken to avoid the development of exogenous Cushing's syndrome (Nieman et al., 2015). The final option for endogenous Cushing's syndrome is radiotherapy to destroy the tumour or adenoma responsible (Nieman et al., 2015, Lacroix et al., 2015). The options for treating exogenous Cushing's syndrome are less extensive. At present the treatment strategy is to gradually reduce the dose of exogenous glucocorticoid given, with care taken to ensure this does not worsen the original condition the glucocorticoids were prescribed for (NHS, 2021, AANS, 2022). Treatment of the metabolic issues caused by glucocorticoid excess runs in parallel with this.

1.10 Further research into the metabolic effects of glucocorticoid excess and its treatment

Despite this extensive knowledge of glucocorticoid excess, the understanding of the metabolic complications caused by sustained glucocorticoid excess is incomplete and gaps in

the literature remain. Due to limited and conflicting literature, summarised in table 1.1, it is presently unclear if glucocorticoid excess, as well as the plethora of tissue specific and global effects that come with it, are reflected in markers of global energy metabolism which can be indicative of global metabolic health. As markers of energy metabolism are often closely linked with, and altered by, the previously mentioned metabolic conditions (Carneiro et al., 2016, Caron et al., 2016) it remains likely these markers are disrupted by glucocorticoid excess. The primary of these markers is energy expenditure (EE) and is often termed as metabolic rate. Shown as a measure of calorie expenditure it is calculated from heat output which can be measured directly, or indirectly via gas exchange. Presently, there is no clear consensus on whether EE is increased (Bessey et al., 1984, Chong et al., 1994, Tataranni et al., 1996), decreased (Poggioli et al., 2013), or even unaltered (Horber et al., 1991, Gravholt et al., 2002, Short et al., 2004, Burt et al., 2006, Radhakutty et al., 2016) by glucocorticoid treatment or glucocorticoid excess. The same is true of a second marker, the respiratory exchange ratio (RER). This is a function of oxygen consumption and carbon dioxide production which creates a value between 0 and 1 giving an indirect measure of substrate utilisation. A value of 0.7 indicates primarily lipid usage, whereas a value towards 1 indicates primarily carbohydrate usage. Much like EE, it is unclear is this is increase (Chong et al., 1994), decreased (Bessey et al., 1984, Tataranni et al., 1996, Poggioli et al., 2013), or unaltered (Horber et al., 1991, Brillon et al., 1995, Gravholt et al., 2002, Short et al., 2004) by glucocorticoid treatment or glucocorticoid excess. The effect of glucocorticoid treatment or glucocorticoid excess is also unclear on the constituent parts of RER, oxygen consumption and carbon dioxide production. Whether they increase (Bessey et al., 1984), or remain unaltered (Horber et al., 1991, Brillon et al., 1995, Short et al., 2004, Poggioli et al., 2013) is not clear.

Table 1.1: The effects of glucocorticoid treatments on energy metabolism

Authors	Model	Treatment protocol	Effect on energy metabolism
Bessey et al. (1984)	Male healthy humans, N=9	Intravenous infusion of 98mg HC for 74hours	↑ EE ↑ O_2 consumption ↑ CO_2 production ↓ RER
Horber et al. (1991)	Healthy humans, N=8	Three times per day oral 0.8mg/kg PRED for 7 days	No effect on EE No effect on O_2 consumption No effect on CO_2 production No effect on RER
Chong et al. (1994)	Female healthy humans, N=7	Twice daily oral 1mg BEM for 14 days	↑ EE ↑ RER
Brillon et al. (1995)	Male and female healthy humans, N=8 and 1	Intravenous infusion of 200µg/kg/hr of HC for 20hours	↑ EE No effect on O_2 consumption No effect on CO_2 production No effect on RER
Tataranni et al. (1996)	Male healthy humans, N=20	Intravenous infusion of 125mg METH for 30 minutes	↑ EE ↓ RER
Gravholt et al. (2002)	Male healthy humans, N=8	Twice daily oral 15mg PRED for 7 days	No effect on EE No effect on RER
Short et al. (2004)	Male and female healthy humans, N=3 and 3	Daily oral 0.5mg/kg PRED for 6 days	No effect on EE No effect on O_2 consumption No effect on RER

Table 1.1: continued

Authors	Model	Treatment protocol	Effect on energy metabolism
Burt et al. (2006)	Male and female cushingoid patients, N=6 and 12	N/A	No effect on EE
Poggioli et al. (2013)	Male C57BL/6J mice, N=6	Daily intraperitoneal injections of 5mg/kg DEX for 7 weeks	↓ EE ↓ RER No effect on O_2 consumption
Radhakutty et al. (2016)	Male and female RA patients, N=6 and 12	Daily oral 6mg/day PRED for 7 days (acute) and 6 months (chronic)	No effect of acute or chronic on EE

DEX, dexamethasone; PRED, prednisone; HC, hydrocortisone; BEM, betamethasone; METH, methylprednisolone; EE, energy expenditure; RER, respiratory exchange ratio; O_2, oxygen; CO_2, carbon dioxide; RA, rheumatoid arthritis

In addition to this unanswered questions, current treatment strategies are far from simple and not always effective. Alternate therapeutic approaches are therefore required to both deal with the consequences of existing glucocorticoid excess and mitigate the development of the phenotype whilst still facilitating the beneficial effects of endogenous or exogenous glucocorticoids. Treatment strategies including nutritional, lifestyle or exercise-based approaches must therefore be considered alongside medical drugs and surgical intervention. However, to develop these new approaches a greater understanding of the underlying mechanisms of glucocorticoid excess is required. Whether these be global or tissue specific in nature, focus must be given to how key metabolic molecules that have far reaching

metabolic importance, like glucocorticoids, are themselves effected. Whilst several of these molecules are known to exist, initial investigation should prioritise molecules that are commonly linked with metabolic conditions caused by glucocorticoid excess. One such candidate, that already has therapeutic potential for other metabolic conditions, is nicotinamide adenine dinucleotide (NAD^+) and its metabolome. Reported decreased in several metabolic conditions that can be caused by glucocorticoid excess (Wu et al., 2016, Lin et al., 2021, Dall et al., 2022) it is presently unclear whether the far reaching metabolic control of glucocorticoids overlaps or interacts with the wide reaching metabolic importance of NAD^+ and its metabolome. It is equally unclear whether the two share a regulatory relationship or if alteration to one influences the other. Exploring the impact on this vastly important metabolic molecule might therefore provide insights into the mechanisms of glucocorticoid excess as well as prove to be a valid therapeutic target.

1.11 Nicotinamide Adenine Dinucleotide

Nicotinamide adenine dinucleotide (NAD^+) is a vital molecule that serves to maintain metabolic function and homeostasis (Xie et al., 2020a). In fact, NAD^+ has a complex metabolome (Fig. 1.10) that is central to the regulation of a plethora of metabolic processes including energy metabolism, circadian clock function, inflammation and more (Xie et al., 2020a). First discovered by Harden and James in 1906 (Manchester, 2000) it was later identified as a key redox cofactor in 1936 by Warburg and Christian, confirming its metabolic importance (Meyerhof and Oesper, 1947). Since then, the growing understanding of NAD^+ has cemented its metabolic importance further. Now known to also be a vital substrate for poly-ADP ribose polymerases (PARPs) (Chambon et al., 1963), sirtuins (SIRT1-7) (Frye, 1999, Imai et al., 2000, Landry et al., 2000) and cyclic ADP-ribose synthases (Malavasi et al., 2008)

making NAD^+ crucial for metabolic signalling. Existing in an oxidised (NAD^+) and reduced (NADH) form when carrying electrons, it is kept in a tightly controlled NAD^+/NADH ratio, determined by cellular location. Additionally, NAD^+ can be phosphorylated by NAD kinase (NADK) to NADP and then further reduced to NADPH, acting in a similar way to NAD^+/NADH (Agledal et al., 2010). The concentration of NAD^+ varies between 300-800µM depending on the tissue, cellular location, or organelle (Dolle et al., 2010, Stein and Imai, 2012, Cambronne et al., 2016) and is highly responsive to changes in metabolic demand.

1.12 NAD^+ synthesis

Nicotinamide adenine dinucleotide is endogenously synthesised or salvaged in a tissue or subcellular location dependent manner from multiple sources; tryptophan (Trp) or the vitamin B3 precursors nicotinic acid (NA), nicotinamide riboside (NR), reduced nicotinamide riboside (NRH) and nicotinamide (NAM) as well as the intermediates nicotinamide mononucleotide (NMN) and reduced nicotinamide mononucleotide (NMNH), all of which can be acquired in the diet (Bogan and Brenner, 2008, Houtkooper et al., 2010, Stein and Imai, 2012, Trammell et al., 2016a, Ummarino et al., 2017) (Fig. 1.10). Each of these sources, and the biosynthetic enzymes that convert them to NAD^+ are often tissue or subcellular location dependent, thus limiting the activity of some pathways whilst increasing the importance of others in certain tissues (Houtkooper et al., 2010, Nikiforov et al., 2011). For example, both de novo biosynthesis (section 1.12.1) and the Preiss- Handler (section 1.12.2.1) pathways are negligible in skeletal muscle but are prominent in the liver, especially de novo biosynthesis (Liu et al., 2018). Whereas the NRK2 salvage (section 1.12.2.2) pathway is thought to predominantly be in skeletal muscle (Liu et al., 2018). As for subcellular location, NMNAT3 is found in the mitochondria, whereas NRK1 and 2 are both localised to the cytosol (Nikiforov

et al., 2011). These pathways are crucial for maintaining cellular NAD^+ levels as exogenous NAD^+ cannot enter the cell directly (Davila et al., 2018). Therefore, without these synthesis pathways to maintain cellular NAD^+ levels and to counter NAD^+ degrading processes, the cell would have completely depleted NAD^+ levels within hours (Yang and Sauve, 2016).

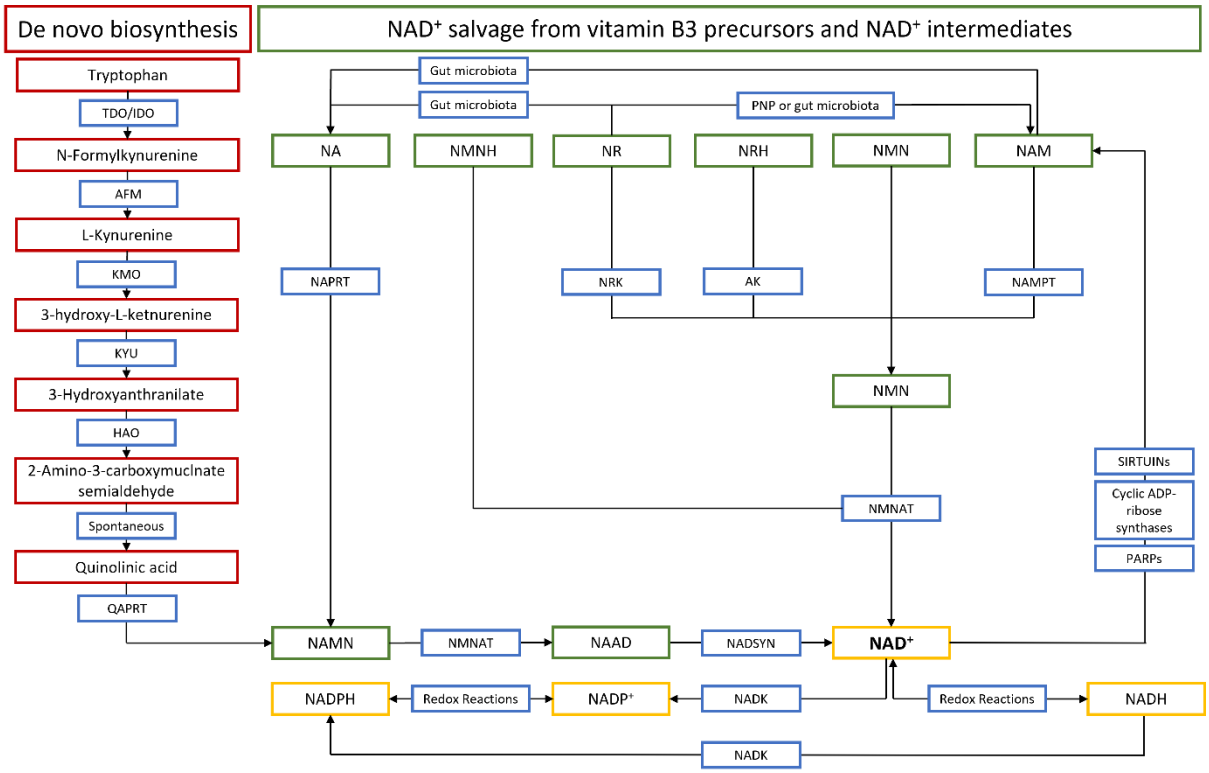

Figure 1.10: The NAD^+ metabolome and its cellular NAD^+ synthesising pathways, de novo biosynthesis and salvage from NAD^+ precursors and intermediates. Red, kynurenine intermediate; green, NAD^+ intermediate; blue, enzyme. Abbreviations: TDO, tryptophan 2,3-dioxygenase; IDO, indoleamine 2,3-dioxygenase; AFM, kynurenine formamidase; KMO, kynurenine 3-monooxygenase; KYU, kynureninase; HAO, 3-HAA 3,4-dioxygenase; QAPRT, quinolinate phosphoribosyltransferase; NMNAT, nicotinamide adenylyl tranferase; NADSYN, NAD^+ synthetase; NADK, NAD^+ kinase; NAMN, nicotinic acid mononucleotide; NAAD, nucleic acid dinucleotide; NA, nicotinic acid; NMNH, reduced nicotinamide mononucleotide; NR, nicotinamide riboside; NRH, reduced nicotinamide riboside; NMN, nicotinamide mononucleotide; NAM, nicotinamide; NAPRT, nicotinic acid phosphoribosyltransferase; NRK, nicotinamide riboside kinase; AK, adenosine kinase; PNP, purine nucleoside phosphorylase; NAMPT, nicotinamide phosphoribosyltranferase; PARPs, poly-ADP ribose polymerases; NAD^+, nicotinamide adenine dinucleotide; NADH, reduced NAD^+; $NADP^+$, NAD^+ phosphate; NADPH, reduced $NADP^+$.

1.12.1 De novo biosynthesis

De novo biosynthesis refers to the kynurenine pathway (Fig. 1.11) and starts with Trp being converted to N-formylkynurenine by either indoleamine 2,3-dioxygenase (IDO) or tryptophan 2,3-dioxygenase (TDO). This is then converted to α-amino-β-carboxymuconate-ε-semialdehyde (ACMS) by four enzymatic reactions (Nikiforov et al., 2011). ACMS is then converted to quinolinic acid (QA) by quinolinate phosphoribosyltransferase (QPRT) before it becomes nucleic acid mononucleotide (NAMN). Conversion to nucleic acid dinucleotide (NAAD) by nicotinamide mononucleotide adenylyltransferase (NMNAT) then follows (Nikiforov et al., 2011) before conversion to NAD^+ by NAD synthase (NADSyn) (Hara et al., 2003).

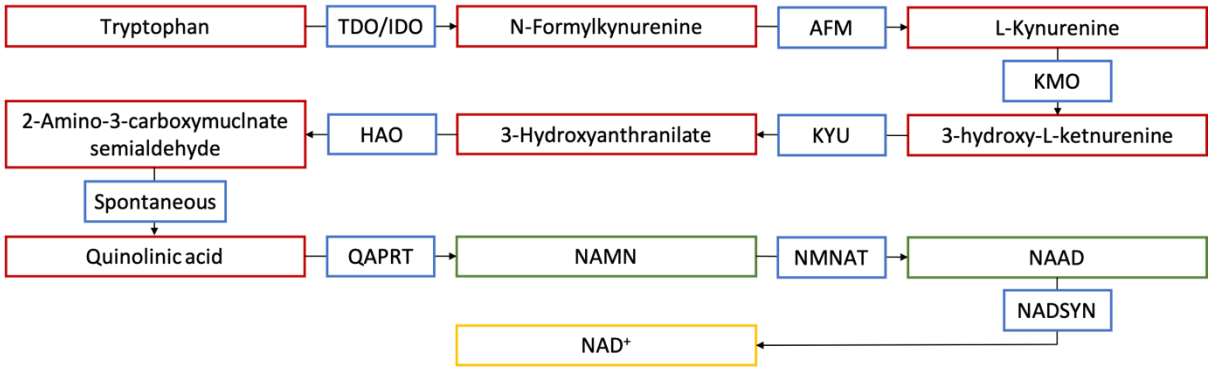

Figure 1.11: De-novo biosynthesis from dietary tryptophan. Red, kynurenine intermediate; green, NAD^+ intermediate; blue, enzyme. Abbreviations: TDO, tryptophan 2,3-dioxygenase; IDO, indoleamine 2,3-dioxygenase; AFM, kynurenine formamidase; KMO, kynurenine 3-monooxygenase; KYU, kynureninase; HAO, 3-HAA 3,4-dioxygenase; QAPRT, quinolinate phosphoribosyltransferase; NMNAT, nicotinamide adenylyl tranferase; NADSYN, NAD^+ synthetase; NAMN, nicotinic acid mononucleotide; NAAD, nucleic acid dinucleotide

1.12.2 Vitamin B3 and intermediate salvage pathways

Whilst both de novo biosynthesis and the Preiss-Handler pathway effectively produce NAD^+, additional pathways are required to meet the demand of the body (Nikiforov et al., 2011). Therefore NAD^+ is also salvaged from vitamin B3 precursors; NA, NR and NAM, as well as an

additional intermediate NMN (Fig. 1.12). These sources are known to be far more effective at generating NAD^+ than Trp (Fricker et al., 2018).

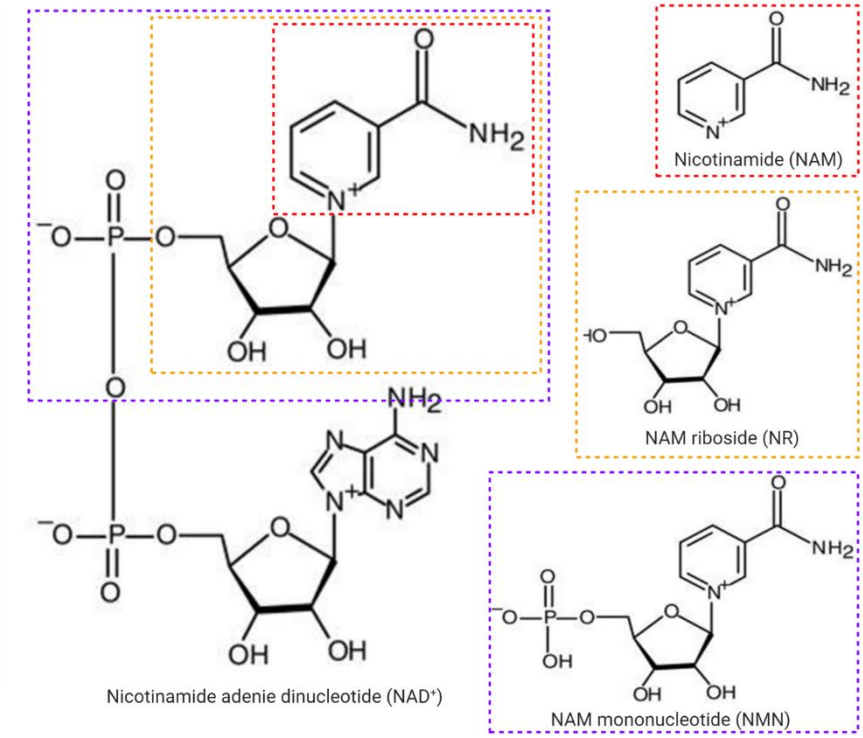

Figure 1.12 Nicotinamide adenine dinucleotide, it's precursors and molecular structures.

1.12.2.1 Nicotinic acid salvage pathway

The first of these precursors, NA, is synthesised to NAD^+ via the Preiss-Handler pathway (Fig. 1.13). To enter this pathway NA first enter the cell through a transporter-mediated pathway (Ma et al., 2014). Once in the Preiss-Handler pathway NA is converted to NAMN with NA phosphoribosyltransferase (NAPRT). Much like in de novo biosynthesis NAMN is then converted to nucleic acid dinucleotide (NAAD) by nicotinamide mononucleotide adenylyltransferase (NMNAT) (Nikiforov et al., 2011) before conversion to NAD^+ by NAD synthase (NADSyn) (Hara et al., 2003). To date NA remains the most widely used, and researched, exogenous supplement to increase endogenous NAD^+ in humans (Hara et al., 2007).

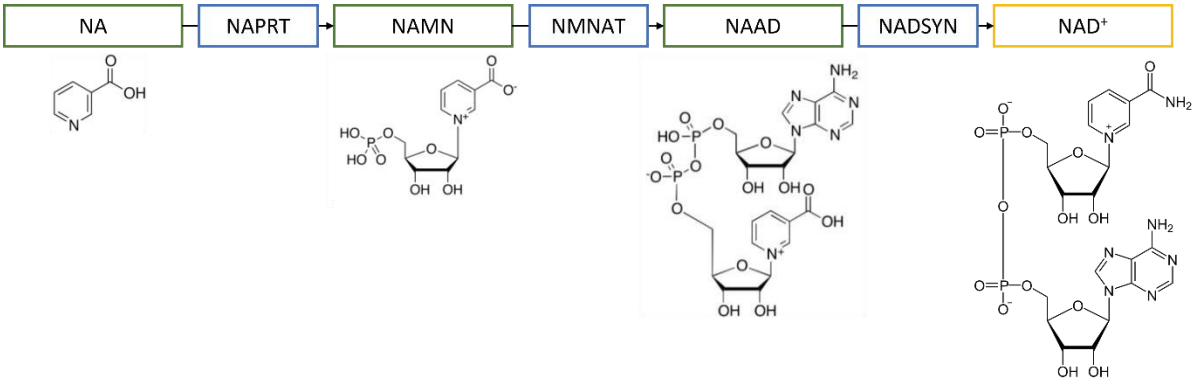

Figure 1.13: Nicotinic acid salvage pathway. Green, NAD^+ intermediates; blue, enzyme. Abbreviations: NA. nicotinic acid; NAMN, nicotinic acid mononucleotide; NAAD, nucleic acid dinucleotide; NAPRT, nicotinic acid phosphoribosyltransferase NMNAT, nicotinamide mononucleotide adenylyltransferase; NADSYN, NAD^+ synthetase.

1.12.2.2 Nicotinamide riboside salvage pathway

Another precursor, NR, is converted to NAD^+ via the nicotinamide riboside kinase (NRK) salvage pathway (Fig. 1.14). Able to cross the plasma membrane of a cell through equilibrative nucleoside transporters (ENTs) (Felici et al., 2015), NR enters the pathway and is converted nicotinamide mononucleotide (NMN) by phosphorylation via NRK1 and/or NRK2, depending on the tissue (Tempel et al., 2007). This is subsequently converted to NAD^+ by NMNAT (Bieganowski and Brenner, 2004). NR can be converted to NAM by purine nucleoside phosphorylase (PNP) (Belenky et al., 2009) or if orally consumed by gut microbiota (Shats et al., 2020) at which point it enters the nicotinamide salvage pathway. Alternatively, orally consumed NR can also be converted to NA by gut microbiota, as observed in mice colons (Shats et al., 2020). However, unless otherwise inhibited, phosphorylation by NRK1/2 remains the most prominent path (Belenky et al., 2009). The reduced form of NR (NRH) has recently been identified as a NAD^+ precursor, in the liver, is converted to NAD^+ in a different pathway (Yang et al., 2020). Firstly, NRH is phosphorylated by adenosine kinase (AK) to the reduced form of NMN (NMNH), that is subsequently converted to NAD^+ by NMNAT (Yang et al., 2020).

NR remains a relatively new exogenous NAD^+ boosting precursor and as such has undergone significantly less trials on humans than NA, with optimal treatment modality in rodents yet to be established (Liu et al., 2018). However, there is considerable evidence that NR can boost NAD^+ levels in cells (Bieganowski and Brenner, 2004), multiple mouse tissues (Canto et al., 2012) and to a lesser extent in humans (Trammell et al., 2016c, Martens et al., 2018). The NR salvage pathway, sufficiently supplied with supplemental NR, has also been reported to recover NAD^+ levels when other synthesising pathways have been inhibited (Ratajczak et al., 2016, Fletcher et al., 2017).

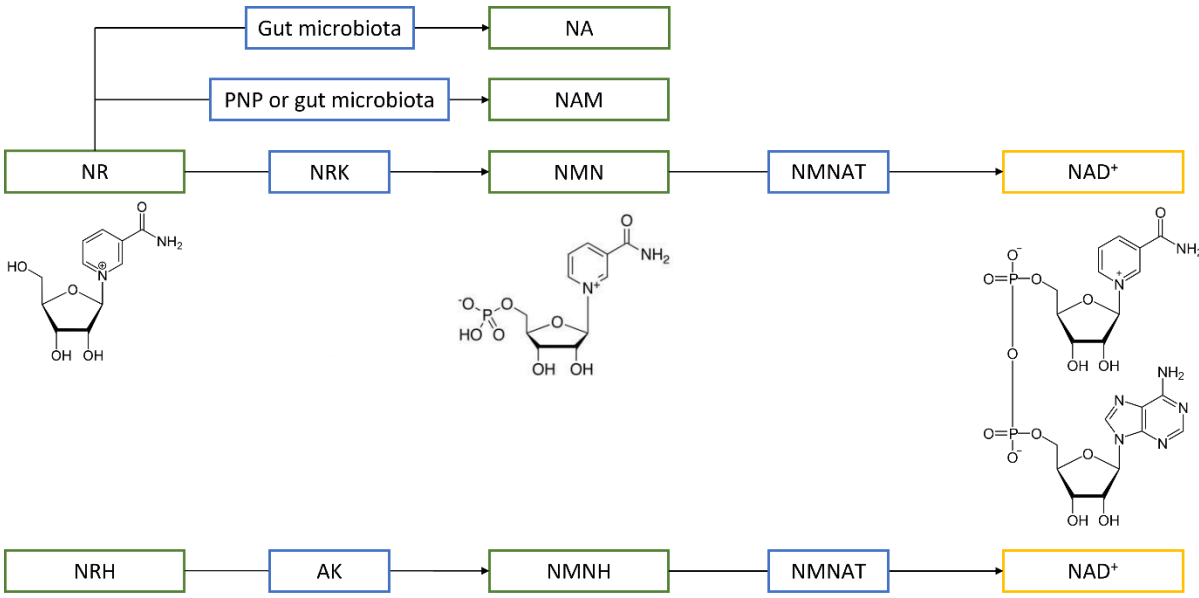

Figure 1.14: Nicotinamide riboside salvage pathway. Green, NAD^+ intermediates; blue, enzyme. Abbreviations: NR, Nicotinamide riboside; NMN, nicotinamide mononucleotide; NRH, reduced NR; NMNH, reduced NMN; NRK, nicotinamide riboside kinase; NMNAT, nicotinamide mononucleotide adenylyltransferase; AK, adenosine kinase; PNP, purine nucleoside phosphorylase.

1.12.2.3 Nicotinamide salvage pathway

Nicotinamide is another prominent precursor that can be synthesised to NAD^+ via the NAMPT dependent pathway (Fig. 1.15). Either entering the cell directly by crossing the plasma

membrane (Felici et al., 2015), or being made available by NAD^+ degradation, making it the primary source of NAD^+ recycling (Burgos et al., 2013). NAM is converted in the cell to NMN via NAMPT (Tan et al., 2013) before NMN is converted to NAD^+ by NMNAT (Bieganowski and Brenner, 2004). Importantly, NAMPT is known as the key rate limiting enzyme in NAD^+ synthesis (Tan et al., 2013). In fact, due to this and its ubiquitous expression, it remains vital for NAD^+ synthesis as inhibition of NAMPT can cause a drastic decline in cellular NAD^+ (Hasmann and Schemainda, 2003). Complete knock out (KO) of NAMPT activity is even lethal for embryonic mice (Zhang et al., 2016). However, orally consumed NAM can bypass NAMPT by first being converted to NA by gut microbiota, at which point it enters the Preiss-Handler pathway (Shats et al., 2020). In fact, NA has been shown to greatly increase in the colon, small intestine, liver and kidney following an oral gavage or labelled NAM (Shats et al., 2020). Up to 70% of colon, 30% of small intestine, 85% of liver and 90% of kidney NAD^+ synthesised from an oral dose of labelled NAM was first converted to NA and entered the Preiss-Handler pathway (Shats et al., 2020). Therefore, much like NA and NR, exogenous NAM supplementation has also been reported to elevate NAD^+ levels; primarily in mice (Klaidman et al., 1996, Liu et al., 2009, Mitchell et al., 2018). Like NR the research in humans is limited to date. Additionally, to protect against NAM overaccumulation, which can inhibit SIRT and PARP activity (Clark et al., 1971, Bitterman et al., 2002, Avalos et al., 2005), NAM can also be methylated to methylated NAM (MeNAM) by the enzyme nicotinamide N-methyltransferase (NNMT) (Pissios, 2017) (Fig. 1.15). This is subsequently cleared from the body, primarily in the urine (Pissios, 2017).

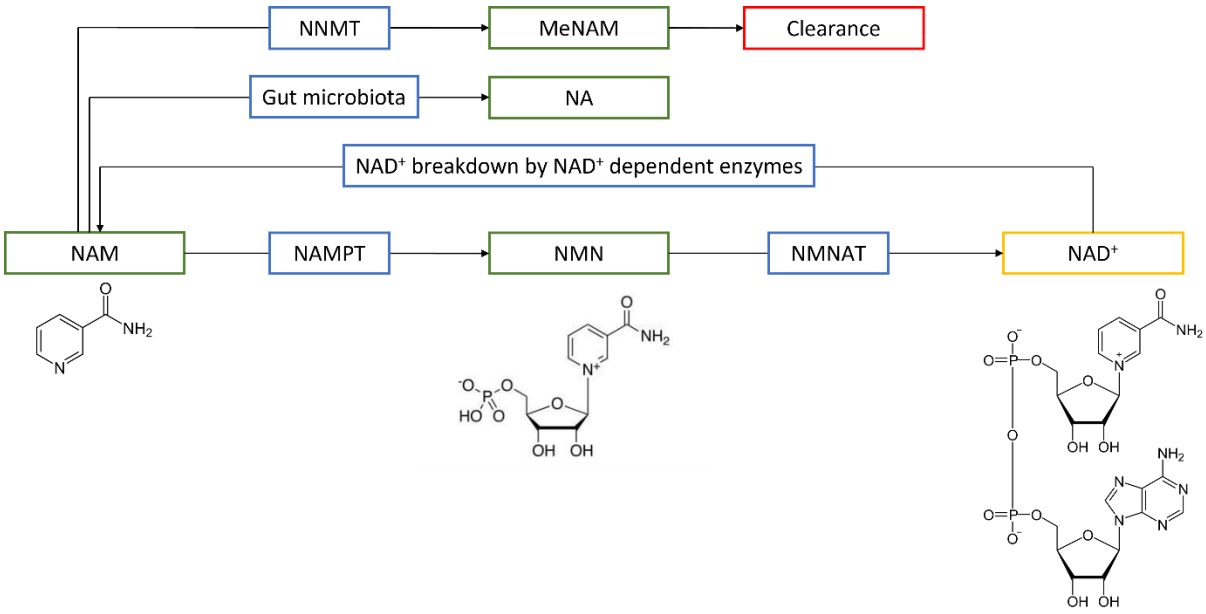

Figure 1.15: Nicotinamide salvage and clearance pathways. Green, NAD^+ intermediates; blue, enzyme. Abbreviations: NAM, Nicotinamide; NMN, nicotinamide mononucleotide; MeNAM, methylated NAM; NAMPT, nicotinamide phosphoribosyltranferase; NMNAT, nicotinamide mononucleotide adenylyltransferase; NNMT, nicotinamide N-methyltransferase.

1.12.2.4 Nicotinamide mononucleotide salvage pathway

As previously mentioned NMN is produced when NR is phosphorylated by NRK1 and/or NRK2 in the nicotinamide riboside pathway (Tempel et al., 2007), and when NAM is converted to NMN by NAMPT in the nicotinamide salvage pathway (Tan et al., 2013). Unlike NA, NR and NAM, NMN is not considered a vitamin B3 precursor due to the attached phosphate group. However, like these three exogenous NMN from the diet or supplementation can enter the cell directly via a SLC12A8 transporter in the cell membrane (Grozio et al., 2019). Alternatively, NMN can also be dephosphorylated extracellularly to NR, which is subsequently transported in the cell (Yoshino et al., 2018). Once in the cell, NMN is converted directly to NAD^+ by NMNAT (Bieganowski and Brenner, 2004) (Fig. 1.16). As with the vitamin B3 precursors exogenous NMN supplementation has been shown the boost NAD^+ levels, primarily in mice with limited humans studies conducted (Ratajczak et al., 2016, Fletcher et al., 2017).

Interestingly, supplementation with NMNH has been reported to boost NAD^+ at a faster rate in mice, despite also being converted to NAD^+ by NMNATs (Zapata-Perez et al., 2021).

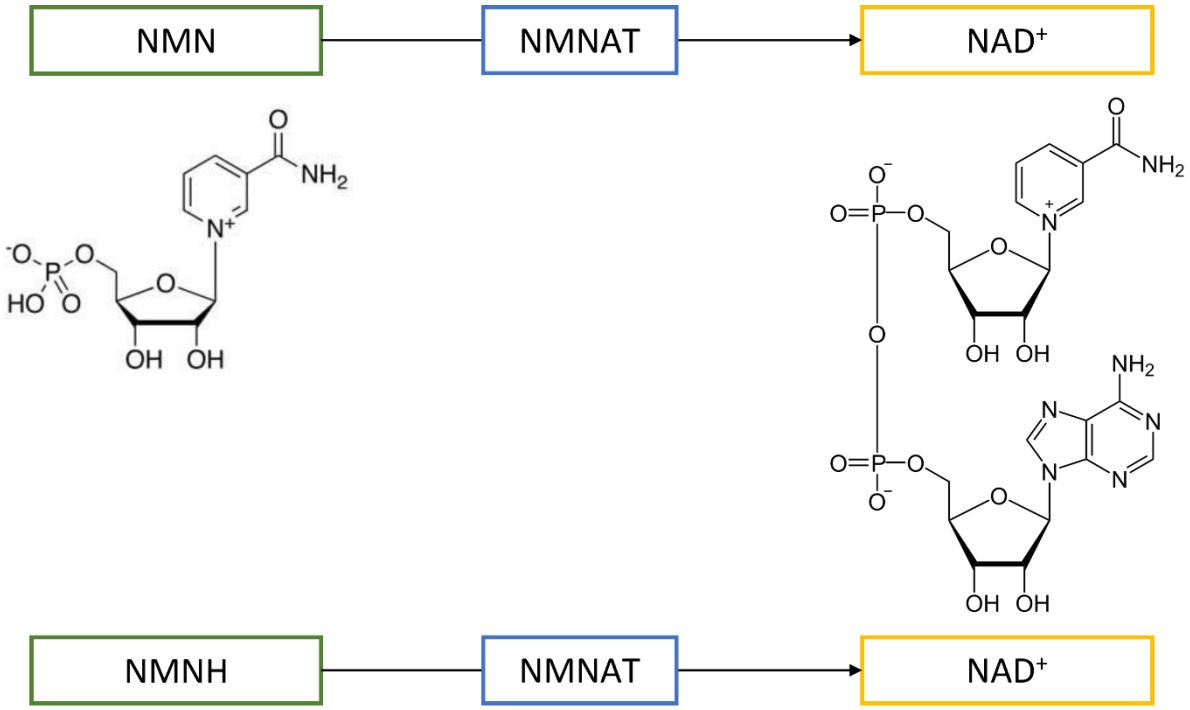

Figure 1.16: Nicotinamide mononucleotide salvage pathway. Green, NAD^+ intermediates; blue, enzyme. Abbreviations: NMN, nicotinamide mononucleotide; NMNH, reduced NMN; NMNAT, nicotinamide mononucleotide adenylyltransferase.

1.13 $NADP^+$ and NADPH

Nicotinamide adenine dinucleotide phosphate ($NADP^+$) is produced by the enzyme NAD kinase (NADK) which removes a phosphate group from ATP and attaches it to NAD^+ (Fig. 1.17) (Agledal et al., 2010). This process is highly dependent on NAD^+ availability and can be considered a NAD^+ depleting process, making up approximately 10% of total NAD^+ consumption (Agledal et al., 2010, Liu et al., 2018). Once phosphorylated, $NADP^+$ can be converted to NADPH by reversible redox reactions (Fig. 1.17) (Agledal et al., 2010), much like NAD^+ and NADH. However, in humans there remains a preference for the latter two with exceedingly large increases in NADK expression required for small increases in $NADP^+$/NADPH

(Pollak et al., 2007, Agledal et al., 2010). NADPH is the more prevalent of the two, as high concentrations are required for use in anabolic redox reactions that contribute to multiple pathways such as fatty acid synthesis, some amino acid synthesis and even steroid hormone synthesis (Agledal et al., 2010). This same redox function is also vital for liver detoxification (Agledal et al., 2010). Interestingly, NADPH serves a vital oxidative defence role against reactive oxygen species (ROS) whilst also contributing to ROS production to facilitate signalling process used for both cell growth and apoptosis (Agledal et al., 2010). As for $NADP^+$, besides its role in NADPH production and redox reactions, it also serves to contribute to key calcium signalling and second messenger processes (Agledal et al., 2010).

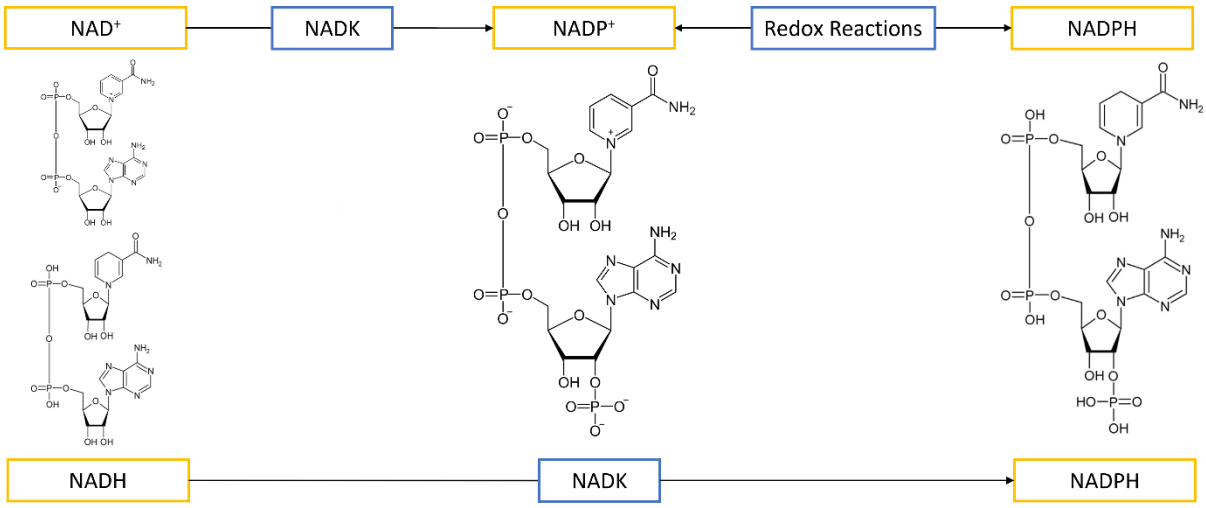

Figure 1.17: Nicotinamide adenine dinucleotide phosphate production pathway. Blue, enzyme. Abbreviations: NADK, NAD^+ kinase; NAD^+, nicotinamide adenine dinucleotide; NADH, reduced NAD^+; $NADP^+$, NAD^+ phosphate; NADPH, reduced $NADP^+$.

1.14 Subcellular localisation

Within the cell the distribution of NAD^+ is not even between the cytosol and organelles (Fig. 1.18). The same is true for the synthesis pathways and biosynthetic enzymes previously described (Fig. 1.18). Therefore, distinct subcellular pools of NAD^+ exists in three primary organelles; the mitochondria, cytosol or nucleus (Tischler et al., 1977, Houtkooper et al., 2010,

Nikiforov et al., 2011, Stein and Imai, 2012, Davila et al., 2018). The total NAD^+ content, and the redox ratio (NAD^+/NADH), varies between these pools and is largely determined by the metabolic functions they facilitate (Stein and Imai, 2012, Dolle et al., 2013). The largest concentration of up to 70% of total NAD^+ can be found in the mitochondria and is typically greater than 250µM (Yang et al., 2007, Covarrubias et al., 2021). The cytosol and nucleus have a much lower concentrations total NAD^+ that remains similar between the two and together exceeds no more than 100µM (Stein and Imai, 2012, Dolle et al., 2013, Covarrubias et al., 2021). However, these concentrations can vary with tissue type and their metabolic functions, with the concentration of mitochondrial total NAD^+ varying between 40-70% (Stein and Imai, 2012). The redox ratio also differs between these organelles, again varying with tissue type. Typically, the mitochondrial redox ratio is more reductive, ranging between 7-8 (number of NAD^+ for each NADH), whereas in the cytosol and nucleus it ranges between 60-700 (Stein and Imai, 2012, Dolle et al., 2013). NAD^+ and NADH can easily from the nucleus to the cytosol, and back, through pores in the nuclear membrane, hence why concentrations are very similar. However, they cannot as easily cross the mitochondrial membrane which results in a more isolated pool (Cambronne et al., 2016). This had caused the long-held belief that NAD^+ or NADH could not cross the mitochondrial membrane at all, despite some theorising (Davila et al., 2018). Recent findings however have shown that NAD^+ can in fact cross the mitochondrial membrane in through a SLC25A51 transporter (Luongo et al., 2020). It is likely that this transporter is tightly regulated to maintain the separate pool of mitochondrial NAD^+, that appears critical for survival (Yang et al., 2007). In fact, the pool of mitochondrial NAD^+ is so well protected that depletion of cytosolic NAD^+ is not reflected in the mitochondrial pool which is completely maintained for an additional 24 hours and maintains metabolic function for 72 hours (Pittelli et al., 2010). This is despite the now known existence of the

aforementioned transporter. In addition to the transporter, crosstalk between the cytosolic and mitochondrial pools is facilitated by both the glyceraldhyde-3-phosphate (G3P) and the malate-aspartate shuttles which takes electrons from cytosolic NADH and transports them into the mitochondria forming mitochondrial NADH (Easlon et al., 2008).

As for subcellular localisation of NAD^+ synthesising enzymes it is known that almost all enzymes localise to the nucleus and cytoplasm, with the only exceptions being NMNAT3, NMNAT1 and NRK, which are only found within the mitochondria, nucleus, or cytosol respectively (Nikiforov et al., 2011). Only one other enzyme, NAMPT, is found in the mitochondria, but unlike NMNAT3, it is found in all subcellular compartments (Covarrubias et al., 2021). The localisation of the NAD^+ precursors and intermediates; NR, NAM and NMN, are reflected by the location of the biosynthetic enzymes that use them to form NAD^+. All appear to be present in the cytosol (Nikiforov et al., 2011, Covarrubias et al., 2021). NAM can both be found in all compartments, however within the mitochondria it is only made available as a product of NAD^+ degradation (Nikiforov et al., 2011, Covarrubias et al., 2021, Amjad et al., 2021). NMN is also present in all three compartments either from translocating between them or by NAM salvage by NAMPT (Amjad et al., 2021).

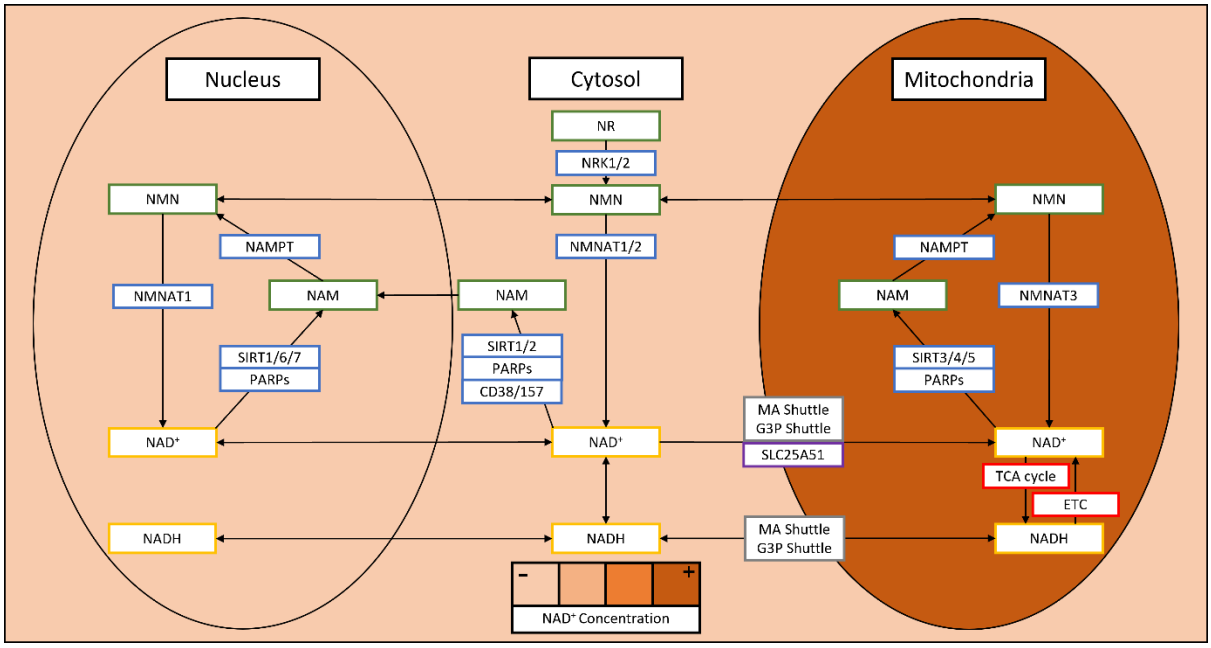

Figure 1.18: Subcellular localisation of NAD^+, biosynthetic enzymes, precursors and intermediates. Green, NAD^+ intermediates; blue, enzyme; grey, electron shuttle; purple, NAD^+ transporter; red, metabolic process. Abbreviations: NR, nicotinamide riboside; NMN, nicotinamide mononucleotide; NAM, nicotinamide; NRK, nicotinamide riboside kinase; NAMPT, nicotinamide phosphoribosyltranferase; NMNAT, nicotinamide adenylyl tranferase; PARPs, poly-ADP ribose polymerases; SIRT, sirtuins NAD^+, nicotinamide adenine dinucleotide; NADH, reduced nicotinamide adenine dinucleotide; MA, malate-aspartate; G3P, glyceraldhyde-3-phosphate; TCA, tricarboxylic acid; ETC, electron transport chain.

1.15 NAD^+ as a redox cofactor

Nicotinamide adenine dinucleotide was first identified as a key redox cofactor by Warburg and Christian in 1936 (Meyerhof and Oesper, 1947). As a redox cofactor NAD^+ is vital for oxidoreductase and transhydrogenase reactions in which it transfers electrons to drive metabolic process (Fig. 1.19) (Stein and Imai, 2012). In this role NAD^+ is found in either an oxidised (NAD^+) or reduced (NADH) form, the latter of which contains two additional bound electrons. Conversion between the two is facilitated by reversible redox reactions (Fig. 1.19) (Pollak et al., 2007). This makes NAD^+ redox function essential for the generation of ATP in the cytosol and mitochondria, through both glycolysis and oxidative phosphorylation (Di

Stefano and Conforti, 2013). The production of ATP requires glucose, lipids or proteins. In glycolysis glyceraldhyde-3-phosphate is converted to 1,3-biphosphoglycerate by glyceraldhyde-3-phosphate dehydrogenase (GAPDH) which uses NAD^+ as a cofactor to drive to reaction, reducing it to NADH (Fig. 1.20)(Baker et al., 2014). The final product of glycolysis, pyruvate, is converted to acetyl-CoA by pyruvate dehydrogenase (PDH), reducing NAD^+ to NADH in the process (Kerbey et al., 1977). Indeed NAD^+ is vital for maintaining the rate of glycolysis as a depletion effectively blocks it (Stein and Imai, 2012). Production of acetyl-CoA by beta oxidation also reduces NAD^+ to NADH as the enzyme 3-hydroxyacyl-CoA dehydrogenase requires NAD^+ as a cofactor (Rindler et al., 2013). Within the tricarboxylic acid (TCA) cycle the enzymes isocitrate dehydrogenase, α-ketoglutarate dehydrogenase and malate dehydrogenase function as redox enzymes requiring NAD^+ as a cofactor and therefore reducing it to NADH (Fig. 1.21)(Chen and Russo, 2012). Within the electron transport chain, the accumulated NADH is essential as the bound electrons are taken and used to create a proton gradient to produce ATP, thus oxidizing NADH to NAD^+ (Fig. 1.22) (Rindler et al., 2013). The importance of NAD^+ as a redox cofactor is highlighted by reduced ATP production and even cell death when NAD^+ is depleted (Tan et al., 2013, Frederick et al., 2016, Ju et al., 2016). This is also because the redox function of NAD^+ is not limited to the aforementioned roles (Elhassan et al., 2017). Similarly, NAD^+ can be phosphorylated to NADP, a process that consumes roughly 12pmol of NAD^+ per million cells per hour (Liu et al., 2018). This can also be used as a redox cofactor and reduced to NADPH in the pentose phosphate pathway (Stincone et al., 2015).

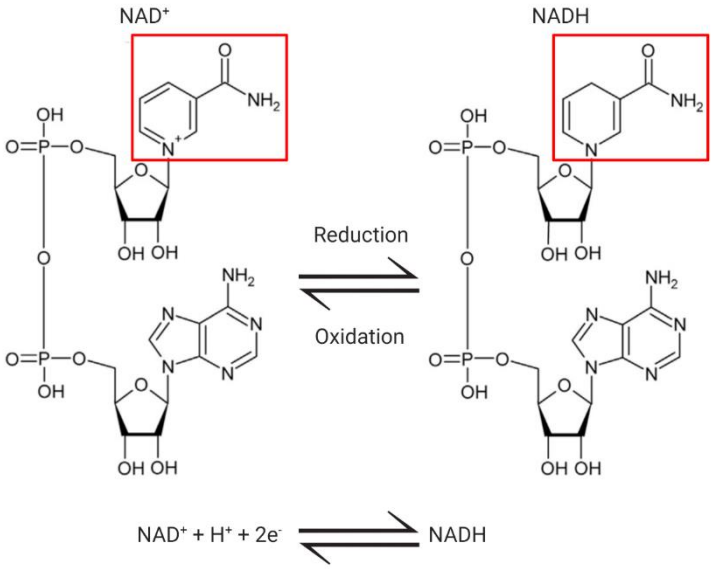

Figure 1.19: NAD^+, NADH and the reversible conversion between the two

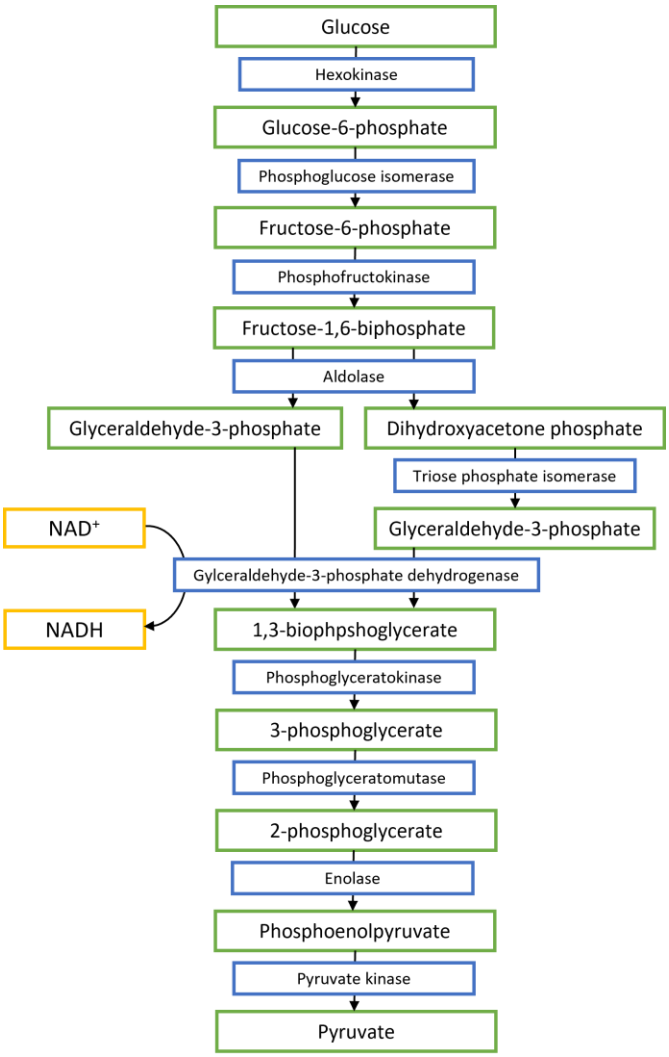

Figure 1.20: The glycolysis pathway and the role of NAD^+ within it. Green, glycolytic intermediate; blue, enzyme.

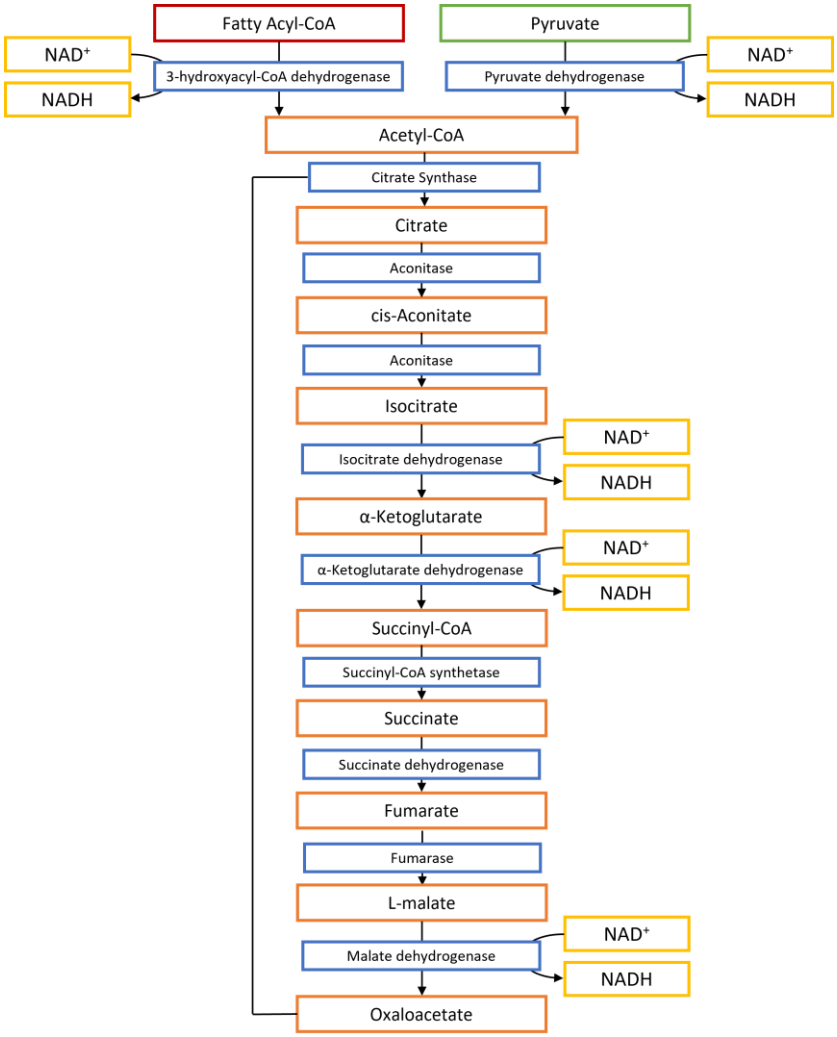

Figure 1.21: The tricarboxylic acid (TCA) cycle with entry points from glycolysis and beta oxidation, as well and the role of NAD^+. Green, glycolytic endpoint; red, beta oxidation end point; blue, enzyme.

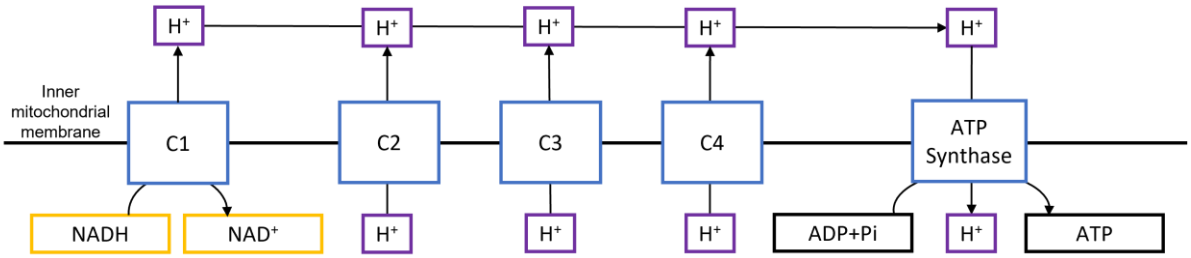

Figure 1.22: The electron transport chain and the election donating role of NAD^+ within it. NADH donates at C1. Other elections at C2-4 are donated from other sources, enabling the pumping of protons (hydrogens) across the inner mitochondrial membrane, creating a proton gradient to generate ATP through ATP synthase. Abbreviations: C1, NADH dehydrogenase, ubiquinone; C2, succinate dehydrogenase; C3, ubiquinol-cytochrome c reductase; C4, cytochrome c oxidase; ADP, adenosine diphosphate; Pi, phosphate; ATP, adenosine triphosphate.

1.16 NAD^+ as a signalling molecule

Nicotinamide adenine dinucleotide has more recently been recognised for its role as a signalling molecule (Houtkooper et al., 2010, Elhassan et al., 2017). Acting as a substrate NAD^+ is consumed by three main families of enzymes: sirtuins (SIRTs), poly ADP-ribose polymerases (PARPs) and cyclic ADP-ribose synthases, enabling their metabolic functions (Fig. 1.23) and leaving behind NAM for NAD^+ salvage (Haigis and Sinclair, 2010). The use of NAD^+ by these enzymes serves as the primary NAD^+ degrading mechanisms. In fact, combined they consume roughly 106pmol of NAD^+ per million cells per hour (Liu et al., 2018). In addition, all three of these enzymes compete with each other for NAD^+ availability. Changes to the activity or expression of one enzyme can exhibit an effect on another (Bai et al., 2011, Mohamed et al., 2014). The signalling elicited by these enzymes is often dependent on the subcellular location where both the enzyme and NAD^+ are found (Fig. 1.23).

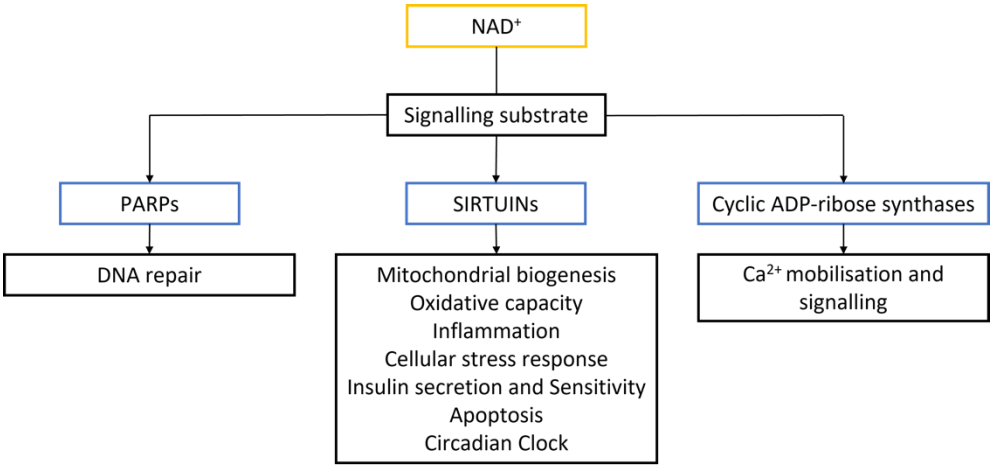

Figure 1.23: NAD^+ as a signalling substrate and the metabolic effects it enables. Adapted from Elhassan et al. (2017).

1.16.1 Sirtuins

A total of seven sirtuins (SIRT1-7) make up the NAD^+ dependent family of deacetylase enzymes. Each sirtuin serves different roles depending on the tissue or subcellular location in

which they are found. Most of the metabolic functions served by sirtuins involve deacetylation which cleaves off acetyl groups from proteins to alter their activity. In this process NAD^+ is used as a substrate and broken down to NAM, for NAD^+ salvage, and ADP ribose (ADPr) (Tong and Denu, 2010). Recently the knowledge of sirtuins has expanded to include the metabolic functions they facilitate and their importance for energy metabolism (Canto et al., 2009, Li, 2013). Whilst they all enable different functions, at least one of the sirtuins (1-7) is now known to be critical for metabolic effects (Dali-Youcef et al., 2007, Elhassan et al., 2017) including mitochondrial biogenesis (Li et al., 2011), increased insulin secretion and sensitivity (Erion et al., 2009), gluconeogenesis (Erion et al., 2009), muscle growth (Lee and Goldberg, 2013), inflammation (Nakamura et al., 2017), DNA repair (Vazquez et al., 2016), circadian rhythm (Nakahata et al., 2009), autophagy (Ou et al., 2014) and even longevity (Imai and Guarente, 2014). The location of each sirtuin determines their contribution to each function. Within the nuclei SIRT 1, 6 and 7 regulate nuclear transcription factors, whereas in the cytoplasm, cytoplasmic transcription factors are regulated by SIRT2 (Kupis et al., 2016). Mitochondrial function and homeostasis are maintained by SIRT3, 4 and 5 in response to changes in the redox environment (Kupis et al., 2016).

1.16.2 Poly ADP-ribose polymerases

Poly ADP-ribose polymerases are another family of 17 NAD^+ dependent enzymes with most knowledge focusing around PARP1 and 2 (Canto et al., 2015). Like sirtuins, PARPs use NAD^+ as a substrate, however with a higher affinity (Canto et al., 2015). Using NAD^+, PARPs transfer poly ADP-ribose to target proteins, leaving behind NAM for NAD^+ salvage (Morales et al., 2014). This process allows them to elicit post-translational modification of proteins, gene transcription and carry out their main function which is DNA repair (Durkacz et al., 1980, El-

Khamisy et al., 2003, Tallis et al., 2014, Elhassan et al., 2017). Whilst it is thought DNA damage itself is a more potent activator of PARP activity than NAD^+, it is still estimated that PARPs account for approximately 1/3 of total NAD^+ consumption (Liu et al., 2018). Inhibition of PARPs is known increased cellular NAD^+ concentrations (Sims et al., 1983, Kauppinen et al., 2013, Mohamed et al., 2014), whilst elevated PARP activity is known to greatly reduce NAD^+ bioavailability (Bai et al., 2011). Additionally excessive PARP activity results in an accumulation of NAM, from NAD^+ breakdown, resulting in an inhibition of SIRT activity (Pillai et al., 2005, Bai et al., 2011). In fact, PARP2 directly inhibits SIRT1 expression (Bai et al., 2011). Interestingly however, SIRT1 activity reduces PARP expression, thereby showing the direct competition between the two for NAD^+ bioavailability (Kolthur-Seetharam et al., 2006).

1.16.3 Cyclic ADP ribose synthases

Cyclic ADP-ribose synthases, primarily CD38 and CD157 consume NAD^+ to produce second messengers that are then used to regulate metabolic processes (Camacho-Pereira et al., 2016). A primary function of these membrane bound enzymes is to produce cADP-ribose (cADPR) which acts as a second messenger to increase intracellular calcium (Ca^{2+}) mobilisation and signalling (Elhassan et al., 2017). It is estimated that for CD38 to produce a single cADPR molecule it must consume up to 100 NAD^+ molecules, making it a key controller of cellular NAD^+ bioavailability (Aksoy et al., 2006). In fact, NAD^+ content increases 10-20 fold following inhibition of CD38 in mice (Aksoy et al., 2006).

1.17 Consequences of NAD^+ depletion and redox imbalance

Given the vital role of NAD^+ in maintaining energy metabolism and homeostasis, it is unsurprising that a deficiency is observed in and/or causal to metabolic and health conditions

in several tissues (Frederick et al., 2016, Okabe et al., 2019, Lin et al., 2021). Resulting from decreased NAD^+ synthesis, increased breakdown or both, a deficiency in NAD^+, its precursors or other disruption to its metabolome can ultimately result in the condition Pellagra, which is characterised by dermatologic, gastrointestinal and neuropsychiatric complications (Holubiec et al., 2021). If inadequately treated this condition can even result in severe organ failure and death (Holubiec et al., 2021). Metabolic conditions such as type II diabetes and obesity are now known to be accompanied by NAD^+ deficiency (Yoshino et al., 2011, Kuang et al., 2018, Okabe et al., 2019). In the case of diabetes an insufficient supply of NAD^+ results in both decreased insulin secretion and sensitivity (Okabe et al., 2019) disrupting glucose metabolism and promoting hyperglycaemia (Kuang et al., 2018). Due to the lack of NAD^+, SIRT6 function is inhibited (Kuang et al., 2018) causing disruption to both glycolysis (Aragones et al., 2009) and gluconeogenesis (Dominy et al., 2012). As for obesity it is unclear if NAD^+ deficiency is a causative factor, but the two often occur in parallel (Okabe et al., 2019). An increase in obesity driven inflammatory cytokines has been shown to deplete NAMPT expression (Kralisch et al., 2005, Dahl et al., 2010, Gaddipati et al., 2010), specifically intracellular NAMPT (iNAMPT) (Okabe et al., 2019), contributing to a global NAD^+ decline. The extent of this decline in tissue dependent but varies from up to 85% in the liver (Trammell et al., 2016b), 85% in skeletal muscle (Frederick et al., 2016) and 20% in adipose tissue (Yoshino et al., 2011). Like the extent of the decline, the metabolic consequences are also tissue dependent. Hepatic steatosis and non-alcoholic fatty liver disease (NAFLD) are both partly attributed to a decrease in SIRT1 and 3 activity, brought about from insufficient supply of NAD^+ (Hirschey et al., 2010, Xu et al., 2010, Kendrick et al., 2011, Min et al., 2012, Okabe et al., 2019). Cardiovascular conditions including atherosclerosis (Lin et al., 2021), ischaemia (Di Lisa et al., 2001), hypertension (Guo et al., 2019), arrhythmia (Kilfoil et al., 2013), heart failure (Xiao et al., 2005), coronary heart

disease (Mericskay, 2016) as well as myocardial energy metabolism disorders (Lin et al., 2021) can all be attributed to NAD^+ deficiency. These conditions are commonly caused by alteration to the activity of NAD^+ consuming enzymes; PARP1, CD38, CD157 and SIRT1-7 (Xiao et al., 2005, Baxter et al., 2014, Mericskay, 2016, Guo et al., 2019, Lin et al., 2021), however in the case of arrhythmia NAD^+ decline dysregulates ion channels in the heart (Kilfoil et al., 2013). Skeletal muscle atrophy (Frederick et al., 2016), sarcopenia (Migliavacca et al., 2019) and even muscular dystrophy (Ryu et al., 2016) are also partly attributed to NAD^+ deficiency. These are accompanied by a reduction of muscular strength and endurance performance that is attributed to reduced ATP productions from NAD^+ dependent pathways (Frederick et al., 2016). It is also theorised that immune function might be reduced by NAD^+ deficiency, possibly exacerbating the severity of diseases such as COVID-19 (Miller et al., 2020, Brenner, 2022).

Interestingly NAD^+ deficiency is also thought to contribute to the ageing process with a decline of up to 90% in the liver (Yoshino et al., 2011, Zhou et al., 2016), 40% in the heart (Braidy et al., 2011), 85% being reported in skeletal muscle (Yoshino et al., 2011), 75% in adipose tissue (Yoshino et al., 2011), and up to 90% in the brain (Zhu et al., 2015). However, the extent, or even existence of this decline is increasingly debate (Peluso et al., 2021). Regardless, the potential decrease in NAD^+ bioavailability is can be attributed with several mechanisms. It has been reported that NAMPT concentrations decrease with age, therefore reducing NAD^+ synthesis from NAM (van der Veer et al., 2007, Yoshino et al., 2011). This can likely be attributed to age related increase in inflammation which are suggested to reduce NAMPT expression (Imai and Yoshino, 2013). Degradation of NAD^+ is also induced by age related DNA damage which, as previously mentioned, requires increased PARP activation and therefore

increased NAD^+ consumption (Massudi et al., 2012). Age related PARP1 activity is also associated with increased ROS production, which further restricts NAD^+ (Mohamed et al., 2014). However, it is debated whether PARP activity does increase with age (Bakondi et al., 2011, Braidy et al., 2011). The expression of CD38 has been reported to increase with age, potentially as a result of age-related inflammation (Chini et al., 2017), further reducing cellular NAD^+ concentrations to a greater extent than PARPs (Camacho-Pereira et al., 2016). These reductions in NAD^+ concentration as well as the increased ROS are likely to inhibit SIRT1-7 activity (Massudi et al., 2012, Mohamed et al., 2014). Therefore, the potential age-related decline in NAD^+ might lessen metabolic activity, mitochondrial efficiency (Bai et al., 2011, Imai and Guarente, 2014, Camacho-Pereira et al., 2016) as well as cause or exacerbate metabolic conditions, including those previously mention (Yoshino et al., 2018).

In a similar vein to NAD^+ deficiency, imbalance in the NAD^+/NADH redox ratio, or alteration to the homeostatic norm can also cause metabolic conditions in several tissues (Wu et al., 2016, Lin et al., 2021). Firstly, an accumulation of NADH inhibits the glycolytic enzymes which would normally convert NAD^+ to NADH (Wilkinson and Williams, 1981). This can then lead to an accumulation of reactive oxygen species (ROS) as well as overwhelming the electron transport chain (ETC) with electron donors (NADH) contributed to further ROS production (Galloway and Yoon, 2012, Quinlan et al., 2014). This alters mitochondrial membrane permeability (Yan et al., 2005), causes mitochondrial dysfunction and oxidising molecules such as protein and lipids (Berlett and Stadtman, 1997, Anderson et al., 2012). All this can then contribute to insulin resistance and diabetes (Kim et al., 2008, Henriksen et al., 2011), obesity (Abel, 2010), cardiac tissue dysfunction (Lin et al., 2021) and even cell death (Seo et al., 2014).

1.18 Glucocorticoid and NAD^+ metabolome interactions

As previously covered, both glucocorticoids and NAD^+ are key metabolic factors. Regulated levels of both are required to maintain metabolic function and health with disruption to either causing metabolic problems. Given their individual importance it remains unclear whether the two regulate one another or if disruption to the regulation of one influence the other.

1.19 Potential mechanisms of interaction

Glucocorticoids and NAD^+ are known to indirectly interact through 11β-HSD1 and 2 (Agarwal and Auchus, 2005) and there is growing evidence they might also interact through sirtuins (Suzuki et al., 2018, Huang and Tao, 2020, Wang et al., 2021). Additional interaction might theoretically be possible through oxidative stress and extracellular NAMPT (eNAMPT), however the evidence for this is yet to be uncovered.

1.19.1 11β-Hydroxysteroid dehydrogenase 1 and 2

As mentioned in section 1.3 and Fig. 1.3, it is well established that glucocorticoids and NAD^+ do interact through 11β-HSD1 and 2. These enzymes activate and inactivate glucocorticoids, requiring NAD^+ in a reduced, oxidised, or phosphorylated form for use as redox cofactors to drive these reactions (Agarwal and Auchus, 2005). 11β-HSD1 is dependent on phosphorylated NAD^+ (NADP), requiring the reduced from (NADPH) to act as a reductase that converts inactive cortisone to active cortisol, converting NADPH to NADP (Lakshmi et al., 1993, Burton et al., 1998, Agarwal and Auchus, 2005). Alternatively, and to a lesser extent, 11β-HSD1 can act as a dehydrogenase to drive the reaction in the other direction, using NADP as the cofactor,

converting it to NADPH (Lakshmi et al., 1993, Burton et al., 1998, Agarwal and Auchus, 2005). Similarly, 11β-HSD2 also acts as a dehydrogenase to convert active cortisol to inactive cortisone but instead using NAD^+ as a redox cofactor, converting it to NADH (Rusvai and Naray-Fejes-Toth, 1993, Agarwal and Auchus, 2005). It is likely that changes to the ratio of active to inactive cortisol or oxidised to reduced $NAD(P)^+$ will affect one another. A review by Agarwal and Auchus (2005) concluded that the activity of 11β-HSD1/2, and therefore glucocorticoid flux, is highly dependent on the cofactor availability, gradient and redox ratio. For example, sufficient resupply of NADPH, by the enzyme hexose-6-phospate dehydrogenase (H6PDH) (Fig. 1.4) enhanced 11β-HSD1 activity, resulting in almost complete conversion of cortisone to cortisol (Agarwal and Auchus, 2005). It is also interesting to note that in the absence of 11β-HSD1 activity the cushingoid phenotype that results from prolonged and excessive glucocorticoid exposure, is absent (Tomlinson et al., 2002, Morgan et al., 2009). As $NAD(P)^+$ is required for 11β-HSD1 activity it is possible that reduced $NAD(P)^+$ availability might also result in attenuated glucocorticoid activity and its subsequent metabolic effects. Beyond 11β-HSD1 and 2 other interactions between glucocorticoids and NAD^+ are less well established and at present might only be theoretical.

1.19.2 Sirtuins

Sirtuins are another possible mechanism of interaction between glucocorticoids and NAD^+. Whilst the understanding is less conclusive than 11β-HSD1 and 2 there is growing evidence that through sirtuins, NAD^+ might be able to influence the potency of glucocorticoids (Dali-Youcef et al., 2007, Elhassan et al., 2017, Suzuki et al., 2018, Huang and Tao, 2020, Wang et al., 2021, Mishra et al., 2022). In mouse bone tissue it has been reported that increasing NAD^+,

through NMN supplementation, prevented dexamethasone inhibition of osteogenesis via increased deacetylation of SIRT1 (Huang and Tao, 2020). There is also *in vitro* (Suzuki et al., 2018) and *in vivo* (Wang et al., 2021) evidence that SIRT1 might be able to directly modulate the activity of the GR, increasing transactivation or transrepression, through a deacetylase independent mechanism (Suzuki et al., 2018, Wang et al., 2021). As shown in Fig. 1.24, SIRT1 is thought to bind to the GR in response to glucocorticoid induced GR binding to the GRE (Suzuki et al., 2018, Wang et al., 2021). It is important to note that SIRT1 only serves as an enhancer of glucocorticoid action at the GR and cannot independently activate the GR (Suzuki et al., 2018). In fact, in the absence of SIRT1 the activity of the GR activity might be attenuated by up to 30% (Suzuki et al., 2018). However, given the deacetylase independent nature of SIRT1 and GR interaction (Suzuki et al., 2018) it is possible this might not be NAD^+ driven as NAD^+ is consumed by sirtuins to fuel their deacetylase activity (Elhassan et al., 2017). SIRT2 however is thought to influence the GR via a deacetylase, and therefore NAD^+, dependent mechanism (Sun et al., 2020). Upon glucocorticoid binding to the GR in the cytoplasm, SIRT2 is reported to deacetylate HSP90 which subsequently dissociates from the GR, allowing the GR and bound glucocorticoid to translocate to the nucleus (Fig. 1.25) (Sun et al., 2020). This translocation is increased by SIRT2 overexpression and inhibited by a knock-down of SIRT2 expression (Sun et al., 2020). Therefore, like SIRT1, SIRT2 helps to facilitate the transcriptional activity of the GR, but only following glucocorticoid and GR binding (Sun et al., 2020). Finally, SIRT6 has also been implemented in facilitating glucocorticoid induced transcription, specifically with regards to glucocorticoid excess (Mishra et al., 2022). As previously mentioned in section 1.5 glucocorticoid excess is known to induce skeletal muscle atrophy. In the absence of SIRT6 this atrophy is not seen, both *in vitro* and *in vivo* (Mishra et al., 2022). It is thought that SIRT6 deficiency results in the hyperactivity of insulin growth factor,

phosphatidylinositol-3-kinase and protein kinase B which inhibits transcription of forkhead box protein O1 which is a key skeletal muscle atrophy protein. Therefore, like SIRT1 and SIRT2, SIRT6 might influence the genomic mechanism of glucocorticoids.

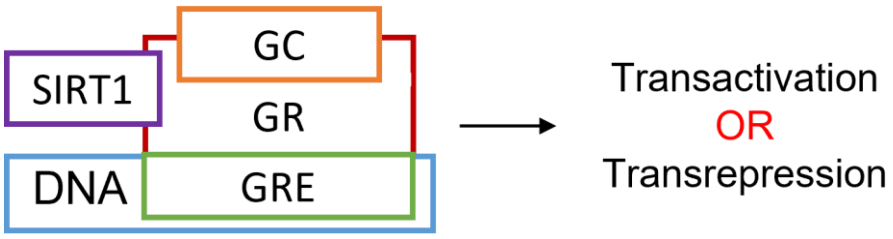

Figure 1.24: Mechanism of interaction between SIRT1 and GR to modulate glucocorticoid transactivation and transrepression. Adapted from Suzuki et al. (2018).

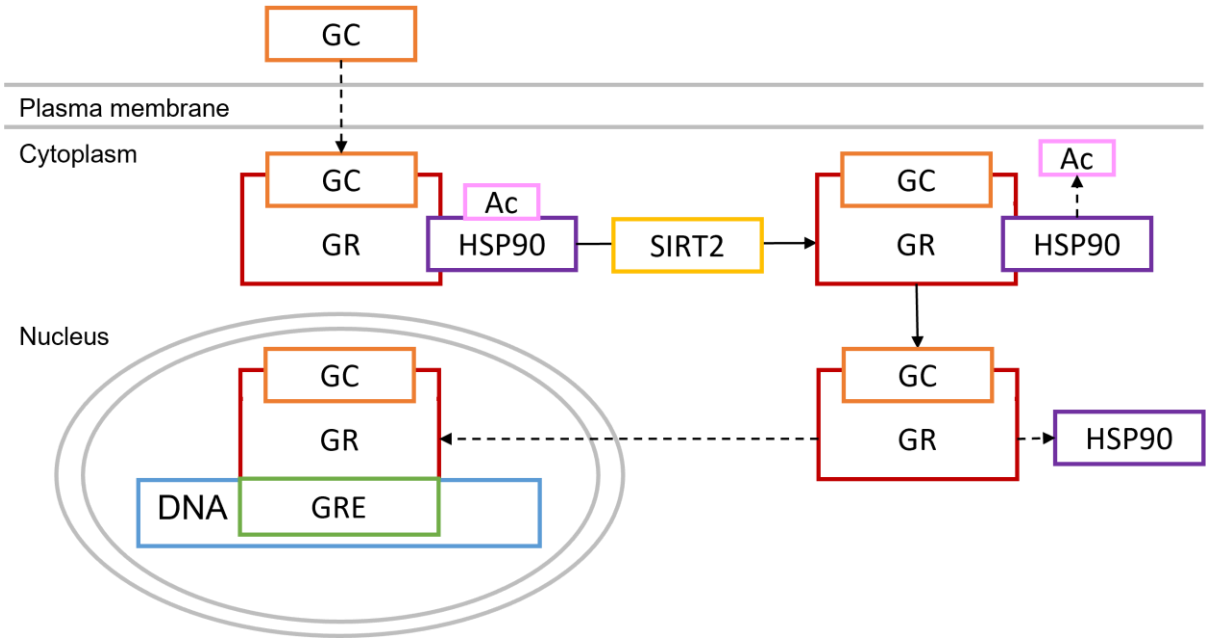

Figure 1.25: Deacetylase mechanism of interaction between SIRT2 and the GR to facilitate GR and glucocorticoid translocation to the nucleus. Ac, acetyl group. Adapted from Sun et al. (2020).

1.19.3 Oxidative stress

Another possible, at present theoretical, point of interaction between glucocorticoids and NAD^+ might be oxidative stress. In theory glucocorticoid induced oxidative stress might have the ability to increase NAD^+ consumption, possible decreasing NAD^+ availability.

Glucocorticoids increase ROS production, even more so during glucocorticoid excess (Roma et al., 2012, Tang et al., 2013, Spiers et al., 2014), whilst also attenuating the activity of the antioxidant superoxide dismutase (SOD) (Tang et al., 2013). Therefore NAD^+ consuming enzymes, SIRTs and PARPs, are increasingly required to act as antioxidants to combat oxidative stress (Singh et al., 2018). Specifically, SIRT1/3/5 directly combat ROS to protect the cell and SIRT2/6/7 alter the activity and expressions of antioxidant genes (Singh et al., 2018). PARPs are required to combat ROS induced DNA damage (Durkacz et al., 1980, El-Khamisy et al., 2003, Elhassan et al., 2017, Singh et al., 2018). Separate to these two NAD^+ consuming enzymes, NAD^+ in the form of NADPH is directly used to combat oxidative stress through reduction of glutathione (Singh et al., 2018). These reactions are likely to decrease the NAD^+ pool as more is consumed to meet the threat of accumulating ROS. Additionally, the NAD^+/NADH ratio is likely to be affected as glucocorticoid induced ROS are known to induce metabolic and mitochondrial dysfunction (Rani et al., 2016) which affects the redox reactions needed to convert NAD^+ to NADH and vice versa.

1.19.4 Extracellular nicotinamide phosphoribosyltransferase

Another potential, and mostly theoretical, mechanism of interaction could be through eNAMPT induced glucocorticoid production. Aspects of the HPA axis (Fig. 1.2) have been reported to be upregulated be increased eNAMPT availability (Celichowski et al., 2018, Celichowski et al., 2021). Specifically, POMC expression in the pituitary has been reported increased *in vivo* by increasing serum concentrations of eNAMPT, which has led to increased serum corticosterone (Celichowski et al., 2018). Inhibition of eNAMPT with FK866 prevents this effect both *in vitro* and *in vivo* (Celichowski et al., 2018). ACTH production is also reported

to be elevated by eNAMPT, contributing to increase corticosterone production (Celichowski et al., 2021). However, the relationship between eNAMPT and the HPA might not necessarily involve NAD^+. Whilst NAMPT is a NAD^+ biosynthetic enzyme, eNAMPT serves as an extracellular hormone with pro-inflammatory effects (Celichowski et al., 2021). Therefore, increased serum eNAMPT concentrations might not be producing NAD^+ at the HPA, especially as eNAMPT often requires liberation from extracellular vesicles and uptake by the cell, becoming intracellular NAMPT (iNAMPT), to produce NAD^+ (Carbone et al., 2017). However, eNAMPT can exist in two forms, dimeric and monomeric, with the former able to synthesize NAD^+ (Sayers et al., 2020). However, as concentrations of eNAMPT increase it progressively becomes more monomeric, reducing and eventually extinguishing its NAD^+ biosynthetic capabilities (Sayers et al., 2020), something that is worth noting with regards to the previously discussed findings (Celichowski et al., 2018, Celichowski et al., 2021). Interestingly Sayers et al. (2020) report elevated eNAMPT in type 2 diabetes, a condition that can be brought on by glucocorticoid excess. It is therefore possible that NAD^+ might not be a factor when considering the effect of eNAMPT on the HPA, or alternatively the transition of eNAMPT to its monomeric form might partly be a compensatory mechanism to reduce eNAMPT stimulated production of glucocorticoids, implying NAD^+ could be involved.

1.20 Direct evidence for glucocorticoid and NAD^+ metabolome interaction

Direct evidence that glucocorticoids can alter the NAD^+ metabolome and that alterations to the NAD^+ metabolome can alter glucocorticoid flux remain scarce. In fact, there is only a handful of published data for the former (table 1.2), and none for the latter. However, at present there is no clear consensus with data on the NAD^+ metabolome being a secondary

focus. For example, whilst conducting research on type 2 diabetes in pancreatic islets Roma et al. (2012) reported that 1mg/kg/day of dexamethasone injected intraperitoneally into rats for 5 days caused a 23.35% decrease in mitochondrial NAD(P)H production leading to a more oxidised $NAD(P)^+$/NAD(P)H ratio. In contrast, whilst researching glucocorticoid induced osteoarthritis Yang et al. (2017) reported a shift in the $NAD(P)^+$/NAD(P)H ratio to a more reduced state following treatment of mouse chondrocytes with 1µM dexamethasone for 24 hours. Two other studies, both Xiao et al. (2019) and Xie et al. (2020b) used daily subcutaneous injections of 20mg/kg of corticosterone for 6 weeks to induce depression like symptoms in mice. Both studies subsequently reported a decrease in liver NAD^+, an increase in liver NAM and a decrease in the expression of NAD^+ biosynthetic enzymes NAMPT and NMNAT3. Xie et al. (2020b) also reported a decrease in liver tryptophan content and decreased activity of the de novo biosynthesis pathway. Whilst at first glance this appears to show the signs of a consensus in the published literature, it must be interpreted carefully as both studies were conducted by the same research group. In addition to this another study reported that 50µg/kg/day of dexamethasone for 2 weeks had no effect on skeletal muscle NAD^+ (Herrera et al., 2020a), however once again this was a secondary measure with the primary focus of the study being glucocorticoid induced hypertension. However, another *in vivo* study that focused on NAD^+ as a primary measure reported an increase in skeletal muscle NAD^+ following weekly intraperitoneal (IP) injections of 1mg/kg prednisone, a far more acute dose (Quattrocelli et al., 2022). Two other *in vitro* studies reported an increase in NAMPT expression following dexamethasone treatment (25nM and 100nM) with or without 100nM of hydrocortisone (Kralisch et al., 2005, Friebe et al., 2011). Whilst the current literature provides glimpses into the relationship between glucocorticoids and the NAD^+ metabolome it is clear more research is needed.

Table 1.2: The effects of glucocorticoid treatments on the NAD^+ metabolome

Authors	Model	Treatment protocol	Effect on the NAD^+ metabolome
Roma et al. (2012)	*in vitro* Male Wistar rat islet, N=5	Daily intraperitoneal injections of 1mg/kg DEX for 5 days	↓ Mitochondrial NAD(P)H production leading to a more oxidised state
Yang et al. (2017)	*in vitro* C57BL/6N mice chondrocytes	1µM DEX for 24 hours	↓ $NAD(P)^+$/NAD(P)H ratios to a more reduced state
Xiao et al. (2019)	*in vivo* Male C57BL/6J mice, N=8	Daily subcutaneous injections of 20mg/kg CORT for 6 weeks	↓ Liver NAD^+ content ↑ Liver NAM content ↓ Liver NAMPT and NMNAT3 expression
Xie et al. (2020b)	*in vivo* Male C57BL/6J mice, N=8	Daily subcutaneous injections of 20mg/kg CORT for 6 weeks	↓ Liver NAD^+ content ↑ Liver NAM content ↓ Liver NAMPT and NMNAT3 expression ↓ Liver tryptophan content ↓ de novo biosynthesis pathway activity
Herrera et al. (2020a)	*in vivo* Male Wistar rats, N=10	Daily subcutaneous injections of 50µg/kg/day DEX for 14 days	No effect on skeletal muscle NAD^+
Quattrocelli et al. (2022)	in vivo Male and female C57BL/6J mice, N=5	Weekly intraperitoneal injections of 1mg/kg PRED for 12 weeks	↑ Skeletal muscle NAD^+

Table 1.2: continued

Authors	Model	Treatment protocol	Effect on the NAD^+ metabolome
Kralisch et al. (2005)	in vitro 3T3-L1 adipocytes	100nM DEX for 3 days	↑ NAMPT gene expression
Friebe et al. (2011)	*in vitro* Human preadipocytes and adipocytes	100nM HC and 25nM DEX for ≤ 12 days	↑ NAMPT gene expression

CORT, corticosterone; DEX, dexamethasone; PRED, prednisone; HC, hydrocortisone

1.21 Evidence that an altered NAD^+ metabolome might alter the effects of glucocorticoids

Despite no direct published data showing the NAD^+ metabolome alters glucocorticoid flux, there is some limited data suggesting increasing NAD^+ through supplementation might help combat some of the consequences of glucocorticoids, specifically glucocorticoid excess. Is has been reported that boosting NAD^+ with the precursor NMN can help combat glucocorticoid induced hyperglycaemia (Uto et al., 2021) as well of glucocorticoid induced osteoporosis (Huang and Tao, 2020). However, at present the data is confined to *in vitro* investigation. Therefore, the question of whether altering the NAD^+ metabolome can combat the effects of glucocorticoids very much remains. Given the findings of Uto et al. (2021) and Huang and Tao (2020) it remains possible that enhancing the NAD^+ metabolome might combat other glucocorticoid induced conditions, or even Cushing's syndrome/disease. This is furthered by the fact that conditions that can be caused by, or independently of, glucocorticoid excess have been associated with a disrupted NAD^+ metabolome or improved by elevating NAD^+. Diabetes (Wu et al., 2016), hypertension (Lin et al., 2021) and non-alcoholic fatty liver disease (NAFLD) (Dall et al., 2022) all fall into one of these categories.

1.22 Remaining questions and project rationale

A definitive answer as to the mechanisms behind glucocorticoid and the NAD^+ metabolome interaction is yet to be established. Whilst some are well understood, like 11β-HSD1/2 (section 1.19.1) and others such as sirtuins (section 1.19.2) are increasing in evidence, others such as oxidative stress (section 1.19.3) or eNAMPT (section 1.19.4), and potentially more, are only theoretically plausible at present. Regardless of how they might interact the direct effect one has on the other and any subsequent effects of any direct interaction remains unclear and a key focus of this thesis. As stated in section 1.20 and table 1.2 there remains a lack of research and no clear consensus on how glucocorticoids, specifically glucocorticoid excess, effects the NAD^+ metabolome. Additionally, whether this contributes to glucocorticoid induced metabolic conditions is also unknown. Likewise, as stated in section 1.6 and table 1.1 there remains a similar lack of research, and no clear consensus on how glucocorticoid excess effects markers of energy metabolism, which are also influenced by the NAD^+ metabolome. Finally, the effect of altering the NAD^+ metabolome, through precursor supplementation, on glucocorticoids also remains unclear. Given the listed benefits of NAD^+ on metabolic functions and the reported benefits of boosting NAD^+ to combat metabolic conditions the question whether boosting NAD^+ can counter the effects of glucocorticoid excess and Cushing's syndrome remains.

1.23 Hypothesis and objectives

NAD^+ decline has been reported in conditions linked to glucocorticoid excess. As have alterations to energy metabolism which have are closely interlined with the NAD^+ metabolome (Canto et al., 2015, Xie et al., 2020a). Additionally, enhancing the NAD^+ content

through precursor supplementation is reported to alleviate some instances of metabolic dysfunction. Finally, many of the known effects of glucocorticoid excess are known to be mediated by the enzyme 11β-HSD1. Therefore, it is hypothesised that glucocorticoid excess will decrease the availability of NAD^+, alter its metabolome and disrupt markers of energy metabolism via a 11β-HSD1 dependent mechanism, and that it is possible to alleviate both these effects and other known metabolic effects of glucocorticoid excess through NR supplementation.

Therefore, the primary aims of this project are:

- To comprehensively establish if glucocorticoid excess disrupts markers of energy metabolism (Chapter 3)
- To comprehensively establish if glucocorticoid excess disrupts aspects of the NAD^+ metabolome which is closely linked to energy metabolism (Chapter 4)
- To determine if any effects of glucocorticoid excess, both known and novel, can be altered by NAD^+ precursor supplementation (Chapter 4).
- To determine if any effects of glucocorticoid excess on markers of energy metabolism, or the NAD^+ metabolome, are facilitated by the enzyme 11β-HSD1 (Chapter 5).

CHAPTER 2 – MATERIALS AND METHODS

2.1 Animal care

All animal procedures were performed at the Biomedical Service Unit at the University of Birmingham (PPL: PP1816482, PIL: I83124981) unless otherwise stated.

2.1.1 Animal housing

Mice were housed in standard IVC cages (Green Line IVC Sealsafe PLUS, Techniplast, USA), containing standardised sawdust along with paper bedding and a red tinted shelter. Mice were kept in sex and litter matched cages of groups 2-4. Mice were fed *ad libitum* with standard chow feed (EURodent Diet 14%, Labdiet, St Louis, Missouri, USA) but water differed depending on treatment group (detailed in each chapter). Mice were kept on a uniform light/dark cycle (06:00 lights on, 18:00 lights off) and kept at a standardised temperature.

2.1.2 Animal sacrifice and tissue collection

Following treatment mice were sacrificed by schedule 1 cervical dislocation with death confirmed by cessation of the heartbeat. Tissue collection began immediately following death with tissues being placed into 1ml cryotubes (Starsedt, Germany) and immediately snap-frozen in liquid nitrogen before storage at -80°C. Tissues were weighed prior to snap-freezing, or in the case of the skeletal muscle beds of the hindlimb, one hindlimb worth of skeletal muscle was immediately collected and snap-frozen, whilst the skeletal muscles of the other were weighed before snap-freezing. This process was completed as fast as possible to minimise biological degradation of samples. The majority of tissues were collected in this way. If another method was used this is detailed where relevant. Tail samples were also collected and flash frozen from genetically altered mice in case subsequent genotyping was required.

2.1.3 Tissue preparation

Tissue samples were removed from -80°C storage and placed on dry ice. A polystyrene box was filled with liquid nitrogen (approximately 1cm deep). The equipment required (pestle and mortar, samples tubes, tweezers, micro spoon and a metal funnel) was placed into the box to cool to a temperature that will ensure samples remain frozen. Once at temperature the mortar was lined with a piece of tin foil and the frozen sample added to be pulverised into a powder. Powdered tissue was then weighed in a pre-cooled sample tube on a calibrated scale (Accuris Instruments Analytical Series W3100-210, Dublin, Ireland) before quickly being placed back into liquid nitrogen. The amount of powdered tissue required depended on the procedure it was to be used for. Excess powder was returned to the original sample tube (cryotube) for storage (-80°C) in case it should be needed in the future.

Extreme care was taken throughout to make sure samples remained frozen to avoid biological degradation. The majority of tissues were prepared in this way. If another method was used this is detailed where relevant.

2.2 Indirect calorimetry

Indirect calorimetry was performed on mice during the final week of treatment using a TSE PhenoMaster 8 cage system (TSE Systems, Bad Homburg, Germany) shown in Fig. 2.1. Mice were placed into the system with their original litter mates in cages for 48 hours to acclimatise to the new environment. Following this, mice were separated and housed individually for 120 hours within the PhenoMaster. The first 24 hours were for acclimation to isolation, while the subsequent 96 hours were for data collection. Energy expenditure (EE), respiratory exchange ratio (RER), oxygen consumption, carbon dioxide production, food and water intake were all measured. In addition, locomotor and ambulatory activity was also measured using a TSE Phenomaster at the University of Edinburgh.

Sufficient food and water was given and only replaced at the start of group acclimatisation and at isolation. Data was analysed using CalR (version 1.2) (Mina et al., 2018).

Figure 2.1: TSE Phenomaster 8 cage system

2.3 Body composition analysis

Body composition was assessed via time domain nuclear magnetic resonance (TD-NMR). This was done with a Bruker minispec LF50 (7.5MHz, 0.175T) system (Bruker, Billerica, Massachusetts, USA). TD-NMR works by applying a low magnetic field that excites hydrogens and aligns their spin states within the tissues of a mouse causing them to shift from a low to high energy state. This shift creates a nuclear magnetic resonance that reflects the composition of each mouse due to the differing number of hydrogens in each tissue. Fat mass (FM), lean body mass (LBM), free bodily fluid (FBF) and

bone mass (BM) were all assessed. FM, LBM and FBF were all assessed directly, whilst BM was calculated by subtracting FM, LBM and FBF away from bodyweight.

2.4 NAD^+/NADH fluorescence assay

NAD^+/NADH quantification from tissue samples was done using a self-developed fluorescence assay based on one previously developed by Graeff and Lee (2002). This involves exciting prepared samples that contain a fluorophore at a set wavelength to induce a chemical reaction, resulting in the generation of resorufin which subsequently produces a fluorescence proportional to the amount of NAD^+ or NADH in the sample.

2.4.1 NAD^+/NADH quantification

Tissue samples were pulverised as detailed in section 2.1.3. Approximately 25-50mg of powdered tissue was placed in a tube for NAD^+ analysis and another tube for NADH analysis (approximately 50-100mg of tissue total). All subsequent sample preparation steps were performed on ice. For NAD^+ quantification 500µl of ice cold 0.6M perchloric acid was added to each sample. For NADH quantification 500µl of ice cold 0.25M KOH in 50% ethanol was added. Samples were homogenised using a TissueLyser II (QIAGEN, Germany) before being centrifuged at 4°C, 12000rpm for 10 minutes. The supernatant of each sample was transferred to a new tube and diluted in ice cold 100mM Na-phosphate buffer. NAD^+ quantification required a dilution factor of 1:100. NADH quantification required a dilution factor of 1:50. Diluted samples were then added to a 96 well plate in duplicate at 5µl per well. Standards consisting of 0, 0.0625, 0.125, 0.25, 0.5 and 1µM of NAM were also added in duplicate at 5µl per well. An ice cold cycling mix was prepared with the reagents listed in in table 2.1, and 95µl was immediately added to each well. The plate was then immediately loaded into an Infinite 200 PRO plate reader (TECAN, Switzerland), “excite” was set at 530nm and “count” at 590nm. This acquired a baseline fluorescence reading for each sample. The plate was subsequently read every 5

minutes for the next 20 minutes whilst it developed. NAD^+ and NADH concentration was then calculated by subtracting the baseline fluorescence away from 20 minutes fluorescence (if samples were too developed at 20 minutes the 15 minutes fluorescence was used). The known standards were used to plot a standard curve which samples were plotted against. Values were then multiplied by the dilution factor and normalised to original pulverised tissue weight. This gave concentrations of μM/mg of tissue for NAD^+ and NADH.

Table 2.1: Cycling mix

dH_2O	8.4ml
1M phosphate pH 8	1ml
BSA (50mg/ml)	20μl
1M nicotinamide	100μl
100% ethanol	200μl
10mM flavin mononucleotide	10μl
20mM resazurin	10μl
Alcohol dehydrogenase (10mg/ml)	110μl
Diaphorase (1mg/ml)	110μl

*Ingredients were combined in the order listed and volumes are sufficient to make 10ml

2.5 Ribonucleic acid extraction and analysis

Ribonucleic acid (RNA) was extracted from tissue samples before being converted to complementary DNA (cDNA) to analyse messenger RNA (mRNA) levels to determine gene expression of specified genes of interest.

2.5.1 Tissue sample preparation

Tissue samples were pulverised as detailed in section 2.1.3. Approximately 10mg of powdered tissue was transferred into a 2ml Eppendorf tube alongside 800μl of TRIzol (Invitrogen, UK) and a pre-cooled

(on dry ice) metal bead. Tubes were then homogenised using a TissueLyser II (QIAGEN, Germany). Samples were then immediately placed onto dry ice before storage at -80°C.

2.5.2 RNA extraction

Samples were thawed on ice before use. Once thawed 200µl of chloroform per 1ml of TRIzol was added to the samples before being vortexed for 5 seconds and then centrifuged for 10 minutes at 12000rpm and 4°C. The clear uppermost layer was then transferred to another Eppendorf tube and the rest was discarded. 500µl of isopropanol (propan-2-ol) per 1ml of TRIzol was then added before samples were vortexed for 5 seconds and placed in -20°C overnight to precipitate. Samples were then immediately centrifuged for 10 minutes at 12000rpm and 4°C to generate a pellet of RNA, meaning the supernatant could be discarded. 500µl of 75% ethanol per 1ml of TRIzol was added to wash the pellet before centrifugation for 10 minutes at 12000rpm and 4°C, after which the ethanol was removed. Pellets were then left at room temperature for 5 minutes so any remaining ethanol could evaporate. Pellets were then resuspended in 10µl of nuclease free water (NFW).

2.5.3 RNA quantification

RNA content of each sample was determined using a NanoDrop (ND, Labtech international). 1µl of NFW was applied to the NanoDrop and measured as a blank sample to calibrate it. This was then cleaned off and 1µl of each sample was then added in turn, with the NanoDrop being cleaned between samples. RNA with a 260/280 nm ration between 1.7-2 was determined to be a sufficient quality.

2.5.4 Reverse transcription

Reverse transcription (RT) converts RNA to cDNA used for analysis. Samples were made up to 1µg of RNA each in NFW with a total volume of 10µl. A high-capacity cDNA RT kit (Applied Biosystems, USA)

consisting of reagents, listed in table 2.2, was used to create a RT master mix. 10μl of RT master mix and 10μl of each sample were combined, briefly vortexed and then placed in a thermal cycler with the following program: 10 minutes at 25°C, 120 minutes at 37°C, 5 minutes at 85°C and then indefinitely at 4°C. 30μl of NFW was added to the generated cDNA before being stored at 4°C.

Table 2.2: High capacity cDNA RT master mix

Reagent	Volume per sample (μl)
RT buffer	2
Random primers	2
Deoxynucleotide (dNTP) mix	0.8
RNase inhibitors	1
Multiscribe® reverse transcriptase	1
Nuclease free water	3.2

2.5.5 Real-time PCR

Real-time PCR (qPCR) quantifies genes of interest via their 5'-3' regions, using TaqMan probes (Life Technologies, UK). The probes are made up of a fluorophore and quencher which attach to the 5' and 3' ends respectively. During the reaction the fluorophore and quencher become separated resulting in fluorescence proportional to the quantity of gene of interest. Cycle threshold (Ct) values are generated which refer to the number of amplifications (cycles) taken for fluorescence to occur. Probes were thawed on ice whilst protected from light before being briefly vortexed. For each probe a master mix was created as detailed in table 2.3). 9μl of probe specific master mix was then added to a 96 or 384 well plate with 1μl cDNA, leaving 10μl per well. All samples were run in duplicate. A film was added to the top of the plate to seal it before it was briefly centrifuged to ensure the master mix and cDNA had mixed and were at the bottom of each well. All plate preparation was done on ice. 96 well plates were loaded onto the QuantStudio 5 Real-time-PCR (Thermofisher, UK). 384 well plates were loaded onto the 7900HT Real-time-PCR (Thermofisher, UK). The settings for each system are shown in table 2.4. Collected Ct values were normalised using one of the following reference genes: 18S,

GAPDH, HPRT1 or GUSB shown in table 2.5. This involved subtracting the reference gene Ct value away from the gene of interest resulting in deltaCt (dCt) (Schmittgen and Livak, 2008). Should none of these provide a stable reference the Genorm method was used (Vandesompele et al., 2002).

Table 2.3: TaqMan probe master mix

Reagent	Volume per sample (μl)
qPCR master mix - HiRox for 384 well plates - LowRox for 96 well plates	5
Nuclease free water	3.5
Probe for gene of interest	0.5

Table 2.4: 96 and 384 well plate qPCR run settings

96 well plate (QuantStudio 5 Real-time-PCR)		384 well plates (7900HT Real-time-PCR)	
Step 1: 90°C for 2 minutes Step 2: 95°C for 10 seconds Step 3: 60°C for 20 seconds	Cycle 40x	Step 1: 95°C for 10 minutes Step 2: 95°C for 15 seconds Step 3: 60°C for 1 minute	Cycle 40x

Table 2.5: TaqMan probe using as reference genes

Gene	Assay ID
18S	4333760T (Cat no.)
GAPDH	Mm99999915_g1
HPRT1	Mm03024075_m1
GUSB	Mm01197698_m1

2.6 Haematoxylin and eosin staining

Haematoxylin and eosin (H&E) staining was used to get a visual representation of triglyceride accumulation in the tissues of interest, as shown in Fig. 2.2.

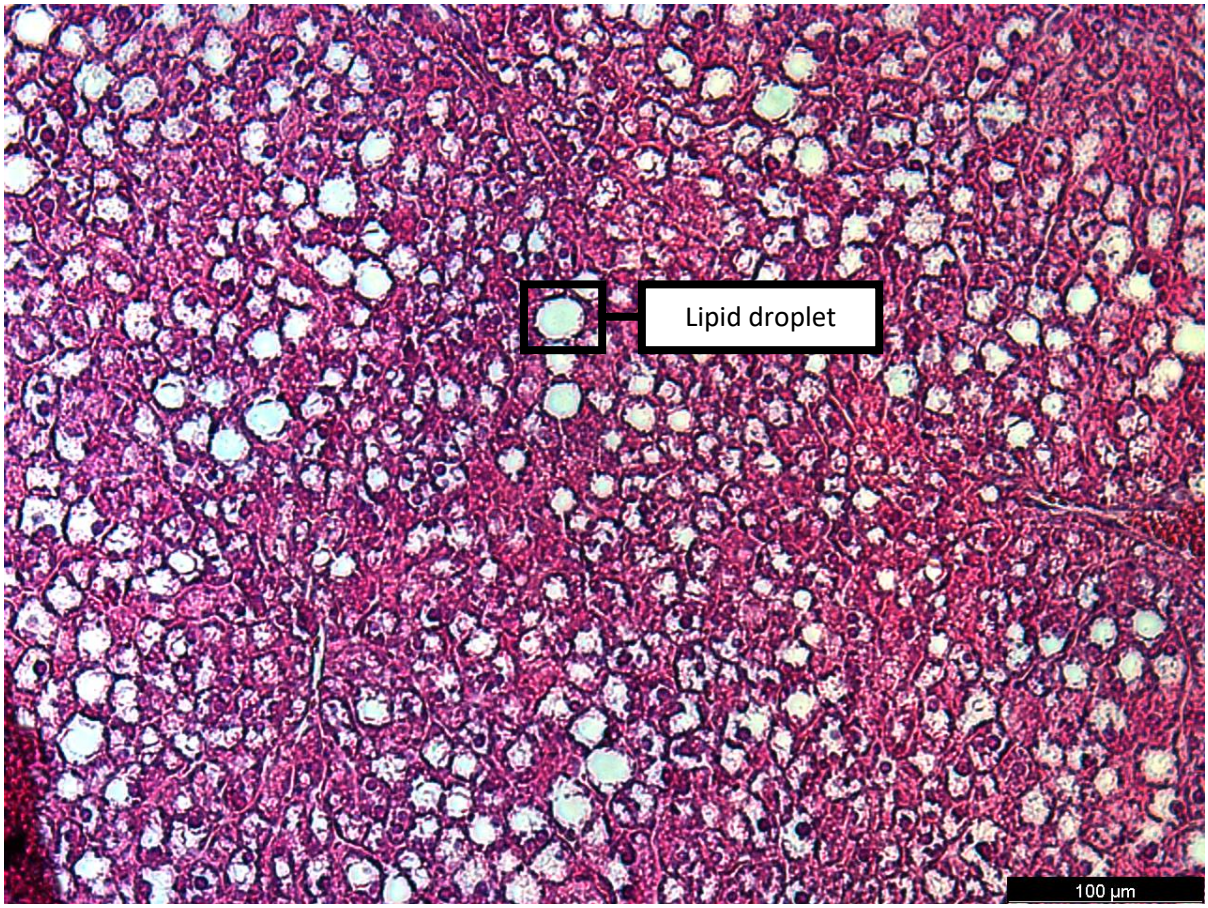

Figure 2.2: An example of a H&E stained tissue section (liver) giving a visual representation of lipid accumulation.

2.6.1 Tissue preparation

Immediately upon dissection tissues were placed in a 5ml bijoux tube containing 1-2ml of formalin (10% formaldehyde solution, 90% dH_2O). Samples were then stored at 4°C until needed.

2.6.2 Paraffin wax embedding

Sample were loaded into individual cassettes and remained in them until stated otherwise. First samples were washing in PBS for 5 minutes. They were then placed in 40% ethanol for 1 hour. Then 70% ethanol for another hour before 100% ethanol for another hour. The 100% ethanol step was then repeated in fresh ethanol. Samples were then placed in xylene for 30 minutes with care taken to

minimise ethanol transfer into the xylene. Sample were then moved into fresh xylene for another 30 minutes before being moving into more xylene for a final 30 minutes. Samples were then transferred into molten paraffin wax (65°C) for 1 hour with care taken to minimise xylene transfer into the wax. Samples were then moved into more molten paraffin wax for another hour before being transferred into another pot of molten paraffin wax for a final hour. Following this samples were removed from cassettes and mounted into embedding moulds with molten paraffin wax. Moulds were left to cool until the wax had fully solidified. A wax block containing the sample was then removed from the mould and stored at room temperature until needed.

2.6.3 Microtome sectioning

Samples were placed into a rotary microtome (Leica Biosystems, UK) allowing 5μm sections to be cut. These were placed into a 50°C dH_2O water bath and mounted on microscope slides. These were left overnight at room temperature or placed into a 40°C oven for 1 hour to facilitate adherence of each section to the slides.

2.6.4 Haemotoxylin and eosin staining

Mounted tissue sections were placed in a series of baths to first remove paraffin wax from embedding and sectioning and then to stain sections. Sections were submerged in xylene for 3 minutes, 3 times. Then into 100% ethanol twice for 2 minutes at a time. This was followed by 2 minutes in 70% ethanol and then 2 minutes in 40% ethanol. Sections were then submerged in haemotoxylin for 5 minutes before being washed in scott's water for 2 minutes and briefly dipped into acid alcohol. Sections were then placed under gently running tap water for 5 minutes, followed by eosin for 5 minutes and brief dip into 100% ethanol. Lastly sections were placed in 100% ethanol twice for 2 minutes each before being placed in xylene 3 times for 2 minutes at a time. Once stained sections were fixed with a cover slide and depex before being left overnight in a fume hood to dry.

2.6.5 Imaging

Stained sections were imaged use an Olympus BX53 microscope with cellSens software (Olympus Lifescience, UK). This generated images as shown in Fig. 2.3.

2.7 Triglyceride analysis

Triglyceride quantification was performed using a triglyceride quantification colorimetric kit (BioVision, USA). Components are listed in table 2.6.

Table 2.6: Triglyceride quantification colorimetric kit components

Components
Triglyceride assay buffer
Triglyceride probe
Lipase
Triglyceride enzyme mix
Triglyceride standard

2.7.1 Triglyceride quantification

Firstly, 100mg of powder tissue was weighed out as detailed in section 2.1.3. Samples were then homogenised in 1ml of dH_20 containing 5% NP-40, before being place in a water bath at 95°C for 5 minutes. Samples were then cooled to room temperature, then returned to the water bath for another 5 minutes before a final cooling to room temperature. Samples were then centrifuged at max speed for 2 minutes. Each sample was then diluted 10-fold in dH_20 before 50µl was added to in duplicate to a 96 well plate. A standard curve was also added to the plate as well as a background control. 220µl of buffer was added to the lipase with 2µl of subsequent mix added to all wells containing a sample, standard or background control. The plate was briefly mixed on an orbital shaker before incubating at room temperature for 20 minutes. A reaction mix was then prepared containing 46µl of buffer, 2µl triglyceride probe and 2µl enzyme mix per sample. The probe was heated to 37°C for 5 minutes before

adding to the reaction mix. 50µl of reaction mix was added to all wells containing a sample, standard or background control. The plate was wrapped in foil to protect it from light and left to incubate at room temperature for 60 minutes. Once developed plates were loaded into a Victor3 1420 multilable plate reader (PerkinElmer, USA) at an optical density of 570nm. The background control was subtracted from all samples and standards giving final concentrations of triglycerides. These were then normalised using the original powdered tissue weight of each sample.

2.8 High resolution respirometry

Mitochondrial respiratory capacity, from permeabilised tissue samples, was quantified via respirometry with an OROBOROS Oxygraph-2k (O2K) system (OROBOROS Instruments, Innsbruck, Austria). The maximal oxidative capacity of each sample is determined as a measure of O_2 flux. The greater the rate of O_2 flux, the greater the rate of oxygen consumption/oxidative phosphorylation. Additionally, each stage of oxidative phosphorylation can be determined through injection of respiratory substrates (suspended in dH_2O) or mitochondrial complex inhibitors (suspended in 100% ethanol). Protocols to permeabilised skeletal muscle fibres and liver tissue were adapted from Doerrier et al. (2018) and Canto and Garcia-Roves (2015) respectively.

2.8.1 Tissue preparation

Skeletal muscle and liver tissue was collected immediately after mice were culled. Tissues of interest were immediately places into ice colds biopsy preservation mediums (BIOPS), detailed in table 2.7. Both skeletal muscle and liver tissue samples were then prized apart by hand before being incubated in BIOPS containing 5mg/ml of saponin for 30 minutes at 4°C. Samples were then incubated in mitochondrial respiration buffer (MIR05), detailed in table 2.8, for 10 minutes at 4°C. Tissue samples

were then briefly dried and weighed, with a target weight of 1-3mg. Weighed samples were then immediately places into an O2k chamber containing 2ml of MIR05.

Table 2.7: Biopsy preservation medium (BIOPS) recipe

Chemical compound	Volume added to buffer*
2.77mM Calcium-potassium-egtazic acid (CaK_2EGTA)	72.3ml
7.23mM Potassium-egtazic acid (K_2EGTA)	27.7ml
Adenosine 5'-triphosphate disodium salt hydrate (Na2ATP)	3.18g
Magnesium chloride hexahydrate ($MgCl_2.6H_2O$)	1.334g
Taurine	2.502g
Na2 phosphocreatine	3.827g
Imidazole	1.362g
Dithiothreitol (DTT)	0.077g
2-[N-morpholino]ethanesulfonic acid (MES)	9.76g
dH^2O	900ml

*Quantities sufficient to make 1L. pH 7.1 using 5M potassium hydroxide (KOH) to adjust

Table 2.8: Mitochondrial respiration buffer (MIR05) recipe

Chemical compound	Required concentration
Egtazic acid (EGTA)	0.5mM
Magnesium chloride hexahydrate ($MgCl_2.6H_2O$)	3mM
Lactobionic acid	60mM
Taurine	20mM
Potassium dihydrogen phosphate (KH_2PO_4)	10mM
4-(2-hydroxyethyl)-1-piperazineethanesulfonic acid (HEPES)	20mM
D-sucrose	110mM
Fatty acid free BSA	1g/L

pH 7.1 using 5M potassium hydroxide (KOH) to adjust

2.8.2 OROBOROS Oxygraph-2k protocol

Following tissue preparation and loading into the O2k 5μl of catalase (280 units/ml) was added to the chamber. This was followed by 2.5μl of 200mM H_2O_2 to oxygenate the chamber to 380-400nmol/ml.

Additionally, 2.5µl of H_2O_2 was added throughout the experiment should oxygen concentration fall below 250nmol/ml. Baseline oxygen flux measured before the first respiratory substrates, 10µl of 0.01M malate and 4µl of 0.1M octanoyl-carntine, was added to induce β-oxidation and subsequently determine proton leak, proton slip and electron leak prior to ATP synthase activity, otherwise termed as FAO leak (Fig. 2.3). Sequential addition of 200mM ADP then followed steps until maximal oxidative phosphorylation/O_2 flux was reached, termed FAO OXPHOS (Fig. 2.3). This involved an initial 30µl followed by multiple 10µl injections and was signified by no additional increase in O_2 flux after a subsequent ADP injection. Following this 10µl of 0.4M malate and 10µl of 2M glutamate were added to assess complex I respiration before cytochrome c, termed CI before cyt c (Fig. 2.3). The subsequent addition of 5µl of 4mM cytochrome c then maximised complex I respiration, termed CI OXPHOS (Fig. 2.3). Total complex I and II respiration, termed CI+II OXPHOS (Fig. 2.3) was then assessed through addition of 20µl of 1M succinate. The first of the mitochondrial complex inhibitors, 0.5mM carbonyl cyanide-4-(trifluoromethoxy)phenylhydrazone (FCCP) was then sequentially added in 1µl steps, until maximal O_2 flux was reached, in order to remove the influence of ATP synthase, phosphate transporters and adenine nucleoside translocase on the ETC. The resulting electron transport state, termed ETS (Fig. 2.3) determined maximal oxidative capacity. The second inhibitor, 1µl of 1mM rotenone was then added to inhibit complex I and assess complex II respiration only, termed CII ETS (Fig. 2.3). Finally, 1µl of 5mM antimycin A was added to inhibit complex III and the ETC to determine non-mitochondrial respiration, termed ROX (Fig. 2.3).

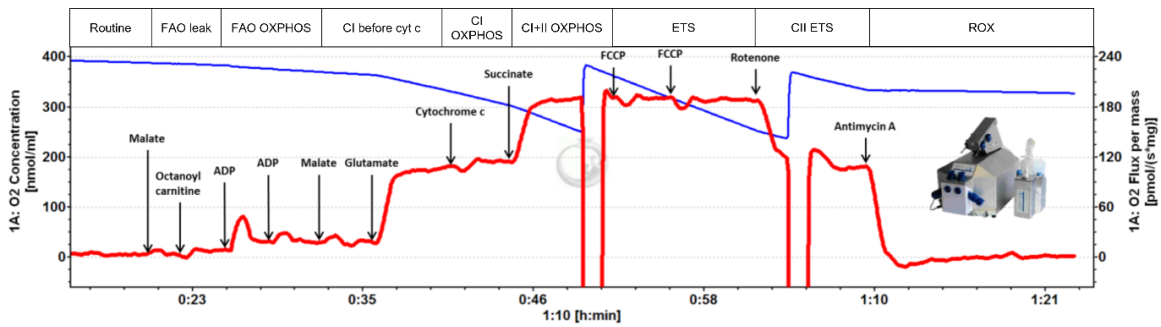

Figure 2.3: Visual representation and real time readout of the OROBOROS Oxygraph-2k protocol. Red line, oxygen concentration of chamber (left axis); blue line, oxygen flux/consumption (right axis).

2.9 Statistical analysis

Statistical significance was tested for using GraphPad Prism version 9 (GraphPad Software, LLC) as well as CalR (version 1.3) in the case of indirect calorimetry measures (Mina et al., 2018). Two-way ANOVAs, or unpaired t-tests, were used to analyse all quantitative measures. Indirect calorimetry measures were also analysed using linear regression and analysis of covariance (ANCOVA) which used body weight as the covariant that was compared to each measure to determine whether the effect of bodyweight was statistically significant. Statistical power was ensured with two-sided student's tests, with an alpha set at 0.05 and a power set at 0.8. Data detailing EE or NAD^+ content in control animals from previous experiments within the lab group were used for calculations. As such energy metabolism assessment required a group size of at least 10, whilst NAD^+ metabolome assessment required a group of at least 8.

CHAPTER 3 – THE IMPACT OF SUSTAINED GLUCOCORTICOID EXCESS ON ENERGY METABOLISM

3.1 Introduction

It is presently unclear what the effect of glucocorticoid excess is on global markers of energy metabolism as the existing literature is both limited and lacking in consensus. As previously mentioned, the primary of these markers is EE, which is greatly influenced by activity and thermogenesis, specifically BAT thermogenesis (van Baak, 1999, Crichton et al., 2017). Another marker of energy metabolism, as well as substrate utilisation is the respiratory exchange ratio (RER), which is influenced by oxygen consumption and carbon dioxide production. Using these markers, it is reported that natural circadian fluctuations in glucocorticoid production do not alter energy metabolism in mice (Dlugosz et al., 2012) or humans (Jobin et al., 1996). However, both acute and short-term low dose glucocorticoid treatment has been reported to increase EE, RER, oxygen consumption and carbon dioxide production in humans (Bessey et al., 1984, Chong et al., 1994, Brillon et al., 1995, Tataranni et al., 1996). Conflicting literature however, reports either no effect on energy metabolism (Chong et al., 1994) or even a decrease to one or more of these markers (Bessey et al., 1984, Horber et al., 1991, Gravholt et al., 2002, Short et al., 2004, Radhakutty et al., 2016). When it comes to investigating the effects of sustained glucocorticoid excess the limited nature of the existing literature is even more noticeable. At present, only three chronic studies exist, two in humans and one in mice. Chronic low dose glucocorticoid treatment in humans is reported to have no effect on EE (Radhakutty et al., 2016). This is also reported in patients with pre-diagnosed Cushing's syndrome (Burt et al., 2006). However, in a mouse model of Cushing's syndrome both EE and RER were reported decreased (Poggioli et al., 2013). In addition to global measures of energy metabolism, the impact of sustained glucocorticoid excess on mitochondrial respiratory capacity remains unclear. Given the functions of mitochondria (Javadov et al., 2020), and the known mitochondrial disfunction caused by glucocorticoid

excess (Tang et al., 2013, Magomedova and Cummins, 2016), respiratory capacity requires investigation.

Therefore, the aim of this chapter is to establish if glucocorticoid excess alters global markers of energy metabolism by exposing male and female mice to an established *in vivo* model of sustained glucocorticoid excess (Morgan et al., 2014). This will also determine if sex differences exists as this has been continuously overlooked by the existing literature. In addition, this chapter will also aim to establish the effect of sustained glucocorticoid excess on mitochondrial respiratory capacity. Together the findings of this chapter will further the understanding of the metabolic effects of glucocorticoid excess whilst also providing clarity to the existing literature.

3.2 Materials and methods

3.2.1 Animal housing

C57BL/6J mice (purchased from Charles River) were housed as detailed in section 2.1.1 for the first two weeks of treatment. For the final week of treatment mice were housed in a TSE Phenomaster 8 cage system as detailed in section 2.2.

3.2.2 Indirect calorimetry

Indirect calorimetry was performed using a TSE Phenomaster 8 cage system as detailed in section 2.2. Both male and female mice (n=12) were assessed by indirect calorimetry, however, activity was only assessed in females (n=8).

3.2.3 Animal treatments

C57BL/6J mice were treated *ab libitum* through their drinking water. Treatments are shown in table 3.1. Treatments lasted for 3 weeks and water was changed every 2 days to keep the animals supplied and to minimise any degradation of treatment. Water bottles were either opaque or wrapped in tin foil to prevent light from degrading the substance within. Both male and female (n=12) mice were treated.

Table 3.1: Animal treatments

Treatment	Dose	Preparation
Corticosterone	100mg/L (≈300µg/day)	100mg of corticosterone (Sigma-Aldrich, St Louis, Missouri, US) was dissolved in 6ml of 100% ethanol and then added to 1L of autoclaved water
Vehicle control	n/a	6ml of 100% ethanol was added to 1L of autoclaved water

Corticosterone treatment was set at 100mg/L based on the findings of Morgan et al. (2014). This dose is sufficient to elevate circulating daytime serum corticosterone by approximately 150% compared to controls over the specified treatment duration (nighttime and tissue specific values not reported), whilst circulating plasma concentrations have been shown to increase by as much as 400% in the day and 650% at night (Karatsoreos et al., 2010). This therefore results in supraphysiological levels and induces a significant Cushingoid phenotype. Length of treatment was restricted to 3 weeks to prevent additional suffering and loss of animals which can occur if treatment is extended to beyond 4 weeks.

3.2.4 Animal sacrifice and tissue collection

Following treatment and indirect calorimetry mice were sacrificed and tissues collected as detailed in section 2.1.2.

3.2.5 Tissue preparation

Tissue samples were prepared for subsequent analysis as detailed in section 2.1.3.

3.2.6 Body composition analysis

Body composition was assessed pre and post treatment as detailed in section 2.3.

3.2.7 Haematoxylin and eosin staining

Haematoxylin and eosin (H&E) staining was used to get a visual representation of triglyceride accumulation in liver samples, as detailed in section 2.6.

3.2.8 Triglyceride assay

Triglyceride quantification was performed using a triglyceride quantification colorimetric kit (BioVision, USA) as detailed in section 2.7.

3.2.9 High resolution respirometry

High resolution respirometry was performed using an OROBOROS Oxygraph-2k (O2K) system as detailed in section 2.8. Skeletal muscle and liver tissue samples from female mice treated with corticosterone or the vehicle control only (n=5) were assessed.

3.2.10 Statistical analysis

Statistical analysis was performed as detailed in section 2.9.

3.3 Results

3.3.1 Corticosterone treatment successfully generated a phenotype typical of glucocorticoid excess

Following corticosterone treatment, a phenotype typical of glucocorticoid excess was generated in both male and female mice as assessed by tissue and bodyweight analysis. Lipid accumulation (Peckett et al., 2011, Gasparini et al., 2019) (Fig. 3.1B and H), skeletal muscle atrophy/reduced lean body mass accrual (Schakman et al., 2013, Gasparini et al., 2016, Sato et al., 2018) (Fig. 3.1D-F, J-L) and spleen atrophy (Patel et al., 2011) (Fig. 3.1C and I) were all observed as expected, confirming the effectiveness of the model. Interestingly female mice accumulated significantly more fat than males with corticosterone treatment (Fig. 3.1H). Female mice also experienced a significant increase in bodyweight with corticosterone treatment (Fig. 3.1G), but males did not (Fig. 3.1A). Additional body composition analysis, of female mice only (due to time restrictions with collaborators), observed typical signs of glucocorticoid excess, further confirming the effectiveness of the model. Following corticosterone treatment skeletal muscle atrophy (Fig. 3.2B), fat accumulation (Fig. 3.2C) and bone atrophy (Hardy et al., 2018) (Fig. 3.2D) were all observed. Finally, another typical sign of glucocorticoid excess, hepatic triglyceride (TAG) accumulation, was also observed, as assessed by a TAG assay and H&E stain. Both male and female mice had significantly increased liver TAG content following corticosterone treatment (Fig. 3.3A-D). However, only female mice showed significantly increased liver weight (Fig. 3.3F).

3.3.2 Corticosterone treatment elevated energy expenditure in male and female mice

Assessment of EE, using the TSE Phenomaster, revealed that corticosterone treatment elevated EE in both male and female mice (Fig. 3.4). This effect was more pronounced during

the day and in female mice. Whilst EE was elevated in male mice it only reached significance at 10 hours (Fig. 3.4A). In female mice however corticosterone resulted in significant elevations at 2, 12, 25, 26, 28, 32, 33 and 36 hours (Fig. 3.4C), as well as on average during the day (Fig. 3.4D). In both males and females EE decreased less from night to day in corticosterone treated mice, compared to controls (Fig. 3.4C and D). Linear regression and subsequent ANCOVA determined no significant differences in slope angle between treatments revealing no significant effect of body weight on EE (Fig. 3.4). Whilst not significantly different female control mice did however exhibit a more positive correlation between EE and bodyweight than corticosterone treated mice (Fig. 3.10C).

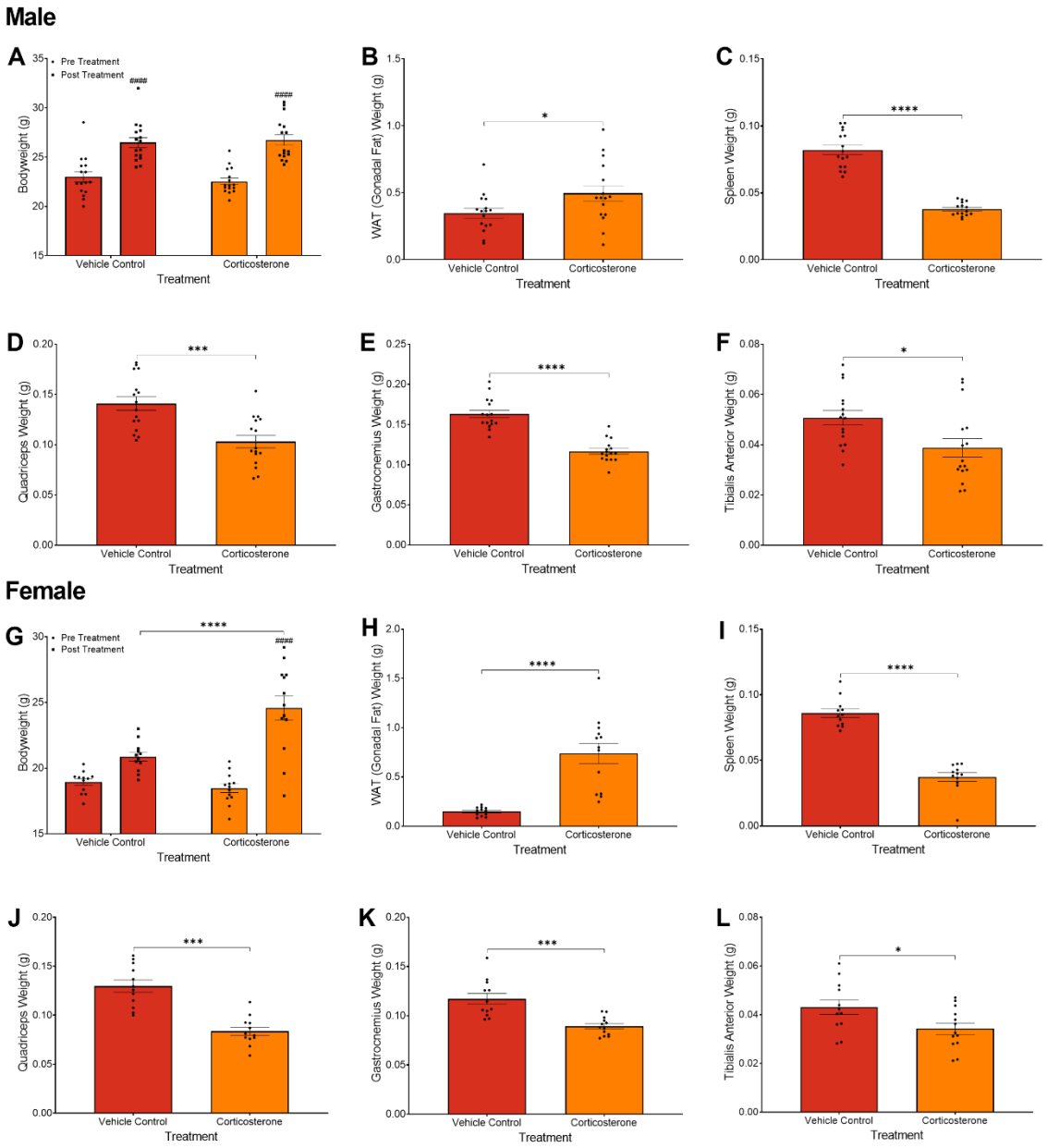

Figure 3.1: Bodyweight and tissue weight following 3 weeks of corticosterone treatment. **A**: Male bodyweight. **B**: Male WAT (gonadal fat) weight. **C**: Male spleen weight. **D**: Male quadriceps weight. **E**: Male gastrocnemius weight. **F**: Male tibialis anterior weight. **G**: Female bodyweight. **H**: Female WAT (gonadal fat) weight. **I**: Female spleen weight. **J**: Female quadriceps weight. **K**: Female gastrocnemius weight. **L**: Female tibialis anterior weight. Data is presented as mean with individual values ± SD, n=12-16. Significance determined via unpaired t-test or two-way ANOVA (A). * significantly different to control, # significantly different to pre. *p<.05, ** p<.01, *** p<.001, **** p<.0001. Abbreviations: WAT, white adipose tissue.

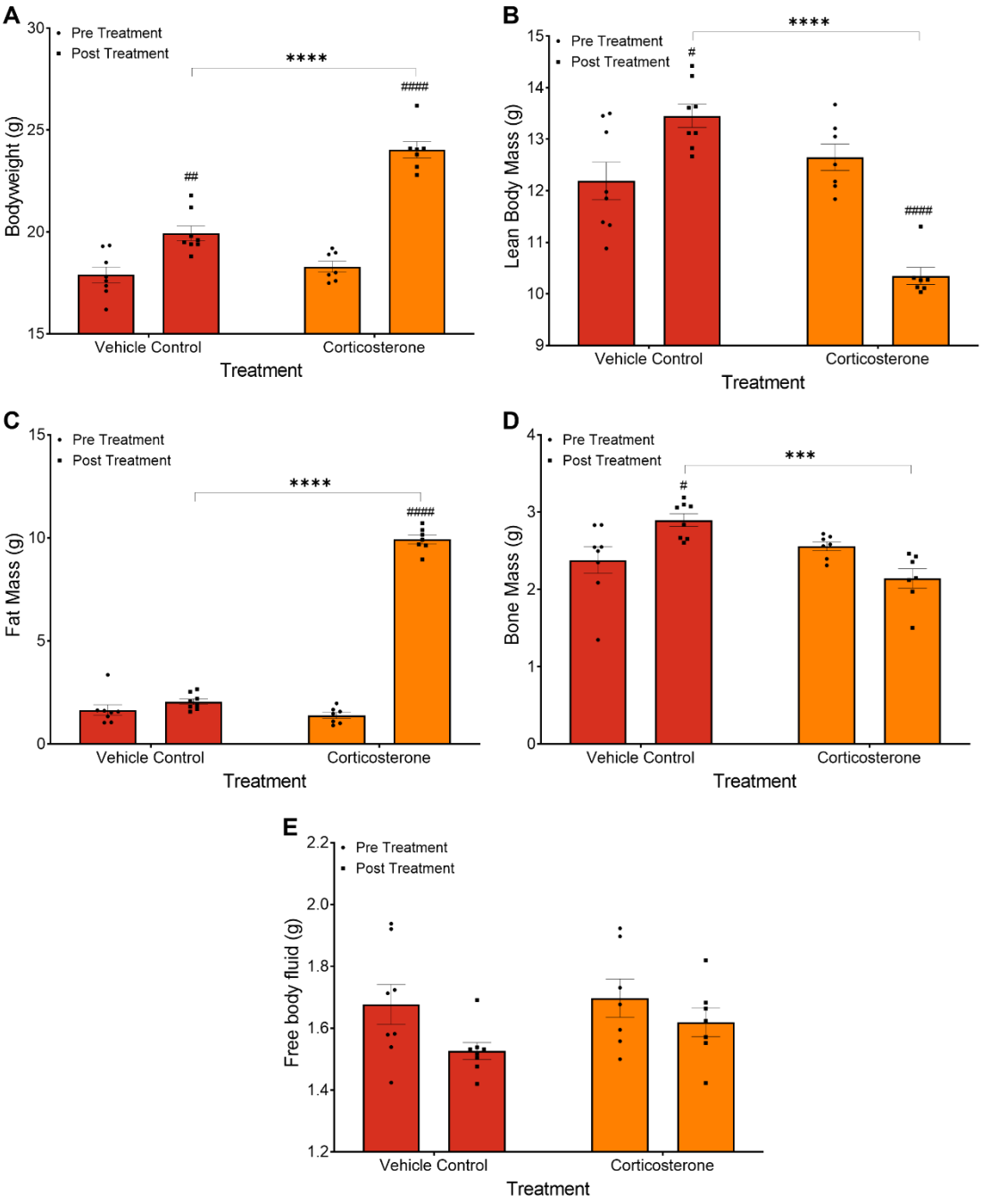

Figure 3.2: Body composition, of female mice only, before and after 3 weeks of corticosterone treatment as assessed by TD-NMR. **A**: Bodyweight. **B**: Lean body mass. **C**: Fat mass. **D**: Bone Mass. **E**: Free body fluid. Data is presented as mean with individual values ± SD, n=7-8, female only. Significance determined via two-way ANOVA. * significantly different to control, # significantly different to pre. *p<.05, ** p<.01, *** p<.001, **** p<.0001.

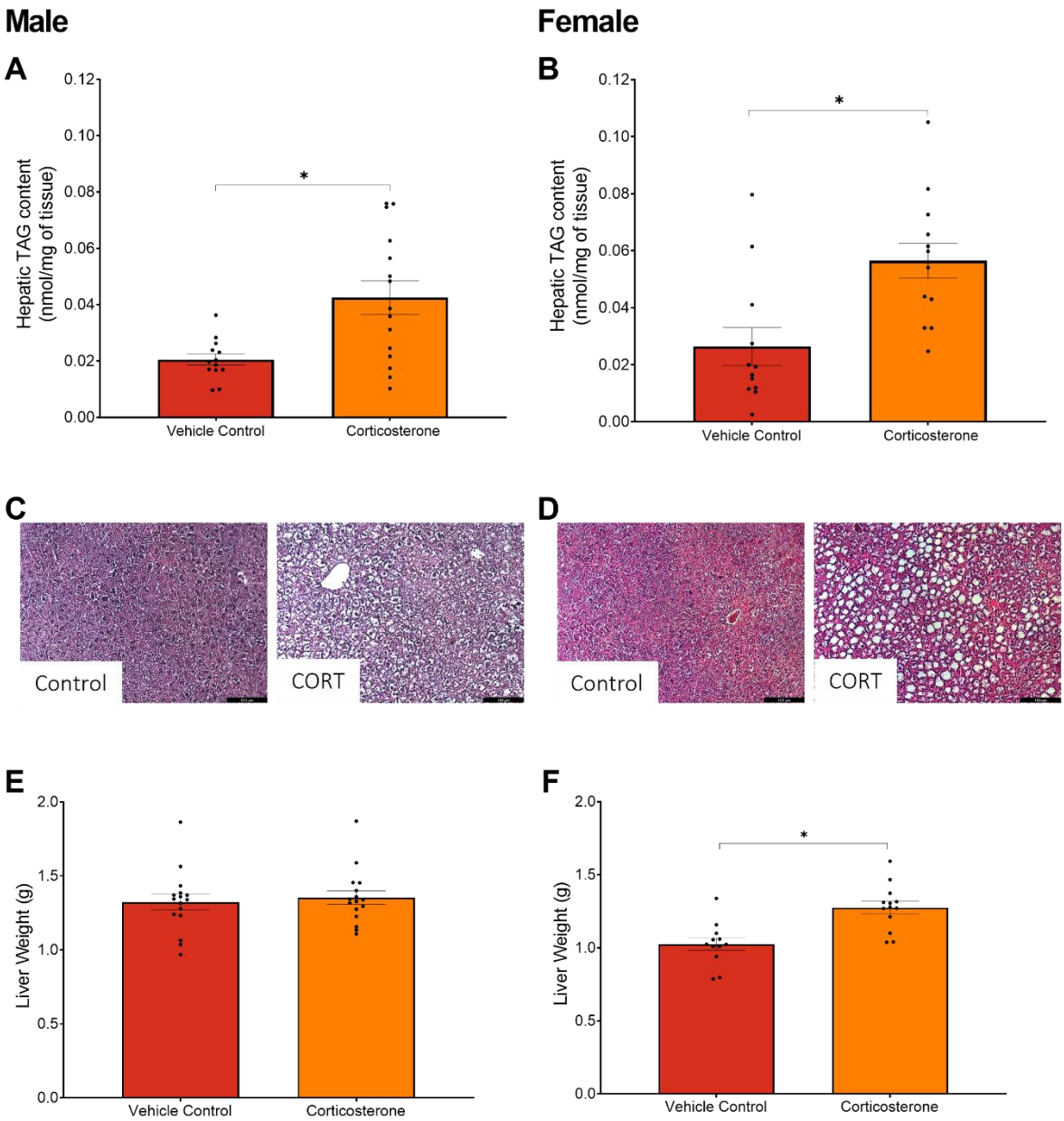

Figure 3.3: Hepatic TAG content after 3 weeks of corticosterone treatment as assessed by TAG assay and H&E staining. **A**: TAG content of male livers. **B**: TAG content of female livers. **C**: Male H&E stained livers. **D**: Female H&E stained livers. **E**: Male liver weight. **F**: Female liver weight. Data is presented as mean with individual values ± SD, n=12-16. Significance determined via unpaired t-test. * significantly different to control. *p<.05, ** p<.01, *** p<.001, **** p<.0001. Abbreviations: TAG, triglyceride; H&E, haematoxylin and eosin; CORT, corticosterone.

3.3.3 Corticosterone treatment elevated the respiratory exchange ratio in male and female mice

Assessment of RER, using the TSE Phenomaster, revealed that corticosterone treatment elevated RER in both male and female mice (Fig. 3.5). This effect was more pronounced during the day and in female mice. However, in both males and females average RER remained significantly elevated across the full 24-hour period, during the 12-hour dark (night) cycle and during the 12-hour light (day) cycle (Fig. 3.5B and D). In females RER did not significantly decrease in corticosterone treated mice from night to day (Fig. 3.5D) but did in male mice (Fig. 3.5B). Linear regression and subsequent ANCOVA determined no significant differences in slope angle between treatments revealing no significant effect of body weight on RER (Fig. 3.10B and D).

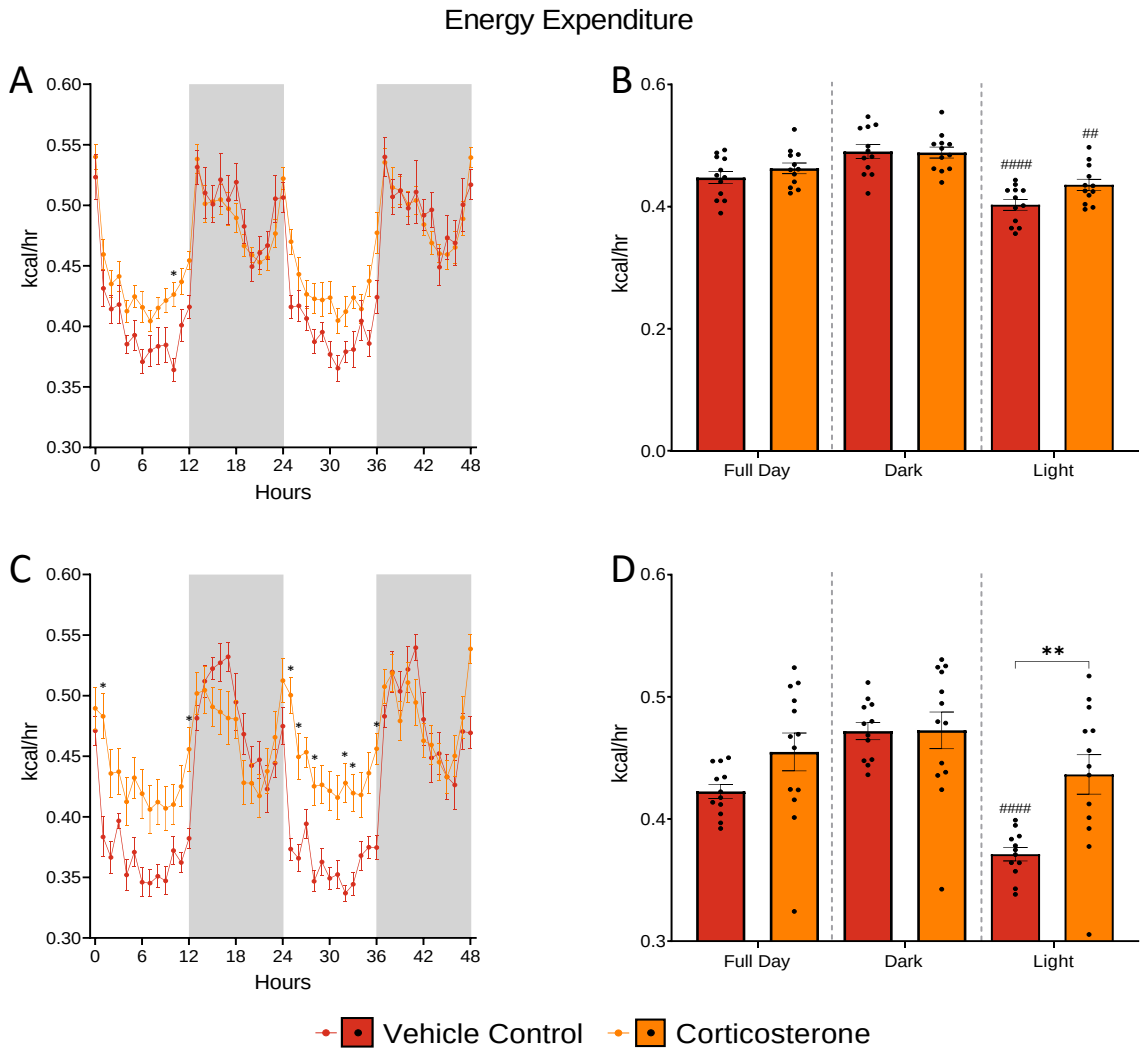

Figure 3.4: Energy expenditure following 3 weeks of corticosterone treatment. **A**: Male hourly energy expenditure. **B**: Male average energy expenditure. **C**: Female hourly energy expenditure. **D**: Female average energy expenditure. Line graphs are presented as mean ± SD, n=11-12. Bar charts are presented as mean with individual values ± SD, n=11-12. Significance determined via two-way ANOVA. * significantly different to control, # significantly different to dark. *p<.05, ** p<.01, *** p<.001, **** p<.0001.

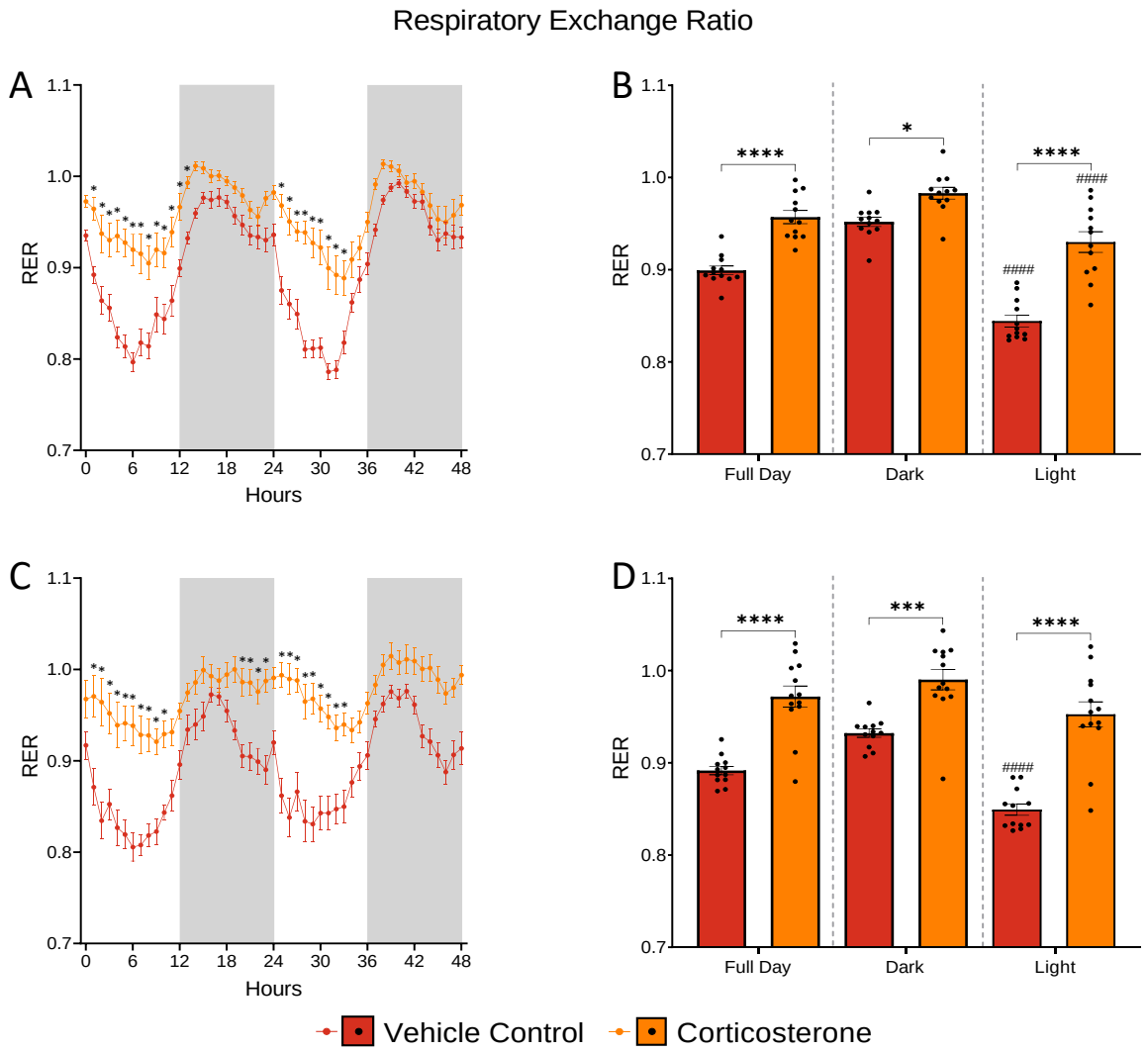

Figure 3.5: Respiratory exchange ratio following 3 weeks of corticosterone treatment. **A**: Male hourly RER. **B**: Male average RER. **C**: Female hourly RER. **D**: Female average RER. Line graphs are presented as mean ± SD, n=11-12. Bar charts are presented as mean with individual values ± SD, n=11-12. Significance determined via two-way ANOVA. * significantly different to control, # significantly different to dark. *p<.05, ** p<.01, *** p<.001, **** p<.0001.

3.3.4 Corticosterone treatment elevated oxygen consumption and carbon dioxide production in sex specific manner

Assessment of the two constituent parts of RER, oxygen consumption and carbon dioxide production, using the TSE Phenomaster, revealed that corticosterone treatment elevated both female mice but only carbon dioxide production in male mice (Fig. 3.6 and 3.7). Once

again, this effect was more pronounced in the day and in female mice. In male oxygen consumption was not significantly different during the dark or light phase (Fig. 3.6B). However, in female mice oxygen consumption was significantly elevated in corticosterone treated mice during the light phase (Fig. 3.6D). Carbon dioxide production was however significantly elevated during the light phase in both male and female mice treated with corticosterone (Fig. 3.7B and D). Linear regression and subsequent ANCOVA determined no significant differences in slope angle between treatments revealing no significant effect of body weight on oxygen consumption or carbon dioxide production (Fig. 3.10E-H). Whilst not significantly different female control mice did however exhibit a more positive correlation between oxygen consumption and bodyweight, as well as carbon dioxide production and bodyweight, than corticosterone treated mice (Fig. 3.10G and H).

3.3.5 Corticosterone treatment induced hyperphagia and polydipsia in male and female mice

Assessment of food and water intake, using the TSE Phenomaster, revealed that corticosterone treatment elevated both in male and female mice (Fig. 3.8 and 3.9), resulting in both hyperphagia and polydipsia. Both cumulative food intake (Fig. 3.8A and C) as well as average food intake (Fig. 3.8B and D), in males and females, revealed that corticosterone treated mice were eating significantly more during both the night and day. Whilst food intake was less during the day, it remained significantly elevated compared to controls in both males and females (Fig 3.8B and D). Linear regression and subsequent ANCOVA determined no significant differences in slope angle between treatments revealing no significant effect of body weight on food intake (Fig. 3.10I and k). As for water intake, both cumulative water

intake (Fig 3.9A and C) as well as average water intake (Fig 3.9B and D), in males and females, revealed that corticosterone treated mice were drinking significantly more during both the night and day. Whilst water intake was less during the day, it remained significantly elevated compared to controls in both males and females (Fig 3.9B and D). Linear regression and subsequent ANCOVA determined no significant differences in slope angle between treatments revealing no significant effect of body weight on water intake (Fig. 3.10J and L).

3.3.6 Corticosterone treatment reduced activity in female mice

Assessment of both locomotor and ambulatory activity in female mice only, using the TSE Phenomaster, revealed that corticosterone treatment decreased both (Fig. 3.11). Both hourly and average locomotor and ambulatory activity were significantly reduced by corticosterone during the night (Fig. 3.11A, B, C and D). During the day both locomotor and ambulatory activity were the same in corticosterone and control mice as activity significantly decreased from night to day in the controls. Activity in corticosterone treated mice did not differ between night and day (Fig. 3.11A, B, C and D).

3.3.7 Corticosterone treatment does not significantly alter mitochondrial respiratory capacity in female mice

Assessment of mitochondrial respiratory capacity in female tissue only revealed that corticosterone treatment does not significantly alter mitochondrial respiration capacity in either the quadriceps or liver (Fig. 3.12A and B). However, there was a trend towards increased oxygen consumption, indicating a slightly increased respiratory capacity in liver samples taken from corticosterone treated mice (Fig. 3.12B).

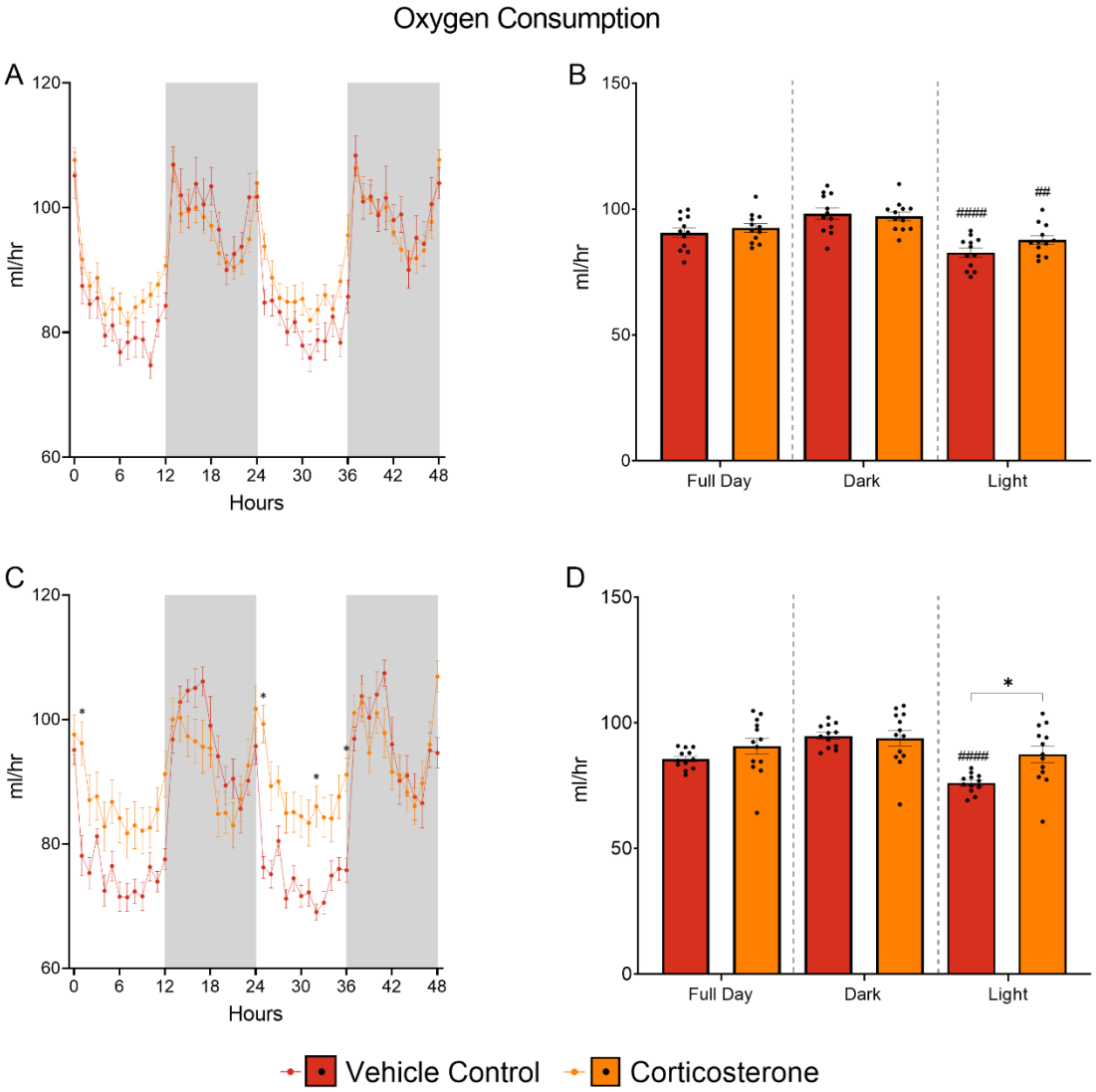

Figure 3.6: Oxygen consumption following 3 weeks of corticosterone treatment. **A**: Male hourly oxygen consumption. **B**: Male average oxygen consumption. **C**: Female hourly oxygen consumption. **D**: Female average oxygen consumption. Line graphs are presented as mean ± SD, n=11-12. Bar charts are presented as mean with individual values ± SD, n=11-12. Significance determined via two-way ANOVA. * significantly different to control, # significantly different to dark. *p<.05, ** p<.01, *** p<.001, **** p<.0001.

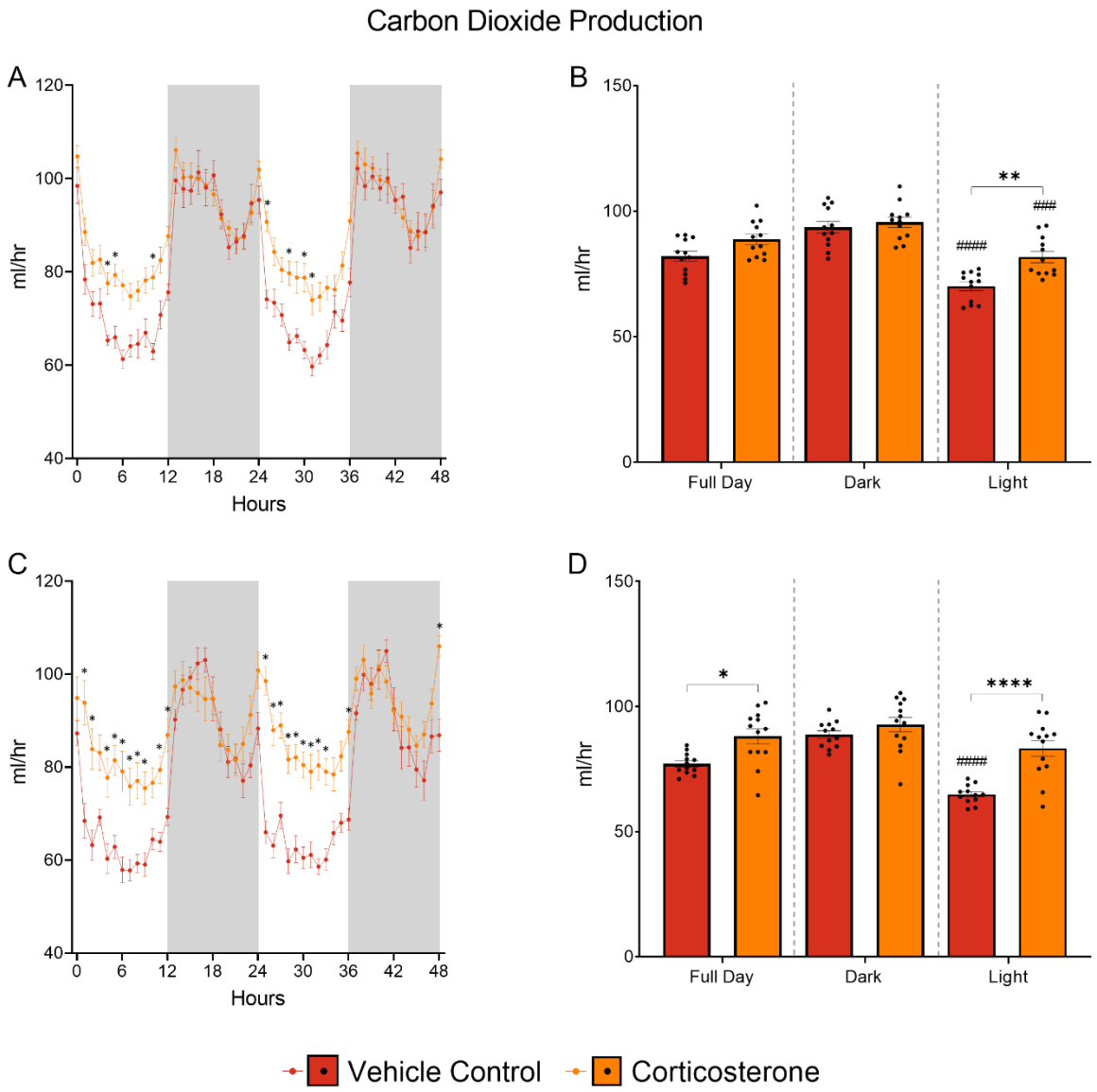

Figure 3.7: Carbon dioxide production following 3 weeks of corticosterone treatment. **A**: Male hourly carbon dioxide production. **B**: Male average carbon dioxide production. **C**: Female hourly carbon dioxide production. **D**: Female average carbon dioxide production. Line graphs are presented as mean ± SD, n=11-12. Bar charts are presented as mean with individual values ± SD, n=11-12. Significance determined via two-way ANOVA. significantly different to control, # significantly different to dark. *p<.05, ** p<.01, *** p<.001, **** p<.0001.

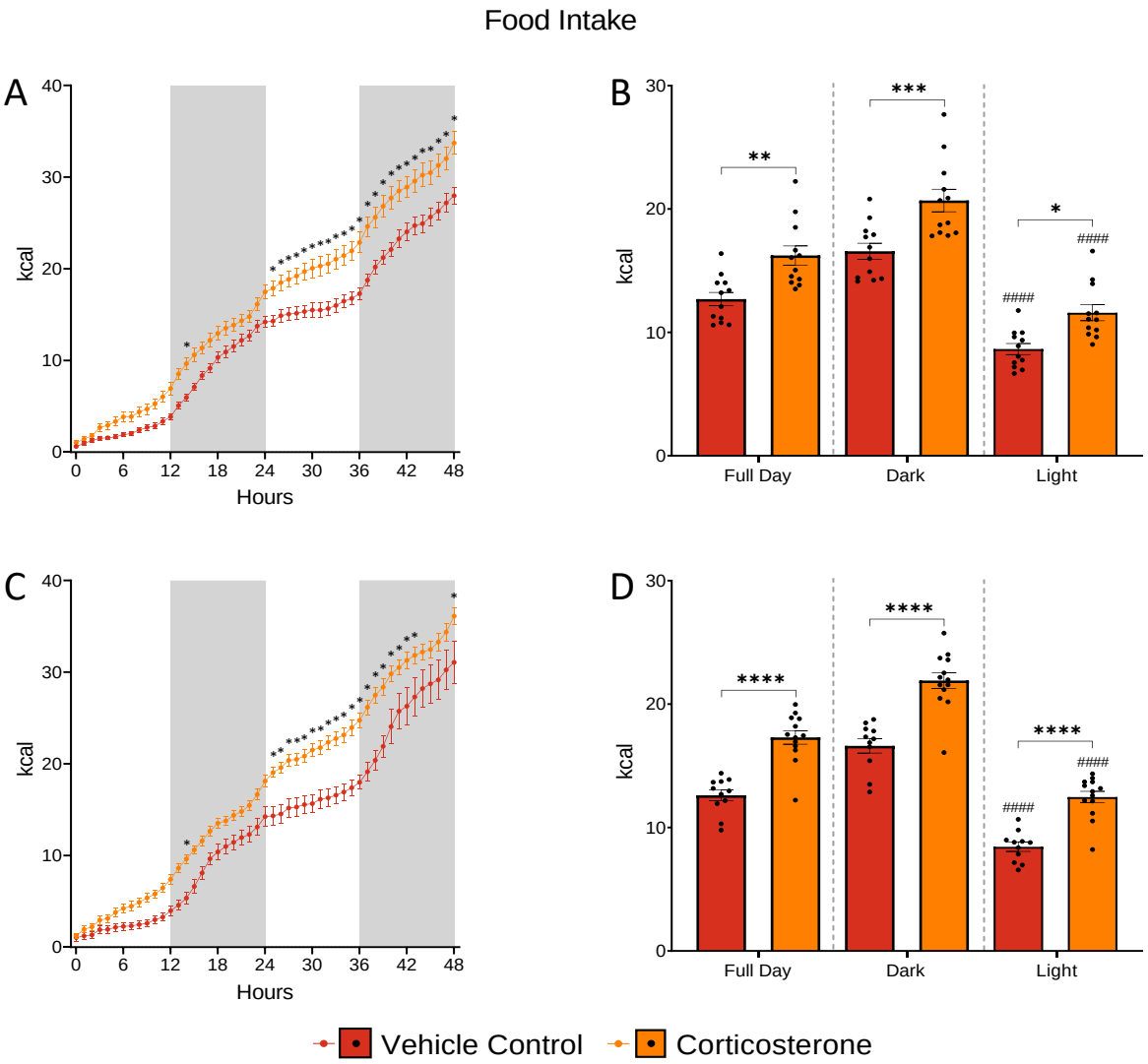

Figure 3.8: Food intake following 3 weeks of corticosterone treatment. **A**: Male cumulative hourly food intake. **B**: Male average food intake. **C**: Female cumulative hourly food intake. **D**: Female average food intake. Line graphs are presented as mean ± SD, n=11-12. Bar charts are presented as mean with individual values ± SD, n=11-12. Significance determined via two-way ANOVA. * significantly different to control, # significantly different to dark. *p<.05, ** p<.01, *** p<.001, **** p<.0001.

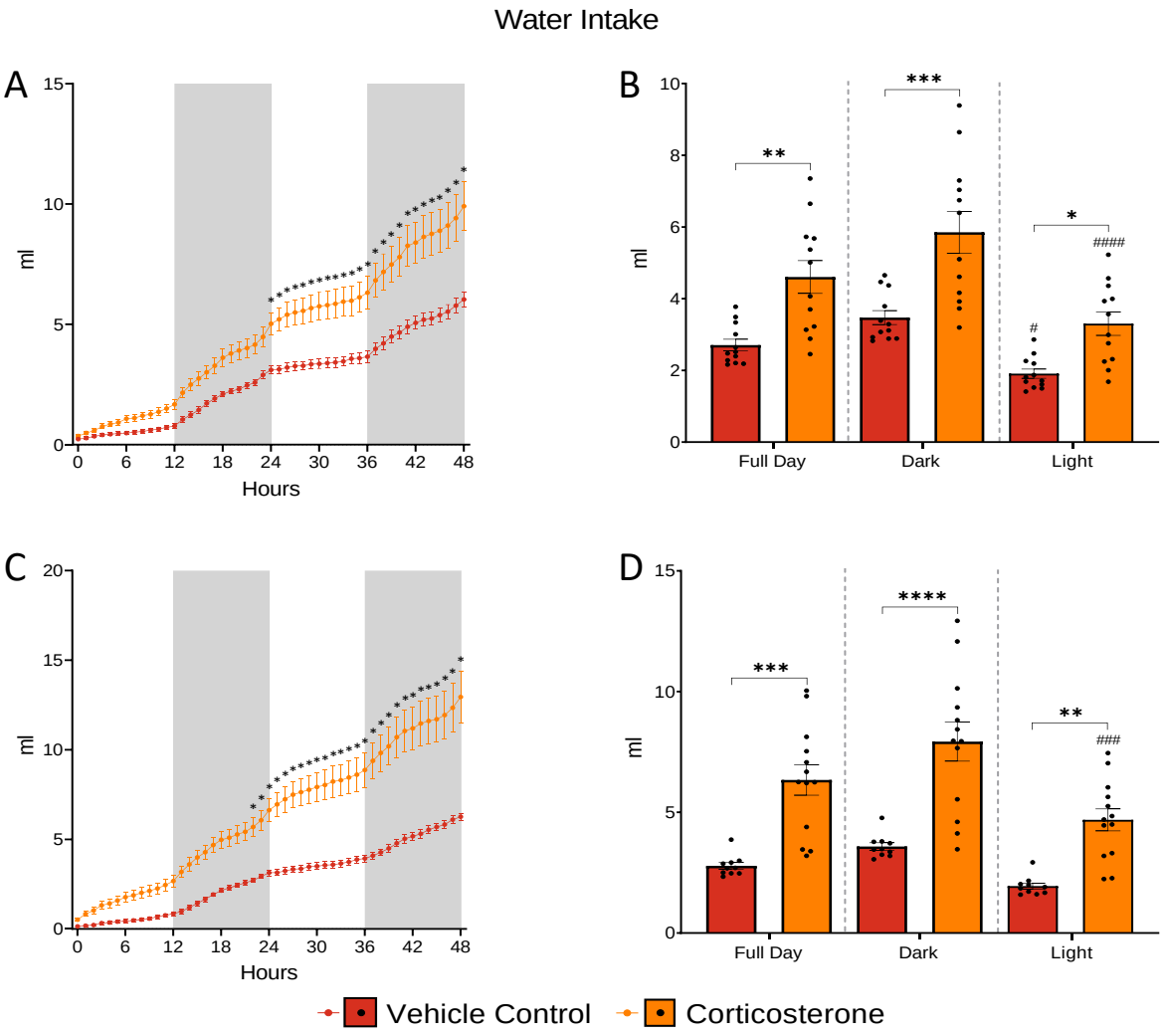

Figure 3.9: Water intake following 3 weeks of corticosterone treatment. **A**: Male cumulative hourly water intake. **B**: Male average water intake. **C**: Female cumulative hourly water intake. **D**: Female average water intake. Line graphs are presented as mean ± SD, n=11-12. Bar charts are presented as mean with individual values ± SD, n=11-12. Significance determined via two-way ANOVA. * significantly different to control, # significantly different to dark. *p<.05, ** p<.01, *** p<.001, **** p<.0001.

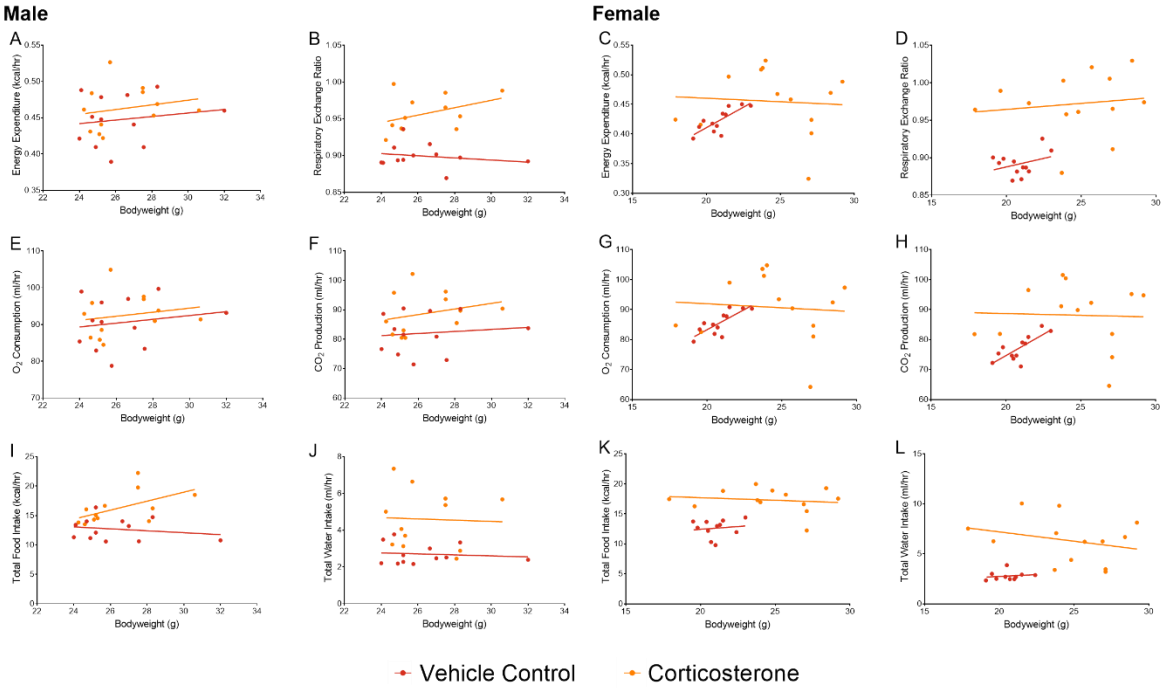

Figure 3.10: Analysis of covariance to determine the influence of bodyweight on markers of energy metabolism following 3 weeks of corticosterone treatment. **A**: Male energy expenditure. **B**: Male respiratory exchange ratio. **C**: Female energy expenditure. **D**: Female respiratory exchange ratio n=12. **E**: Male oxygen consumption. **F**: Male carbon dioxide production. **G**: Male oxygen consumption. **H**: Male carbon dioxide production. **I**: Male food intake. **J**: Male water intake. **K**: Female food intake. **L**: Female water intake. Significance determined via ANCOVA. * significantly different, *p<.05, ** p<.01, *** p<.001, **** p<.0001. Abbreviations: O_2, oxygen; CO_2, carbon dioxide.

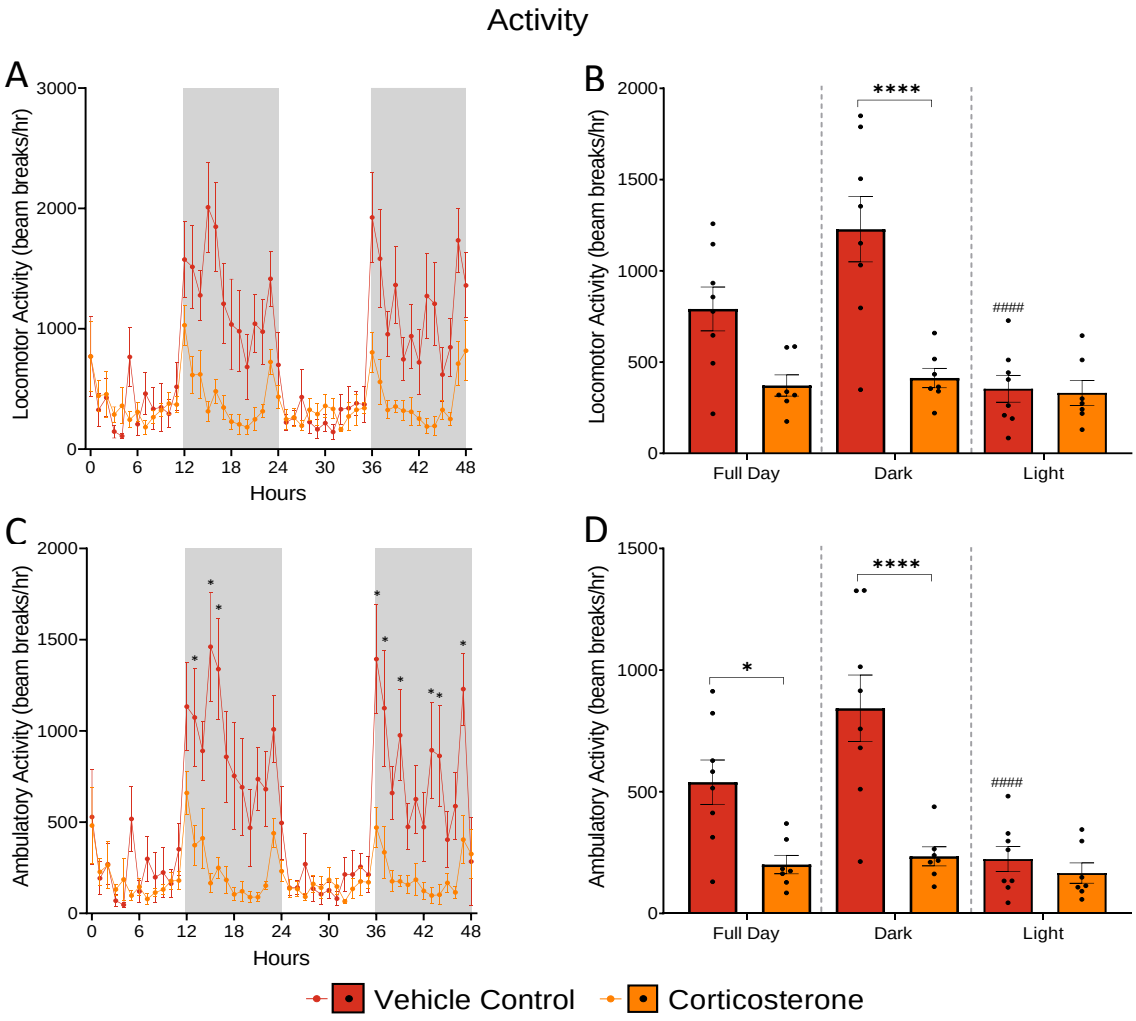

Figure 3.11: Animal activity following 3 weeks of corticosterone treatment. **A**: Hourly locomotor activity. **B**: Average locomotor activity. **C**: Hourly ambulatory activity. **D**: Average ambulatory activity. Line graphs are presented as mean ± SD, n=7-8. Bar charts are presented as mean with individual values ± SD, n=7-8. Significance determined via two-way ANOVA. * significantly different to control, # significantly different to dark. *p<.05, ** p<.01, *** p<.001, **** p<.0001.

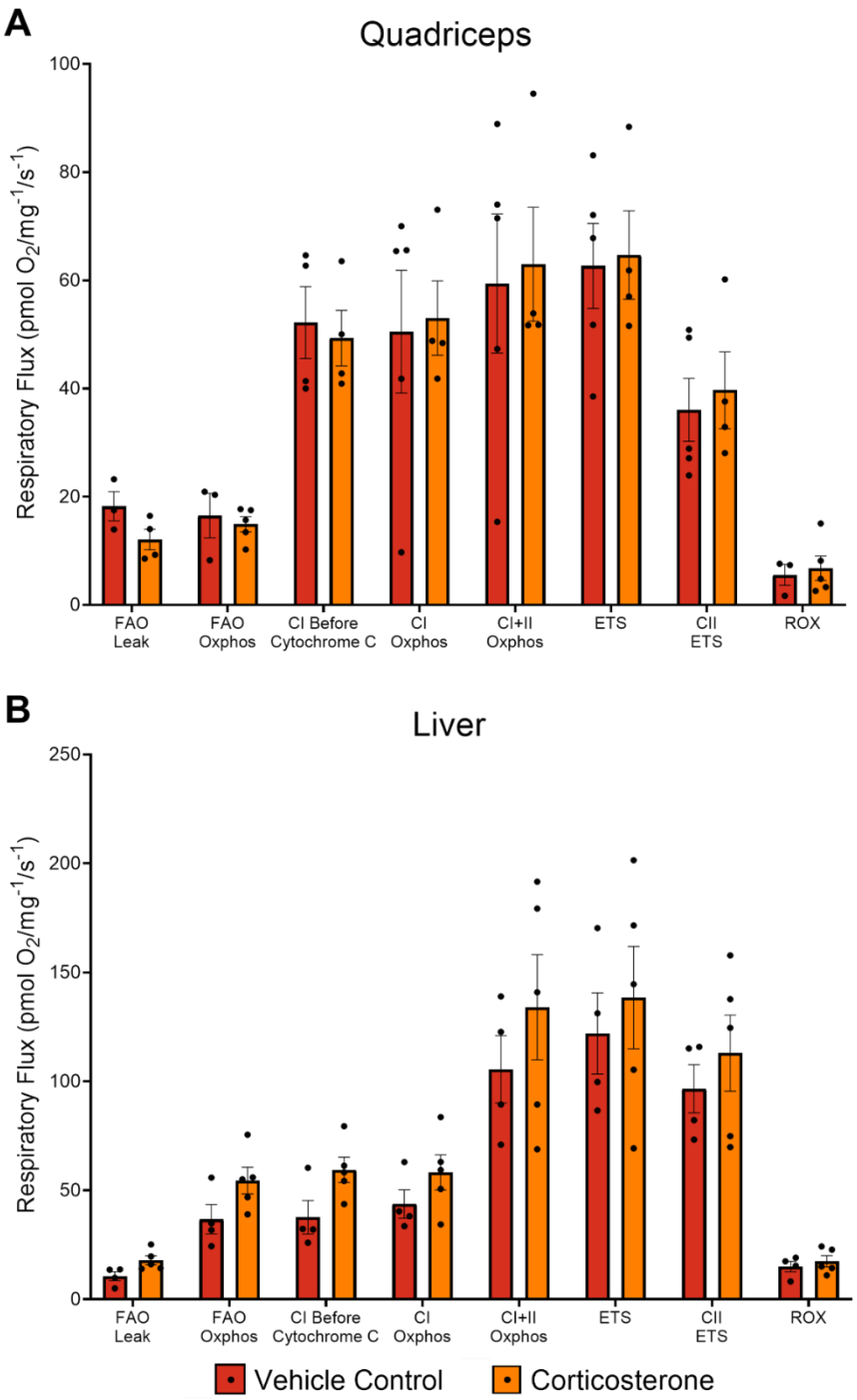

Figure 3.12: Mitochondrial respiratory capacity in female mice following 3 weeks of corticosterone treatment. **A**: Quadriceps mitochondrial respiratory capacity. **B**: Liver mitochondrial respiratory capacity. Data is presented as mean with individual values ± SD, n=4-5. Significance determined via individual unpaired t-tests for each stage. * significantly different to control. *p<.05, ** p<.01, *** p<.001, **** p<.0001.

3.4 Discussion

The findings presented in this chapter firstly confirm the effectivness of glucocorticoid treatment as a classic phenotype of sustained glucocorticoid excesss was observed. However, greater fat accumulation and bodyweight gain was identified in female mice treated with corticosterone. This chapter identifies the role of glucocorticoid excess in elevating markers of energy metabolism *in vivo*, as assessed by a TSE Phenomaster. The data indicates that elevations to EE and RER, as well as the constituent parts of RER, oxygen consumption and carbon dixoide production, are most pronounced during the day and interestingly, in female mice, again revealing a clear sex difference. This also shows that cushingoid mice are seen to expel more energy, despite accumulating more fat. An elevated RER also shows altered substrate utlisation as cushingoid mice are less able to utilise lipid oxidation for energy production and are instead restricted to carbohydrate oxidation. Additonally, at a more tissue specific level these findings are not necessarily mirrored as mitochondrial respiratory capacity is mostly unaltered, but trend towards a slight increase in the liver.

Whilst being one of the first studies to investigate the effect of sustained glucocorticoid excess on energy metabolism, and potentially only the second in mice, there is exisiting literature to compare the present findings with. Whilst a few studies do at face value agree with the present findings (Bessey et al., 1984, Chong et al., 1994, Brillon et al., 1995, Tataranni et al., 1996), it is important to note that these are all in humans studies given acute doses of glucocoritocoids. The closest existing study to the present one found a decrease in both EE and RER in C57BL/6J mice (Poggioli et al., 2013), the same strain used in this chapter. Treating mice with 5mg/kg of dexamthasone every other day for 7 weeks mice developed a cushingoid phenotype similar to that presented in this chapter. This dose is equivalent to approximately

375µg of corticosterone per mouse per day, given that dexamethaosne is approximately 25 times more potent that corticosterone, making it only slightly more than the dose used in this chapter (Table 3.1) meaning that dose is probaly not the reason for the conflicting findings. It is possible that the greater length of treatment used by Poggioli et al. (2013) might be responsible, suggesting that an even more prolonged model of glucocorticoid excess might evoke a different result, however this is hard to confirm and requires further investigation. The use of dexamethasone, whilst an approximately equivalent dose might also explain the differences. Dexamethasone is known to almost exclusively bind to and activate the GR, whilst corticosterone binds to both the GR and MR (Grossmann et al., 2004). This could explain the contrasting findings, but alternatively might not as dexamethasone and corticosterone have previously been reported to induce similar results *in vitro* (Menconi et al., 2008). Additionaly, Poggioli et al. (2013) might also be reporting a decrease in EE and RER as mice were given a high fat diet, which is known to cause a decrease on its own (Cartwright et al., 2021). Two further studies can also be used as reasonably close comparisons to the present study. Both Radhakutty et al. (2016) and Burt et al. (2006) reported no effect on EE or RER in human volunteers treated with chronic glucocortioicd excess, or those with pre-diagnosed Cushing's syndrome. As this evidence is in humans it can't be directly comapred to the findings in this chapter, but it might suggest that the effect of glucocorticoid excess on energy metabolism differs between mice and humans. Unfortunately, only further investigations and contributions to the literature can confirm this.

As for the mitochondrial respiratory capacity it is not possible to draw direct comparisons to the literature due to the novel nature of the findings presented in this chapter. It is interesting to observe little to no effect of glucocorticoid excess on the tissue specific oxygen

consumption of both the quadriceps and liver as glucocorticoid excess is known to cause global mitochondrial dysfunction (Tang et al., 2013, Magomedova and Cummins, 2016) and reduced substrate oxidation in both tissues (Magomedova and Cummins, 2016). In theory this should contribute to decreased oxygen consumption and respiratory capacity, which makes it more surprising that in the liver there is an upward trend towards increased mitochondrial oxygen consumption, including β-oxidation and ETC respiration. It is especially suprising that β-oxidation trends towards an increase in corticosterone treated livers, as this contradicts the previously mentioned elevated RER, which implies a reduction in lipid oxidation. However, this might be a consequence of the global and hepatic fat accumulation reported in this previous as rodent models of obesity and hepatic steatosis have reported increased rates β-oxidation in the liver (Brady et al., 1985, Diao et al., 2018). Whilst this is all difficult to categorically explain, some literature does report increased liver mitochondrial efficiency, but not necessarily oxygen consumption, in a rodent model of fatty liver (Crescenzo et al., 2013). Additionally, it does appear to coincide with the global increase in oxygen consumption that was observed.

Regardless of comparisons with the existing literature, the glucocorticoid excess induced elevations to both EE and RER require explaination. Potential explainations can be theorised from examining traditional explainations for altered energy metabolism. Traditionally EE in the context of gas exchange indirect calorimetry is seen as a measure of heat output which as previsouly mentioned is primarily driven in rodents by activty or thermogenesis within BAT. Increased activity is well understood to increase EE as assessed by indirect calorimetry (van Baak, 1999). However, the findings presented in this chapter show that both locomotor and ambulatory activity are decreased in mice treated with a sustained glucocorticoid excess,

keeping them in a continuosly inactive state. Importantly, during the day, when differences in EE are greatest between corticosterone and control treated mice, activity is no different. Additionally during the night when differences in EE are smallest, the difference in activity is greatest. Therefore, in this model, activity is not responsible for increasing EE. In line with the traditional perspective BAT thermogenesis is another possible explaination. This process is highly dependent on uncoupling protein 1 (UCP1) which enables heat production in BAT by "uncoupling" substrate oxidation and subsequent ATP synthesis through ATP synthase (Crichton et al., 2017). The proton gradient that would ordinarily go through ATP synthase (Fig. 1.22) is instead diverted to cross the inner mitochondrial membrane through UCP1, generating heat (Crichton et al., 2017). However, in rodents treated with glucocorticoid excess, including those treated with the exact same treatment protocol utilised in this chapter, both UCP1 protein content and gene expression are suppressed, thus inhibiting BAT thermogenesis (Poggioli et al., 2013, Doig et al., 2017). Another thermogenic mechanism within BAT, the futile creatine cycle, might also be suppressed but indirectly by glucocorticoid excess. This cycle involves the repeated phosphorylation and subsequent dephosphorylation of creatine, the latter of which generates heat (Rahbani et al., 2021). It has been reported that in mice that feed during the inactive phase of the 24 hour cycle, creatine mediated thermogeneis is decreased (Rahbani et al., 2021). As mice treated with glucocortocoid excess in this chapter are continuously in an inactive state, as well as continuosly eating it is likely the futile creatine cycle is also inhibited. Therefore it is also unlikely that thermogenesis is responsible for the increase in EE. An explaination or theory outside of the traditional perspective is therefore required. One has been proposed by Ho (2018). Ho (2018) propose that EE in the context of gas exchange indirect calorimetry should be thought of as EE and post-prandial EE. They propose post-prandial EE is actually a measure of heat output as well

as both the chemical energy stored post meal and the cost of storing this energy. This is thought to be primarily driven by lipid synthesis and storage, or de novo lipogenesis. To test this healthy human volunteers were treated with 15mg/day prednisolone for 1 week followed by a meal. Post-prandial (<2 hours post meal) skin temperature was reduced in prednisolone treated volunteers but not in placebo treated controls, showing reduced thermogenesis. However post prandial EE was elevated in prednisolone treated volunteers compared to the controls, as was lipid synthesis. A similar process is likely happening in the mouse model utilised in this chapter. Glucocorticoid excess induced hyperphagia was observed in agreement with existing literature (Tataranni et al., 1996). This is because glucocortiocid excess elevates levels within the hypothalamus, including in rodents models comparible to that used in this chapter, resulting an overexpression and transcription of agouti-related protein (AgRP), a potent regulator of energy balance and appetite (Ilnytska and Argyropoulos, 2008, Sefton et al., 2016). This then drives increased energy/food intake as it tricks the mouse, or human, into thinking they are in a severe calorie deficit (Sefton et al., 2016). Importantly in this chapter, this mehcanims resulted in consistent hyperphagia during both the night and day, keeping mice in a continuous post-prandial state from a majority carbohydrate based food. This is likely to be driving de novo lipogenesis, which is known to be increased by glucocorticoid excess (Magomedova and Cummins, 2016, Pranger et al., 2018, Garcia-Eguren et al., 2020), and also contributes to the fat accumulation seen in the this chapter (Fig. 3.1). This is then elevating EE through the chemical energy storage of lipids and the energy costs associated with storage and sythesis. Thus explaining how these mice are able to accumlated fat despite having a greatly increased energy expenditure. This theory could also explain the elevated RER seen in corticosterone treated mice. As previously mentioned, RER is a function of oxygen consumption and carbon dioxide production and is represented by a value normally

ranging from 0 to 1, giving an indication of the primary substrate utilisation. However values can exceed 1, as seen in this chapter, which can also be attributed to an increase in de novo lipogeneisis (Talal et al., 2021). Additionally, this theory might also explain why female mice experienced greater elevations in EE and RER as they were seen to accumulate more fat following corticosterone treatment which is likely caused by increased de novo lipogeneis compared to male mice. Finally, to further this theory the upward trend of mitochondrial oxygen consumption observed in female liver samples might also be indicative, but not definitively, of increased de novo lipogenesis. Whilst glucocorticoid excess is known to cause mitochondrial dysfunction (Tang et al., 2013, Magomedova and Cummins, 2016), evidence from a rodent model of de novo lipogenesis reports increase mitochondrial efficiency in order to facilitate increased de novo lipogenesis (Crescenzo et al., 2013). Whilst this does not necessarily imply increased liver mitochondrial oxygen consumption, it could play a role.

Whilst revealing significant insight into the effects of sustained glucocorticoid excess on energy metabolism *in vivo*, this chapter raises additional questions. The first of these is regarding the observed sex differences. As discussed in section 1.4.1 it is known that androgens and estrogens, as well as their respective receptors, can modulate the activtiy of the GR (Dakin et al., 2015, Spaanderman et al., 2018, Kroon et al., 2020). However, this same literature indicates that elevated androgens in rodent models of glucocorticoid excess enhance metabolic dysfunction (Spaanderman et al., 2018, Kroon et al., 2020) whilst increased estrogen has a protective, but not preventitve, effect (Dakin et al., 2015). It is therefore puzzling that females in this chapter experienced exaggerated effects, however this does coincide with literature reporting differing presentation of cushingoid symptoms in humans, including increased weight gain in female Cushing's patients (Pecori Giraldi et al.,

2003, Valassi et al., 2011, Broersen et al., 2019), as well as findings in female mice reported increased WAT accumulation and weight gain compared to males (Kaikaew et al., 2019). To fully answer this question is beyond the scope of this thesis but future investigation could look to repeat the approaches taken in this chapter with male mice given estrogen, female mice given testosterone or even ovariectomised female mice. The second question raised by this chapter is whether the theory proposed by Ho (2018) does in fact explain the elevations to EE and RER. Given the observed decrease in activity and known suppression of BAT thermogenesis it remains a primary candidate, but without future investigation this cannot be confirmed. Complete removal of food, time restricted feeding or even pair matched feeding are all possible options to explore this further. The final question raised by this chapter is how glucocorticoid excess is able to induce these effects. Whislt the mechanisms of glucocorticoid action are well understood (Groeneweg et al., 2012, Ramamoorthy and Cidlowski, 2016), the exact cause of the findings observed in this chapter are not immediately clear and require extensive investigation.

In conclusion, this chapter provides evidence that glucocorticoid excess elevates EE, RER, food and water intake in male and female C57BL/6J mice. Interestingly it also reveals a more pronounced effect in female mice. Both of these findings expand the understandiong of the phenotype typical of glucocorticoid excess. Given the effects observed in the chapter, the following chapter will investigate whether the NAD^+ metabolome is also disrupted by glucocorticoid excess as it is known to be strongly linked with both energy metabolism and other metabolic processes that are altered by glucocorticoid excess (Canto et al., 2015, Xie et al., 2020a, Levine et al., 2021). The following chapter will also investigate whether an NAD^+

precursor, NR, reported to augment the NAD^+ metabolome (Canto et al., 2012) is an effect treatment strategy to attenuate the effects of sustained glucocorticoid excess.

CHAPTER 4 –THE IMPACT OF SUSTAINED GLUCOCORTICOID EXCESS ON THE NAD^+ METABOLOME AND FEASIBILITY OF NR SUPPLEMENTATION AS A TREATMENT STRATEGY

4.1 Introduction

Findings in the previous chapter comprehensively established that markers of energy metabolism are altered in an *in vivo* model of sustained glucocorticoid excess. Whilst a potential explanation for this was discussed, other mechanisms, or molecules might also be involved, at least theoretically. One such candidate is NAD^+ and its metabolome. Known to be crucial for healthy metabolic function and linked to energy metabolism (Canto et al., 2015, Xie et al., 2020a) it is plausible that an alteration to the NAD^+ metabolome might be involved in the effects observed in the previous chapter. In fact, EE has been reported to be directly altered by changes within the NAD^+ metabolome (Canto et al., 2015, Xie et al., 2020a). However, whether this is the case with sustained glucocorticoid excess requires investigation. At present the relationship between sustained glucocorticoid excess and the NAD^+ metabolome remains poorly defined. The most basic knowledge of whether glucocorticoids alter NAD^+ content, the expression of its biosynthetic enzymes or other aspects of the NAD^+ metabolome remains inconclusive. Limited existing investigation, discussed in section 1.20 and summarised in table 1.2, provides a glimpse, however one that is extremely sparse, lacking in clarity and not always focusing specifically on glucocorticoid excess (Kralisch et al., 2005, Friebe et al., 2011, Roma et al., 2012, Yang et al., 2017, Xiao et al., 2019, Herrera et al., 2020b, Xie et al., 2020b, Quattrocelli et al., 2022). For example, both Kralisch et al. (2005) and Friebe et al. (2011) indicate an increase in NAMPT expression, the key rate limiting enzyme in NAD^+ biosynthesis, in cultured adipocytes and preadipocytes. However, preliminary data from our lab in C2C12 myotubes (Fig. 4.1A), as well as *in vivo* findings within the livers of mice, suggest the opposite (Xiao et al., 2019, Xie et al., 2020b). Roma et al. (2012) and Yang et al. (2017) provide evidence for alterations to the $NADP^+$/NADPH ratio in cultured rat islet and mouse chondrocytes respectively, however one reports a shift to a more oxidised ratio (Roma

et al., 2012) whilst the other reports a more reduced ratio (Yang et al., 2017). As for NAD^+ content itself it is unclear if it is decreased (Xiao et al., 2019, Xie et al., 2020b), undisturbed (Herrera et al., 2020b) or even increased (Quattrocelli et al., 2022). Importantly several questions remain due to the lack of clarity and because much of the NAD^+ metabolome, summarised in Fig. 1.10, remains untouched. However, these studies do give preliminary indications of a relationship between glucocorticoid treatment, whether it be excess or not, and alterations to the NAD^+ metabolome, thus meriting extensive further investigation.

Additionally, there is a need to investigate if altering the NAD^+ metabolome through NAD^+ precursor or intermediate supplementation *in vivo* can alter any of the effects of glucocorticoid excess, including those identified in the previous chapter and any effects on the NAD^+ metabolome if indeed there are any. Limited existing literature indicates the plausibility of this. Both Uto et al. (2021) and Huang and Tao (2020) report that NAD^+ precursor NMN, discussed in section 1.12.2.4 is able to attenuate glucocorticoid excess induced hyperglycaemia and osteoporosis respectively. It is therefore possible supplementing another NAD^+ precursor, NR, which was discussed in section 1.12.2.2, might also be of benefit. Shown to boost NAD^+ *in vivo* (Canto et al., 2012, Doig et al., 2020, Cartwright et al., 2021) it has also been attributed with helping combat some metabolic conditions that can be caused independent of glucocorticoid excess (Canto et al., 2012, Diguet et al., 2018, Dall et al., 2022). Preliminary data from our lab in C2C12 myotubes also indicates NR might be able to influence glucocorticoid flux as it increased the conversion of exogenous 11-dehydrocorticosterone to corticosterone (Fig. 4.1B). However, whether NR is able to alter the metabolic conditions and dysfunction caused by glucocorticoid excess, and therefore be viable treatment strategy, remains to be seen.

Therefore, the aims of this chapter are to firstly characterise the effect of glucocorticoid excess on aspects of the NAD^+ metabolome, *in vivo*. This will provide further evidence for the relationship between the two, addressing the lack of clarity in the limited existing literature. The second aim of this chapter is to test if NR supplementation can alter some of the known effects of glucocorticoid excess, including the novel effects identified in the previous chapter, as well as any effects on the NAD^+ metabolome should they be identified in this chapter.

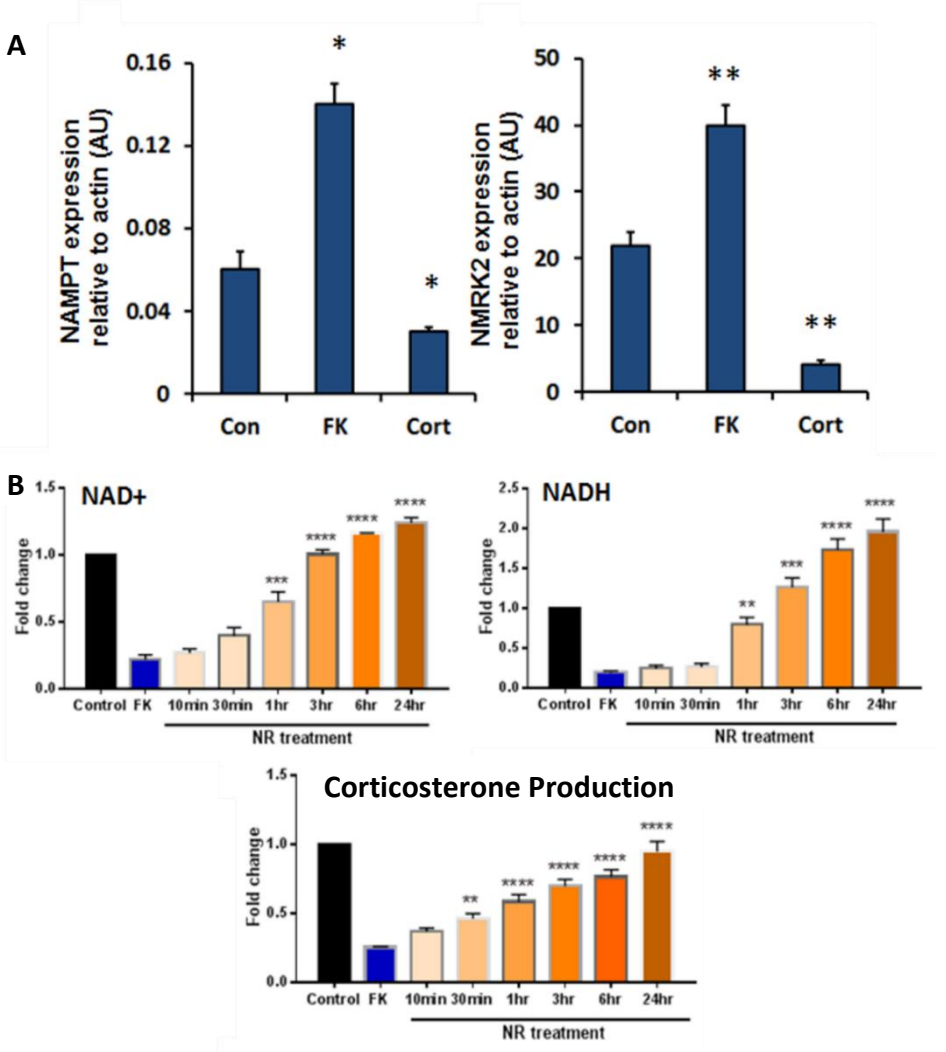

Figure 4.1: Preliminary data showing crosstalk between glucocorticoids and the NAD^+ metabolome the effect of glucocorticoid excess and the NAD^+ metabolome in C2C12 myotubes. **A**. Corticosterone induced NAMPT and NRK2 depletion *in vitro*. **B**. NAD^+ replenishment modulates glucocorticoid flux *in vitro*. Abbreviations: Con, control, FK, FK866 (NAMPT inhibitor); Cort, corticosterone.

4.2 Materials and methods

4.2.1 Animal housing

C57BL/6J mice (purchased from Charles River) were housed as detailed in section 2.1.1 for the duration of treatment.

4.2.2 Animal treatments

C57BL/6J mice were treated *ab libitum* through their drinking water. Treatments are shown in table 4.1. Treatments lasted for 3 weeks and water was changed every 2 days to keep the animals supplied and to minimise any degradation of treatment. Water bottles were either opaque or wrapped in tin foil to prevent light from degrading the substance within. Both male and female (n=12) mice were treated.

Table 4.1: Animal treatments

Treatment	Dose	Preparation
Corticosterone	100mg/L (≈300µg/day)	100mg of corticosterone (Sigma-Aldrich, St Louis, Missouri, US) was dissolved in 6ml of 100% ethanol and then added to 1L of autoclaved water
Nicotinamide riboside	5g/L (≈400µg/day)	5g of nicotinamide riboside (Chromadex, California, USA) was dissolved in 1L of autoclaved water
Corticosterone + nicotinamide riboside	100mg/L + 5g/L	100mg of corticosterone was dissolved in 6ml of 100% ethanol and then added to 1L of autoclaved water. 5g of nicotinamide riboside was then dissolved in the same water
Vehicle control	n/a	6ml of 100% ethanol was added to 1L of autoclaved water

4.2.3 Indirect calorimetry

Indirect calorimetry was performed using a TSE Phenomaster 8 cage system as detailed in section 2.2. Both male and female mice (n=12) were assessed by indirect calorimetry.

4.2.4 Animal sacrifice and tissue collection

Following treatment mice were sacrificed and tissues collected as detailed in section 2.1.2.

4.2.5 Tissue preparation

Following animal sacrifice and tissue collection tissues were prepared for subsequent analysis as detailed in section 2.1.3.

4.2.6 NAD^+/NADH fluorescence assay

NAD^+ and NADH quantification was performed via a NAD^+/NADH fluorescence assay as detailed in section 2.4.

4.2.7 RNA extraction and analysis

Gene expression of samples was assessed as detailed in section 2.5 with reference genes listed in table 2.5 used. Genes specific to this chapter are detailed in table 4.2.

Table 4.2: TaqMan probes used in this chapter

Gene	Assay ID
Trim63 (MuRF1)	Mm01185221_m1
NAMPT	Mm00451938_m1
NMRK1 (NRK1)	Mm00521051_m1
NMRK2 (NRK2)	Mm01172899_g1
NMNAT1	Mm01257929_m1
NMNAT3	Mm00513791_m1

Table 4.2: continued

Gene	Accession number
NADSYN1 (NADSYN)	Mm00513448_m1
NAPRT	Mm00553802_m1
NADK	Mm00446804_m1
PNP	Mm00840006_m1
QPRT	Mm00504998_g1
HAAO (HAO)	Mm00517945_m1
KYNU (KYU)	Mm00551012_m1
KMO	Mm01321343_m1
AFMID (AFM)	Mm00510774_m1
IDO1 (IDO)	Mm00492590_m1
TDO2 (TDO)	Mm00451269_m1

4.2.8 Haematoxylin and eosin staining

Haematoxylin and eosin (H&E) staining was used to get a visual representation of triglyceride accumulation in liver samples, as detailed in section 2.6.

4.2.9 Triglyceride analysis

Triglyceride quantification was performed using a triglyceride quantification colorimetric kit (BioVision, USA) as detailed in section 2.7.

4.2.10 Statistical analysis

Statistical analysis was performed as detailed in section 2.9.

4.3 Results

4.3.1 Corticosterone treatment significantly decreases NAD^+ in a tissue and sex specific manner

Following corticosterone treatment NAD^+ was depleted in a tissue specific and even sex specific manner, as assessed by NAD^+ fluorescence assay. However, it was only decreased in female WAT (Fig. 4.2F). Within male and female skeletal muscle (tibialis anterior), liver and male WAT corticosterone treatment did not significantly alter NAD^+ content (Fig. 4.2A-E).

4.3.2 Corticosterone treatment significantly increases NADH in a tissue specific manner

Like NAD^+ corticosterone treatment also altered NADH in a tissue specific manner as assessed by a NADH fluorescence assay. Within skeletal muscle (tibialis anterior) corticosterone elevated NADH content in both male and female mice (Fig. 4.3A and B). In WAT (gonadal) NADH was also significantly increased in male and female mice (Fig. 4.3E and F). However, in the liver NADH was unaffected by corticosterone in male and female mice but may trend towards a slight decrease (Fig. 4.3C and D).

4.3.3 Corticosterone treatment significantly alters the NAD+/NADH ratio in a tissue and sex specific manner

Following corticosterone treatment, the NAD**+**/NADH ratio was mostly unchanged in male and female tissue (Fig. 4.4A-E). However, in female WAT tissue only the ratio was shifted to a more reductive state (Fig, 4.4F).

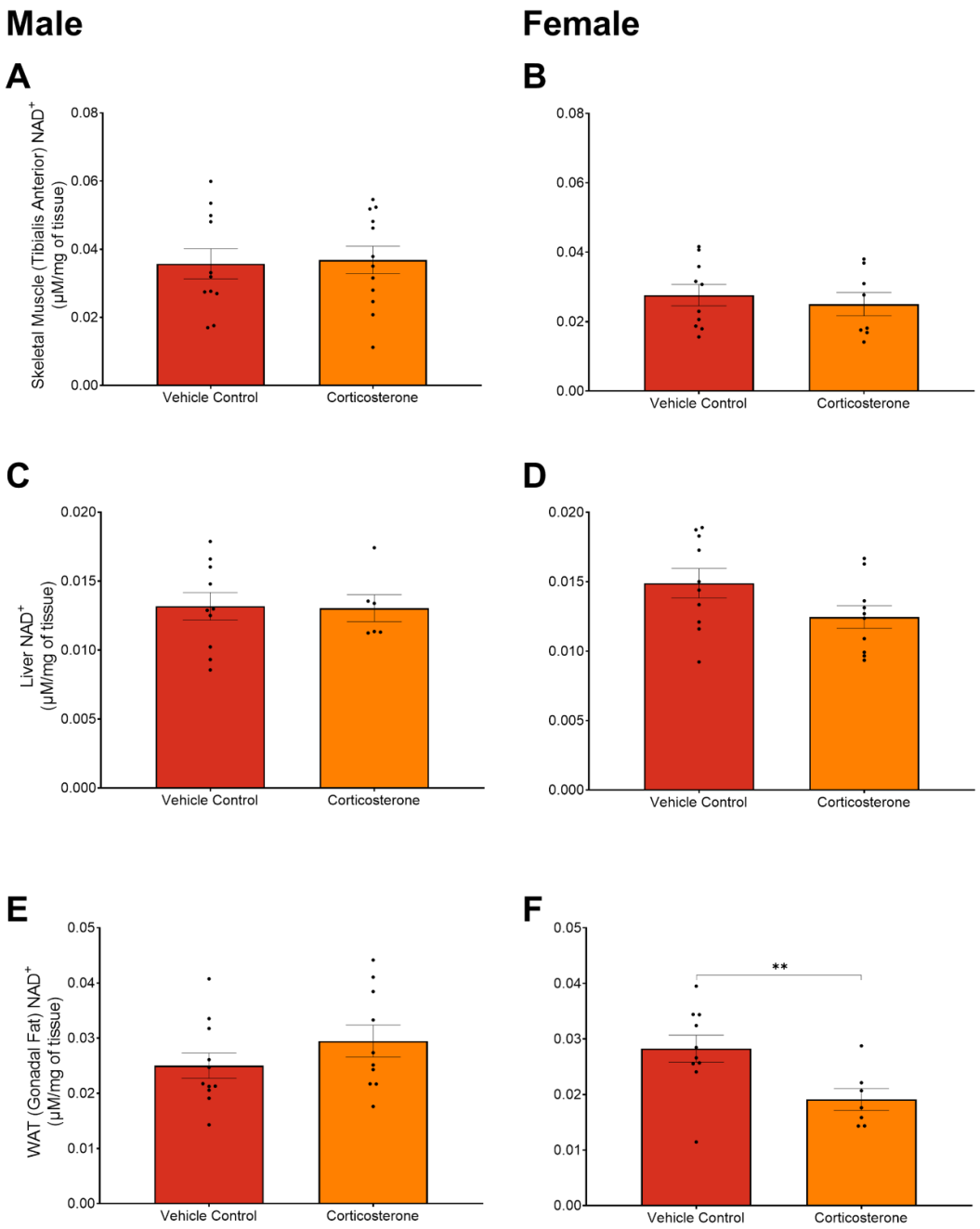

Figure 4.2: NAD^+ content 3 weeks of corticosterone treatment as assessed by NAD^+ fluorescence assay. **A**: Male skeletal muscle NAD^+ content. **B**: Female skeletal muscle NAD^+ content. **C**: Male liver NAD^+ content. **D**: Female liver NAD^+ content. **E**: Male WAT NAD^+ content. F: Female WAT NAD^+ content. Data is presented as mean with individual values ± SD, n=8-12. Significance determined via unpaired t-test. * significantly different to control. *p<.05, ** p<.01, *** p<.001, **** p<.0001. Abbreviations: WAT, white adipose tissue.

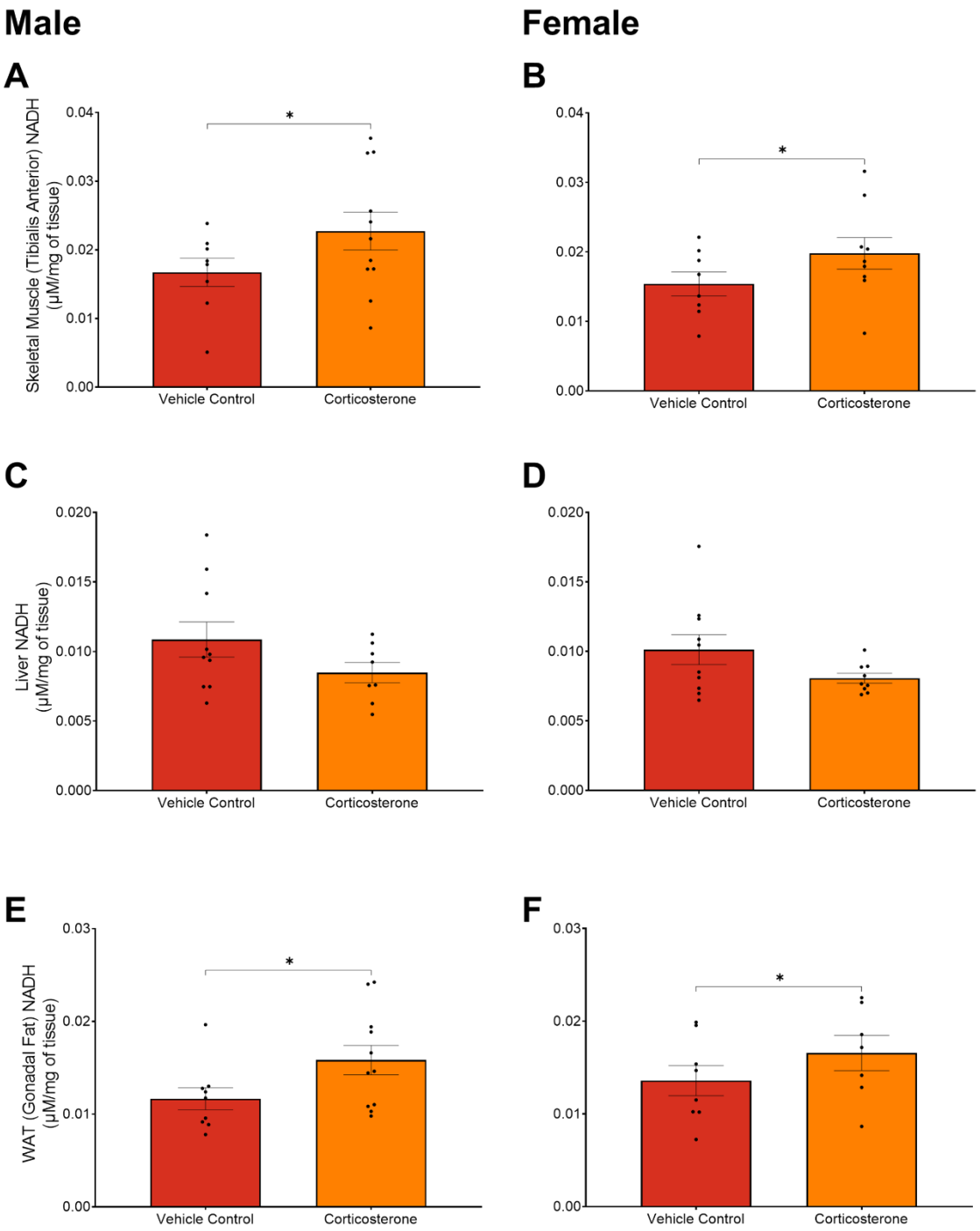

Figure 4.3: NADH content 3 weeks of corticosterone treatment as assessed by NADH fluorescence assay. **A**: Male skeletal muscle NADH content. **B**: Female skeletal muscle NADH content. **C**: Male liver NADH content. **D**: Female liver NADH content. **E**: Male WAT NADH content. F: Female WAT NADH content. Data is presented as mean with individual values ± SD, n=8-12. Significance determined via unpaired t-test. * significantly different to control. *p<.05, ** p<.01, *** p<.001, **** p<.0001. Abbreviations: WAT, white adipose tissue.

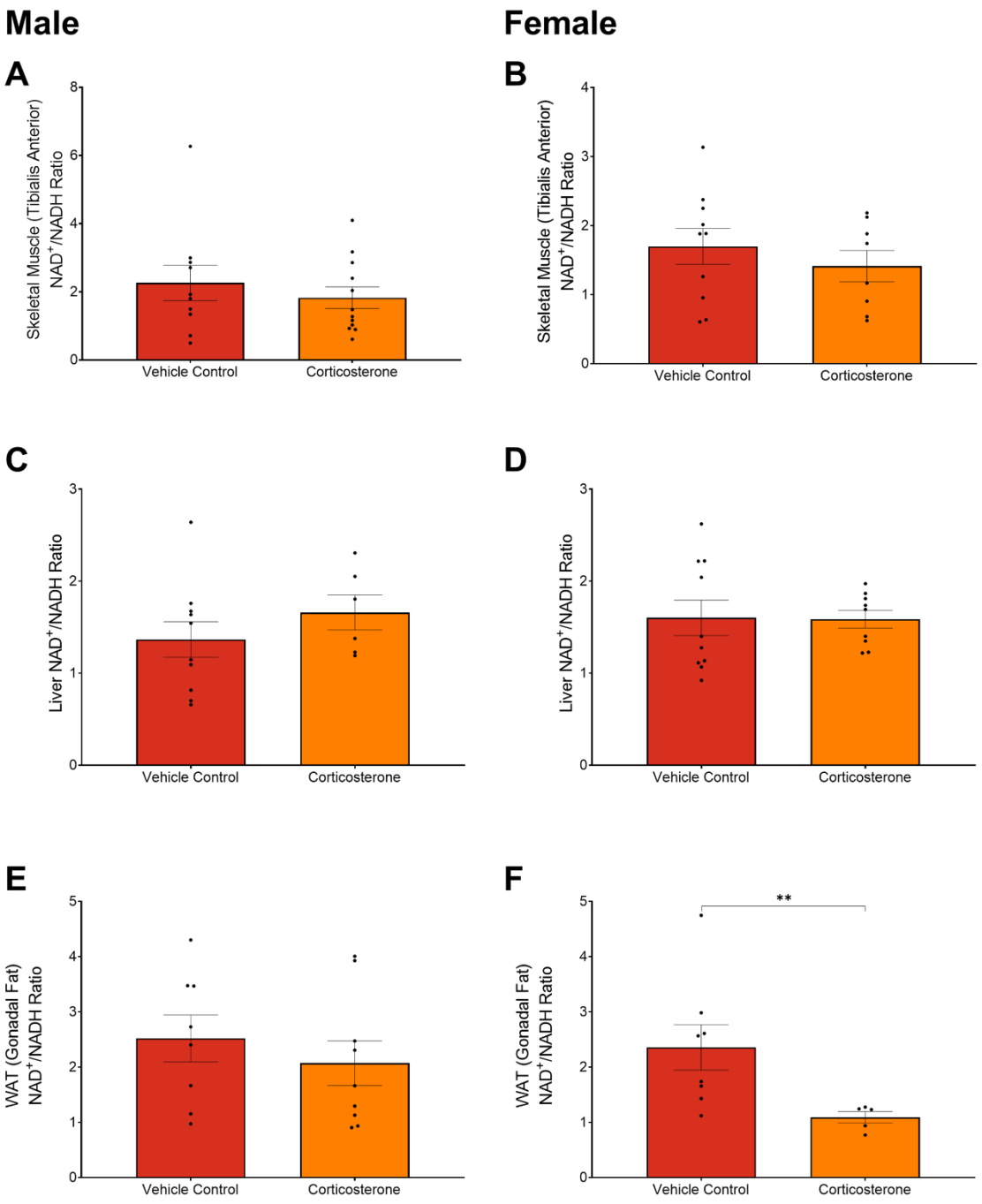

Figure 4.4: NAD^+/NADH ratio following 3 weeks of corticosterone treatment as assessed by NAD^+ fluorescence assay. **A**: Male skeletal muscle NAD^+/NADH ratio. **B**: Female skeletal muscle NAD^+/NADH ratio. **C**: Male liver NAD^+/NADH ratio. **D**: Female liver NAD^+/NADH ratio. **E**: Male WAT NAD^+/NADH ratio. **F**: Female WAT NAD^+/NADH ratio. Data is presented as mean with individual values ± SD, n=12. * significantly different to control. *p<.05, ** p<.01, *** p<.001, **** p<.0001. Abbreviations: WAT, white adipose tissue.

4.3.4 Corticosterone treatment significantly alters gene expression of the NAD^+ biosynthetic network in a gene and tissue specific manner

Following corticosterone treatment the gene expression of NAD^+ biosynthetic enzymes were altered in a tissue specific manner. Within skeletal muscle (quadriceps) only NAMPT and NRK2 expression were altered by corticosterone treatment. The former being elevated, and the latter being decreased in both male and female mice (Fig. 4.5A and B). The expression of all other biosynthetic enzymes was unaffected (Fig. 4.5A and B). MuRF1 expression, assessed as a known control, was also increased by corticosterone treatment (Fig. 5.4A and B), as expected (Morgan et al., 2016a). In the liver of male and female mice the impact of corticosterone was more pronounced. NRK1, NMNAT1, NMNAT3, NADSYN, NAPRT, NADK, QPRT, HAO, KYU, KMO and AFM were all significantly decreased by corticosterone in male and female mice (Fig. 4.6A and B). IDO was significantly decreased in male mice by corticosterone (Fig. 4.6A) and but non-significantly decreased in female mice (Fig. 4.6B). Conversely, PNP was only significantly decreased in female mice by corticosterone (Fig. 4.6B) and non-significantly decreased in male mice (Fig. 4.6A). NAMPT was the only enzyme with unaltered gene expression in male and female liver (Fig. 4.6A and B). In WAT (gonadal) only NMNAT3 was significantly decreased in male and female mice by corticosterone (Fig. 4.7A and B). In males only, NMNAT1 and NADK were also significantly decreased by corticosterone treatment (Fig. 4.7A). The expression of all other enzymes within WAT was unaltered by corticosterone.

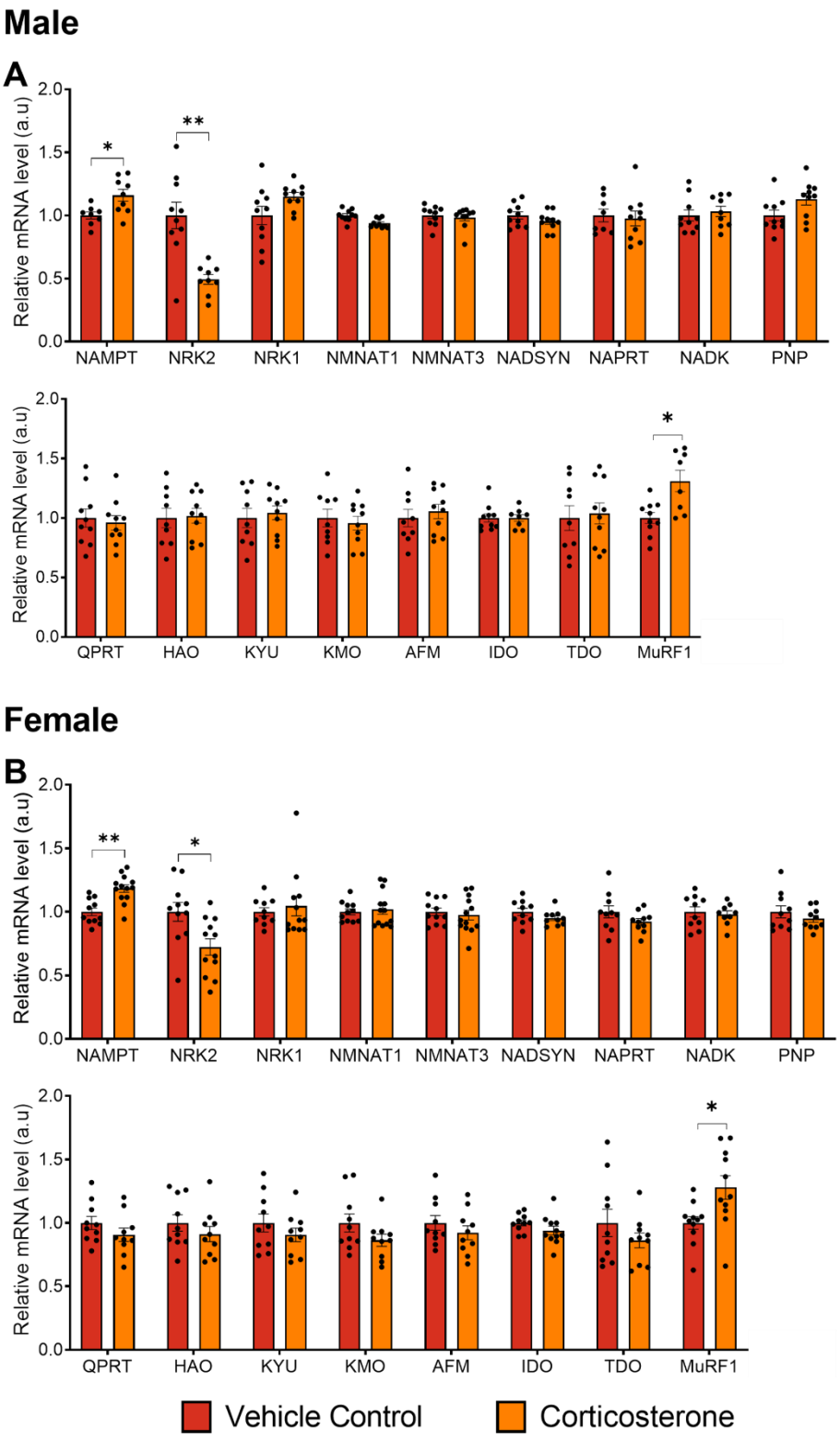

Figure 4.5: Skeletal muscle (quadriceps) NAD^+ biosynthetic gene expression after 3 weeks of corticosterone treatment as assessed by qPCR. **A**: Male NAD^+ biosynthetic gene expression. **B**: Female NAD^+ biosynthetic gene expression. Data is presented as mean with individual values ± SD, n=8-12. Significance determined via individual unpaired t-tests for each gene. * significantly different to control. *p<.05, ** p<.01, *** p<.001, **** p<.0001.

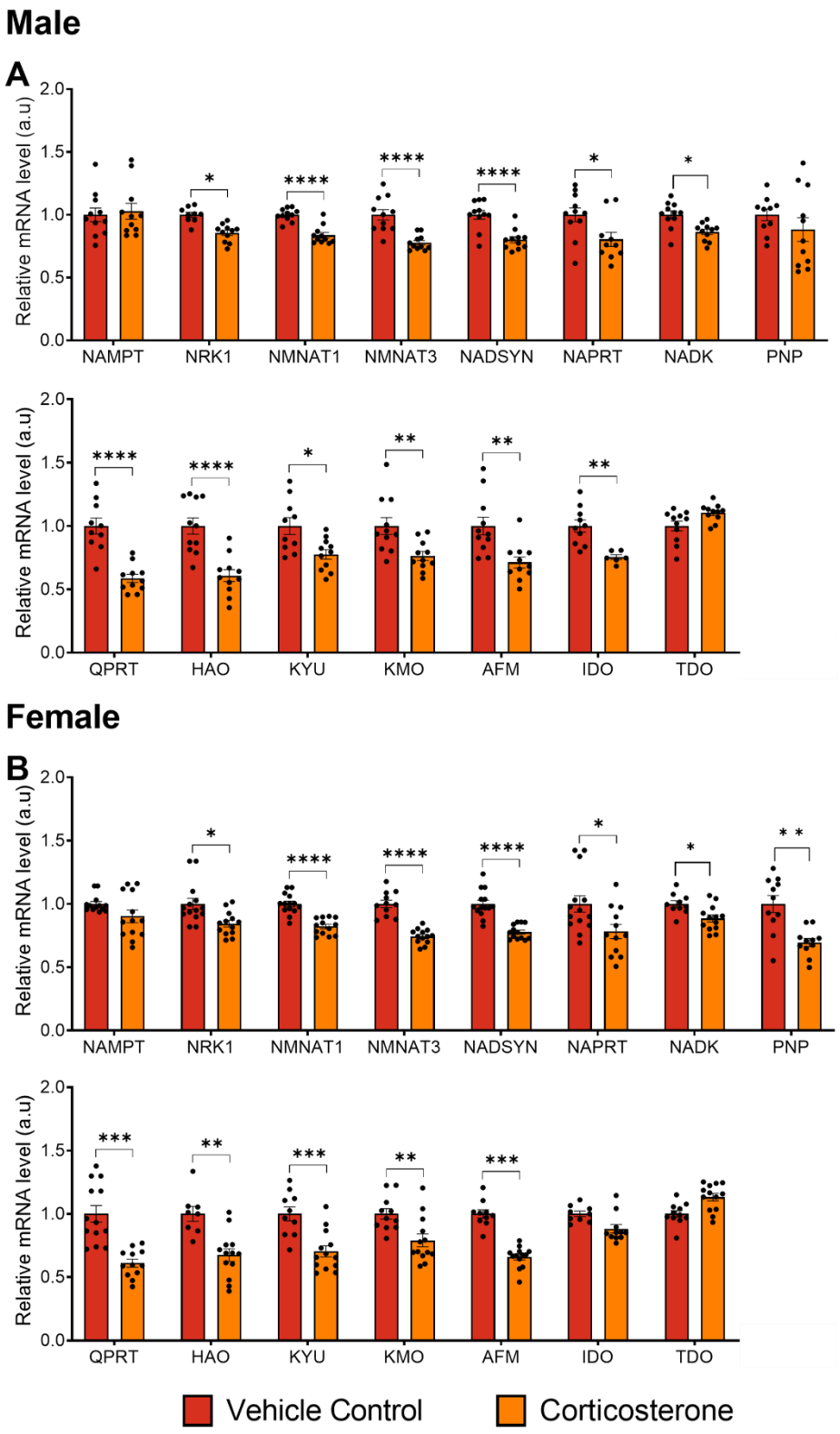

Figure 4.6: Liver NAD^+ biosynthetic gene expression after 3 weeks of corticosterone treatment as assessed by qPCR. **A**: Male NAD^+ biosynthetic gene expression. **B**: Female NAD^+ biosynthetic gene expression. Data is presented as mean with individual values ± SD, n=8-12. Significance determined via individual unpaired t-tests for each gene. * significantly different to control. *p<.05, ** p<.01, *** p<.001, **** p<.0001.

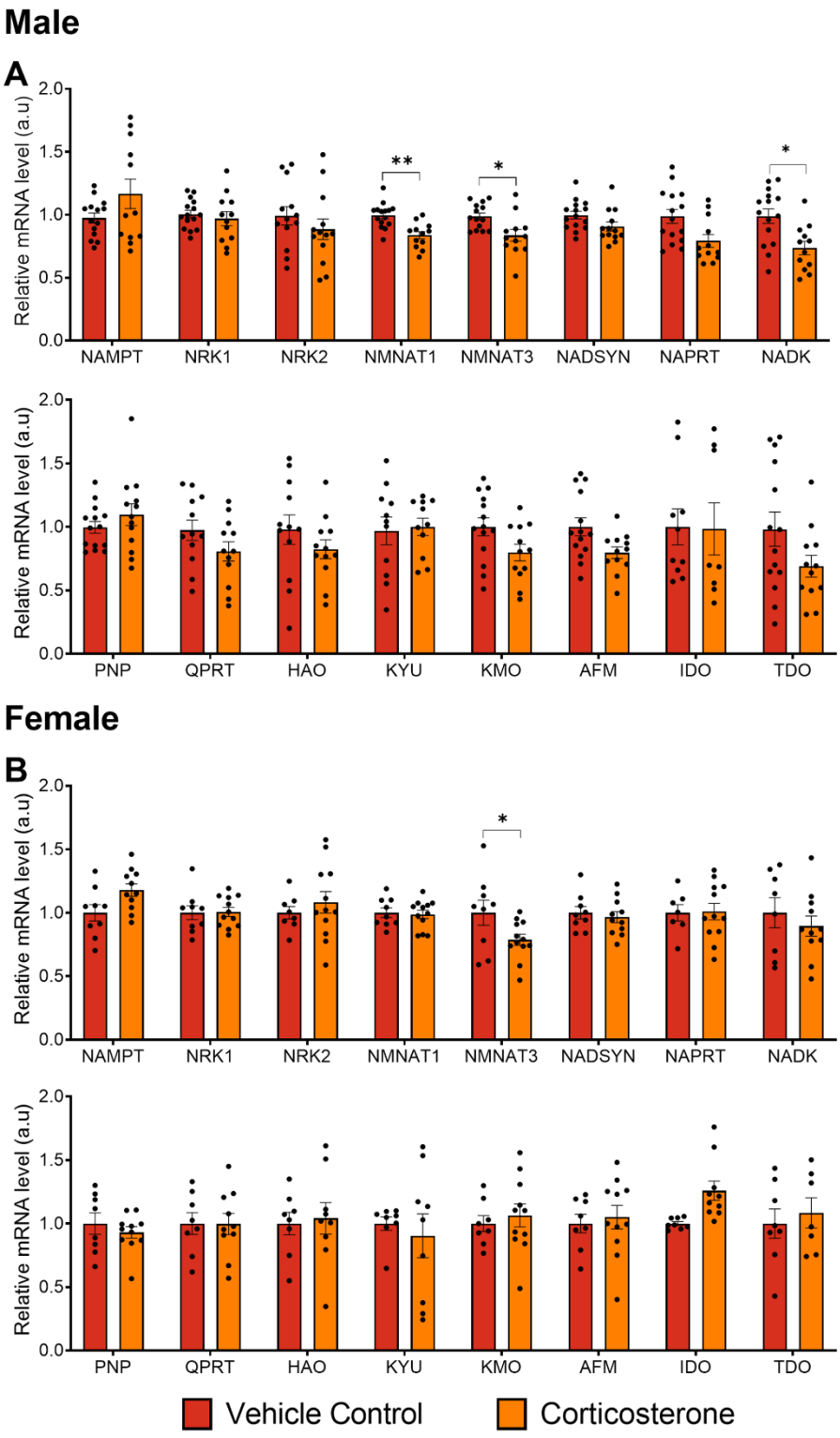

Figure 4.7: WAT NAD^+ biosynthetic gene expression after 3 weeks of corticosterone treatment as assessed by qPCR. **A**: Male NAD^+ biosynthetic gene expression. **B**: Female NAD^+ biosynthetic gene expression. Data is presented as mean with individual values ± SD, n=8-12. Significance determined via individual unpaired t-tests for each gene. * significantly different to control. *p<.05, ** p<.01, *** p<.001, **** p<.0001. Abbreviations: WAT, white adipose tissue.

4.3.5 Nicotinamide riboside supplementation partially alters some of the effects of corticosterone treatment on the NAD^+ metabolome

Within male and female skeletal muscle (tibialis anterior) concurrent treatment with NR, alongside corticosterone, as well as NR alone did not significantly alter NAD^+ content compared to both the control or corticosterone (Fig. 4.8A and B). However, surprisingly both NR alone and in combination with corticosterone did show a downward trend with regards to NAD^+ content. Unfortunately, concurrent corticosterone and NR treatment could not be assessed in male skeletal muscle due to loss of samples. Within male and female livers NR surprisingly did not alter NAD^+ content compared to the control or corticosterone (Fig. 4.8C and D). Concurrent NR and corticosterone treatment also did not differ from control or corticosterone in male or female livers (Fig. 4.8C and D). Finally, within male and female WAT (gonadal) NR and concurrent NR and corticosterone treatment decreased NAD^+ content compared to controls and corticosterone (Fig. 4.8E and F). In female WAT the combination of NR and corticosterone decreased NAD^+ further than corticosterone alone (Fig. 4.8F).

As for NADH, assessed by a NADH fluorescence assay, both NR treatment alone and concurrent NR and corticosterone treatment significantly reduced NADH content compared to the vehicle control and corticosterone in male and female skeletal muscle (tibialis anterior) (Fig. 4.9A and B). In male and female livers NR alone, or in combination with corticosterone did not alter NADH content compared to the control or corticosterone treated mice (Fig. 4.9C and D). Within male and female WAT (gonadal) the effect of NR alone or in combination with corticosterone on NADH content was the same as in skeletal muscle (Fig. 4.9E and F).

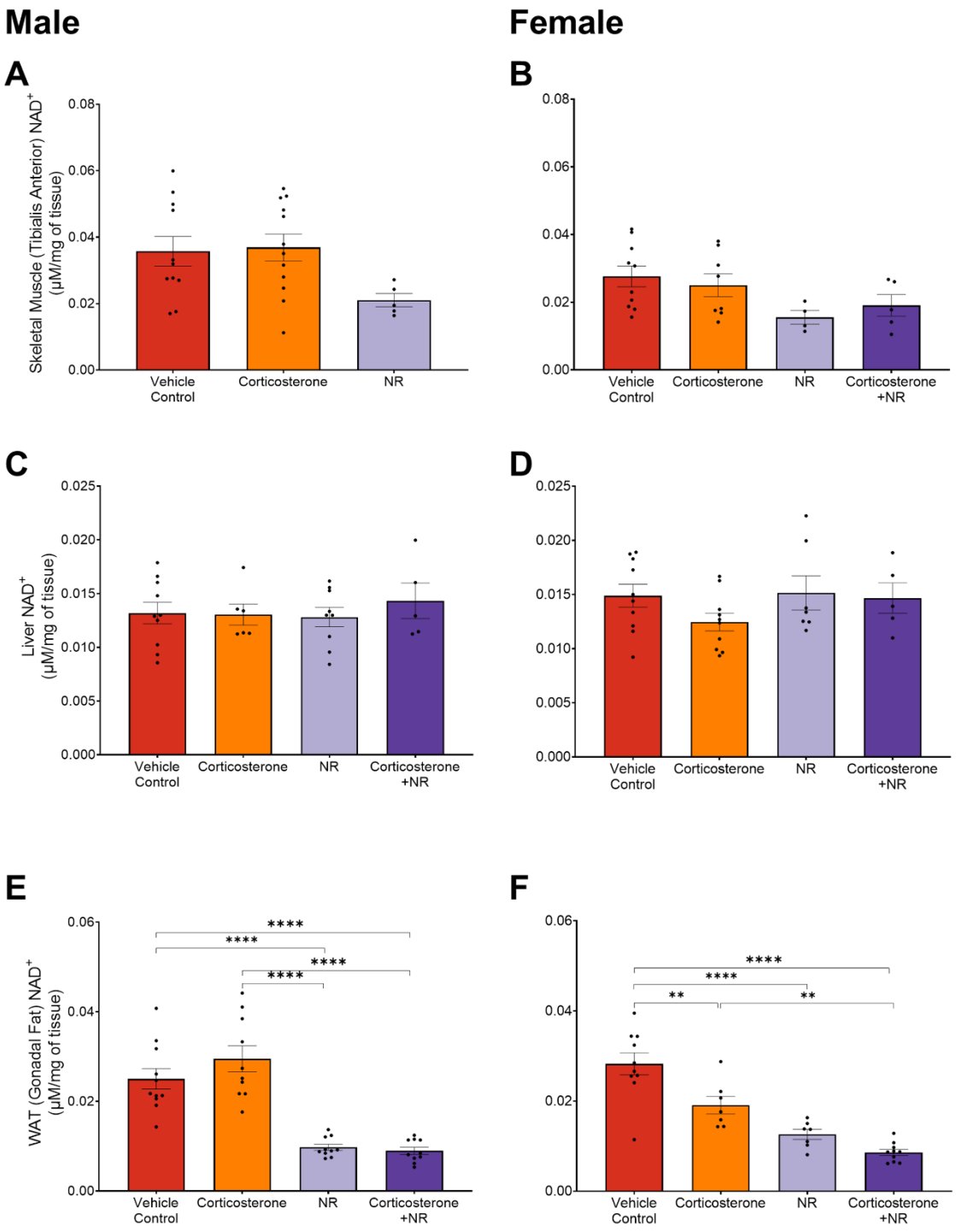

Figure 4.8: NAD^+ content 3 weeks of corticosterone and nicotinamide riboside treatment as assessed NAD^+ fluorescence assay. **A**: Male skeletal muscle NAD^+ content. **B**: Female skeletal muscle NAD^+ content. **C**: Male liver NAD^+ content. **D**: Female liver NAD^+ content. **E**: Male WAT NAD^+ content. F: Female WAT NAD^+ content. Data is presented as mean with individual values ± SD, n=4-12. Significance determined via two-way ANOVA. * significantly different to control. *p<.05, ** p<.01, *** p<.001, **** p<.0001. Abbreviations: WAT, white adipose tissue.

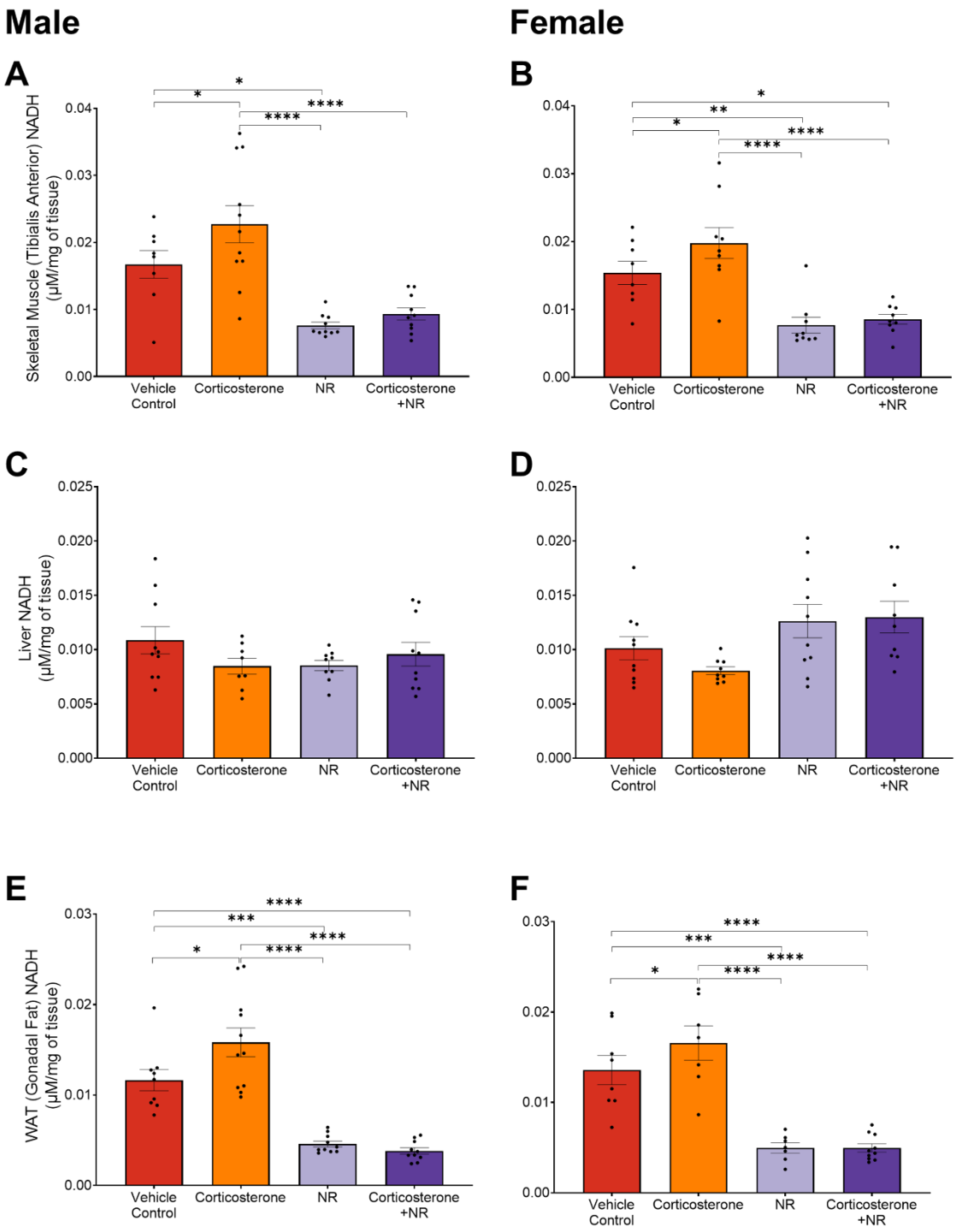

Figure 4.9: NADH content 3 weeks of corticosterone and nicotinamide riboside treatment as assessed by NADH fluorescence assay. **A**: Male skeletal muscle NAD^+ content. **B**: Female skeletal muscle NAD^+ content. **C**: Male liver NAD^+ content. **D**: Female liver NAD^+ content. **E**: Male WAT NAD^+ content. F: Female WAT NAD^+ content. Data is presented as mean with individual values ± SD, n=8-12. Significance determined via two-way ANOVA. * significantly different to control. *p<.05, ** p<.01, *** p<.001, **** p<.0001. Abbreviations: WAT, white adipose tissue.

Concurrent NR treatment alongside corticosterone did not alter the effect of corticosterone on the gene expression of the NAD^+ biosynthetic network in male or female skeletal muscle (quadriceps) (Fig. 4.10A and B). NR treatment alone did not differ from the control in male and females (Fig. 4.10A and B) apart from NRK1 expression which was elevated in male skeletal muscle (Fig. 4.10A). Within male and female liver, the effect of concurrent NR and corticosterone treatment was the same as in skeletal muscle. NR did not alter the effects of corticosterone on the gene expression of the NAD^+ biosynthetic network (Fig 4.11A and B). However, in male liver concurrent NR and corticosterone treatment decreased PNP expression, an effect not seen with corticosterone treatment alone (Fig. 4.11A). Like skeletal muscle NR treatment alone did not differ from control in both male and female liver, apart from NADSYN and NAPRT which had decreased gene expression as a result of NR treatment in male mice (Fig. 4.11A and B). Finally, within male and female WAT (gonadal), concurrent NR treatment with corticosterone did not alter the gene expression effects of corticosterone (Fig. 4.12A and B). NR treatment alone did not differ from control treatment in male or female WAT (Fig. 4.12A and B).

4.3.6 Nicotinamide riboside supplementation does not alter the phenotype induced by corticosterone treatment

Following concurrent NR and corticosterone treatment the phenotype induced by corticosterone alone was not altered. Tissue and bodyweight analysis revealed that fat accumulation, skeletal muscle atrophy/reduced lean body mass accrual and spleen atrophy were all still present in female mice (Fig. 4.13H-L) despite NR treatment alongside corticosterone. In male mice skeletal muscle atrophy/reduced lean body mass accrual and

spleen atrophy were also not prevented by simultaneous NR and corticosterone treatment (Fig. 4.13C-F). However, fat accumulation was attenuated by NR treatment alongside corticosterone (Fig. 4.13B). Therefore, as with corticosterone treatment alone, female mice treated with both corticosterone and NR accumulated significantly more fat, resulting in significantly greater bodyweight gain (Fig. 4.13G). NR treatment alone did not differ from control treatment in male or female mice (Fig. 4.13). Hepatic TAG accumulation, assessed via a TAG assay and H&E stain, seen in male and female mice treated with corticosterone was also not prevented by simultaneous NR treatment (Fig. 4.14A-D). NR treatment alone did not differ to control treated mice.

4.3.7 Nicotinamide riboside did not alter the effects of corticosterone on energy expenditure

NR treatment, alongside corticosterone, did not prevent the effects of corticosterone on EE in male and female mice (Fig. 4.15). EE remained elevated, compared to control, following concurrent corticosterone and NR treatment and did not differ from corticosterone treatment alone. NR treatment alone did not differ to control. Linear regression and subsequent ANCOVA also determined no significant differences in slope angle between treatments revealing no significant effect of body weight on EE (Fig. 4.21A and C).

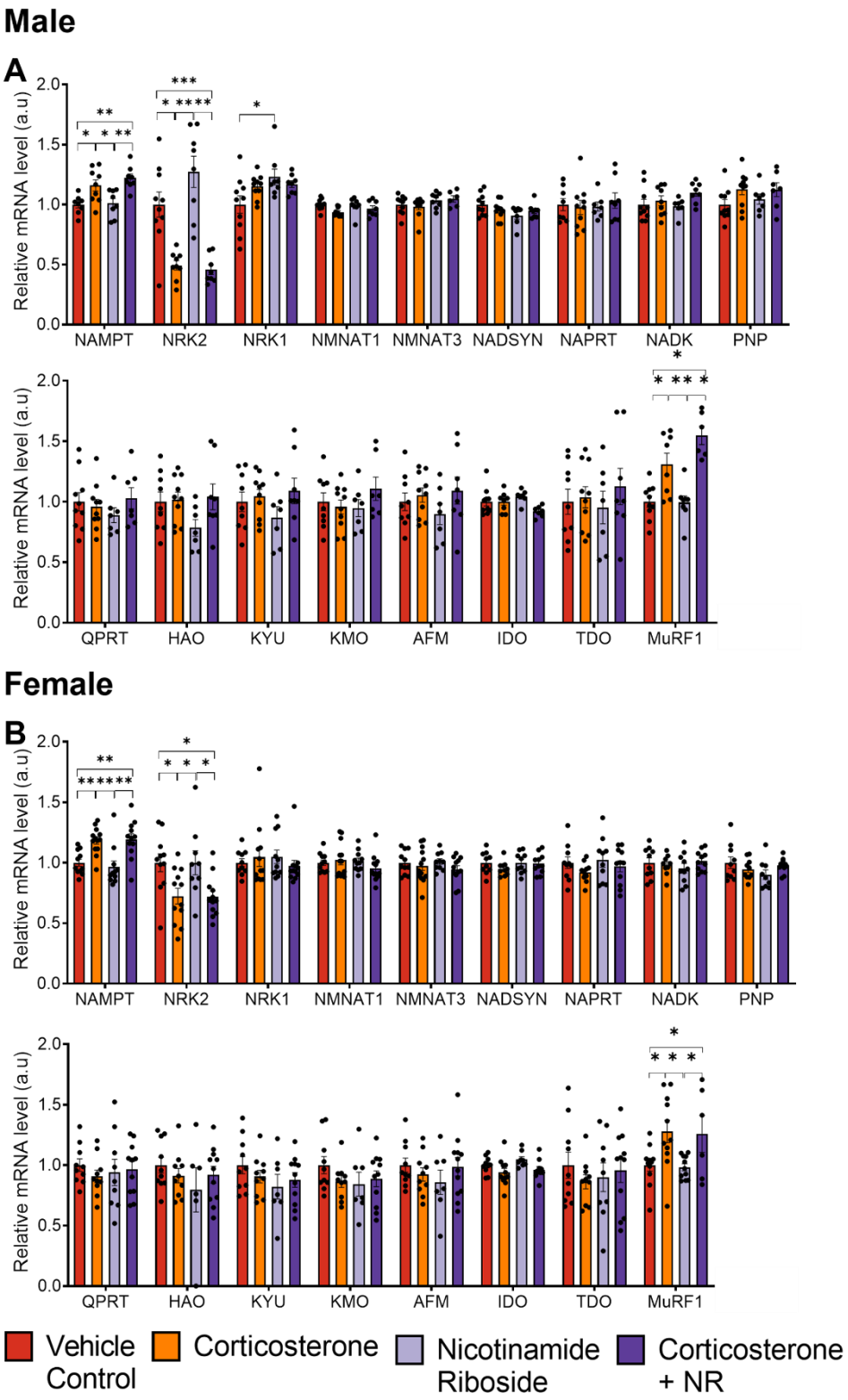

Figure 4.10: Skeletal muscle (quadriceps) NAD^+ biosynthetic gene expression after 3 weeks of corticosterone and nicotinamide riboside treatment as assessed by qPCR. **A**: Male NAD^+ biosynthetic gene expression. **B**: Female NAD^+ biosynthetic gene expression. Data is presented as mean with individual values ± SD, n=8-12. Significance determined via two-way ANOVA for each gene. * significantly different to control. *p<.05, ** p<.01, *** p<.001, **** p<.0001.

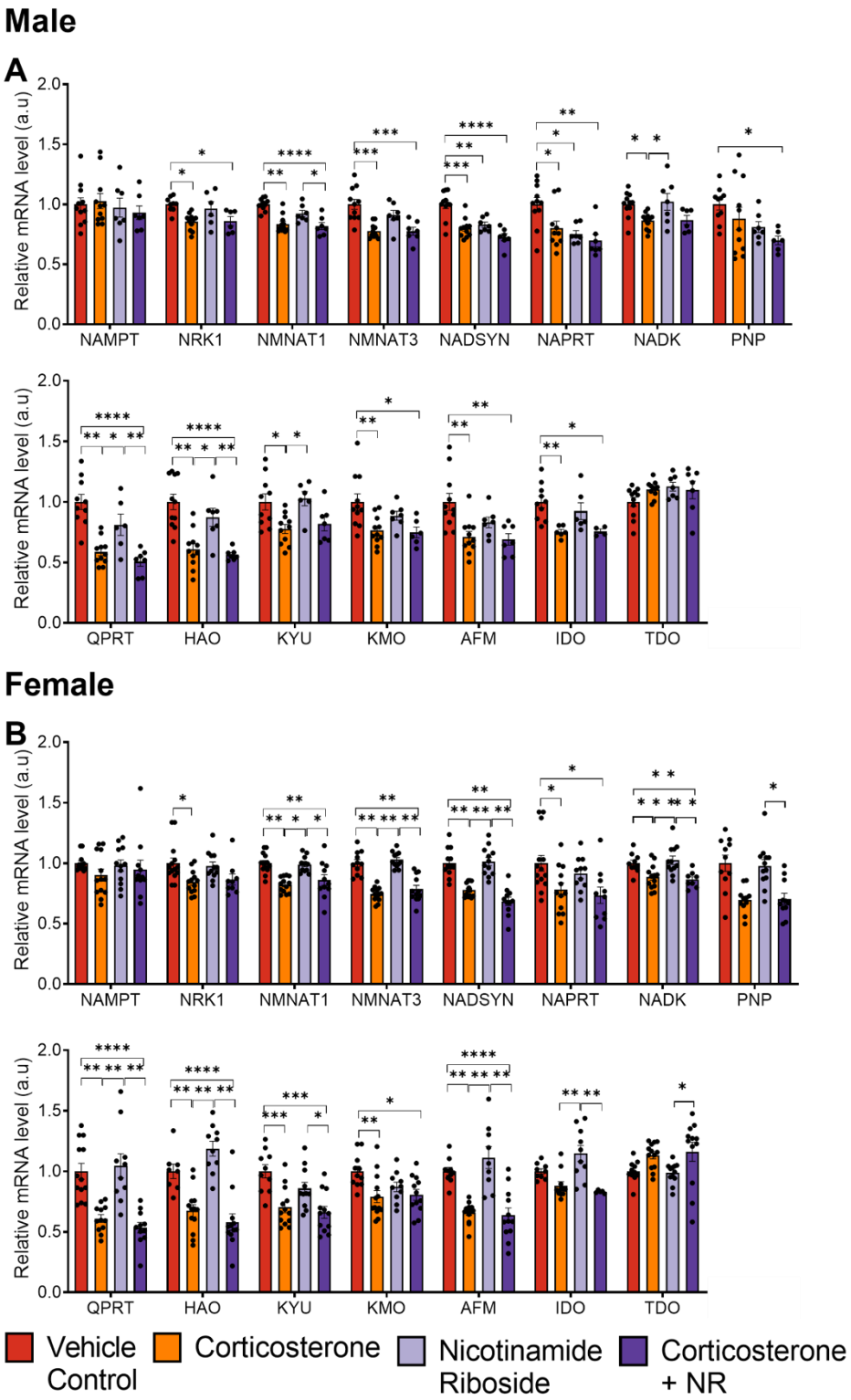

Figure 4.11: Liver NAD^+ biosynthetic gene expression after 3 weeks of corticosterone and nicotinamide riboside treatment as assessed by qPCR. **A**: Male NAD^+ biosynthetic gene expression. **B**: Female NAD^+ biosynthetic gene expression. Data is presented as mean with individual values ± SD, n=8-12. Significance determined via two-way ANOVA for each gene. * significantly different to control. *p<.05, ** p<.01, *** p<.001, **** p<.0001.

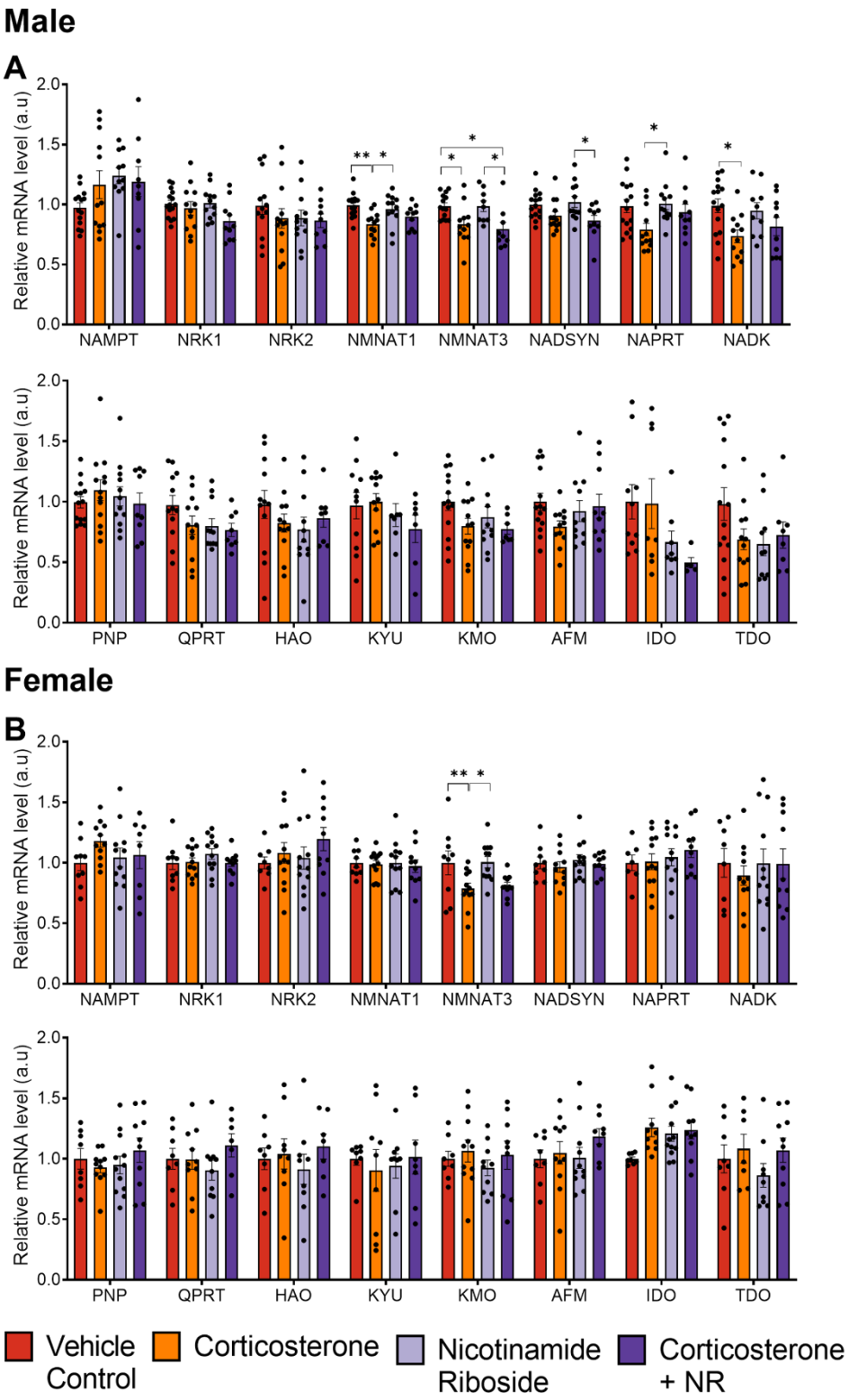

Figure 4.12: WAT NAD^+ biosynthetic gene expression after 3 weeks of corticosterone and nicotinamide riboside treatment as assessed by qPCR. **A**: Male NAD^+ biosynthetic gene expression. **B**: Female NAD^+ biosynthetic gene expression. Data is presented as mean with individual values ± SD, n=8-12. Significance determined via two-way ANOVA for each gene. * significantly different to control. *p<.05, ** p<.01, *** p<.001, **** p<.0001. . Abbreviations: WAT, white adipose tissue.

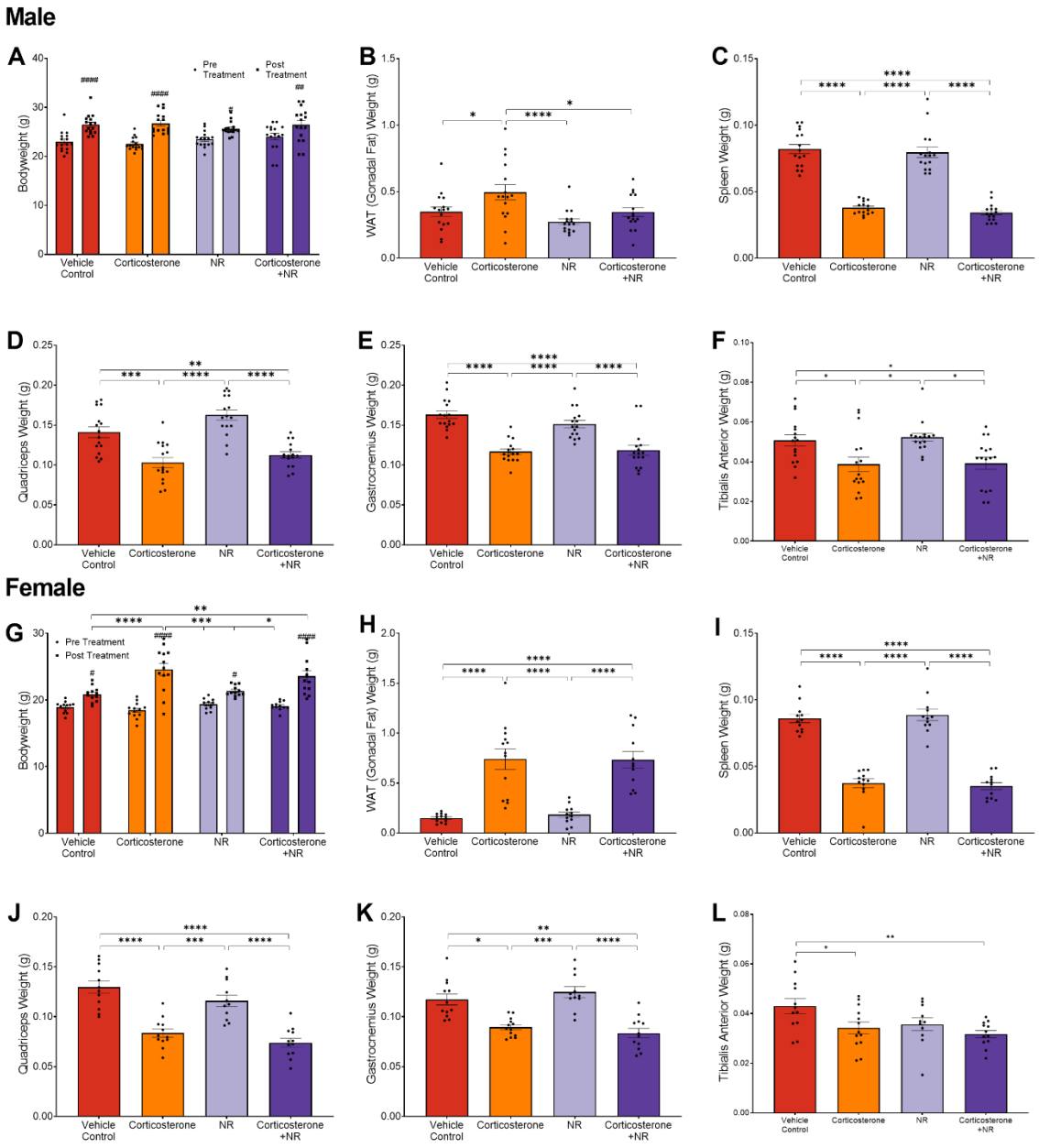

Figure 4.13: Bodyweight and tissue weight following 3 weeks of corticosterone and nicotinamide riboside treatment. **A**: Male bodyweight. **B**: Male WAT (gonadal fat) weight. **C**: Male spleen weight. **D**: Male quadriceps weight. **E**: Male gastrocnemius weight. **F**: Male tibialis anterior weight. **G**: Female bodyweight. **H**: Female WAT (gonadal fat) weight. **I**: Female spleen weight. **J**: Female quadriceps weight. **K**: Female gastrocnemius weight. **L**: Female tibialis anterior weight. Data is presented as mean with individual values ± SD, n=12-16. Significance determined via two-way ANOVA. * significantly different, # significantly different to pre. *p<.05, ** p<.01, *** p<.001, **** p<.0001. Abbreviations: WAT, white adipose tissue.

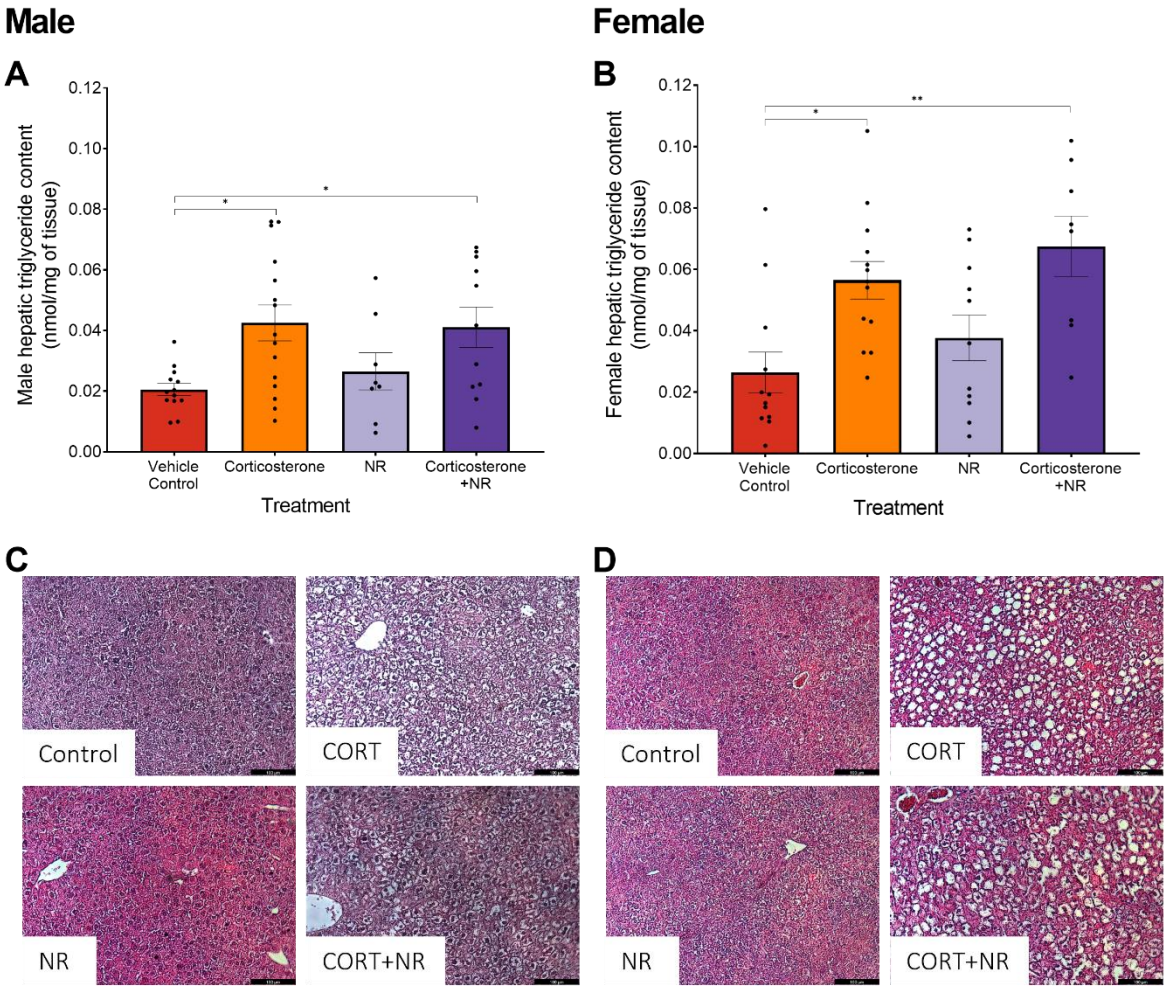

Figure 4.14: Hepatic TAG content after 3 weeks of corticosterone and nicotinamide riboside treatment as assessed by TAG assay and H&E staining. **A**: TAG content of male livers. **B**: TAG content of female livers. **C**: Male H&E stained livers. **D**: Female H&E stained livers. Data is presented as mean with individual values ± SD, n=8-12. Significance determined via two-way ANOVA. * significantly different to control. *p<.05, ** p<.01, *** p<.001, **** p<.0001. Abbreviations: TAG, triglyceride; H&E, haematoxylin and eosin; CORT, corticosterone.

4.3.8 Nicotinamide riboside did not significantly alter the effects of corticosterone on the respiratory exchange ratio

NR treatment, alongside corticosterone, did not significantly alter the effects of corticosterone on the RER in male or female mice (Fig. 4.16). However, in female mice it did

slightly reduce RER compared to corticosterone alone during the day and night, however this difference was non-significant and RER was still significantly different to control (Fig. 4.16C and D). NR treatment alone did not differ to control. Linear regression and subsequent ANCOVA also determined no significant differences in slope angle between treatments revealing no significant effect of body weight on the RER (Fig. 4.21B and D).

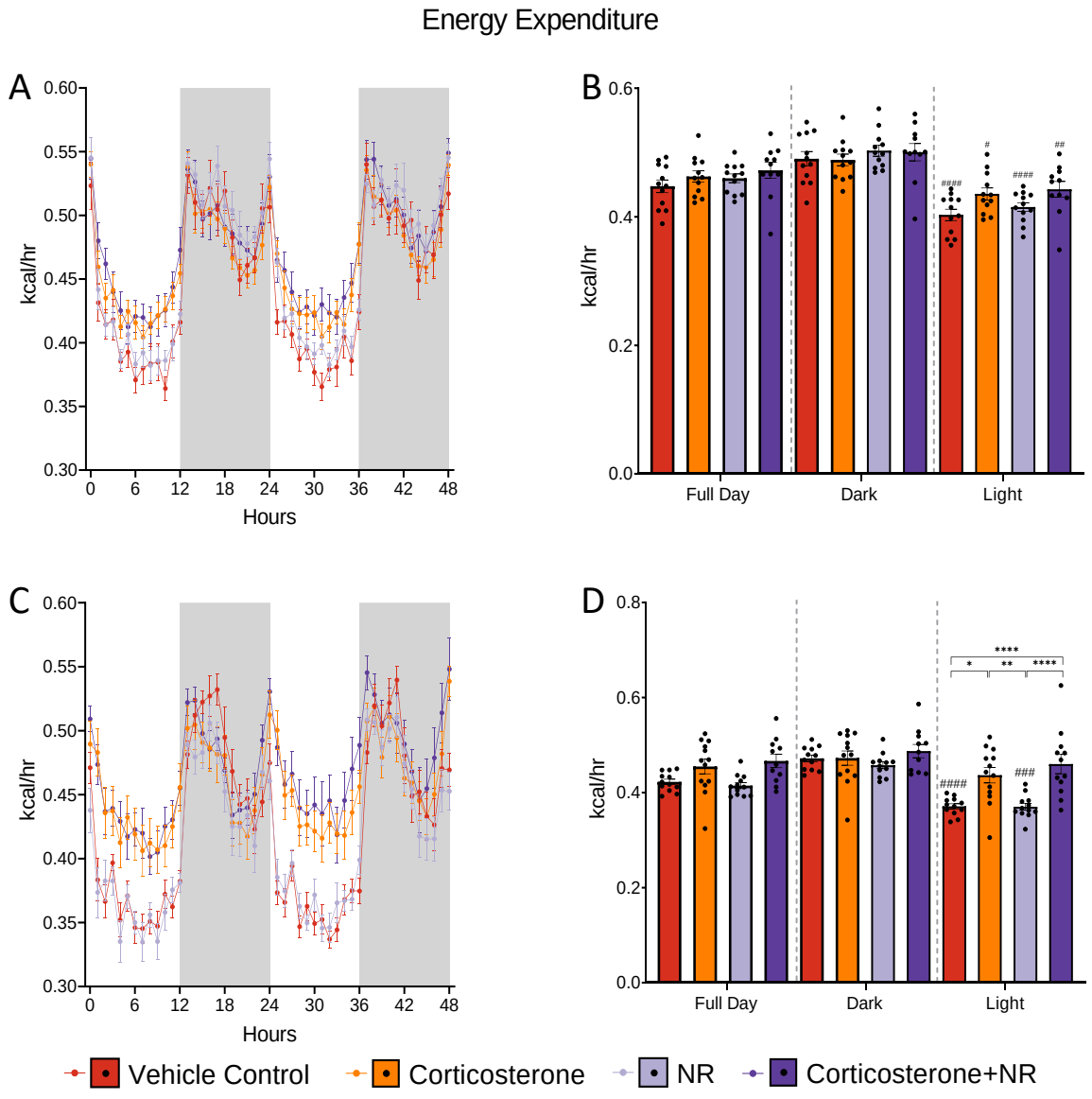

Figure 4.15: Energy expenditure following 3 weeks of corticosterone and NR treatment. **A**: Male hourly energy expenditure. **B**: Male average energy expenditure. **C**: Female hourly energy expenditure. **D**: Female average energy expenditure. Line graphs are presented as mean ± SD, n=9-12. Bar charts are presented as mean with individual values ± SD, n=9-12. Significance determined via two-way ANOVA. * significantly different, # significantly different to dark. *p<.05, ** p<.01, *** p<.001, **** p<.0001.

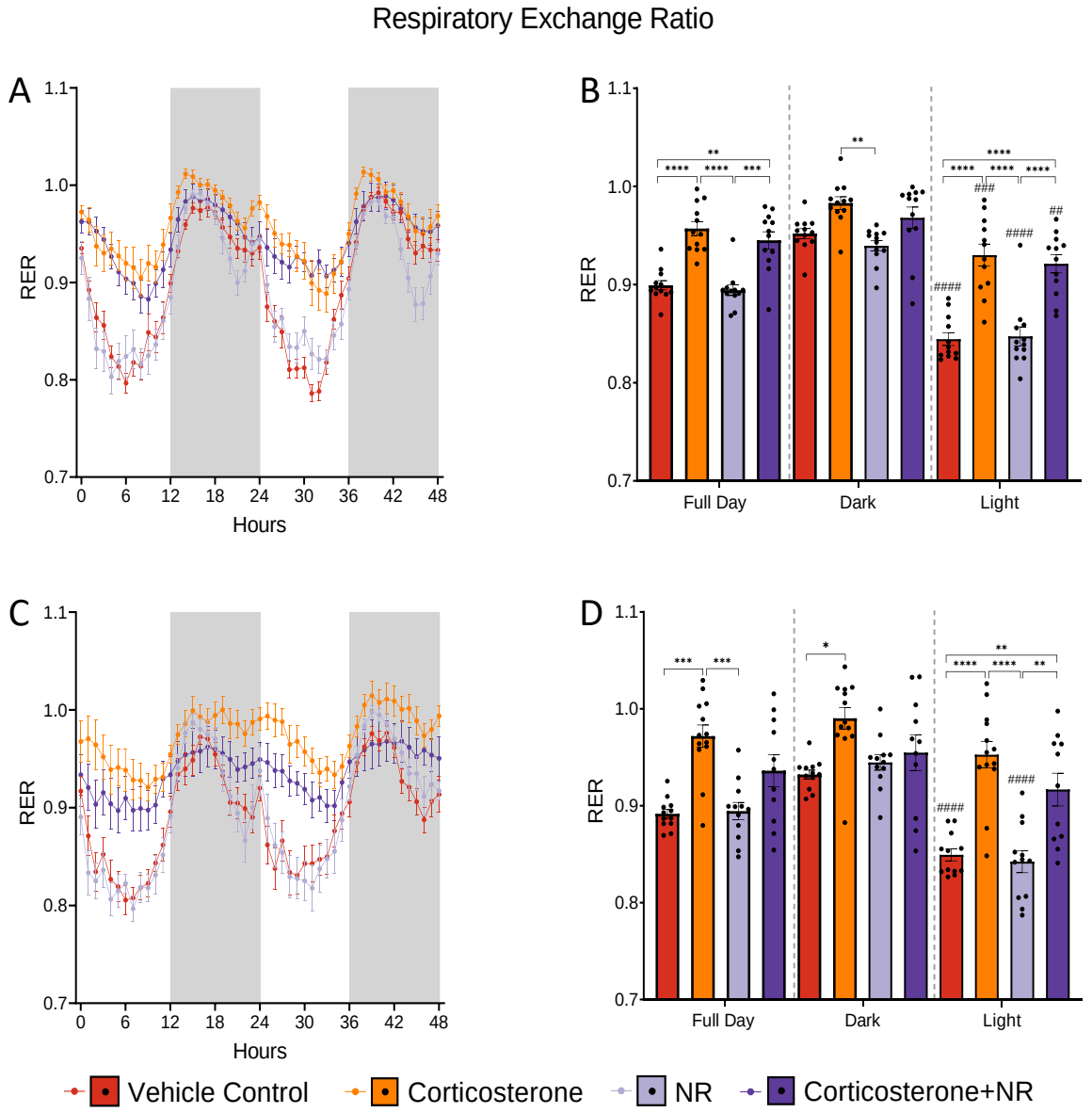

Figure 4.16: Respiratory exchange ratio following 3 weeks of corticosterone and NR treatment. **A**: Male hourly RER. **B**: Male average RER. **C**: Female hourly RER. **D**: Female average RER. Line graphs are presented as mean ± SD, n=11-12. Bar charts are presented as mean with individual values ± SD, n=11-12. Significance determined via two-way ANOVA. * significantly different, # significantly different to dark. *p<.05, ** p<.01, *** p<.001, **** p<.0001.

4.3.9 Nicotinamide riboside did not significantly alter the effects of corticosterone on oxygen consumption or carbon dioxide production

NR treatment, alongside corticosterone, did not prevent the effects of corticosterone on oxygen consumption or carbon dioxide production in male and female mice (Fig. 4.17 and 4.18). Both remained elevated, compared to control, following concurrent corticosterone and NR treatment and did not differ from corticosterone treatment alone. NR treatment alone did not differ to control. Linear regression and subsequent ANCOVA also determined no significant differences in slope angle between treatments revealing no significant effect of body weight on oxygen consumption or carbon dioxide production (Fig. 4.21E-H).

4.3.10 Nicotinamide riboside did not prevent corticosterone induced hyperphagia or polydipsia

NR treatment, alongside corticosterone, did not prevent corticosterone induced hyperphagia (Fig. 4.19A and B) and polydipsia (Fig. 4.20A and B) in male mice. However, in female mice corticosterone and NR treatment did result in a significant decrease in water intake, during the night, compared to corticosterone alone (Fig. 4.20C and D). Whilst water consumption was decreased it remained non-significantly elevated compared to control. Corticosterone induced hyperphagia was not prevented by simultaneous NR treatment in female mice (Fig. 4.20C and D). NR treatment alone did not differ to control. Linear regression and subsequent ANCOVA also determined no significant differences in slope angle between treatments revealing no significant effect of body weight on food or water intake (Fig. 4.21I-L).

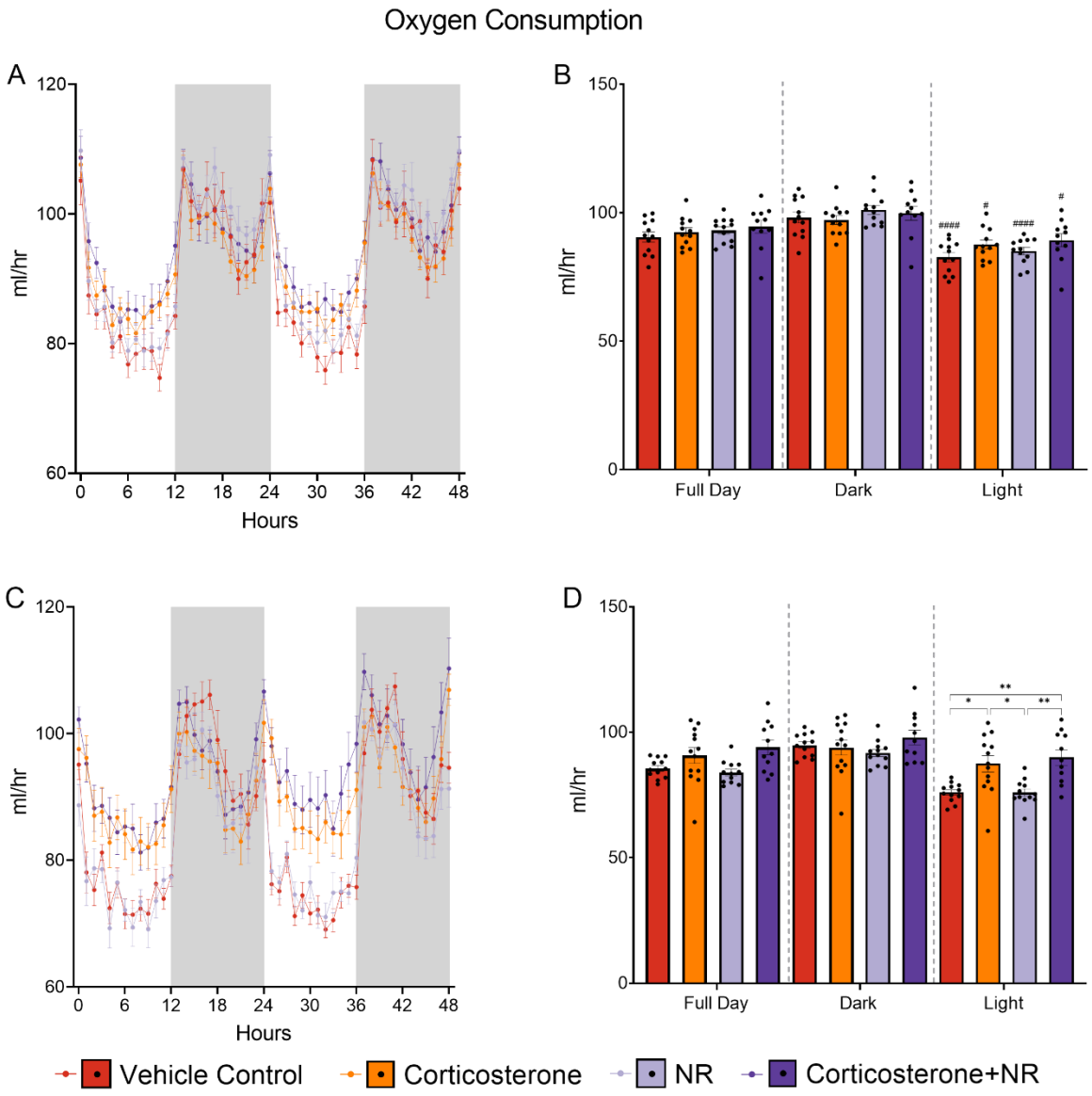

Figure 4.17: Oxygen consumption following 3 weeks of corticosterone and NR treatment. **A**: Male hourly oxygen consumption. **B**: Male average oxygen consumption. **C**: Female hourly oxygen consumption. **D**: Female average oxygen consumption. Line graphs are presented as mean ± SD, n=11-12. Bar charts are presented as mean with individual values ± SD, n=11-12. Significance determined via two-way ANOVA. * significantly different to control, # significantly different to dark. *p<.05, ** p<.01, *** p<.001, **** p<.0001.

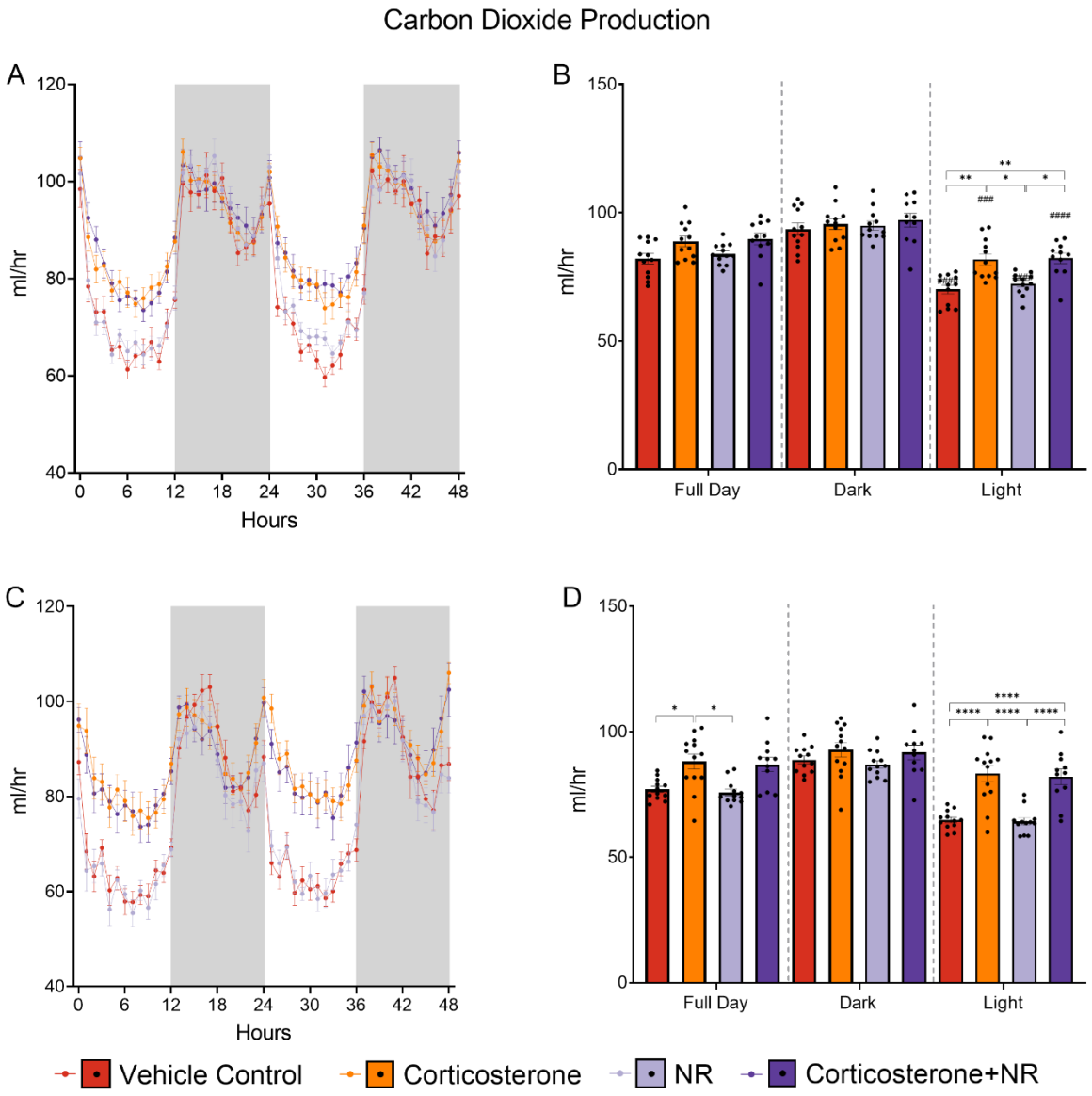

Figure 4.18: Carbon dioxide production following 3 weeks of corticosterone and NR treatment. **A**: Male hourly carbon dioxide production. **B**: Male average carbon dioxide production. **C**: Female hourly carbon dioxide production. **D**: Female average carbon dioxide production. Line graphs are presented as mean ± SD, n=11-12. Bar charts are presented as mean with individual values ± SD, n=11-12. Significance determined via two-way ANOVA. * significantly different to control, # significantly different to dark. *p<.05, ** p<.01, *** p<.001, **** p<.0001.

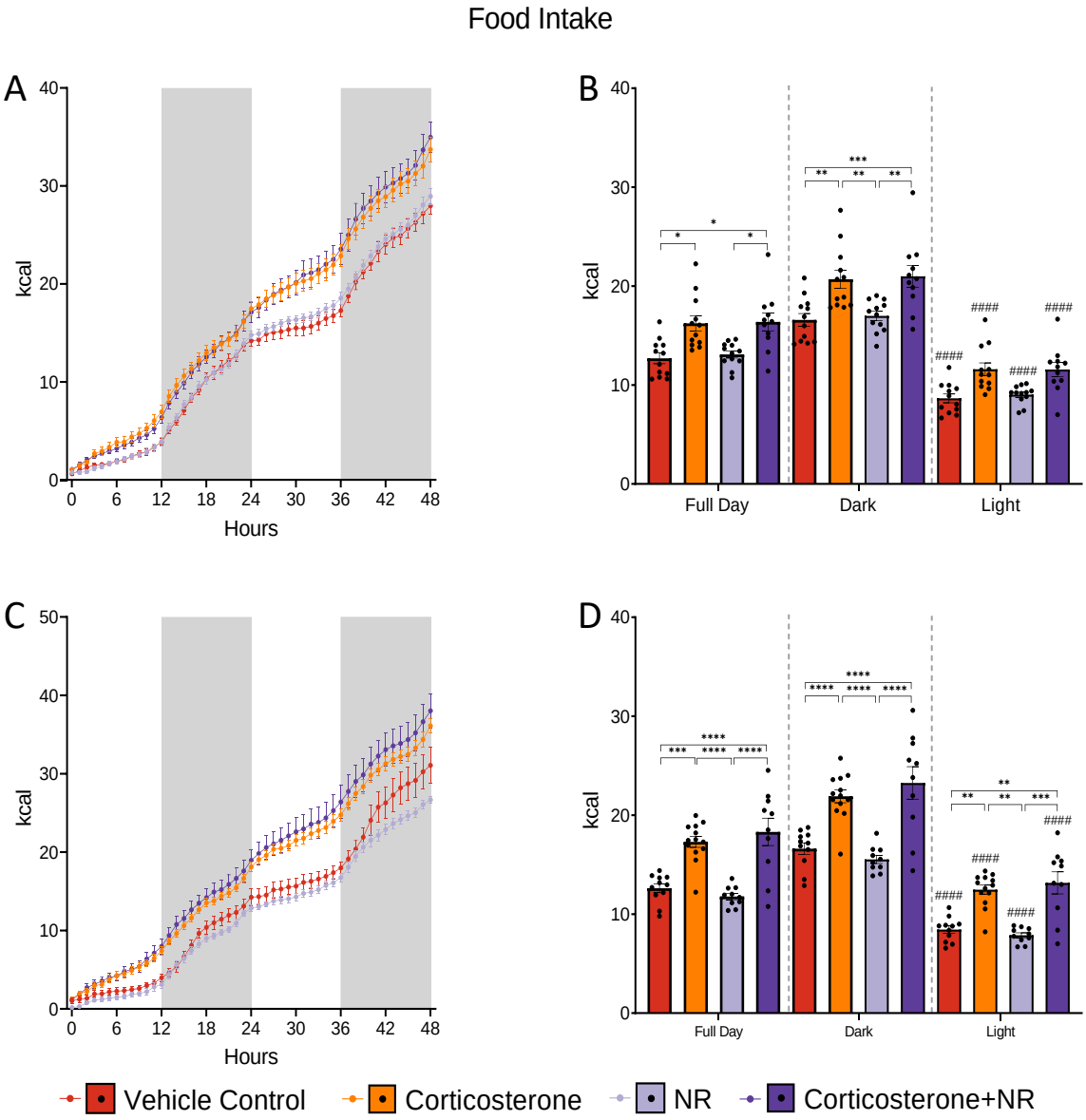

Figure 4.19: Food intake following 3 weeks of corticosterone and NR treatment. **A**: Male cumulative hourly food intake. **B**: Male average food intake. **C**: Female cumulative hourly food intake. **D**: Female average food intake. Line graphs are presented as mean ± SD, n=10-12. Bar charts are presented as mean with individual values ± SD, n=10-12. Significance determined via two-way ANOVA. * significantly different, # significantly different to dark. *p<.05, ** p<.01, *** p<.001, **** p<.0001.

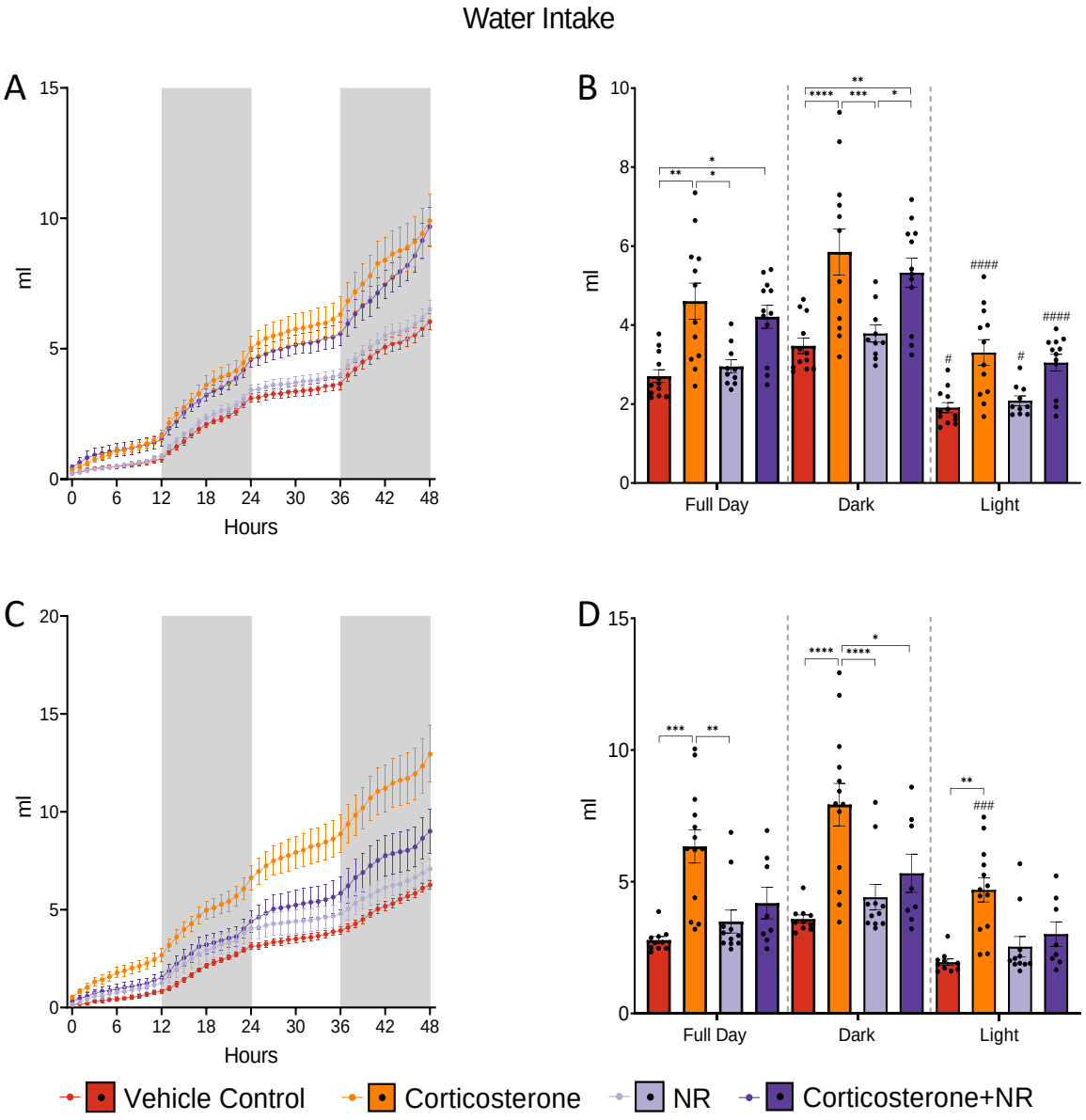

Figure 4.20: Water intake following 3 weeks of corticosterone and NR treatment. **A**: Male cumulative hourly water intake. **B**: Male average water intake. **C**: Female cumulative hourly water intake. **D**: Female average water intake. Line graphs are presented as mean ± SD, n=11-12. Bar charts are presented as mean with individual values ± SD, n=11-12. Significance determined via two-way ANOVA. * significantly different, # significantly different to dark. *p<.05, ** p<.01, *** p<.001, **** p<.0001.

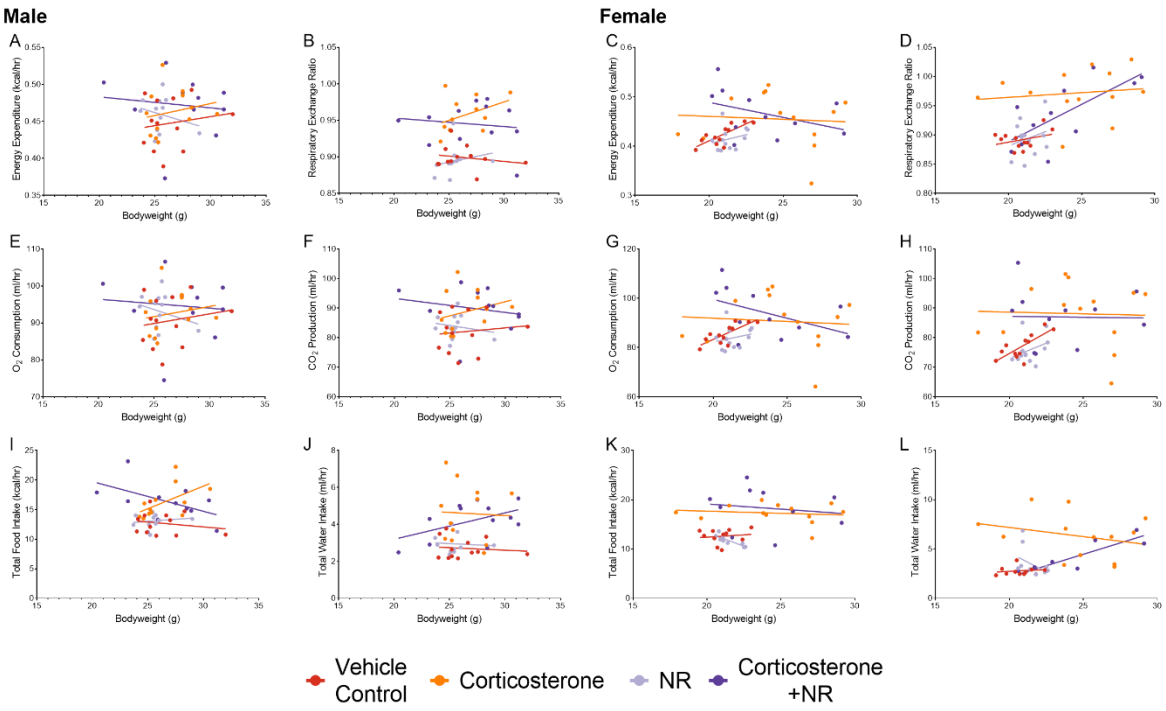

Figure 4.21: Analysis of covariance to determine the influence of bodyweight on markers of energy metabolism following 3 weeks of corticosterone and NR treatment. **A**: Male energy expenditure. **B**: Male respiratory exchange ratio. **C**: Female energy expenditure. **D**: Female respiratory exchange ratio n=12. **E**: Male oxygen consumption. **F**: Male carbon dioxide production. **G**: Male oxygen consumption. **H**: Male carbon dioxide production. **I**: Male food intake. **J**: Male water intake. **K**: Female food intake. **L**: Female water intake. Significance determined via ANCOVA. * significantly different, *p<.05, ** p<.01, *** p<.001, **** p<.0001. Abbreviations: O_2, oxygen; CO_2, carbon dioxide.

4.4 Discussion

The initial findings presented in this chapter characterise the impact of sustained glucocorticoid excess on the NAD^+ metabolome *in vivo*, as assessed by a NAD^+/NADH fluorescence assay and qPCR. The data indicates that sustained glucocorticoid excess does not alter NAD^+ content, apart from in female WAT. Interestingly it does appear to increase NADH in a tissue specific manner. Finally, the gene expression of enzymes within the NAD^+ biosynthetic network is also altered by sustained glucocorticoid excess in a tissue specific manner. Subsequent findings also show that supplementation with the NAD^+ precursor NR

can partially alter some of the effects of sustained glucocorticoid excess on the NAD^+ metabolome. Specifically reversing the corticosterone induced tissue specific increase in NADH, ultimately resulting in a decrease. However, the final data presented in this chapter shows that this, and therefore NR supplementation, does not alter the phenotype induced by sustained glucocorticoid excess, including alterations to markers of energy metabolism first identified in the previous chapter.

The first finding of this chapter is that sustained glucocorticoid excess alters parts NAD^+ metabolome in a tissue specific, and even sex specific manner. This involves a significant decrease in female WAT NAD^+, as well as an increase in WAT NADH in male and female mice. Whilst NAD^+ is unaltered in skeletal muscle, both male and female mice also exhibited increased skeletal muscle NADH. However, within male and female liver both NAD^+ and NADH were unaltered. Within skeletal muscle, and WAT, it is interesting to see an increase in NADH, as well a decrease in NAD^+ in female WAT, as this will result in a more reductive NAD^+/NADH ratio which suggests one or more of the many redox reactions within skeletal muscle and WAT are disrupted by glucocorticoid excess. However, at present it is beyond the scope of this thesis to determine which. Regardless of exact cause any change in the NAD^+/NADH ratio will likely result in further metabolic disruption (Wu et al., 2016, Lin et al., 2021), possibly contributing to conditions attributed to glucocorticoid excess. Energy producing pathways such as glycolysis, TCA cycle and ETC, shown in Fig. 1.20, 1.21 and 1.22, are among those likely effected (Canto et al., 2015). Therefore, this could also be a contributing factor to the findings of the previous chapter. The increase in NADH in male and female skeletal muscle and male WAT alone is likely to cause further metabolic disruption. Accumulation of NADH is known to cause a subsequent accumulation of ROS and mitochondrial disfunction (Galloway and Yoon,

2012, Quinlan et al., 2014) which might contribute to glucocorticoid excess induced oxidative stress and mitochondrial disfunction (Roma et al., 2012, Tang et al., 2013, Spiers et al., 2014). In addition, evidence is now emerging that an accumulation of NADH also inhibits SIRT1 deacetylation, reducing the expression of key metabolic enzymes such as brain and muscle Arnt-like protein-1 (BMAL1) and peroxisome proliferator-activated receptor alpha (PPARα) (Levine et al., 2021) which might further exacerbate the metabolic complications of glucocorticoid excess. With this in mind, the observed NADH accumulation might be a contributing factor to the findings of the previous chapter as disruption of homeostatic genes, such as BMAL1 can attenuate circadian regulation of energy metabolism (Levine et al., 2021) which was evident in corticosterone treated mice. However, the impact of NADH accumulation on SIRT1 deacetylation has presently only been investigated in *in vitro* and *in vivo* liver cells and tissue (Levine et al., 2021). As for the decline in female WAT NAD^+, it is possible this too will cause metabolic disruption (Frederick et al., 2016, Okabe et al., 2019, Lin et al., 2021), and potentially contribute to conditions caused by glucocorticoid excess, many of which NAD^+ decline has already been separately attributed to (Yoshino et al., 2011, Kuang et al., 2018, Okabe et al., 2019). However, as NAD^+ is unaltered in all but female WAT, it is possible these effects might be mitigated. Interestingly, the mostly unaffected state of NAD^+ content suggests that both NAD^+ synthesis and degradation might be unaltered by sustained glucocorticoid excess. Alternatively, it could suggest both are altered, cancelling out any alteration to the other. This is potentially the case with regards to NAD^+ degradation as the activity, expression and/or protein content of the primary NAD^+ consuming enzymes (SIRTs, PARPs and CD38) is reported decreased be glucocorticoid excess both *in vitro* and *in vivo* (Kang et al., 2008, Lee et al., 2018a, Jiang et al., 2019, Pan et al., 2019, Pasquereau et al., 2021). Additionally, increased NADH is reported to inhibit SIRT1 deacetylation, however

presently only in the liver (Levine et al., 2021). Taken together this could indicate that NAD^+ degradation is decreased. As for NAD^+ synthesis, it is possible that as NADH is seen to increase and NAD^+ remains unaltered, NAD^+ synthesis is in fact elevated to compensate for the increased reduction of NAD^+ to NADH. The observed elevation in skeletal muscle NAMPT expression would appear to support this as it is the key rate limiting enzyme in NAD^+ biosynthesis (Houtkooper et al., 2010). However, data in healthy overweight humans revealed that eNAMPT content was unaffected by a dexamethasone dose (0.5mg every 6 hours for 48 hours) that was sufficient to induce insulin resistance (Marcinkowska et al., 2007). Whilst eNAMPT and iNAMPT perform different roles it is possible iNAMPT content, and potentially NAD^+ synthesis, is equally unaffected. Without comprehensive assessment of enzyme content and activity within the NAD^+ biosynthetic network the effect on NAD^+ synthesis and breakdown cannot be confirmed. Additionally, as NAD^+ declined in female WAT, it is possible sexual differences regarding NAD^+ synthesis and/or consumption do exist in the presence of sustained glucocorticoid excess. This theory appears plausible as the gene expressions of enzymes involved in NAD^+ biosynthesis was impacted differently in male and female WAT. Whilst both had decreased NMNAT3 expression, only male WAT reported decreased NMNAT1 and NADK expression. Whilst it is not presently possible to confirm this theory, other sex related differences in the presentation of Cushing's syndrome/disease have been observed in humans (Pecori Giraldi et al., 2003, Valassi et al., 2011, Broersen et al., 2019), meaning this could be another one. As for the liver, it is also unclear why liver NAD^+ and NADH are unaffected by sustained glucocorticoid excess, despite the extensive inhibition of gene expression within the NAD^+ biosynthetic network. This includes reduced expression of enzymes involved in the primarily liver specific de novo biosynthesis pathway. Whilst a decrease in expression does not always represent a decrease in activity, which might explain

why NAD^+ and NADH are unaltered, some data does exist to suggest the activity of the de novo biosynthesis pathway is decreased by glucocorticoid excess *in vivo* (Xie et al., 2020b). Additionally, it is unclear if one or more enzymes are compensating for any disruption to the biosynthetic network to maintain NAD^+ and NADH levels.

As previously mentioned, there is limited conflicting research, especially *in vivo*, regarding the effect of glucocorticoid excess on the NAD^+ metabolome. However, the initial findings presented in this chapter do find limited agreement with the existing literature, specifically the lack of effect on skeletal muscle NAD^+. Herrera et al. (2020b) reported no effect of dexamethasone injected subcutaneously for 14 days (50µg/kg/day) on skeletal muscle NAD^+ in male wistar rats. Whilst methodology differs this does appear to confirm this initial finding. However, beyond this the findings of this chapter provide further conflict as they largely disagree with the published data. In fact, another *in vivo* study, albeit a far more acute one, found that 1mg/kg of prednisone injected once per week in male and female C57BL/6J mice increased skeletal muscle NAD^+ (Quattrocelli et al., 2022). Further disagreement can be found regarding the unaffected nature of liver NAD^+. Two *in vivo* studies, both from the same lab group, reported a decrease in liver NAD^+ in male C57BL/6J mice subcutaneously injected with corticosterone (20m/kg/day) for 6 weeks (Xiao et al., 2019, Xie et al., 2020b). Additional both studies reported a decrease in liver NAMPT expression, which was not observed in this chapter. They did however report a decrease in liver NMNAT3 expression, mirroring the finding in this chapter. Additionally, Xie et al. (2020b) also reported decreased de novo biosynthesis pathway activity, as assessed by tryptophan availability. Whilst this was not assessed in this chapter it does appear to agree with the reduction in NAD^+ biosynthetic gene expression seen in this chapter. Unfortunately, further *in vivo* comparisons are prevented as

no other study has assessed sex differences, gene expression beyond that already mentioned, WAT or NADH content in any tissue. However, some comparison can be made with limited *in vitro* investigation, none of which directly agrees with the findings of this chapter. Firstly, Kralisch et al. (2005) and Friebe et al. (2011) both report increased NAMPT expression *in vitro*, however in in adipocytes and preadipocytes, contrary to this chapter which identified no effect of corticosterone on NAMPT in WAT. Secondly, both Roma et al. (2012) and Yang et al. (2017) report on the redox ratio, specifically the $NADP^+$/NADPH ratio with Roma et al. (2012) reporting a shift to a more oxidised state, whilst Yang et al. (2017) reports a shift to a more reductive environment, similar to the findings in WAT in this chapter. However, whilst the findings of Roma et al. (2012) appear to contradict the findings in this chapter, neither act as direct comparisons as both focused on $NADP^+$/NADPH and are in cultured islets and chondrocytes respectively.

The secondary finding presented in this chapter is that NR does not augment NAD^+ content in any of the tissues assessed, both alone and in the presence of sustained glucocorticoid excess. This was mirrored with NAD^+ biosynthetic enzyme gene expression as NR did not alter any of the effects of corticosterone in any tissue, whilst NR alone did not differ from the controls, as expected from previous findings within the literature (Canto et al., 2012). However, the inability of NR to augment NAD^+ content was not expected as *in vivo* NR supplementation through drinking water is reported to elevate NAD^+ content (Canto et al., 2012, Cartwright et al., 2021). It is therefore even more unexpected that NR, both alone and in combination with corticosterone, resulted in a pronounced decrease in NAD^+ in male and female WAT, something which is difficult to explain. It is however unlikely to be from NAD^+ degradation as NR does not enhance NAD^+ degradation (Canto et al., 2012). Whilst in skeletal muscle and

liver, corticosterone treatment attenuated NRK2 and NRK1 expression respectively, potentially preventing NR conversion to NMN and then NAD^+, NRK1 and 2 were both unaffected in WAT. However, as enzyme activity was not assessed, no solid conclusion can be made. Additionally, as NR was orally consumed it can also easily be converted to NAM either by PNP or the gut microbiota, allowing it to enter the NAMPT pathway (Belenky et al., 2009, Shats et al., 2020) or alternatively to NA by gut microbiota before subsequent conversion to NAD^+ by the enzymes NAPRT, MNMNT and NADSYN (Shats et al., 2020). Therefore, these also require assessment to find a definitive answer. Regardless, this doesn't explain why NR alone did not increase NAD^+ as expected as NR alone is not reported to alter the mechanisms of NAD^+ biosynthesis (Canto et al., 2012). Therefore these findings presently question the use of NR for the purpose of NAD^+ metabolome augmentation, both independently and in the presence of sustained glucocorticoid excess. As for NADH however, NR resulted in a more expected effect by depleting NADH in skeletal muscle and WAT (Canto et al., 2012, Mukherjee et al., 2021) whilst having no effect in the liver. In both skeletal muscle and WAT NR completely reversed the effect of corticosterone when given in combination, promoting a more oxidative, rather than reductive, state. As NADH accumulation is reported to induce metabolic complications (Galloway and Yoon, 2012, Quinlan et al., 2014, Levine et al., 2021) the effects of NR might still yield therapeutic potential in combatting glucocorticoid excess, despite either unaltering or depleting NAD^+, especially as NR has been reported to help combat conditions caused independent of glucocorticoid excess (Frederick et al., 2016, Wu et al., 2016, Okabe et al., 2019, Dall et al., 2022). Additionally, it might be possible to further improve the effects of NR. As previously mentioned, NR alone, surprisingly, did not significantly elevate NAD^+ in any tissue, contrary to existing literature (Canto et al., 2012, Doig et al., 2020, Cartwright et al., 2021). Whilst significant increases in skeletal muscle NAD^+ have

been reported by NR treatment in drinking water (Canto et al., 2012, Cartwright et al., 2021), it is possible this effect was not observed in this chapter due to the first pass effect, causing NR to be partly broken down and utilised before it can get to the target tissues, limiting its bioavailability and ability to increase NAD^+ (Liu et al., 2018, Hayat and Migaud, 2020, Herman and Santos, 2022). An alternate delivery strategy, such as intraperitoneal (IP) injections, which are shown to increase NAD^+ with NR (Doig et al., 2020), might increase the capability of NR to increase NAD^+ in the presence of sustained glucocorticoid excess as it is reported to increase NR bioavailability at the tissue level as the number of the steps NR needs to go through to reach the target tissues is reduced (Liu et al., 2018, Hayat and Migaud, 2020). However, whether this would in fact be of benefit requires further investigation as due to the novel nature of this part of the chapter there is no existing literature to draw direct comparisons to.

The final finding presented in the chapter is that NR supplementation does not prevent the phenotype induced by glucocorticoid excess, despite reversing the increase in NADH seen with corticosterone treatment alone, directly testing the therapeutic potential of the NR for combating sustained glucocorticoid excess. As shown in the previous chapter corticosterone treatment alone developed a classic phenotype of glucocorticoid excess was, including signs such as skeletal muscle atrophy, fat accumulations, spleen atrophy and hepatic TAG accumulation. The findings of the previous chapter also identified altered energy metabolism as part of this phenotype. When NR was supplemented alongside corticosterone however, all these effects were still present. Skeletal muscle atrophy, fat accumulation, bodyweight gain, spleen atrophy and hepatic TAG accumulation were not prevented. However, fat accumulation was slightly attenuated in male mice. In addition, EE, RER, oxygen consumption, carbon dioxide production, as well as food and water intake all remained elevated. These

findings indicate that altering some of the effects of sustained glucocorticoid excess on the NAD^+ metabolome, such as NADH accumulation, is not enough to combat these conditions when glucocorticoid induced. This is interesting as some existing literature suggests NR supplementation improves several metabolic conditions, including skeletal muscle atrophy, diabetes, obesity, and fatty liver disease when caused independent of glucocorticoid excess (Frederick et al., 2016, Wu et al., 2016, Okabe et al., 2019, Dall et al., 2022). This suggests that either altering some of the effects of sustained glucocorticoid excess on the NAD^+ metabolome is unable to counteract the hormonal disruption of glucocorticoid excess, or alternatively that the glucocorticoid excess induced disruption of the NAD^+ metabolome, observed in this chapter, is not causative of the metabolic complications of glucocorticoid excess, but instead just another one of the consequences of glucocorticoid excess.

The findings presented in this chapter therefore question the use of NR supplementation for the purpose of NAD^+ metabolome augmentation and treatment of metabolic conditions induced by glucocorticoid excess. Whilst a number of studies have reported metabolic benefits of NR (Frederick et al., 2016, Wu et al., 2016, Okabe et al., 2019, Dall et al., 2022), several have also reported little to no benefit in other metabolic conditions, some which can be caused by glucocorticoid excess (Elhassan et al., 2019, Remie et al., 2020), much like this chapter. Additionally, NR supplementation has also previously been shown ineffective at altering both EE, RER and food intake in C57BL/6J mice treated with a high fat diet (HFD) or a standard chow (Cartwright et al., 2021). Whilst HFD has the opposite effect to glucocorticoid excess identified in the previous chapter, especially with regards to RER, Cartwright et al. (2021) still show that NR has no effect, despite actually increasing NAD^+ content. Therefore, the findings in the present chapter, and others (Elhassan et al., 2019, Remie et al., 2020,

Cartwright et al., 2021) suggest that augmenting the NAD^+ metabolome might not always be the appropriate strategy for countering metabolic disruption, even if NAD^+ metabolome disruption is observed. However, as the effects of NR observed in this chapter were very minimal it remains possible that another NAD^+ precursor, such as NMN which has been credited with combating glucocorticoid induce hyperglycaemia and osteoporosis (Huang and Tao, 2020, Uto et al., 2021), might be more beneficial. Additionally, further investigation should also include labelled NR, as well as liquid chromatography–mass spectrometry analysis (LCMS) (which was planned for this chapter but was delayed due to complications with collaborators) to fully establish the fate of NR and why it is not augmenting NAD^+ at the tissue level as previously reported. This approach could also be used for supplementation of other NAD^+ precursors as labelling would determine their end points and LCMS would allow all the intermediate steps in NAD^+ biosynthesis, as well as additional metabolites, to be quantified (Liu et al., 2018). Therefore, without further investigation the futility of NR supplementation and the concept of NAD^+ metabolome augmentation for the purpose of combating the effects of glucocorticoid excess cannot be confirmed.

Whilst revealing significant insights into the effect of sustained glucocorticoid excess on the NAD^+ metabolome, as well as the limited ability of NR to counter these effects and the overall phenotype, this chapter raises additional questions. Despite the extensive knowledge of glucocorticoid mechanisms of action, the first question raised by this chapter is what are the exact mechanisms induced by glucocorticoid excess that alter the NAD^+ metabolome? As previously mentioned, it this could be from decreased synthesis, increased degradation, altered redox reactions or more, but how any of these might be bought about remains unclear. A second questions is regarding the observed sex differences. The use of both male

and female mice was a major strength of this chapter as this is often overlooked in rodent cushingoid research. However, this leaves the question why glucocorticoid excess causes different effects with regards to NAD^+ and gene expression in WAT, as well as fat accumulation. Another question raised in by this chapter is this effectiveness of NR and its delivery method for boosting NAD^+, as well as combating the effects of glucocorticoid excess. Whilst it is well tolerated by mice, causing no negative side effects and maximising animal welfare, especially when given non-invasively through drinking water (Canto et al., 2012), it is unclear if another delivery method, such as IP injection would improve its effects or better combat the effects of glucocorticoid excess. In addition to this it is unclear if NR is the most suitable NAD^+ precursor for the job. Alternatives such as NA, NAM and NMN, as well as reduced forms of these precursors, all merit investigation as they have been reported capable of boosting NAD^+ (Hara et al., 2003, Liu et al., 2009, Ratajczak et al., 2016, Fletcher et al., 2017, Zapata-Perez et al., 2021). NMN especially merits investigation as it is both well tolerated by mice and has reported benefits similar to NR (Mills et al., 2016). It has also been credited with combating glucocorticoid excess induced hyperglycaemia and osteoporosis (Huang and Tao, 2020, Uto et al., 2021). As this chapter has only assessed whether NAD^+ metabolome disruption and subsequent NR supplementations effects a few of the metabolic effects of glucocorticoid excess the final question of the chapter is whether additional consequences of sustained glucocorticoid excess can be reversed by NR supplementation, given its reversal of glucocorticoid excess induced NADH elevation. Whilst all these questions all merit investigation, detailed exploration is beyond the scope of this thesis. The following chapter will instead focus on investigating the role of 11β-HSD1 in mediating the novel effects identified in this chapter, as well as the previous, to further explore the mechanisms involved

and explore the therapeutic potential of 11β-HSD1 inhibition for combatting the novel effects identified so far in this thesis.

In conclusion, this chapter provides evidence that sustained glucocorticoid excess alters the NAD^+ metabolome in a tissue specific, and even sex specific manner. It also showed that NR supplementation can partially alter some of the effects of corticosterone on the NAD^+ metabolome, namely reversing NADH elevation, without altering the typical cushingoid phenotype. Finally it also provides further evidence that using NR does not alter the global effects of glucocorticoid excess on energy metabolism identified in the previous chapter. Taken together these findings suggest that alterations to the NAD^+ metabolome, specifically increased NADH, are only a consequence of glucocorticoid excess and not causative factors of the many metabolic conditions it causes. As such, NR supplementation, or NAD^+ metabolome augmentation does not appear to be an effective treatment strategy to counter the effects of sustained glucocorticoid excess. However, further investigation is required to confirm this.

CHAPTER 5 – THE ROLE OF 11B-HSD1 IN MEDIATING THE IMPACT OF SUSTAINED GLUCOCORTICOID EXCESS ON THE NAD^+ METABOLOME AND ENERGY METABOLISM

5.1 Introduction

The findings presented in the previous two chapters identify glucocorticoid excess induced disruption to markers of energy metabolism (Chapter 3) and the NAD^+ metabolome (Chapter 4). Both these chapters therefore raise the same question; what mechanisms are involved that facilitate these effects? Despite the extensive knowledge of glucocorticoid mechanisms of action (section 1.4), without extensive investigation the exact mechanisms behind the novel effects identified thus far are not apparent. However, this is a potentially vast area of investigation. Therefore, this chapter will investigate the role of 11β-HSD1 as it known to be critical in mediating other glucocorticoid excess induced effects (Tomlinson et al., 2002, Morgan et al., 2014, Webster et al., 2021). Acting predominantly as a reductase, 11β-HSD1 activates glucocorticoids at the tissue level (Agarwal and Auchus, 2005). However, should 11β-HSD1 be defective or even deleted, both humans and mice are protected against many of the effects of sustained glucocorticoid excess (Tomlinson et al., 2002, Morgan et al., 2014, Webster et al., 2021). This is despite the fact that circulating active glucocortiocid levels do not differ (Morgan et al., 2014). This includes circulating corticosterone levels that result form the model used througout this thesis (Morgan et al., 2014). Instead both humans and mice are protected due to drastically reduced active glucocorticoid availability at the tissue level, even if the source of glucocorticoid excess is active, exogenous, glucocorticoid treatment (Tomlinson et al., 2004, Morgan et al., 2014). This is because 11β-HSD2 remains active, predominately within the kidneys, driving glucocorticoid deactivation through its dehydrogenase activity (Tomlinson et al., 2004, Morgan et al., 2014). Due to the absence of 11β-HSD1 activity, glucocorticoids cannot be reactivated at the tissue level, thus attenuating the effects of sustained endogenous and exogenous glucocorticoid excess (Tomlinson et al., 2004, Morgan et al., 2014). Given this knowledge it is unsuprising that several glucocorticoid

excess induced metabolic conditions are prevented in a 11β-HSD1 knock out (KO) model. This includes glucocorticoid excess induced obesity, diabetes, insulin resistance, hypertension, skeletal muscle atrophy, hepatic steatosis and many more (Morgan et al., 2009, Morgan et al., 2013, Morgan et al., 2014, Morgan et al., 2016a, Webster et al., 2021). In addition, the cushingoid phenotype as a whole is also prevented (Fig. 1.9) (Tomlinson et al., 2002, Morgan et al., 2014). However, given the novel nature of the findings presented in chapters 3 and 4, it is unknown if these too are also mediated by the prescence of 11β-HSD1.

Therefore, the aims of this chapter are to establish if glucocorticoid excess induced disruption of the NAD^+ metabolome, identified in chapter 4, as well as elevated energy metabolism, identified in chapter 3, are reliant on the presence of 11β-HSD1. Given the ineffectiveness of NR in the previous chapter, exploration into the role of 11β-HSD1 might uncover a more viable theraputic approach for tackling the novel effects identified thus far.

5.2 Materials and methods

5.2.1 Animal housing

C57BL/6J (WT) (purchased from Charles River) and 11β-HSD1KO mice were housed as detailed in section 2.1.1 for the first two weeks of treatment. For the final week of treatment mice were housed in a TSE Phenomaster 8 cage system as detailed in section 2.2.

5.2.2 Indirect calorimetry

Indirect calorimetry was performed using a TSE Phenomaster 8 cage system as detailed in section 2.2. Both male and female C57BL/6J (WT) and 11β-HSD1KO mice (n=8-12) were assessed by indirect calorimetry.

5.2.3 Animal treatments

C57BL/6J (WT) and 11β-HSD1KO mice were treated *ab libitum* through their drinking water. Treatments are shown in table 5.1. Treatments lasted for 3 weeks and water was changed every 2 days to keep the animals supplied and to minimise any degradation of treatment. Water bottles were either opaque or wrapped in tin foil to prevent light from degrading the substance within. Both male and female C57BL/6J (WT) and 11β-HSD1KO mice (n=8-12) were treated.

Table 5.1: Animal treatments

Treatment	Dose	Preparation
Corticosterone	100mg/L (≈300µg/day)	100mg of corticosterone (Sigma-Aldrich, St Louis, Missouri, US) was dissolved in 6ml of 100% ethanol and then added to 1L of autoclaved water
Vehicle control	n/a	6ml of 100% ethanol was added to 1L of autoclaved water

5.2.4 Animal sacrifice and tissue collection

Following treatment and indirect calorimetry mice were sacrificed and tissues collected as detailed in section 2.2.2.

5.2.5 Tissue preparation

Following animal sacrifice and tissue collection tissues were prepared for subsequent analysis as detailed in section 2.1.3.

5.2.6 NAD^+/NADH fluorescence assay

NAD^+ and NADH quantification was performed via a NAD^+/NADH fluorescence assay as detailed in section 2.4.

5.2.7 RNA extraction and analysis

Gene expression of samples was assessed as detailed in section 2.5 with reference genes listed in table 2.5 used. Genes specific to this chapter are detailed in table 5.2.

Table 5.2: TaqMan probe used in this chapter

Gene	Assay ID
NAMPT	Mm00451938_m1
NMRK1 (NRK1)	Mm00521051_m1
NMRK2 (NRK2)	Mm01172899_g1
NMNAT1	Mm01257929_m1
NMNAT3	Mm00513791_m1
NADSYN1 (NADSYN)	Mm00513448_m1
NAPRT	Mm00553802_m1
NADK	Mm00446804_m1
PNP	Mm00840006_m1
QPRT	Mm00504998_g1
HAAO (HAO)	Mm00517945_m1
KYNU (KYU)	Mm00551012_m1
KMO	Mm01321343_m1
AFMID (AFM)	Mm00510774_m1
IDO1 (IDO)	Mm00492590_m1

5.2.8 Statistical analysis

Statistical analysis was performed as detailed in section 2.9.

5.3 Results

5.3.1 11β-HSD1KO mice are protected against the phenotype typical of glucocorticoid excess in a sex specific manner

As expected, male 11β-HSD1KO mice (females not previously assessed) are protected against the phenotype typical of glucocorticoid excess when treated with corticosterone (Fig. 5.1) (Morgan et al., 2014), thus confirming the effectiveness of the knock-out. Increased adiposity (Fig. 5.1B) and skeletal muscle atrophy (Fig. 5.1D-F) were both prevented as male 11β-HSD1KO mice treated with the vehicle control, or corticosterone did not exhibit any different effects to male WT mice treated with the vehicle control. Like males, female 11β-HSD1KO mice were also protected from increased adiposity (Fig. 5.1H) which prevented the bodyweight increase seen in WT mice (Fig. 5.1G). Interestingly, female 11β-HSD1KO mice were not fully protected from skeletal muscle atrophy (Fig. 5.1J-L) as gastrocnemius atrophy was still present (Fig. 5.1K). Spleen atrophy, however, was also still present in male and female 11β-HSD1KO mice treated with corticosterone.

5.3.2 NAD^+ content is unaffected by corticosterone treatment in 11β-HSD1KO mice

Following corticosterone treatment NAD^+ content did not differ in male or female 11β-HSD1KO mice compared to 11β-HSD1KO mice treated with the vehicle control in any tissue, as assessed by NAD^+ fluorescence assay (Fig. 5.2A-F). Additionally, regardless of treatment 11β-HSD1KO mice did not differ to WT mice that had been treated with corticosterone, however this was only assessed in female mice (Fig. 5.2B, D and F). In skeletal muscle

(gastrocnemius) and liver tissue all three of these groups did not differ to WT control mice, however once again this was only assessed in females (Fig. 5.2B and D). However, in female WAT (gonadal fat), 11β-HSD1KO mice treated with corticosterone or the vehicle control, as well as WT mice treated with corticosterone, NAD^+ was significantly less than in WT controls (Fig. 5.2F).

5.3.3 11β-HSD1KO prevented the tissue specific corticosterone induced increase in NADH

Within skeletal muscle (gastrocnemius) corticosterone treatment increase NADH content in WT mice compared to WT controls (Fig. 5.3B). However, 11β-HSD1KO mice treated with corticosterone did not experience this increase and did not differ to WT controls or 11β-HSD1KO controls (Fig. 5.3B). Unfortunately, this was only assessed in female mice. Within the liver, corticosterone did not increase NADH in WT mice, but despite this both corticosterone and control 11β-HSD1KO mice had significantly less NADH than WT corticosterone but not WT controls (Fig. 5.3D). Again, this was only assessed in female mice. In WAT (gonadal fat) however, WT mice treated with corticosterone had decreased NADH compared to WT controls, contrary to chapter 3. In 11β-HSD1KO mice this effect was also seen in those treated with corticosterone and the vehicle control, with both being significantly less than WT controls (Fig. 5.3F). In all three tissues, comparison with WT mice was completed in female mice only. However, regardless of tissue, NADH did not differ between corticosterone or vehicle control treated male and female 11β-HSD1KO mice (Fig. 5.3A-F).

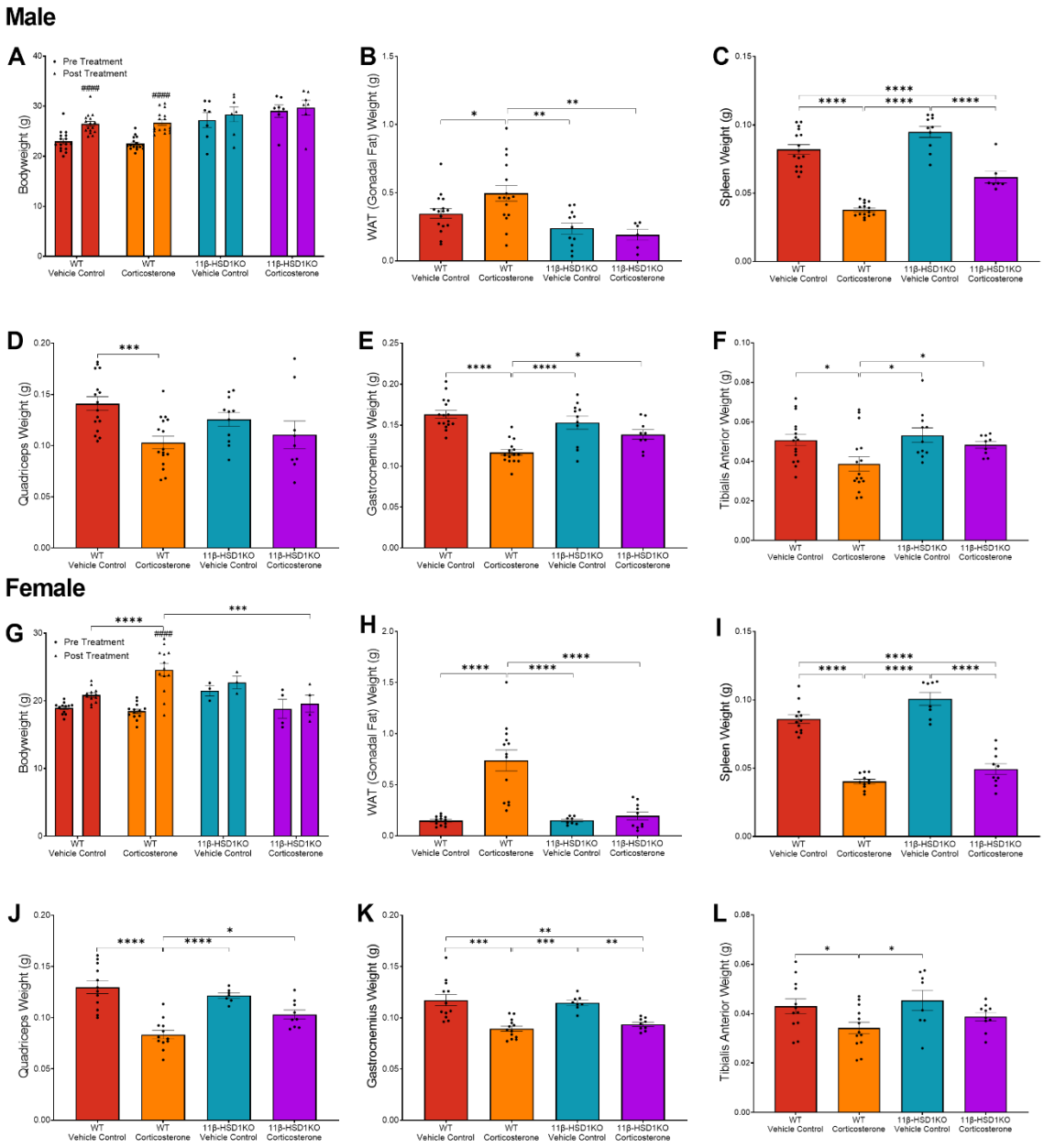

Figure 5.1: Bodyweight and tissue weight of WT and 11β-HSD1KO mice following 3 weeks of corticosterone treatment. **A**: Male bodyweight. **B**: Male WAT (gonadal fat) weight. **C**: Male spleen weight. **D**: Male quadriceps weight. **E**: Male gastrocnemius weight. **F**: Male tibialis anterior weight. **G**: Female bodyweight. **H**: Female WAT (gonadal fat) weight. **I**: Female spleen weight. **J**: Female quadriceps weight. **K**: Female gastrocnemius weight. **L**: Female tibialis anterior weight. Data is presented as mean with individual values ± SD, n=8-12. Significance determined via two-way ANOVA. * significantly different, # significantly different to pre. *p<.05, ** p<.01, *** p<.001, **** p<.0001. Abbreviations: WAT, white adipose tissue.

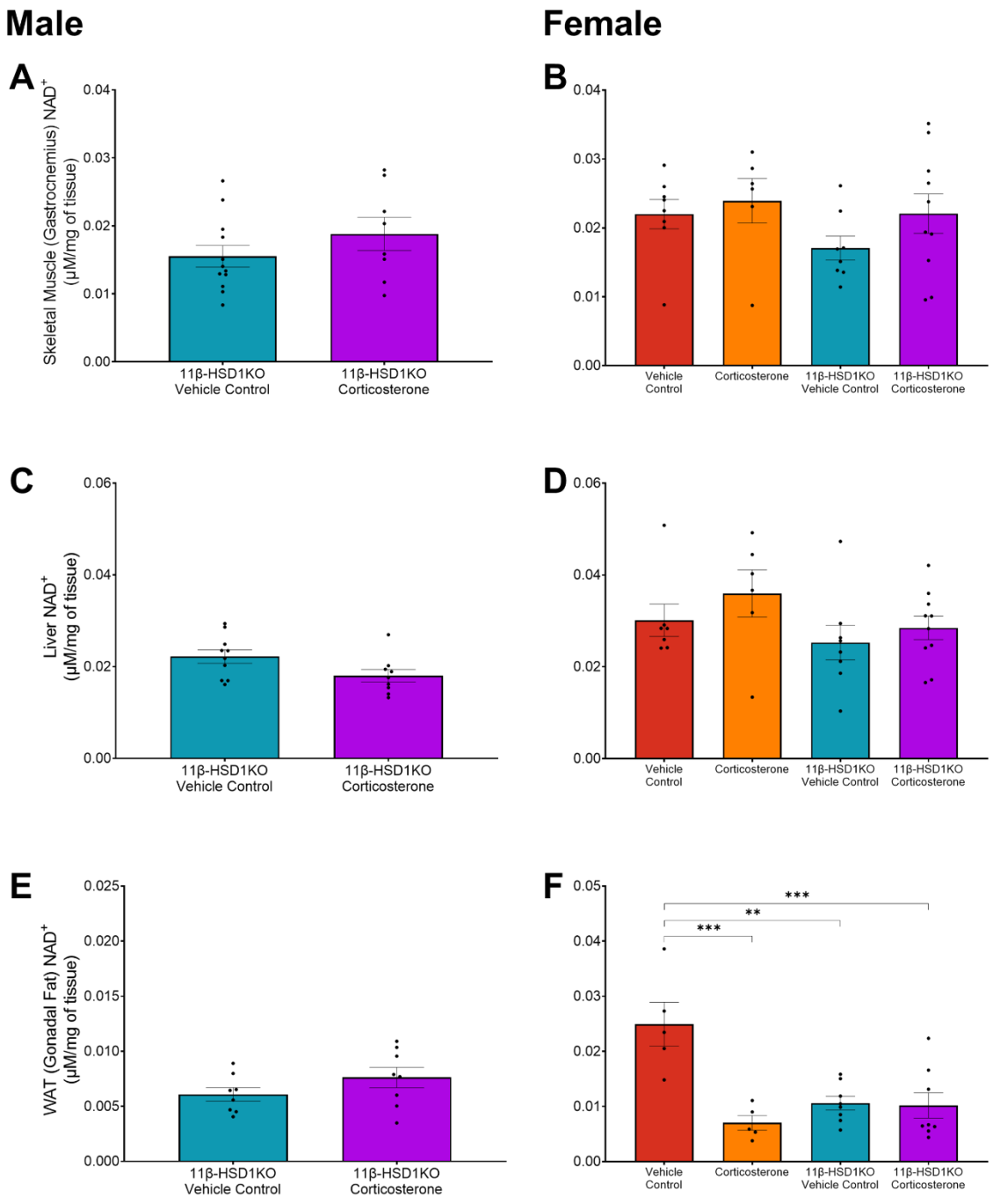

Figure 5.2: NAD^+ content of WT and 11β-HSD1KO mice following 3 weeks of corticosterone treatment as assessed by NAD^+ fluorescence assay. **A**: Male skeletal muscle NAD^+ content. **B**: Female skeletal muscle NAD^+ content. **C**: Male liver NAD^+ content. **D**: Female liver NAD^+ content. **E**: Male WAT NAD^+ content. F: Female WAT NAD^+ content. Data is presented as mean with individual values ± SD, n=6-12. Significance determined via two-way ANOVA.* significantly different. *p<.05, ** p<.01, *** p<.001, **** p<.0001. Abbreviations: WAT, white adipose tissue.

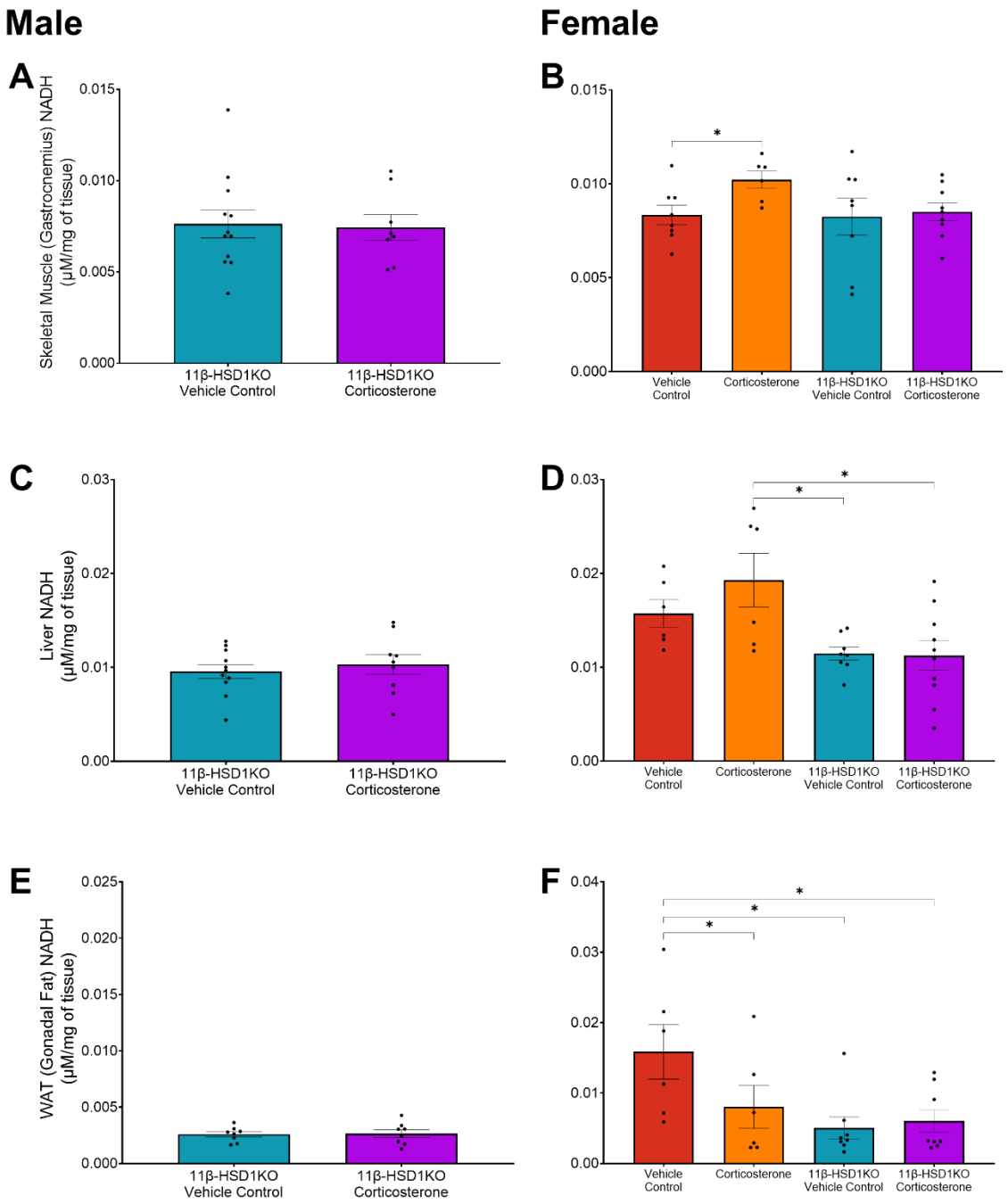

Figure 5.3: NADH content of WT and 11β-HSD1KO mice following 3 weeks of corticosterone treatment as assessed by NADH fluorescence assay. **A**: Male skeletal muscle NADH content. **B**: Female skeletal muscle NADH content. **C**: Male liver NADH content. **D**: Female liver NADH content. **E**: Male WAT NADH content. **F**: Female WAT NADH content. Data is presented as mean with individual values ± SD, n=6-12. Significance determined via two-way ANOVA. * significantly different. *p<.05, ** p<.01, *** p<.001, **** p<.0001. Abbreviations: WAT, white adipose tissue.

5.3.4 11β-HSD1KO mice are largely protected against the effects of corticosterone on the gene expression of the NAD^+ biosynthetic network

The gene expression of NAD^+ biosynthetic enzymes that was previously altered by corticosterone in chapter 3 was assessed in 11β-HSD1KO mice. Unfortunately, only female gene expression was assessed due to availability of samples. Within WT skeletal muscle (quadriceps) NAMPT was increased whilst NRK2 was decreased by corticosterone, as seen in chapter 3. However, in 11β-HSD1KO mice the increase in NAMPT was not seen following corticosterone treatment as it did not differ from WT controls or 11β-HSD1KO controls (Fig. 5.4). However, NRK2 was still decreased by corticosterone in 11β-HSD1KO mice, matching the effect seen in WT mice. 11β-HSD1KO control mice exhibited similar expression levels to WT control mice (Fig. 5.4).

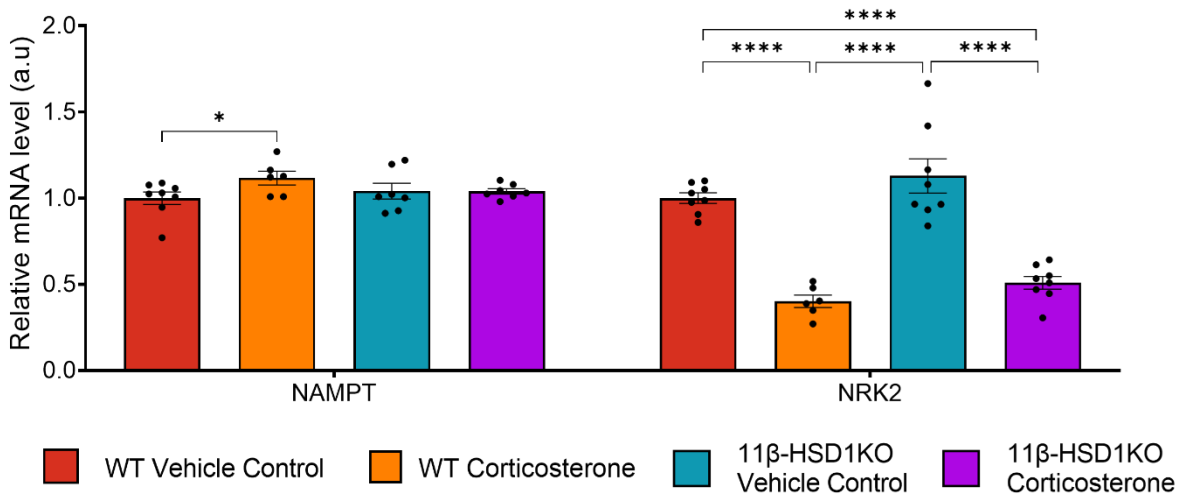

Figure 5.4: Skeletal muscle (quadriceps) NAD^+ biosynthetic gene expression of female WT and 11β-HSD1KO mice only following 3 weeks of corticosterone treatment as assessed by qPCR. Only genes altered previously by corticosterone treatment in chapter 3 were assessed. Data is presented as mean with individual values ± SD, n=8. Significance determined via two-way ANOVA for each gene. * significantly different *p<.05, ** p<.01, *** p<.001, **** p<.0001.

As for the liver corticosterone decreased gene expression in WT mice in NMNAT1, NMNAT3, NADSYN, NAPRT, NADK, PNP, QPRT, HAO, AFM and IDO (Fig. 5.5) as seen in chapter 3. However, NRK1, KYU and KMO expression were not decreased in WT mice (Fig. 5.5) contrary to findings in chapter 3. Of those genes which were still decreased, 11β-HSD1KO prevented the corticosterone induced decrease in all but IDO which decreased to a similar extent as in WT mice (Fig. 5.5). As with skeletal muscle 11β-HSD1KO control mice had similar gene expression as WT control mice (Fig. 5.5).

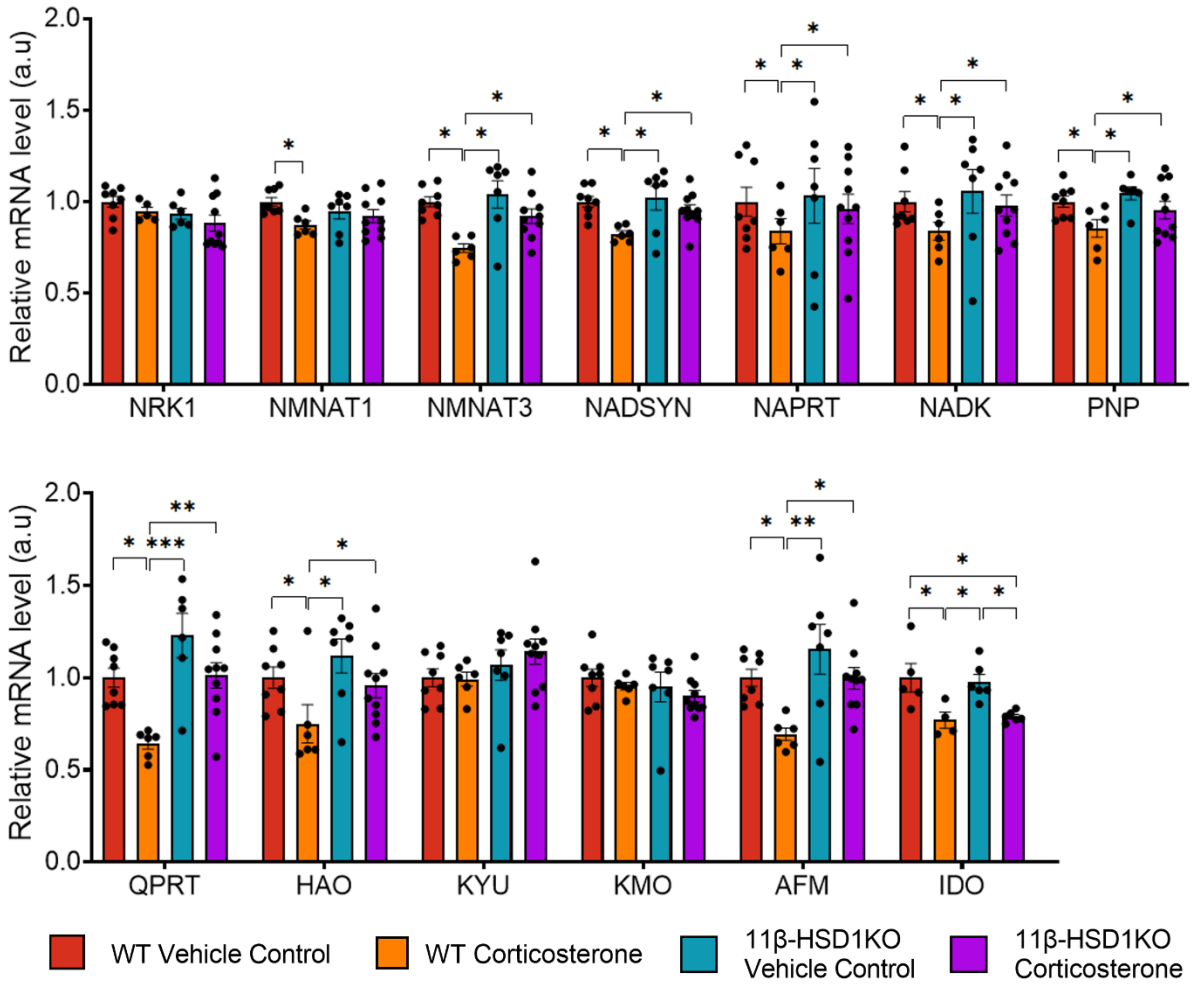

Figure 5.5: Liver NAD^+ biosynthetic gene expression of female WT and 11β-HSD1KO mice only following 3 weeks of corticosterone treatment as assessed by qPCR. Only genes altered previously by corticosterone treatment in chapter 3 were assessed. Data is presented as mean with individual values ± SD, n=6-12, female only. Significance determined via two-way ANOVA for each gene. * significantly different. *p<.05, ** p<.01, *** p<.001, **** p<.0001.

Within WAT (gonadal fat) NMNAT, NMNAT3 and NADK were assessed. However only NMNAT3 expression decreased in WT mice following corticosterone treatment (Fig. 5.6). In contrast to chapter 3, neither NMNAT1 or NADK expression decreased in WT following corticosterone treatment (Fig. 5.6). In 11β-HSD1KO mice corticosterone did not alter the expression of all three of these genes, meaning that they were all equal to WT and 11β-HSD1KO controls (Fig. 5.6). Therefore, in the case of NMNAT3, 11β-HSD1KO prevented the corticosterone induced decrease seen in WT mice (Fig. 5.6).

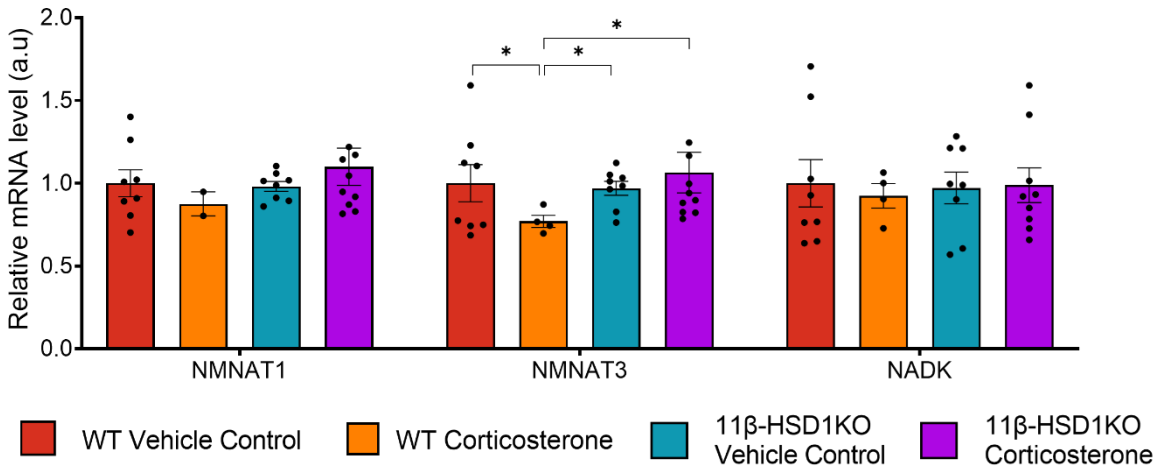

Figure 5.6: WAT (gonadal fat) NAD^+ biosynthetic gene expression of female WT and 11β-HSD1KO mice only following 3 weeks of corticosterone treatment as assessed by qPCR. Only genes altered previously by corticosterone treatment in chapter 3 were assessed. **A**: Male NAD^+ biosynthetic gene expression. **B**: Female NAD^+ biosynthetic gene expression. Data is presented as mean with individual values ± SD, n=4-12. Significance determined via two-way ANOVA for each gene. * significantly different. *p<.05, ** p<.01, *** p<.001, **** p<.0001. Abbreviations: WAT, white adipose tissue.

5.3.5 11β-HSD1KO mice do not experience elevated energy expenditure with corticosterone treatment

Both male and female 11β-HSD1KO mice are protected against the corticosterone induced increase in EE seen in WT mice (Fig. 5.7A-D). Regardless of treatment 11β-HSD1KO mice

maintain an EE similar to WT control mice, which is therefore less, significantly so in female 11β-HSD1KO mice during the light phase, than the values of corticosterone treated WT mice (Fig. 5.7A-D). Linear regression and subsequent ANCOVA determined no significant differences in slope angle between treatments or mouse strains revealing no significant effect of body weight on EE (Fig. 5.13A and C).

5.3.6 11β-HSD1KO mice do not experience an elevated respiratory exchange ratio with corticosterone treatment

As with EE, both male and female 11β-HSD1KO mice are protected against the corticosterone induced increase in RER seen in WT mice (Fig. 5.8A-D). Regardless of treatment 11β-HSD1KO mice maintain a RER similar to WT control mice, which is therefore significantly less, especially during the light phase, than the values of corticosterone treated WT mice (Fig. 5.8A-D). Linear regression and subsequent ANCOVA determined no significant differences in slope angle between treatments or mouse strains revealing no significant effect of body weight on RER (Fig. 5.13B and D).

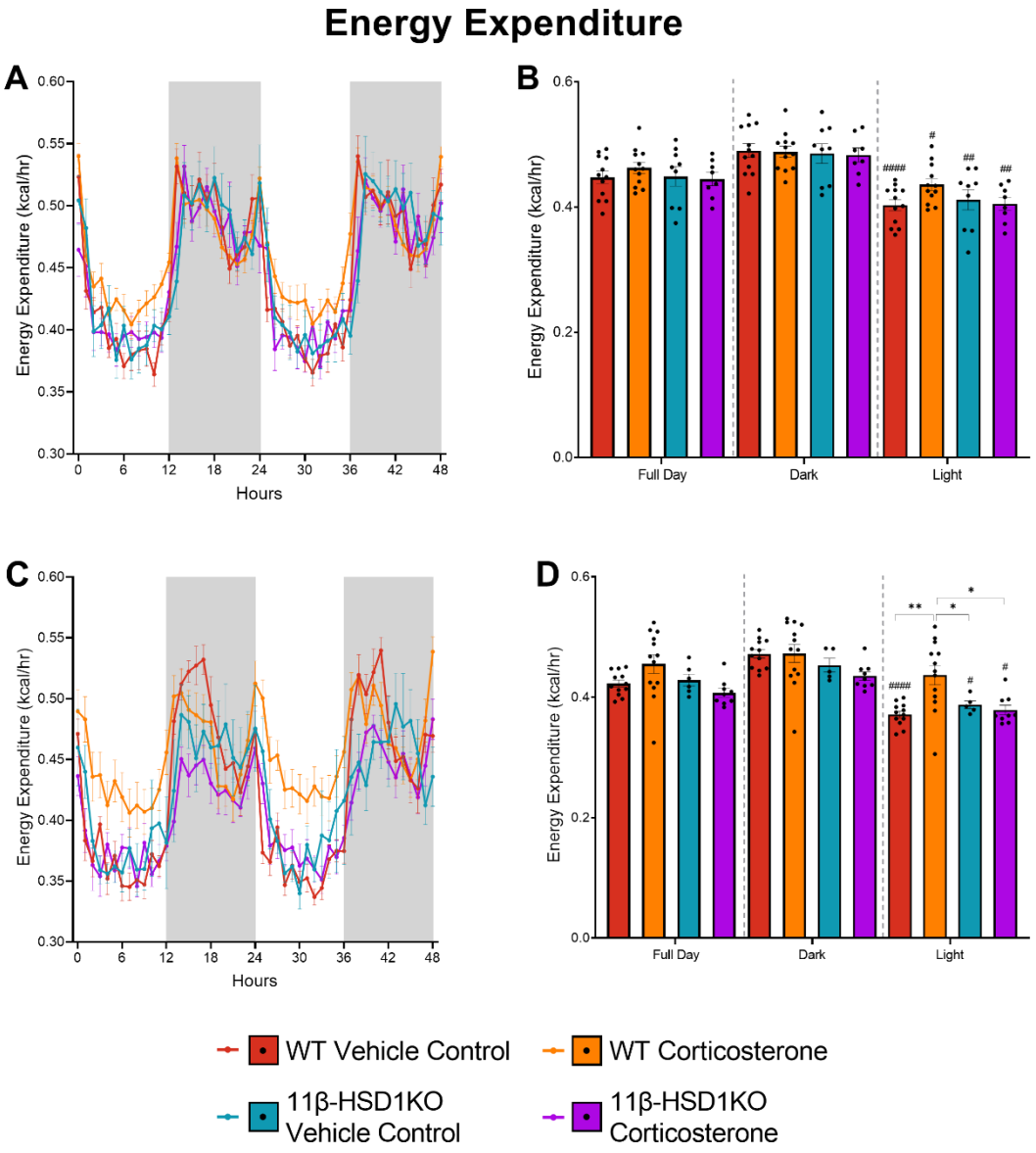

Figure 5.7: Energy expenditure of WT and 11β-HSD1KO mice following 3 weeks of corticosterone treatment. **A**: Male hourly energy expenditure. **B**: Male average energy expenditure. **C**: Female hourly energy expenditure. **D**: Female average energy expenditure. Line graphs are presented as mean ± SD, n=9-12. Bar charts are presented as mean with individual values ± SD, n=9-12. Significance determined via two-way ANOVA. * significantly different, # significantly different to dark. *p<.05, ** p<.01, *** p<.001, **** p<.0001.

5.3.7 11β-HSD1KO mice do not experience an elevated oxygen consumption or carbon dioxide production with corticosterone treatment

Both of the constituent parts of RER, oxygen consumption and carbon dioxide production, were not elevated by corticosterone in male and female 11β-HSD1KO mice (Fig. 5.9 and 5.10). Regardless of treatment 11β-HSD1KO mice maintain oxygen consumption and carbon dioxide production values similar to WT control mice, which are therefore significantly less, especially during the light phase, than the values of corticosterone treated WT mice. However, this effect was more pronounced in female mice (Fig. 5.9 and 5.10). Linear regression and subsequent ANCOVA determined no significant differences in slope angle between treatments or mouse strains revealing no significant effect of body weight on oxygen consumption or carbon dioxide production (Fig. 5.13E-H).

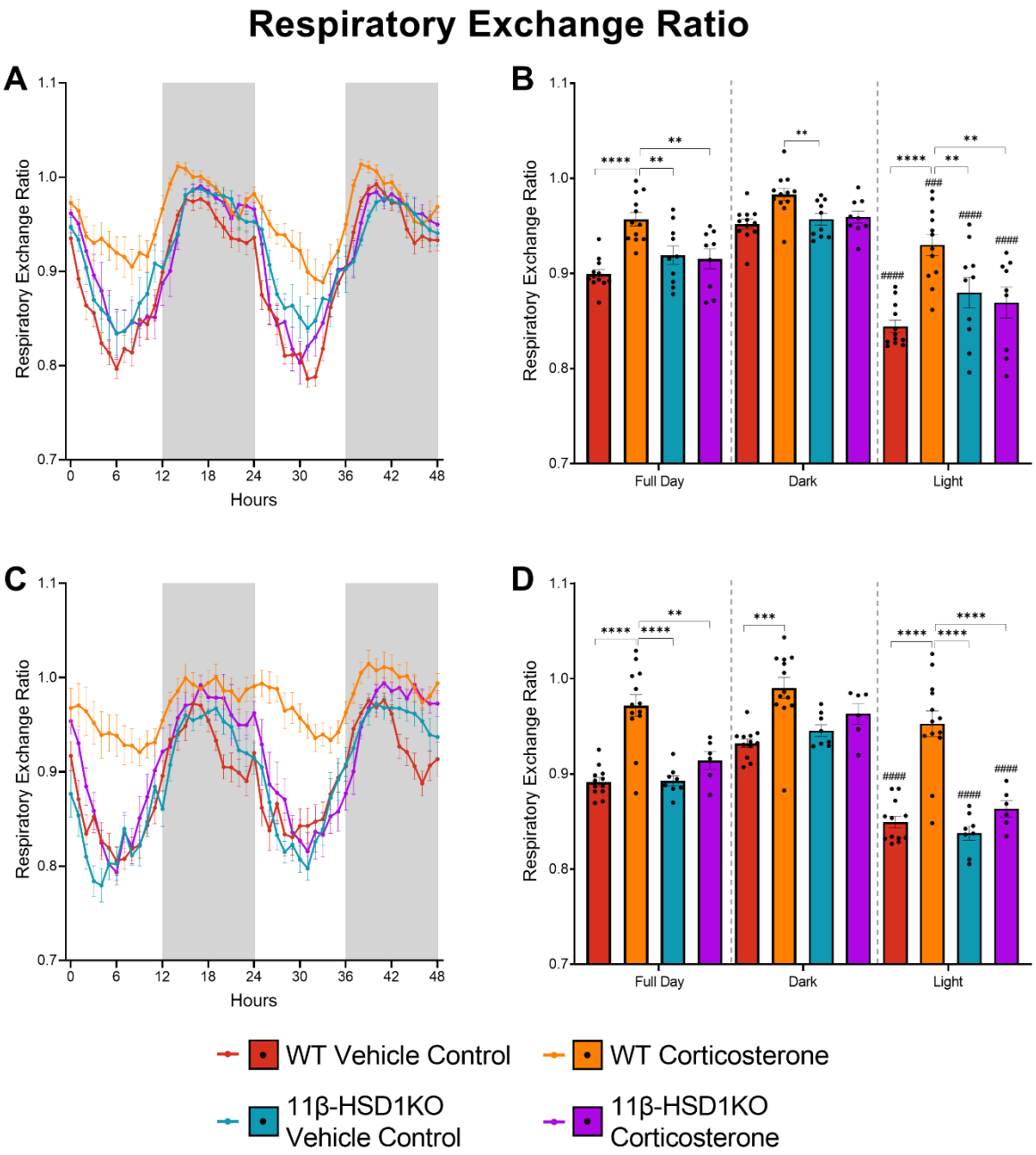

Figure 5.8: Respiratory exchange ratio of WT and 11β-HSD1KO mice following 3 weeks of corticosterone treatment. **A**: Male hourly energy expenditure. **B**: Male average energy expenditure. **C**: Female hourly energy expenditure. **D**: Female average energy expenditure. Line graphs are presented as mean ± SD, n=10-12. Bar charts are presented as mean with individual values ± SD, n=10-12. Significance determined via two-way ANOVA. * significantly different, # significantly different to dark. *p<.05, ** p<.01, *** p<.001, ****

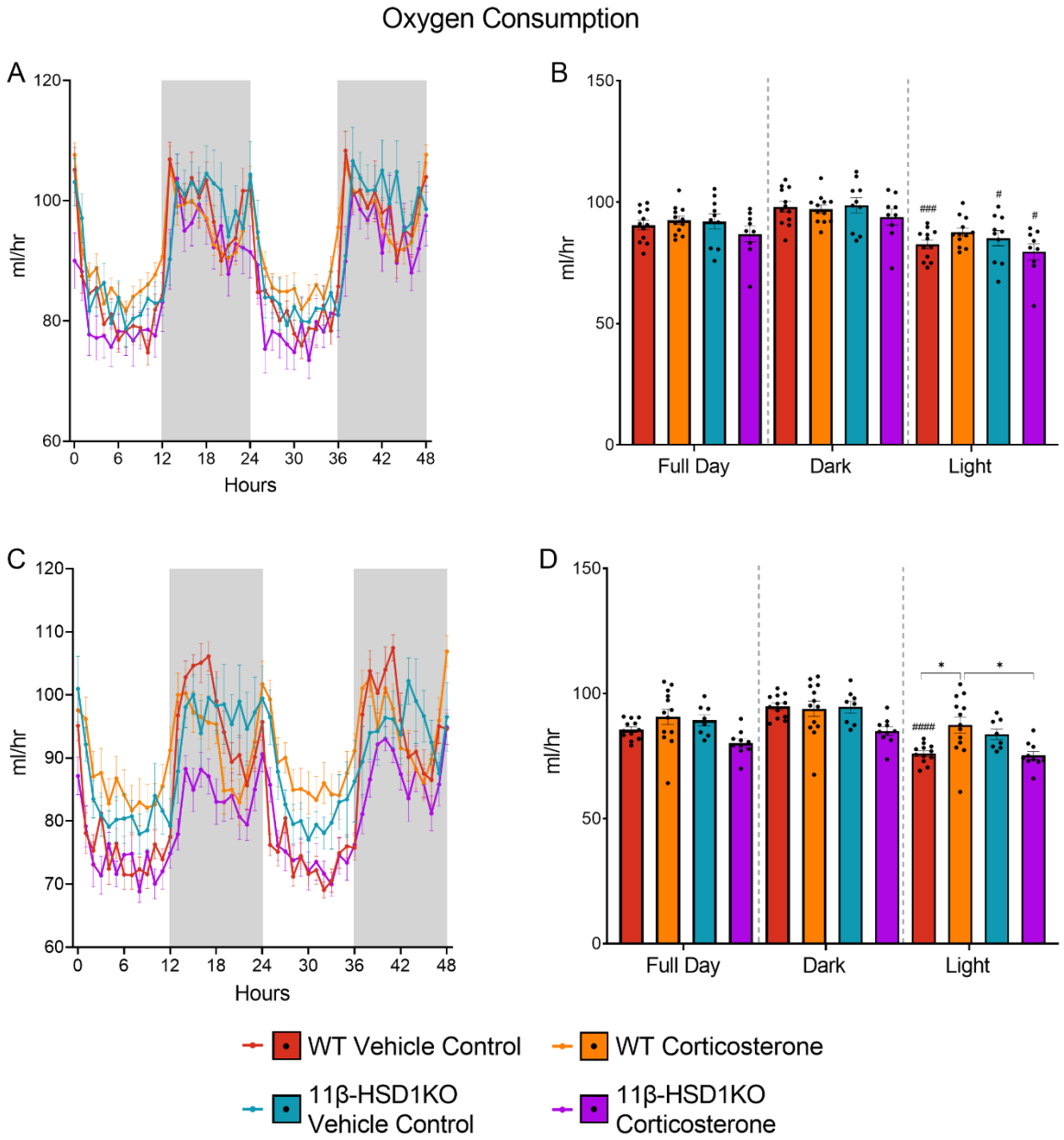

Figure 5.9: Oxygen consumption of WT and 11β-HSD1KO mice following 3 weeks of corticosterone treatment. **B**: Male average oxygen consumption. **C**: Female hourly oxygen consumption. **D**: Female average oxygen consumption. Line graphs are presented as mean ± SD, n=10-12. Bar charts are presented as mean with individual values ± SD, n=10-12. Significance determined via two-way ANOVA. * significantly different to control, # significantly different to dark. *p<.05, ** p<.01, *** p<.001, **** p<.0001.

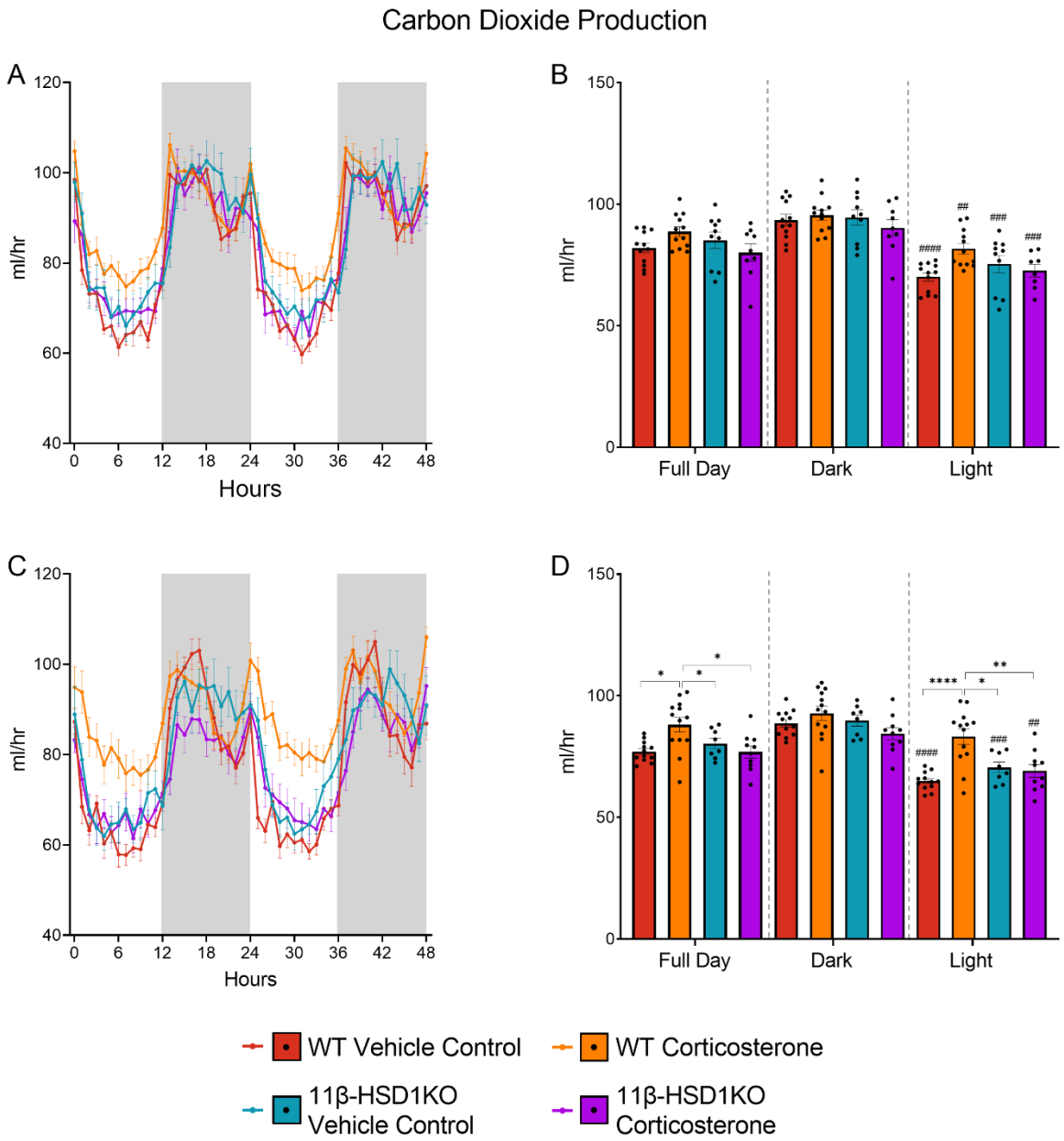

Figure 5.10: Carbon dioxide production of WT and 11β-HSD1KO mice following 3 weeks of corticosterone treatment. **A**: Male hourly carbon dioxide production. **B**: Male average carbon dioxide production. **C**: Female hourly carbon dioxide production. **D**: Female average carbon dioxide production. Line graphs are presented as mean ± SD, n=10-12. Bar charts are presented as mean with individual values ± SD, n=10-12. Significance determined via two-way ANOVA. * significantly different to control, # significantly different to dark. *p<.05, ** p<.01, *** p<.001, **** p<.0001.

5.3.8 11β-HSD1KO mice are largely protected against corticosterone induced hyperphagia and polydipsia

Assessment of food and water intake, using the TSE Phenomaster, revealed that 11β-HSD1KO mice are mostly protected against glucocorticoid induced hyperphagia (Fig. 5.11) and fully protected against glucocorticoid induced polydipsia (Fig 5.12). In male mice 11β-HSD1KO fully prevented corticosterone induced hyperphagia as food intake did not differ from the WT or 11β-HSD1KO controls during the dark or light phases (Fig. 5.11A and B). However, whilst male 11β-HSD1KO treated with corticosterone ate less than their WT counterparts, it was not significantly less at any time point (Fig. 5.11B). In female 11β-HSD1KO mice treated with corticosterone food intake was lower than in WT mice, however not significantly (Fig. 5.11C and D). However, contrary to the findings in male mice food intake was significantly elevated by corticosterone in 11β-HSD1KO mice compared to 11β-HSD1KO controls during the dark phase (Fig. 5.11D). It remained elevated during the light phase, however non-significantly (Fig. 5.11D). Despite this it did not significantly differ to WT controls (Fig. 5.11C and D). Unfortunately, it was only possible to assess food intake in two of the female 11β-HSD1KO controls due to food hopper malfunctions, meaning present findings must be taken cautiously. Additionally, both WT and 11β-HSD1KO controls did not differ (Fig. 5.11C and D). Increased water intake seen in male and female WT mice treated with corticosterone was fully prevented by 11β-HSD1KO as male and female 11β-HSD1KO mice treated with corticosterone or vehicle control, as well as WT controls, all had similar water intake values that were all significantly less that WT mice treated with corticosterone during both the dark and light phases (Fig. 5.12A-D). Linear regression and subsequent ANCOVA determined no significant differences in slope angle between treatments or mouse strains revealing no significant effect of body weight on food or water intake (Fig. 13I-L).

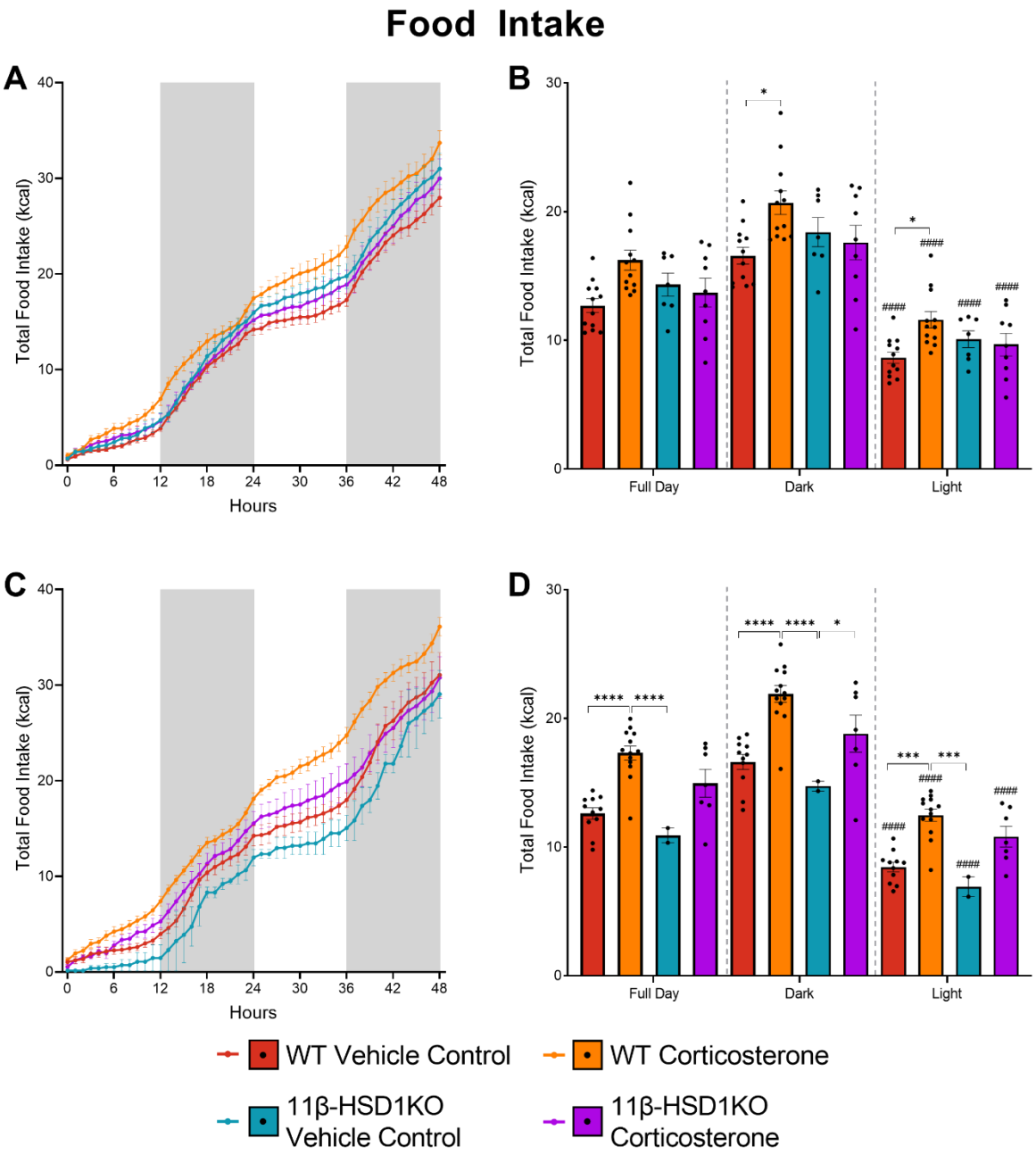

Figure 5.11: Food intake of WT and 11β-HSD1KO mice following 3 weeks of corticosterone treatment. **A**: Male hourly energy expenditure. **B**: Male average energy expenditure. **C**: Female hourly energy expenditure. **D**: Female average energy expenditure. Line graphs are presented as mean ± SD, n=2-12. Bar charts are presented as mean with individual values ± SD, n=2-12. Significance determined via two-way ANOVA. * significantly different, # significantly different to dark. *p<.05, ** p<.01, *** p<.001, **** p<.0001.

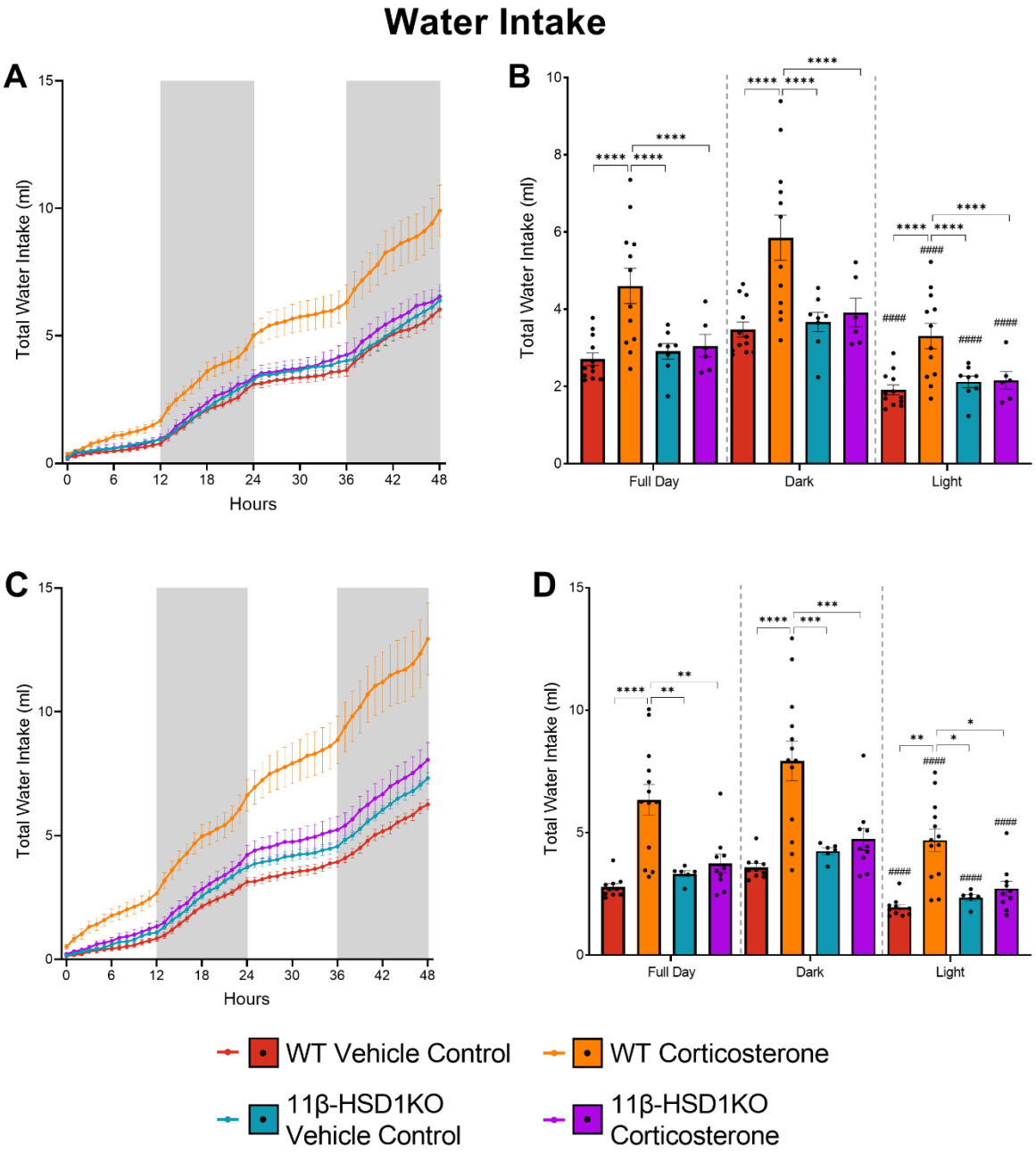

Figure 5.12: Water intake of WT and 11β-HSD1KO mice following 3 weeks of corticosterone treatment. **A**: Male hourly energy expenditure. **B**: Male average energy expenditure. **C**: Female hourly energy expenditure. **D**: Female average energy expenditure. Line graphs are presented as mean ± SD, n=7-12. Bar charts are presented as mean with individual values ± SD, n=7-12. Significance determined via two-way ANOVA. * significantly different, # significantly different to dark. *p<.05, ** p<.01, *** p<.001, **** p<.0001.

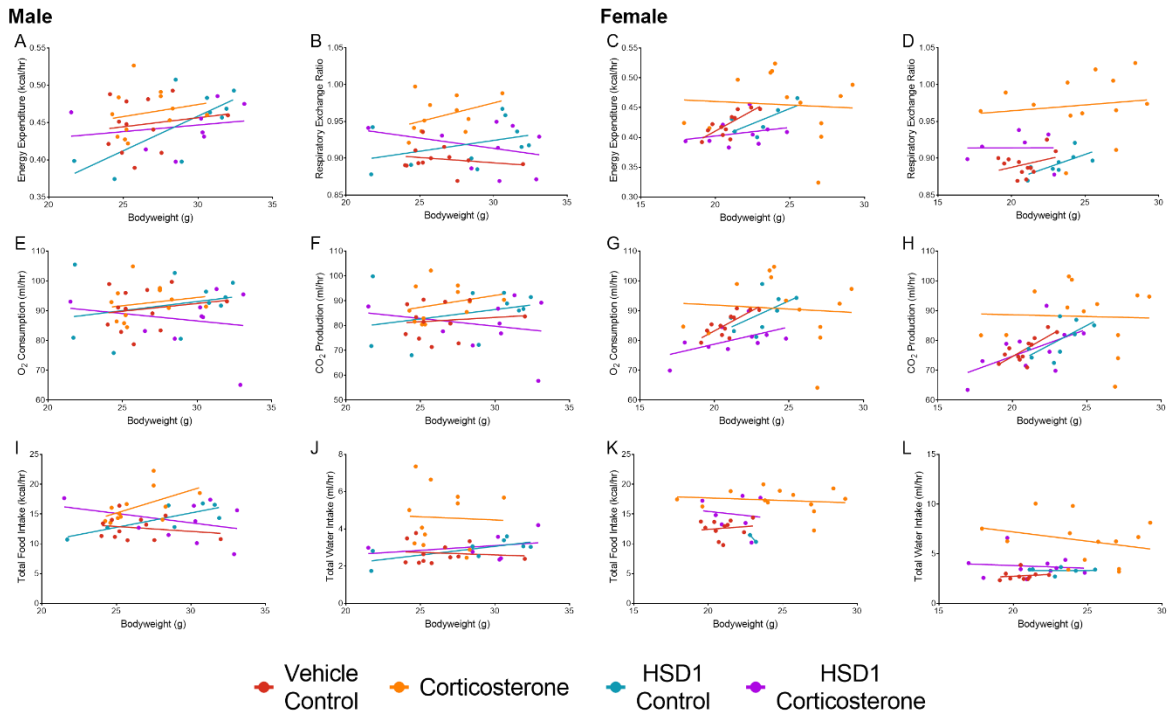

Figure 5.13: Analysis of covariance to determine the influence of bodyweight on markers of energy metabolism following 3 weeks of corticosterone in WT and 11β-HSD1KO mice. **A**: Male energy expenditure. **B**: Male respiratory exchange ratio. **C**: Female energy expenditure. **D**: Female respiratory exchange ratio n=12. **E**: Male oxygen consumption. **F**: Male carbon dioxide production. **G**: Male oxygen consumption. **H**: Male carbon dioxide production. **I**: Male food intake. **J**: Male water intake. **K**: Female food intake. **L**: Female water intake. Significance determined via ANCOVA. * significantly different, *p<.05, ** p<.01, *** p<.001, **** p<.0001. Abbreviations: O_2, oxygen; CO_2, carbon dioxide.

5.4 Discussion

The findings presented in this chapter identify that some of the effects of glucocorticoid excess on the NAD^+ metabolome, first identified in chapter 4, and the effects on energy metabolism, first identified in chapter 3, are reliant on the presence of the enzyme 11β-HSD1 in a rodent model of glucocorticoid excess. These findings indicate that the corticosterone driven tissue specific increase in NADH and alterations to the gene expression of enzymes within the NAD^+ biosynthetic network are, for the most part, mediated by the enzyme 11β-HSD1. Additionally, corticosterone induced elevations to EE, RER, oxygen consumption and

carbon dioxide production, as well as hyperphagia and polydipsia are also influenced to differing extents by the presence of 11β-HSD1. Therefore, the crucial reductase activity of 11β-HSD1, which is required to continually activate glucocorticoids at the tissue level, is involved in some of the underlying mechanism that drive the findings presented in chapters 3 and 4.

Given the novel nature of the findings presented in this chapter it is not possible to draw direct comparisons with any existing literature. Despite this they do continue a series of findings that show 11β-HSD1 inhibition, deletion or a defectiveness attenuates the effects of sustained glucocorticoid excess (Tomlinson et al., 2002, Morgan et al., 2009, Morgan et al., 2013, Morgan et al., 2014, Morgan et al., 2016a, Webster et al., 2021). As 11β-HSD1KO mice in this chapter did not experience increased NADH, altered gene expression (for the most part), elevated EE and RER, polydipsia and hyperphagia (attenuated but not prevented in females), it suggests these might be contributing factors to, or even side effects of, other glucocorticoid excess induced metabolic conditions. This is likely the case with EE at the very least as conditions such as obesity, diabetes and insulin resistance, which can be caused by glucocorticoid excess and subsequently attenuated by 11β-HSD1 inhibition, have been reported to alter EE (Morgan et al., 2009, Morgan et al., 2013, Morgan et al., 2014, Carneiro et al., 2016, Caron et al., 2016). However, without additional investigation to confirm otherwise, these findings might just be additional, separate consequences of sustained glucocorticoid excess. Further investigation into glucocorticoid induced hyperphagia in female WT and 11β-HSD1KO mice is definitely required to determine its impact on other glucocorticoid induced conditions due to food hopper malfunctions which prevented

definitive statistically analysis. Asides from this, given the findings of chapter 4, it is unlikely that increased NADH is causative of other glucocorticoid excess induced effects.

Interestingly the findings of this chapter identify some effects of sustained glucocorticoid excess that are not prevented by 11β-HSD1KO, specifically NRK2 gene expression within skeletal muscle and IDO expression within the liver. Whilst no other study has assessed these with regards to glucocorticoid excess or 11β-HSD1 inhibition, these findings are in contrast to the aforementioned literature reporting the attenuation of the effects of sustained glucocorticoid excess through 11β-HSD1 inhibition (Tomlinson et al., 2002, Morgan et al., 2009, Morgan et al., 2013, Morgan et al., 2014, Morgan et al., 2016a, Webster et al., 2021). It is very interesting to see that NRK2 expression was still decreased by corticosterone in 11β-HSD1KO mice, even though the other gene in skeletal muscle affected by corticosterone, NAMPT, was restored to control levels by 11β-HSD1KO. This implies separate regulatory processes of these genes that are affected differently by glucocorticoid excess. However, the exact reason why NRK2 is decreased, in both WT and 11β-HSD1KO mice requires investigation, especially as in other metabolic conditions, or cases of physiological trauma it is often reported increased (Fletcher and Lavery, 2018). It is also very interesting to see that IDO expression was still decreased by corticosterone in 11β-HSD1KO mice, even though the other affected genes within the liver were restored to control levels by 11β-HSD1KO. Like NRK2 and NAMPT in skeletal muscle, this implies separate regulatory processes of these genes that are affected differently by glucocorticoid excess. The exact reason why IDO expression responded differently is unclear, however this could be due to its role in the immune regulation (Chen, 2011) which can be suppressed by glucocorticoid excess (Oppong

and Cato, 2015). However, why this isn't reversed by 11β-HSD1KO, like other enzymes in the de novo biosynthesis pathway, is unclear.

Another interesting finding in this chapter was that 11β-HSD1KO decreases NAD^+ and NADH in WAT regardless of treatment. These decreases in fact matched the decrease seen in WT mice treated with corticosterone. The reason for this is unclear, especially as 11β-HSD1KO reversed many of the corticosterone induced decreases in gene expression, indicating that NAD^+ synthesis is likely unaltered. However, as this chapter only assessed genes that had previously been altered by corticosterone in chapter 4, it is possible other genes within WAT might be decreased by 11β-HSD1KO. Additionally, enzyme activity, which was not assessed, might have been altered. It is possible 11β-HSD1KO resulted in increased NAD^+ breakdown as an 11β-HSD1 inhibitor drug has been reported to increased SIRT1 activity in the liver (Chen et al., 2022). However, this might be an effect of the specific inhibitor and not the global knock-out used in this chapter. Additionally, this might not be the case within WAT and requires further investigation. Alternatively, the apparent decrease in both NAD^+ and NADH might be down to sample error as the decrease in WT NADH is opposite to the effect seen in chapter 4. However, as the control values between chapters are similar, and the effect in other tissues was similar between chapters, this might not be the case. Regardless, this can be considered a limitation of the chapter as the findings regarding WAT NAD^+ and NADH merit repeat investigation to assure confidence. In addition, some of the genes assessed in this chapter did not respond to corticosterone as observed in chapter 4. The expression of liver NRK1, KYU and KMO, as well as WAT NMNAT1 and NADK did not change it WT mice treated with corticosterone despite previously declining in chapter 4. Whilst this did not prevent

subsequent assessment of these genes in 11β-HSD1KO mice it does cast doubt on some of the NAD^+ metabolome findings that are presented in this chapter and chapter 4. Whilst most of the genes responded the same in both chapters repeat investigation would be beneficial to address this potential limitation and provide further clarity. In addition, to ensure complete confidence in any sex differences repeat investigation should include male WT samples which were unfortunately not available in the present analysis and can be considered another limitation of the chapter.

In conclusion, this chapter provides evidence that the effects of sustained glucocorticoid excess on the NAD^+ metabolome and energy metabolism are for the most part dependent on the presence of the enzyme 11β-HSD1. Therefore, implicating it in the underlying mechanisms that facilitate the effects observed in chapters 3 and 4, whilst also expanding the ever-growing body of 11β-HSD1 inhibition literature. However, this chapter also identifies that some of the effects of sustained glucocorticoid excess, such as decreased skeletal muscle NRK2 and liver IDO gene expression, occur independently of 11β-HSD1 creating further mechanistic questions. Future investigation is required to answer this and address the limitations identified within this chapter.

CHAPTER 6 – FINAL DISCUSSION

The impact of sustained glucocorticoid excess, or Cushing's syndrome has been continually well researched since it was first described by Harvey Williams Cushing in 1912 (Cushing, 1994, Lacroix et al., 2015). Known to cause numerous severe metabolic conditions including hyperglycaemia (Burke et al., 2017), diabetes mellitus (Di Dalmazi et al., 2012), hypertension (Goodwin and Geller, 2012), obesity (Abraham et al., 2013), skeletal muscle atrophy (Schakman et al., 2013, Morgan et al., 2016a), osteoporosis (Hardy et al., 2018), mitochondrial disfunction (Du et al., 2009, Tang et al., 2013, Spiers et al., 2014) and many more (Oray et al., 2016), sustained glucocorticoid excess has a deleterious impact on metabolic health and is ultimately life threatening (Barbot et al., 2020, Hakami et al., 2021). Despite this extensive knowledge, the list of known effects of sustained glucocorticoid excess is far from complete with the impact on global markers of energy metabolism, such as EE and RER, unclear. The knowledge of the impact on the metabolically crucial NAD^+ metabolome (Xie et al., 2020a) is also yet to be established. Serving as both a redox cofactor and signalling substrate (Elhassan et al., 2017), NAD^+ is implicated in the regulation and function of a plethora of metabolic processes that are key to sustained metabolic health and homeostasis (Xie et al., 2020a). Interestingly a decline in NAD^+, or alteration to its metabolome, are attributed to metabolic decline and conditions that can also be caused by sustained glucocorticoid excess (Yoshino et al., 2011, Frederick et al., 2016, Okabe et al., 2019). Therefore, an improved understanding of their interactions, and the impact one has on the other might be beneficial to improving metabolic health through therapeutic, or other, means.

Existing literature regarding the impact of glucocorticoid excess on energy metabolism remains limited, leaving no clear consensus on whether the plethora of metabolic conditions

or the hormonal disruption caused by sustained glucocorticoid excess are reflected in markers such as EE and RER (Burt et al., 2006, Poggioli et al., 2013, Radhakutty et al., 2016). Given this lack of clarity the initial objective of this thesis was to better define the impact of sustained glucocorticoid excess on markers of energy metabolism in male and female mice. Additionally, as the NAD^+ metabolome is crucial to global energy metabolism (Canto et al., 2015, Xie et al., 2020a) and the impact of sustained glucocorticoid excess on the NAD^+ metabolome is also unclear an additional aim of this thesis was to further define the impact of sustained glucocorticoid excess on the NAD^+ metabolome *in vivo*, in multiple tissues and in both male and female mice. Existing literature does highlight some known interactions between glucocorticoids and the NAD^+ metabolome (Agarwal and Auchus, 2005), whilst others provide growing or theorised evidence for other mechanisms of interaction (Suzuki et al., 2018, Huang and Tao, 2020, Wang et al., 2021). Interaction through the enzymes 11β-HSD1 and 2 is well research and critical to glucocorticoid function (Agarwal and Auchus, 2005). Sirtuins are another, less understood, mechanisms of interaction as there is growing evidence that through sirtuins, NAD^+ might be able to influence the potency of glucocorticoids through interaction with the GR (Dali-Youcef et al., 2007, Suzuki et al., 2018, Huang and Tao, 2020, Wang et al., 2021, Mishra et al., 2022). Beyond this further evidence of interactions is lacking and only remains theoretical with factors such as oxidative stress as potential candidates. However, despite the known and theorised mechanisms of interactions, only limited evidence of the impact of glucocorticoid excess on the NAD^+ metabolome exists *in vivo*, either showing no effect, decrease, or even an increase, dependent on the tissue or aspect of the NAD^+ metabolome being investigated (Xiao et al., 2019, Herrera et al., 2020b, Xie et al., 2020b). When combined with the initial aim this would indicate if any glucocorticoid induced changes to the NAD^+ metabolome align with any changes to energy metabolism, potentially

determining whether they are involved in any underlying mechanisms. Furthermore, sustained glucocorticoid excess is known to induce several metabolic effects, some of which has been reported improved by NAD^+ metabolome augmentation when caused independently of glucocorticoid excess (Canto et al., 2012, Wu et al., 2016, Lin et al., 2021, Dall et al., 2022). Additionally, some emerging evidence now suggests that some conditions directly caused by glucocorticoid excess can be counteracted through NAD^+ metabolome augmentation with NAD^+ precursors (Huang and Tao, 2020, Uto et al., 2021). Therefore, another aim of this thesis was to determine if NAD^+ precursor supplementation, specifically NR, can alter the Cushingoid phenotype induced by glucocorticoid excess, or any of the potential effects on the NAD^+ metabolome or markers of energy metabolism uncovered in this thesis. Finally, as many of the effects of glucocorticoid excess are known to be mediated by the enzymes 11β-HSD1 (Tomlinson et al., 2002, Morgan et al., 2009, Morgan et al., 2014, Morgan et al., 2016a, Webster et al., 2021) the final aim of this thesis was to determine if any of the effects of sustained glucocorticoid excess on the NAD^+ metabolome, or markers of energy metabolism can be prevented by 11β-HSD1KO *in vivo*.

Sustained glucocorticoid excess, in the form of excessive corticosterone treatment, result in significant elevations to EE and RER, as well as the constituent parts of RER, oxygen consumption and carbon dioxide production, were observed in male and female mice, largely in disagreement with the existing literature (Burt et al., 2006, Poggioli et al., 2013, Radhakutty et al., 2016). This indicates that mice exposed to sustained glucocorticoid excess expend and increased number of calories, which is fuelled primarily be carbohydrate metabolism, despite developing a pronounced phenotype which includes fat accumulation. Interestingly, the

elevation to energy expenditure, RER, oxygen consumption, carbon dioxide production and fat accumulation, were more pronounced in female mice, potentially aligning with literature reporting differing presentation of Cushing's syndrome symptoms in humans (Pecori Giraldi et al., 2003, Valassi et al., 2011, Broersen et al., 2019). Interestingly, in both males and females, the effect on energy expenditure and RER was more pronounced during the day as it did not decline from night to day to the same extent as controls. This thesis however confirms these effects are not caused by increased activity, at least in females as activity was not assessed in males due to time restraints with collaborators. Literature also indicates it is unlikely to be because of BAT thermogenesis (Doig et al., 2017, Rahbani et al., 2021, Poggioli et al., 2013). This thesis therefore provides further evidence to support another theory that these effects are caused by the observed glucocorticoid excess induced hyperphagia which is keeping mice in a constant post prandial state that increases de novo lipogenesis, which subsequently elevates EE and RER, as well as the constituent parts of RER, oxygen consumption and carbon dioxide production, whilst also causing exaggerated effects in female mice (Ho, 2018) (Fig. 6.1). Unfortunately, this thesis was not able to further investigate or confirm this theory by fasting mice, something that is known to not alter EE in control animals (Liu et al., 2019), due to licence restraints.

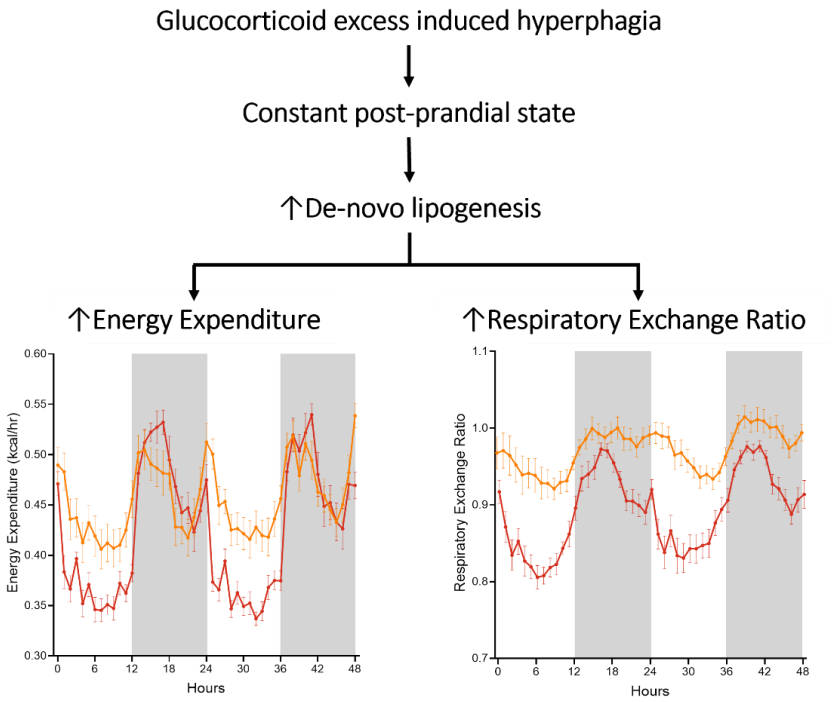

Figure 6.1: The potential role of glucocorticoid excess induced hyperphagia and de-novo lipogenesis in elevating energy expenditure and the respiratory exchange ratio in a mouse model of sustained glucocorticoid excess.

As for the NAD^+ metabolome, this thesis identified tissue specific, and even sex specific, alterations as a result of sustained glucocorticoid excess *in vivo*. The first initial finding was that NAD^+ content was unaltered by corticosterone treatment, apart form in female WAT in which it was decreased. Interestingly however in both male and female skeletal muscle, as well as WAT, NADH content was increased indicating altered redox reactions in these tissues thus shifting the cellular environment to a more reductive state. However, this thesis does not identify which redox reactions are altered or if separate NAD^+ pools within the cell are equally altered. Regardless, it is possible this shift could be involved in further metabolic dysfunction, including conditions induced by sustained glucocorticoid excess (Wu et al., 2016, Levine et al., 2021, Lin et al., 2021). It is also possible that these alterations to the NAD^+ metabolome might contribute to the identified alterations to markers of energy metabolism

as the two are usually closely linked (Canto et al., 2015, Xie et al., 2020a). The observed increase in NADH in particular could be responsible for, or at least contributing towards, altered energy metabolism as NADH accumulation is reported to cause disruption of energy homeostasis and typical circadian patterns (Levine et al., 2021). Whilst no other study had assessed the impact on NADH *in vivo* making it impossible to make direct comparisons, NAD^+ metabolome findings did find some agreement with the existing literature as skeletal muscle NAD^+ remained unaltered (Herrera et al., 2020b). However, beyond this the findings also find disagreement with the literature as liver NAD^+ was found to be unaltered, rather than decreased (Xiao et al., 2019, Xie et al., 2020b). This lack of effect in the liver was especially interesting as the majority of NAD^+ biosynthetic enzyme gene expression was downregulated by corticosterone within the liver. However, as this did not translate to a decline in NAD^+, it suggests that enzyme activity might be preserved. Unfortunately, given that glucocorticoids are primarily transcriptional regulators (Groeneweg et al., 2012), a limitation of this thesis is that enzyme activity was not assessed meaning this informative detail was not revealed. Additionally, other aspects of the NAD^+ metabolome, such as $NADP^+$ or NADPH were not investigated and as such cannot presently be used to further the existing literature.

The impact of NR supplementation on the effects of sustained glucocorticoid excess was largely null throughout this thesis. This was first observed with regards to the NAD^+ metabolome as NR was unable to counter all but one of the effects of corticosterone treatment. It was only able to reverse the increase in NADH seen with corticosterone treatment. In agreement with the literature (Canto et al., 2012), it in fact decreased NADH compared to the control, both alone and in combination with corticosterone, leaving the cell

in an oxidative rather than reductive state. Whilst this might have alluded to a therapeutic potential of NR treatment as it was able to reverse the NADH increase which is known to cause metabolic disruption (Wu et al., 2016, Levine et al., 2021, Lin et al., 2021) this was not the case. The typical phenotype induced by sustained glucocorticoid excess was not altered by NR supplementation and neither were the effects on markers of energy metabolism in male or female mice. This suggests two things. Firstly, that NR supplementation is not an effective therapeutic treatment strategy for combating the effects of glucocorticoid excess, despite its reported benefits in other metabolic conditions (Canto et al., 2012, Wu et al., 2016, Lin et al., 2021, Dall et al., 2022). Secondly, that NAD^+ metabolome disruption, specifically the increase in skeletal muscle and WAT NADH, is not a causative factor in the metabolic consequences of sustained glucocorticoid excess, but likely just another consequence of glucocorticoid excess. This therefore also indicates that glucocorticoid excess causes a disconnect between the normally connected NAD^+ metabolome and markers of energy metabolism (Canto et al., 2015, Xie et al., 2020a). This is because, NR did not alter the effects of sustained glucocorticoid excess on markers of energy metabolism, despite altering NADH content. However, due to disagreement with the literature regarding the impact of NR supplementation on NAD^+ content, these conclusions must be presently taken with caution. Whilst the findings of this thesis regarding the impact of NR on NADH agree with the literature (Canto et al., 2012), the observed lack of impact on NAD^+ content disagrees and does not show increased levels seen in the majority of existing literature (Canto et al., 2012, Doig et al., 2020, Cartwright et al., 2021). This lack of NAD^+ boosting could explain the lack of NR effect as existing studies that report a benefit of NR treatment also report an elevation in NAD^+ (Canto et al., 2012, Gariani et al., 2016). Additionally, as only NR was used throughout this thesis in cannot be definitively concluded that NAD^+ metabolome augmentation with NAD^+

precursors is a fruitless endeavour, especially as another precursor, NMN has been reported to combat some of the effects of sustained glucocorticoids (Huang and Tao, 2020, Uto et al., 2021). Whilst the use of NR throughout this thesis cannot be considered a limitation, the inclusion of NMN treated mice as well would have been considered a strength.

In contrast to NR, 11β-HSD1KO was far more effective at preventing the effects of sustained glucocorticoid excess in both male and female mice. This included the typical phenotype, in agreement with the literature (Tomlinson et al., 2002, Morgan et al., 2009, Morgan et al., 2014, Morgan et al., 2016a), as well as the novel effects on markers of energy metabolism and most of the effects on the NAD^+ metabolome identified in this thesis. In both male and female mice, the protective effect of 11β-HSD1KO with regards to energy metabolism was complete, confirming that glucocorticoid excess induced elevations are reliant on the presence of 11β-HSD1. This also indicates that elevations to markers of energy metabolism are either consequences of the metabolic conditions induced by sustained glucocorticoid excess, or alternatively caused directly by glucocorticoid excess. Additionally, as glucocorticoid excess induced hyperphagia was largely attenuated it provides further evidence for the potential mechanism shown in Fig. 6.1. As for the NAD^+ metabolome, this thesis confirmed that most of the effects of glucocorticoid excess are also dependent on the presence of 11β-HSD1, including the increase in skeletal muscle and WAT NADH. Interestingly however, it was revealed that the corticosterone induced alteration to the expression of two NAD^+ biosynthetic genes was not prevented by 11β-HSD1KO and as such the skeletal muscle NRK2 and liver IDO require further investigation. Unfortunately, due to sample availability this was only fully explored in female samples, which can be considered a limitation of this

part of the thesis. Another interesting finding was that 11β-HSD1KO decreased NAD^+ and NADH in female WAT, something that contrasts with the other findings of the thesis and is not previously reported in the literature. The reason for this decline is unclear and merits further investigation especially as sample error cannot be ruled out. Regardless of this puzzling finding, this thesis provides evidence that in both male and female mice exposed to sustained exogenous glucocorticoid excess, 11β-HSD1 reductase activity is required to maintain glucocorticoid activity and thus its mechanisms of action, which in turn drives most of the novel effects identified (Fig. 6.2). This thesis therefore provides further evidence that 11β-HSD1KO or inhibition is an effective therapeutic approach to counter the effects of sustained glucocorticoid excess. As such it currently appears a far more beneficial approach than NAD^+ metabolome augmentation.

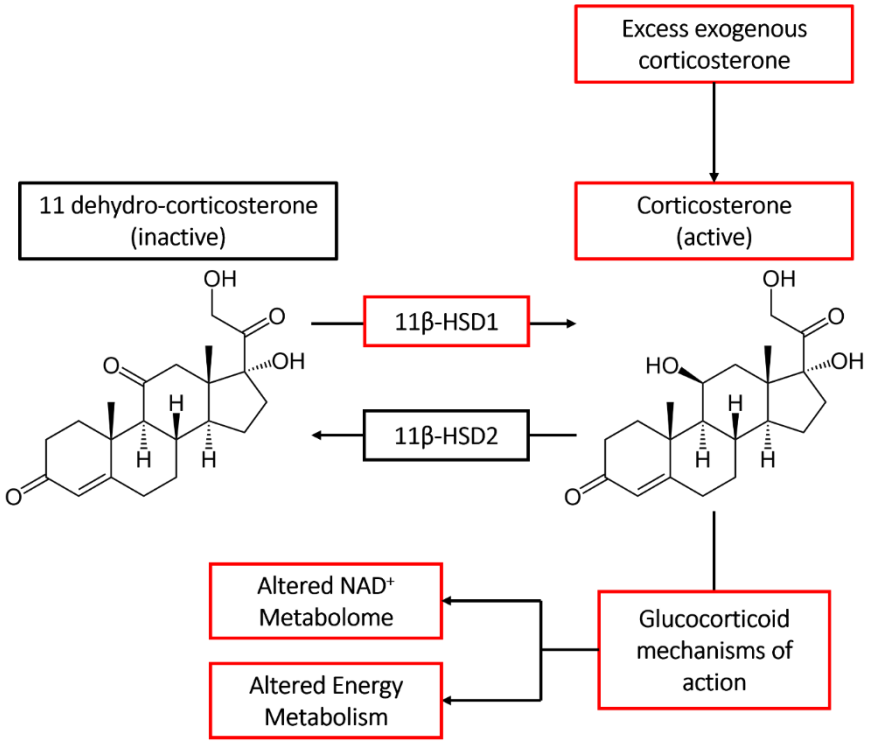

Figure 6.2: The role of 11β-HSD1 in facilitating the effect of sustained glucocorticoid excess on the NAD^+ metabolome and energy metabolism by maintaining glucocorticoid activation.

Despite conclusions being drawn from the findings of this thesis it is evident that some are not definitive and require additional investigation. Additionally, it is evident that a few limitations are present and need addressing through future investigation to both reinforce the existing conclusions as well as provide further insight into glucocorticoid excess, energy metabolism, NAD^+ metabolome and the relationship between them. Firstly, further work is required to complete investigation into the effects of sustained glucocorticoid excess on the NAD^+ metabolome *in vivo*. Whilst the findings in this thesis identify the effects on NAD^+, NADH and the expression of NAD^+ biosynthetic enzymes much is left untouched by this thesis. As previously mentioned, enzyme activity or protein content was not assessed and should be a primary focus of future investigation, especially given that the severe disruption to enzyme expression did not result in NAD^+ or NADH alteration in the liver. Similarly, the expression, protein content and activity of NAD^+ consuming enzymes, discussed in section 1.16, would also be worth investigating further. However, as some literature already exists indicating they are altered by glucocorticoid excess (Kang et al., 2008, Lee et al., 2018a, Jiang et al., 2019, Pan et al., 2019, Pasquereau et al., 2021) this takes less priority than the former point. Other aspects of the NAD^+ metabolome, untouched by this thesis, also merit investigation. Firstly, the content of NAD^+ intermediates within each synthesis and breakdown pathway (Fig. 1.10) should be explored to help determine respective contributions to NAD^+ synthesis and degradation under the influence of sustained glucocorticoid excess. Additionally, NAD^+ clearance (Fig. 1.15) should also be investigated. Whilst the findings presented in this thesis do not appear to indicate altered NAD^+ clearance, as NAD^+ content is mostly unchanged, this cannot be confirmed without the necessary research and would require assessment of MeNAM, as well as NNMT expression, protein content and activity. Similarly, NAD^+ phosphorylation to $NADP^+$ and subsequent redox conversion to NADPH requires further

investigation. Whilst NADK expression was assessed, its protein content and activity, as well as $NADP^+$, NADPH content need assessment to provide a more complete picture. Especially as $NADP^+$ and NADPH are required for 11β-HSD1 function and are also key to redox reactions (Agarwal and Auchus, 2005, Agledal et al., 2010) that could be altered, as indicated by *in vitro* evidence (Roma et al., 2012, Yang et al., 2017), like those involving NAD^+ and NADH. However, in both cases future investigation is required, and should be prioritised, to establish which specific redox reactions are likely altered. Similarly, there is a need to establish if the effects on the NAD^+ metabolome are global across the cell or determined by subcellular location discussed in section 1.14. Beyond the effects of sustained glucocorticoid excess on the NAD^+ metabolome future investigation should also further explore the effect of NAD^+ augmentation on the effects of glucocorticoid excess reported in this thesis or existing literature. Given that oral NR supplementation had little to no effect in this thesis, this could include an alternate NR treatment strategy, such as IP injections which have been shown to boost NAD^+ *in vivo* (Doig et al., 2020). Alternatively further investigation is needed to clarify if other NAD^+ precursors elicit the same or different response, specifically NMN as it has been shown to alter some effect of glucocorticoid excess (Huang and Tao, 2020, Uto et al., 2021). As for the effects of sustained glucocorticoid excess on markers of energy metabolism, future work should prioritise testing the theory proposed by Ho (2018) and supported by the findings in this thesis (Fig. 6.1). This could include fasting mice which theoretically would prevent hyperphagia and subsequent de novo lipogenesis, in turn preventing elevations to EE and RER. Additionally, pair matched feeding could also be tested to investigate this. Beyond this mechanism, future investigation should also seek to determine the exact mechanisms involved in the effects of sustained glucocorticoid excess on the NAD^+ metabolome and energy metabolism that are reported in this thesis. Whether these be genomic or non-

genomic in nature or involves some of the established and theoretical mechanisms of interaction discussed in section 1.19, needs to be established to guide therapeutic development.

Alongside further *in vivo* mouse investigation this thesis also informs future investigation towards translational research in humans and could subsequently inform therapeutic approaches which is the ultimate aim of the research throughout this thesis. As mentioned in section 1.5.5 and indicated when comparing some of the findings of this thesis to the literature, species specific differences exist in the effects of sustained glucocorticoid excess. Therefore, the impact of glucocorticoid excess on energy metabolism and the NAD^+ metabolome within human volunteers is required. As giving high doses of excess glucocorticoids to humans presents an ethical concern given the severity of Cushing's syndrome, human investigation could be conducted in patients who either already have Cushing's syndrome or are undergoing medical treatment with exogenous glucocorticoids. By using methods similar to Burt et al. (2006) and Radhakutty et al. (2016) energy metabolism could be assessed to determine if the findings of this thesis align with human investigation, as currently they do not agree with existing literature. This knowledge could be beneficial for treating patients with glucocorticoid excess, especially if the impact on energy metabolism is hyperphagia driven like it might be in this thesis. If this is the case it might prove fruitful to test dietary interventions in treating the effects of glucocorticoid excess in humans. Likewise, the NAD^+ metabolome could also be assessed from tissue samples from the same patients, by methods employed in this thesis. Additionally, the feasibility of NAD^+ metabolome augmentation with NR or NMN to combat the effects of glucocorticoid excess could also be

assessed in these patients as they are both well tolerated and it is unclear if they will drive different effects to those seen in mice (Elhassan et al., 2019, Cartwright et al., 2021). As outlined in section 1.9 current treatment strategies for glucocorticoid excess are far from perfect, making it important to assess viability of NAD^+ metabolome augmentation in humans before it is discounted. Finally, patients who are undergoing energy metabolism and/or NAD^+ metabolome assessment could also be given 11β-HSD1 inhibitors as there is growing promising research regarding their benefits (Othonos et al., 2023) meaning the findings presented in this thesis might be replicated in humans, thus providing further knowledge of glucocorticoid excess in humans and support for further development of 11β-HSD1 inhibitors.

In summary, this thesis has achieved its aims and provided more evidence that sustained glucocorticoid excess altered both energy metabolism and the NAD^+ metabolome, finding agreement and disagreement with the existing literature. Through identification of both tissue specific and sex specific effects this thesis adds valuable, previously unknown, insights to the literature. It also for the first time shows that these effects are mediated by the enzyme 11β-HSD1, meaning 11β-HSD1 inhibition is potentially of therapeutic benefit. However, this thesis also provides evidence that NAD^+ precursor supplementation might not be of therapeutic benefit, at least for combatting the effects of sustained glucocorticoid excess. Additionally, this thesis also highlights the need for further research that should focus on further characterising the effect of sustained glucocorticoid excess on energy metabolism and the NAD^+ metabolome, as well as explore the specific mechanisms involved.

CHAPTER 7 - REFERENCES

AANS. 2022. *Cushing's Syndrome/Disease* [Online]. Available: https://www.aans.org/en/Patients/Neurosurgical-Conditions-and-Treatments/Cushings-Disease#:~:text=Treatment%20of%20Cushing's%20Syndrome&text=If%20the%20cause%20is%20iatrogenic,for%20control%20of%20that%20disorder [Accessed 15.08.22].

ABAD, V., CHROUSOS, G. P., REYNOLDS, J. C., NIEMAN, L. K., HILL, S. C., WEINSTEIN, R. S. & LEONG, G. M. 2001. Glucocorticoid excess during adolescence leads to a major persistent deficit in bone mass and an increase in central body fat. *J Bone Miner Res,* 16**,** 1879-85.

ABEL, E. D. 2010. Free fatty acid oxidation in insulin resistance and obesity. *Heart Metab,* 48**,** 5-10.

ABRAHAM, S. B., RUBINO, D., SINAII, N., RAMSEY, S. & NIEMAN, L. K. 2013. Cortisol, obesity, and the metabolic syndrome: a cross-sectional study of obese subjects and review of the literature. *Obesity (Silver Spring),* 21**,** E105-17.

AGARWAL, A. K. & AUCHUS, R. J. 2005. Minireview: cellular redox state regulates hydroxysteroid dehydrogenase activity and intracellular hormone potency. *Endocrinology,* 146**,** 2531-8.

AGLEDAL, L., NIERE, M. & ZIEGLER, M. 2010. The phosphate makes a difference: cellular functions of NADP. *Redox Rep,* 15**,** 2-10.

AKSOY, P., WHITE, T. A., THOMPSON, M. & CHINI, E. N. 2006. Regulation of intracellular levels of NAD: a novel role for CD38. *Biochem Biophys Res Commun,* 345**,** 1386-92.

ALEV, K., VAIN, A., ARU, M., PEHME, A., PURGE, P., KAASIK, P. & SEENE, T. 2018. Glucocorticoid-Induced Changes in Rat Skeletal Muscle Biomechanical and Viscoelastic Properties: Aspects of Aging. *J Manipulative Physiol Ther,* 41**,** 19-24.

ALMAWI, W. Y. & MELEMEDJIAN, O. K. 2002. Molecular mechanisms of glucocorticoid antiproliferative effects: antagonism of transcription factor activity by glucocorticoid receptor. *J Leukoc Biol,* 71**,** 9-15.

AMJAD, S., NISAR, S., BHAT, A. A., SHAH, A. R., FRENNEAUX, M. P., FAKHRO, K., HARIS, M., REDDY, R., PATAY, Z., BAUR, J. & BAGGA, P. 2021. Role of NAD(+) in regulating cellular and metabolic signaling pathways. *Mol Metab,* 49**,** 101195.

ANDERSON, E. J., KATUNGA, L. A. & WILLIS, M. S. 2012. Mitochondria as a source and target of lipid peroxidation products in healthy and diseased heart. *Clin Exp Pharmacol Physiol,* 39**,** 179-93.

ARAGONES, J., FRAISL, P., BAES, M. & CARMELIET, P. 2009. Oxygen sensors at the crossroad of metabolism. *Cell Metab,* 9**,** 11-22.

ARNALDI, G., SCANDALI, V. M., TREMENTINO, L., CARDINALETTI, M., APPOLLONI, G. & BOSCARO, M. 2010. Pathophysiology of dyslipidemia in Cushing's syndrome. *Neuroendocrinology,* 92 Suppl 1**,** 86-90.

AVALOS, J. L., BEVER, K. M. & WOLBERGER, C. 2005. Mechanism of sirtuin inhibition by nicotinamide: altering the NAD(+) cosubstrate specificity of a Sir2 enzyme. *Mol Cell,* 17**,** 855-68.

BAI, P., CANTO, C., BRUNYANSZKI, A., HUBER, A., SZANTO, M., CEN, Y., YAMAMOTO, H., HOUTEN, S. M., KISS, B., OUDART, H., GERGELY, P., MENISSIER-DE MURCIA, J., SCHREIBER, V., SAUVE, A. A. & AUWERX, J. 2011. PARP-2 regulates SIRT1 expression and whole-body energy expenditure. *Cell Metab,* 13**,** 450-460.

BAKER, B. Y., SHI, W., WANG, B. & PALCZEWSKI, K. 2014. High-resolution crystal structures of the photoreceptor glyceraldehyde 3-phosphate dehydrogenase (GAPDH) with three and four-bound NAD molecules. *Protein Sci,* 23**,** 1629-39.

BAKONDI, E., CATALGOL, B., BAK, I., JUNG, T., BOZAYKUT, P., BAYRAMICLI, M., OZER, N. K. & GRUNE, T. 2011. Age-related loss of stress-induced nuclear proteasome activation is due to low PARP-1 activity. *Free Radic Biol Med,* 50**,** 86-92.

BARBOT, M., ZILIO, M. & SCARONI, C. 2020. Cushing's syndrome: Overview of clinical presentation, diagnostic tools and complications. *Best Pract Res Clin Endocrinol Metab,* 34**,** 101380.

BARNES, P. J. 1998. Anti-inflammatory actions of glucocorticoids: molecular mechanisms. *Clin Sci (Lond),* 94**,** 557-72.

BARTHEL, A. & SCHMOLL, D. 2003. Novel concepts in insulin regulation of hepatic gluconeogenesis. *Am J Physiol Endocrinol Metab,* 285**,** E685-92.

BARTHOLOME, B., SPIES, C. M., GABER, T., SCHUCHMANN, S., BERKI, T., KUNKEL, D., BIENERT, M., RADBRUCH, A., BURMESTER, G. R., LAUSTER, R., SCHEFFOLD, A. & BUTTGEREIT, F. 2004. Membrane glucocorticoid receptors (mGCR) are expressed in normal human peripheral blood mononuclear cells and up-regulated after in vitro stimulation and in patients with rheumatoid arthritis. *FASEB J,* 18**,** 70-80.

BAXTER, P., CHEN, Y., XU, Y. & SWANSON, R. A. 2014. Mitochondrial dysfunction induced by nuclear poly(ADP-ribose) polymerase-1: a treatable cause of cell death in stroke. *Transl Stroke Res,* 5**,** 136-44.

BEATO, M., CANDAU, R., CHAVEZ, S., MOWS, C. & TRUSS, M. 1996. Interaction of steroid hormone receptors with transcription factors involves chromatin remodelling. *J Steroid Biochem Mol Biol,* 56**,** 47-59.

BELENKY, P., CHRISTENSEN, K. C., GAZZANIGA, F., PLETNEV, A. A. & BRENNER, C. 2009. Nicotinamide riboside and nicotinic acid riboside salvage in fungi and mammals. Quantitative basis for Urh1 and purine nucleoside phosphorylase function in NAD+ metabolism. *J Biol Chem,* 284**,** 158-164.

BERDANIER, C. D. 1989. Role of glucocorticoids in the regulation of lipogenesis. *FASEB J,* 3**,** 2179-83.

BERLETT, B. S. & STADTMAN, E. R. 1997. Protein oxidation in aging, disease, and oxidative stress. *J Biol Chem,* 272**,** 20313-6.

BESSEY, P. Q., WATTERS, J. M., AOKI, T. T. & WILMORE, D. W. 1984. Combined hormonal infusion simulates the metabolic response to injury. *Ann Surg,* 200**,** 264-81.

BETTERLE, C., PRESOTTO, F. & FURMANIAK, J. 2019. Epidemiology, pathogenesis, and diagnosis of Addison's disease in adults. *J Endocrinol Invest,* 42**,** 1407-1433.

BIEGANOWSKI, P. & BRENNER, C. 2004. Discoveries of nicotinamide riboside as a nutrient and conserved NRK genes establish a Preiss-Handler independent route to NAD+ in fungi and humans. *Cell,* 117**,** 495-502.

BITTERMAN, K. J., ANDERSON, R. M., COHEN, H. Y., LATORRE-ESTEVES, M. & SINCLAIR, D. A. 2002. Inhibition of silencing and accelerated aging by nicotinamide, a putative negative regulator of yeast sir2 and human SIRT1. *J Biol Chem,* 277**,** 45099-107.

BLEDSOE, R. K., MONTANA, V. G., STANLEY, T. B., DELVES, C. J., APOLITO, C. J., MCKEE, D. D., CONSLER, T. G., PARKS, D. J., STEWART, E. L., WILLSON, T. M., LAMBERT, M. H., MOORE, J. T., PEARCE, K. H. & XU, H. E. 2002. Crystal structure of the glucocorticoid receptor ligand binding domain reveals a novel mode of receptor dimerization and coactivator recognition. *Cell,* 110**,** 93-105.

BLONDEAU, B., SAHLY, I., MASSOURIDES, E., SINGH-ESTIVALET, A., VALTAT, B., DORCHENE, D., JAISSER, F., BREANT, B. & TRONCHE, F. 2012. Novel transgenic mice for inducible gene overexpression in pancreatic cells define glucocorticoid receptor-mediated regulations of beta cells. *PLoS One,* 7**,** e30210.

BODINE, S. C., STITT, T. N., GONZALEZ, M., KLINE, W. O., STOVER, G. L., BAUERLEIN, R., ZLOTCHENKO, E., SCRIMGEOUR, A., LAWRENCE, J. C., GLASS, D. J. & YANCOPOULOS, G. D. 2001. Akt/mTOR pathway is a crucial regulator of skeletal muscle hypertrophy and can prevent muscle atrophy in vivo. *Nature Cell Biology,* 3**,** 1014-1019.

BOGAN, K. L. & BRENNER, C. 2008. Nicotinic acid, nicotinamide, and nicotinamide riboside: a molecular evaluation of NAD+ precursor vitamins in human nutrition. *Annu Rev Nutr,* 28**,** 115-30.

BONCOMPAGNI, S., ARTHURTON, L., AKUJURU, E., PEARSON, T., STEVERDING, D., PROTASI, F. & MUTUNGI, G. 2015. Membrane glucocorticoid receptors are localised in the extracellular matrix and signal through the MAPK pathway in mammalian skeletal muscle fibres. *J Physiol,* 593**,** 2679-92.

BRADY, L. J., BRADY, P. S., ROMSOS, D. R. & HOPPEL, C. L. 1985. Elevated hepatic mitochondrial and peroxisomal oxidative capacities in fed and starved adult obese (ob/ob) mice. *Biochem J,* 231**,** 439-44.

BRAIDY, N., GUILLEMIN, G. J., MANSOUR, H., CHAN-LING, T., POLJAK, A. & GRANT, R. 2011. Age related changes in NAD+ metabolism oxidative stress and Sirt1 activity in wistar rats. *PLoS One,* 6**,** e19194.

BRENNER, C. 2022. Viral infection as an NAD(+) battlefield. *Nat Metab,* 4**,** 2-3.

BREUNER, C. W. & ORCHINIK, M. 2002. Plasma binding proteins as mediators of corticosteroid action in vertebrates. *J Endocrinol,* 175**,** 99-112.

BRILLON, D. J., ZHENG, B., CAMPBELL, R. G. & MATTHEWS, D. E. 1995. Effect of cortisol on energy expenditure and amino acid metabolism in humans. *Am J Physiol,* 268**,** E501-13.

BROERSEN, L. H. A., VAN HAALEN, F. M., KIENITZ, T., BIERMASZ, N. R., STRASBURGER, C. J., DEKKERS, O. M. & PEREIRA, A. M. 2019. Sex Differences in Presentation but Not in Outcome for ACTH-Dependent Cushing's Syndrome. *Front Endocrinol (Lausanne),* 10**,** 580.

BUREN, J., LAI, Y. C., LUNDGREN, M., ERIKSSON, J. W. & JENSEN, J. 2008. Insulin action and signalling in fat and muscle from dexamethasone-treated rats. *Arch Biochem Biophys,* 474**,** 91-101.

BURGOS, E. S., VETTICATT, M. J. & SCHRAMM, V. L. 2013. Recycling nicotinamide. The transition-state structure of human nicotinamide phosphoribosyltransferase. *J Am Chem Soc,* 135**,** 3485-93.

BURKE, S. J., BATDORF, H. M., EDER, A. E., KARLSTAD, M. D., BURK, D. H., NOLAND, R. C., FLOYD, Z. E. & COLLIER, J. J. 2017. Oral Corticosterone Administration Reduces Insulitis but Promotes Insulin Resistance and Hyperglycemia in Male Nonobese Diabetic Mice. *Am J Pathol,* 187**,** 614-626.

BURT, M. G., GIBNEY, J. & HO, K. K. 2006. Characterization of the metabolic phenotypes of Cushing's syndrome and growth hormone deficiency: a study of body composition and energy metabolism. *Clin Endocrinol (Oxf),* 64**,** 436-43.

BURTON, P. J., KROZOWSKI, Z. S. & WADDELL, B. J. 1998. Immunolocalization of 11beta-hydroxysteroid dehydrogenase types 1 and 2 in rat uterus: variation across the estrous cycle and regulation by estrogen and progesterone. *Endocrinology,* 139**,** 376-82.

BUTTGEREIT, F. & SCHEFFOLD, A. 2002. Rapid glucocorticoid effects on immune cells. *Steroids,* 67**,** 529-34.

CAMACHO-PEREIRA, J., TARRAGO, M. G., CHINI, C. C. S., NIN, V., ESCANDE, C., WARNER, G. M., PURANIK, A. S., SCHOON, R. A., REID, J. M., GALINA, A. & CHINI, E. N. 2016. CD38 Dictates Age-Related NAD Decline and Mitochondrial Dysfunction through an SIRT3-Dependent Mechanism. *Cell Metab,* 23**,** 1127-1139.

CAMBRONNE, X. A., STEWART, M. L., KIM, D., JONES-BRUNETTE, A. M., MORGAN, R. K., FARRENS, D. L., COHEN, M. S. & GOODMAN, R. H. 2016. Biosensor reveals multiple sources for mitochondrial NAD(+). *Science,* 352**,** 1474-7.

CAMPBELL, J. E., PECKETT, A. J., D'SOUZA A, M., HAWKE, T. J. & RIDDELL, M. C. 2011. Adipogenic and lipolytic effects of chronic glucocorticoid exposure. *Am J Physiol Cell Physiol,* 300**,** C198-209.

CANTO, C. & GARCIA-ROVES, P. M. 2015. High-Resolution Respirometry for Mitochondrial Characterization of Ex Vivo Mouse Tissues. *Curr Protoc Mouse Biol,* 5**,** 135-153.

CANTO, C., GERHART-HINES, Z., FEIGE, J. N., LAGOUGE, M., NORIEGA, L., MILNE, J. C., ELLIOTT, P. J., PUIGSERVER, P. & AUWERX, J. 2009. AMPK regulates energy expenditure by modulating NAD+ metabolism and SIRT1 activity. *Nature,* 458**,** 1056-60.

CANTO, C., HOUTKOOPER, R. H., PIRINEN, E., YOUN, D. Y., OOSTERVEER, M. H., CEN, Y., FERNANDEZ-MARCOS, P. J., YAMAMOTO, H., ANDREUX, P. A., CETTOUR-ROSE, P., GADEMANN, K., RINSCH, C., SCHOONJANS, K., SAUVE, A. A. & AUWERX, J. 2012. The NAD(+) precursor nicotinamide riboside enhances oxidative metabolism and protects against high-fat diet-induced obesity. *Cell Metab,* 15**,** 838-47.

CANTO, C., MENZIES, K. J. & AUWERX, J. 2015. NAD(+) Metabolism and the Control of Energy Homeostasis: A Balancing Act between Mitochondria and the Nucleus. *Cell Metab,* 22**,** 31-53.

CARBONE, F., LIBERALE, L., BONAVENTURA, A., VECCHIE, A., CASULA, M., CEA, M., MONACELLI, F., CAFFA, I., BRUZZONE, S., MONTECUCCO, F. & NENCIONI, A. 2017. Regulation and Function of Extracellular Nicotinamide Phosphoribosyltransferase/Visfatin. *Compr Physiol,* 7**,** 603-621.

CARNEIRO, I. P., ELLIOTT, S. A., SIERVO, M., PADWAL, R., BERTOLI, S., BATTEZZATI, A. & PRADO, C. M. 2016. Is Obesity Associated with Altered Energy Expenditure? *Adv Nutr,* 7**,** 476-87.

CARON, N., PEYROT, N., CADERBY, T., VERKINDT, C. & DALLEAU, G. 2016. Energy Expenditure in People with Diabetes Mellitus: A Review. *Front Nutr,* 3**,** 56.

CARTWRIGHT, D. M., OAKEY, L. A., FLETCHER, R. S., DOIG, C. L., HEISING, S., LARNER, D. P., NASTESKA, D., BERRY, C. E., HEASELGRAVE, S. R., LUDWIG, C., HODSON, D. J., LAVERY, G. G. & GARTEN, A. 2021. Nicotinamide riboside has minimal impact on energy metabolism in mouse models of mild obesity. *J Endocrinol,* 251**,** 111-123.

CELICHOWSKI, P., JOPEK, K., MILECKA, P., SZYSZKA, M., TYCZEWSKA, M., MALENDOWICZ, L. K. & RUCINSKI, M. 2018. Nicotinamide phosphoribosyltransferase and the hypothalamic-pituitary-adrenal axis of the rat. *Mol Med Rep,* 17**,** 6163-6173.

CELICHOWSKI, P., JOPEK, K., SZYSZKA, M., MILECKA, P., TYCZEWSKA, M., SAKHANOVA, S., SZAFLARSKI, W., MALENDOWICZ, L. K. & RUCINSKI, M. 2021. Extracellular Nampt (eNampt/visfatin/PBEF) directly and indirectly stimulates ACTH and CCL2 protein secretion from isolated rat corticotropes. *Adv Clin Exp Med,* 30**,** 967-980.

CHAMBON, P., WEILL, J. D. & MANDEL, P. 1963. Nicotinamide mononucleotide activation of new DNA-dependent polyadenylic acid synthesizing nuclear enzyme. *Biochem Biophys Res Commun,* 11**,** 39-43.

CHAUDHRY, H. S. & SINGH, G. 2022. Cushing Syndrome. *StatPearls.* Treasure Island (FL).

CHEN, J. Q. & RUSSO, J. 2012. Dysregulation of glucose transport, glycolysis, TCA cycle and glutaminolysis by oncogenes and tumor suppressors in cancer cells. *Biochim Biophys Acta,* 1826**,** 370-84.

CHEN, T. C., BENJAMIN, D. I., KUO, T., LEE, R. A., LI, M. L., MAR, D. J., COSTELLO, D. E., NOMURA, D. K. & WANG, J. C. 2017. The glucocorticoid-Angptl4-ceramide axis induces insulin resistance through PP2A and PKCzeta. *Sci Signal,* 10.

CHEN, W. 2011. IDO: more than an enzyme. *Nat Immunol,* 12**,** 809-11.

CHEN, Y., LI, J., ZHANG, M., YANG, W., QIN, W., ZHENG, Q., CHU, Y., WU, Y., WU, D. & YUAN, X. 2022. 11beta-HSD1 Inhibitor Alleviates Non-Alcoholic Fatty Liver Disease by Activating the AMPK/SIRT1 Signaling Pathway. *Nutrients,* 14.

CHIMIN, P., FARIAS TDA, S., TORRES-LEAL, F. L., BOLSONI-LOPES, A., CAMPANA, A. B., ANDREOTTI, S. & LIMA, F. B. 2014. Chronic glucocorticoid treatment enhances lipogenic activity in visceral adipocytes of male Wistar rats. *Acta Physiol (Oxf),* 211**,** 409-20.

CHINI, C. C. S., TARRAGO, M. G. & CHINI, E. N. 2017. NAD and the aging process: Role in life, death and everything in between. *Mol Cell Endocrinol,* 455**,** 62-74.

CHO, J. E., FOURNIER, M., DA, X. & LEWIS, M. I. 2010. Time course expression of Foxo transcription factors in skeletal muscle following corticosteroid administration. *J Appl Physiol (1985),* 108**,** 137-45.

CHONG, P. K., JUNG, R. T., SCRIMGEOUR, C. M. & RENNIE, M. J. 1994. The effect of pharmacological dosages of glucocorticoids on free living total energy expenditure in man. *Clin Endocrinol (Oxf),* 40**,** 577-81.

CLARK, J. B., FERRIS, G. M. & PINDER, S. 1971. Inhibition of nuclear NAD nucleosidase and poly ADP-ribose polymerase activity from rat liver by nicotinamide and 5'-methyl nicotinamide. *Biochim Biophys Acta,* 238**,** 82-5.

CLARKE, B. A., DRUJAN, D., WILLIS, M. S., MURPHY, L. O., CORPINA, R. A., BUROVA, E., RAKHILIN, S. V., STITT, T. N., PATTERSON, C., LATRES, E. & GLASS, D. J. 2007. The E3 Ligase MuRF1 degrades myosin heavy chain protein in dexamethasone-treated skeletal muscle. *Cell Metab,* 6**,** 376-85.

CODERRE, L., SRIVASTAVA, A. K. & CHIASSON, J. L. 1992. Effect of hypercorticism on regulation of skeletal muscle glycogen metabolism by insulin. *Am J Physiol,* 262**,** E427-33.

COLE, T. G., WILCOX, H. G. & HEIMBERG, M. 1982. Effects of adrenalectomy and dexamethasone on hepatic lipid metabolism. *J Lipid Res,* 23**,** 81-91.

COLE, T. J., BLENDY, J. A., MONAGHAN, A. P., KRIEGLSTEIN, K., SCHMID, W., AGUZZI, A., FANTUZZI, G., HUMMLER, E., UNSICKER, K. & SCHUTZ, G. 1995. Targeted disruption of the glucocorticoid receptor gene blocks adrenergic chromaffin cell development and severely retards lung maturation. *Genes Dev,* 9**,** 1608-21.

COLE, T. J., SHORT, K. L. & HOOPER, S. B. 2019. The science of steroids. *Semin Fetal Neonatal Med,* 24**,** 170-175.

COOMBES, B. K., BISSET, L. & VICENZINO, B. 2010. Efficacy and safety of corticosteroid injections and other injections for management of tendinopathy: a systematic review of randomised controlled trials. *Lancet,* 376**,** 1751-67.

COVARRUBIAS, A. J., PERRONE, R., GROZIO, A. & VERDIN, E. 2021. NAD(+) metabolism and its roles in cellular processes during ageing. *Nat Rev Mol Cell Biol,* 22**,** 119-141.

CRESCENZO, R., BIANCO, F., FALCONE, I., COPPOLA, P., LIVERINI, G. & IOSSA, S. 2013. Increased hepatic de novo lipogenesis and mitochondrial efficiency in a model of obesity induced by diets rich in fructose. *Eur J Nutr,* 52**,** 537-45.

CRICHTON, P. G., LEE, Y. & KUNJI, E. R. 2017. The molecular features of uncoupling protein 1 support a conventional mitochondrial carrier-like mechanism. *Biochimie,* 134**,** 35-50.

CROXTALL, J. D., CHOUDHURY, Q. & FLOWER, R. J. 2000. Glucocorticoids act within minutes to inhibit recruitment of signalling factors to activated EGF receptors through a receptor-dependent, transcription-independent mechanism. *Br J Pharmacol,* 130**,** 289-98.

CUSHING, H. 1994. The basophil adenomas of the pituitary body and their clinical manifestations (pituitary basophilism). 1932. *Obes Res,* 2**,** 486-508.

DAHL, T. B., HAUKELAND, J. W., YNDESTAD, A., RANHEIM, T., GLADHAUG, I. P., DAMAS, J. K., HAALAND, T., LOBERG, E. M., ARNTSEN, B., BIRKELAND, K., BJORO, K., ULVEN, S. M., KONOPSKI, Z., NEBB, H. I., AUKRUST, P. & HALVORSEN, B. 2010. Intracellular nicotinamide phosphoribosyltransferase protects against hepatocyte apoptosis and is down-regulated in nonalcoholic fatty liver disease. *J Clin Endocrinol Metab,* 95**,** 3039-47.

DAKIN, R. S., WALKER, B. R., SECKL, J. R., HADOKE, P. W. & DRAKE, A. J. 2015. Estrogens protect male mice from obesity complications and influence glucocorticoid metabolism. *Int J Obes (Lond),* 39**,** 1539-47.

DALI-YOUCEF, N., LAGOUGE, M., FROELICH, S., KOEHL, C., SCHOONJANS, K. & AUWERX, J. 2007. Sirtuins: the 'magnificent seven', function, metabolism and longevity. *Ann Med,* 39**,** 335-45.

DALL, M., HASSING, A. S. & TREEBAK, J. T. 2022. NAD(+) and NAFLD - caution, causality and careful optimism. *J Physiol,* 600**,** 1135-1154.

DAVILA, A., LIU, L., CHELLAPPA, K., REDPATH, P., NAKAMARU-OGISO, E., PAOLELLA, L. M., ZHANG, Z., MIGAUD, M. E., RABINOWITZ, J. D. & BAUR, J. A. 2018. Nicotinamide adenine dinucleotide is transported into mammalian mitochondria. *Elife,* 7.

DE GUIA, R. M., ROSE, A. J. & HERZIG, S. 2014. Glucocorticoid hormones and energy homeostasis. *Horm Mol Biol Clin Investig,* 19**,** 117-28.

DEKHUIJZEN, P. N., GAYAN-RAMIREZ, G., BISSCHOP, A., DE BOCK, V., DOM, R. & DECRAMER, M. 1995. Corticosteroid treatment and nutritional deprivation cause a different pattern of atrophy in rat diaphragm. *J Appl Physiol (1985),* 78**,** 629-37.

DHINDSA, S., GHANIM, H., GREEN, K., ABUAYSHEH, S., BATRA, M., MAKDISSI, A., CHAUDHURI, A., SANDHU, S. & DANDONA, P. 2019. Acute effects of insulin on skeletal muscle growth and differentiation genes in men with type 2 diabetes. *Eur J Endocrinol,* 181**,** K55-K59.

DI DALMAZI, G., PAGOTTO, U., PASQUALI, R. & VICENNATI, V. 2012. Glucocorticoids and type 2 diabetes: from physiology to pathology. *J Nutr Metab,* 2012**,** 525093.

DI LISA, F., MENABO, R., CANTON, M., BARILE, M. & BERNARDI, P. 2001. Opening of the mitochondrial permeability transition pore causes depletion of mitochondrial and cytosolic NAD+ and is a causative event in the death of myocytes in postischemic reperfusion of the heart. *J Biol Chem,* 276**,** 2571-5.

DI, S., MALCHER-LOPES, R., HALMOS, K. C. & TASKER, J. G. 2003. Nongenomic glucocorticoid inhibition via endocannabinoid release in the hypothalamus: a fast feedback mechanism. *J Neurosci,* 23**,** 4850-7.

DI, S., MALCHER-LOPES, R., MARCHESELLI, V. L., BAZAN, N. G. & TASKER, J. G. 2005. Rapid glucocorticoid-mediated endocannabinoid release and opposing regulation of glutamate and gamma-aminobutyric acid inputs to hypothalamic magnocellular neurons. *Endocrinology,* 146**,** 4292-301.

DI, S., MAXSON, M. M., FRANCO, A. & TASKER, J. G. 2009. Glucocorticoids regulate glutamate and GABA synapse-specific retrograde transmission via divergent nongenomic signaling pathways. *J Neurosci,* 29**,** 393-401.

DI STEFANO, M. & CONFORTI, L. 2013. Diversification of NAD biological role: the importance of location. *FEBS J,* 280**,** 4711-28.

DIAMANT, S. & SHAFRIR, E. 1975. Modulation of the activity of insulin-dependent enzymes of lipogenesis by glucocorticoids. *Eur J Biochem,* 53**,** 541-6.

DIAO, L., AUGER, C., KONOEDA, H., SADRI, A. R., AMINI-NIK, S. & JESCHKE, M. G. 2018. Hepatic steatosis associated with decreased beta-oxidation and mitochondrial function contributes to cell damage in obese mice after thermal injury. *Cell Death Dis,* 9**,** 530.

DIGUET, N., TRAMMELL, S. A. J., TANNOUS, C., DELOUX, R., PIQUEREAU, J., MOUGENOT, N., GOUGE, A., GRESSETTE, M., MANOURY, B., BLANC, J., BRETON, M., DECAUX, J. F., LAVERY, G. G., BACZKO, I., ZOLL, J., GARNIER, A., LI, Z., BRENNER, C. & MERICSKAY, M. 2018. Nicotinamide Riboside Preserves Cardiac Function in a Mouse Model of Dilated Cardiomyopathy. *Circulation,* 137**,** 2256-2273.

DIMITRIADIS, G., LEIGHTON, B., PARRY-BILLINGS, M., SASSON, S., YOUNG, M., KRAUSE, U., BEVAN, S., PIVA, T., WEGENER, G. & NEWSHOLME, E. A. 1997. Effects of glucocorticoid excess on the sensitivity of glucose transport and metabolism to insulin in rat skeletal muscle. *Biochem J,* 321 (Pt 3)**,** 707-12.

DLUGOSZ, E. M., HARRIS, B. N., SALTZMAN, W. & CHAPPELL, M. A. 2012. Glucocorticoids, aerobic physiology, and locomotor behavior in California mice. *Physiol Biochem Zool,* 85**,** 671-83.

DOERRIER, C., GARCIA-SOUZA, L. F., KRUMSCHNABEL, G., WOHLFARTER, Y., MESZAROS, A. T. & GNAIGER, E. 2018. High-Resolution FluoRespirometry and OXPHOS Protocols for Human Cells, Permeabilized Fibers from Small Biopsies of Muscle, and Isolated Mitochondria. *Methods Mol Biol,* 1782**,** 31-70.

DOIG, C. L., FLETCHER, R. S., MORGAN, S. A., MCCABE, E. L., LARNER, D. P., TOMLINSON, J. W., STEWART, P. M., PHILP, A. & LAVERY, G. G. 2017. 11beta-HSD1 Modulates the Set Point of Brown Adipose Tissue Response to Glucocorticoids in Male Mice. *Endocrinology,* 158**,** 1964-1976.

DOIG, C. L., ZIELINSKA, A. E., FLETCHER, R. S., OAKEY, L. A., ELHASSAN, Y. S., GARTEN, A., CARTWRIGHT, D., HEISING, S., ALSHERI, A., WATSON, D. G., PREHN, C., ADAMSKI, J., TENNANT, D. A. & LAVERY, G. G. 2020. Induction of the nicotinamide riboside kinase NAD(+) salvage pathway in a model of sarcoplasmic reticulum dysfunction. *Skelet Muscle,* 10**,** 5.

DOLINSKY, V. W., DOUGLAS, D. N., LEHNER, R. & VANCE, D. E. 2004. Regulation of the enzymes of hepatic microsomal triacylglycerol lipolysis and re-esterification by the glucocorticoid dexamethasone. *Biochem J,* 378**,** 967-74.

DOLLE, C., NIERE, M., LOHNDAL, E. & ZIEGLER, M. 2010. Visualization of subcellular NAD pools and intra-organellar protein localization by poly-ADP-ribose formation. *Cell Mol Life Sci,* 67**,** 433-43.

DOLLE, C., RACK, J. G. & ZIEGLER, M. 2013. NAD and ADP-ribose metabolism in mitochondria. *FEBS J,* 280**,** 3530-41.

DOMINY, J. E., JR., LEE, Y., JEDRYCHOWSKI, M. P., CHIM, H., JURCZAK, M. J., CAMPOREZ, J. P., RUAN, H. B., FELDMAN, J., PIERCE, K., MOSTOSLAVSKY, R., DENU, J. M., CLISH, C. B., YANG, X., SHULMAN, G. I., GYGI, S. P. & PUIGSERVER, P. 2012. The deacetylase Sirt6 activates the acetyltransferase GCN5 and suppresses hepatic gluconeogenesis. *Mol Cell,* 48**,** 900-13.

DU, J., WANG, Y., HUNTER, R., WEI, Y., BLUMENTHAL, R., FALKE, C., KHAIROVA, R., ZHOU, R., YUAN, P., MACHADO-VIEIRA, R., MCEWEN, B. S. & MANJI, H. K. 2009. Dynamic regulation of mitochondrial function by glucocorticoids. *Proc Natl Acad Sci U S A,* 106**,** 3543-8.

DU, K., HERZIG, S., KULKARNI, R. N. & MONTMINY, M. 2003. TRB3: a tribbles homolog that inhibits Akt/PKB activation by insulin in liver. *Science,* 300**,** 1574-7.

DUCHARME, F. M., ZEMEK, R. L. & SCHUH, S. 2009. Oral corticosteroids in children with wheezing. *N Engl J Med,* 360**,** 1674; author reply 1675.

DURKACZ, B. W., OMIDIJI, O., GRAY, D. A. & SHALL, S. 1980. (ADP-ribose)n participates in DNA excision repair. *Nature,* 283**,** 593-6.

EASLON, E., TSANG, F., SKINNER, C., WANG, C. & LIN, S. J. 2008. The malate-aspartate NADH shuttle components are novel metabolic longevity regulators required for calorie restriction-mediated life span extension in yeast. *Genes Dev,* 22**,** 931-44.

EL-KHAMISY, S. F., MASUTANI, M., SUZUKI, H. & CALDECOTT, K. W. 2003. A requirement for PARP-1 for the assembly or stability of XRCC1 nuclear foci at sites of oxidative DNA damage. *Nucleic Acids Res,* 31**,** 5526-33.

ELHASSAN, Y. S., KLUCKOVA, K., FLETCHER, R. S., SCHMIDT, M. S., GARTEN, A., DOIG, C. L., CARTWRIGHT, D. M., OAKEY, L., BURLEY, C. V., JENKINSON, N., WILSON, M., LUCAS, S. J. E., AKERMAN, I., SEABRIGHT, A., LAI, Y. C., TENNANT, D. A., NIGHTINGALE, P., WALLIS, G. A., MANOLOPOULOS, K. N., BRENNER, C., PHILP, A. & LAVERY, G. G. 2019. Nicotinamide Riboside Augments the Aged Human Skeletal Muscle NAD(+) Metabolome and Induces Transcriptomic and Anti-inflammatory Signatures. *Cell Rep,* 28**,** 1717-1728 e6.

ELHASSAN, Y. S., PHILP, A. A. & LAVERY, G. G. 2017. Targeting NAD+ in Metabolic Disease: New Insights Into an Old Molecule. *J Endocr Soc,* 1**,** 816-835.

ENDOCRINESOCIETY. 2022. *Cushing's Syndrome and Cushing Disease* [Online]. Available: https://www.endocrine.org/patient-engagement/endocrine-library/cushings-syndrome-and-cushing-disease [Accessed 23/02/2023].

ERION, D. M., YONEMITSU, S., NIE, Y., NAGAI, Y., GILLUM, M. P., HSIAO, J. J., IWASAKI, T., STARK, R., WEISMANN, D., YU, X. X., MURRAY, S. F., BHANOT, S., MONIA, B. P., HORVATH, T. L., GAO, Q., SAMUEL, V. T. & SHULMAN, G. I. 2009. SirT1 knockdown in liver decreases basal hepatic glucose production and increases hepatic insulin responsiveness in diabetic rats. *Proc Natl Acad Sci U S A,* 106**,** 11288-93.

FARDET, L. & FEVE, B. 2014. Systemic glucocorticoid therapy: a review of its metabolic and cardiovascular adverse events. *Drugs,* 74**,** 1731-45.

FELICI, R., LAPUCCI, A., CAVONE, L., PRATESI, S., BERLINGUER-PALMINI, R. & CHIARUGI, A. 2015. Pharmacological NAD-Boosting Strategies Improve Mitochondrial Homeostasis in Human Complex I-Mutant Fibroblasts. *Mol Pharmacol,* 87**,** 965-71.

FLETCHER, R. S. & LAVERY, G. G. 2018. The emergence of the nicotinamide riboside kinases in the regulation of NAD+ metabolism. *J Mol Endocrinol,* 61**,** R107-R121.

FLETCHER, R. S., RATAJCZAK, J., DOIG, C. L., OAKEY, L. A., CALLINGHAM, R., DA SILVA XAVIER, G., GARTEN, A., ELHASSAN, Y. S., REDPATH, P., MIGAUD, M. E., PHILP, A., BRENNER, C., CANTO, C. & LAVERY, G. G. 2017. Nicotinamide riboside kinases display redundancy in mediating nicotinamide mononucleotide and nicotinamide riboside metabolism in skeletal muscle cells. *Mol Metab,* 6**,** 819-832.

FREDERICK, D. W., LORO, E., LIU, L., DAVILA, A., JR., CHELLAPPA, K., SILVERMAN, I. M., QUINN, W. J., 3RD, GOSAI, S. J., TICHY, E. D., DAVIS, J. G., MOURKIOTI, F., GREGORY, B. D., DELLINGER, R. W., REDPATH, P., MIGAUD, M. E., NAKAMARU-OGISO, E., RABINOWITZ, J. D., KHURANA, T. S. & BAUR, J. A. 2016. Loss of NAD Homeostasis Leads to Progressive and Reversible Degeneration of Skeletal Muscle. *Cell Metab,* 24**,** 269-82.

FRICKER, R. A., GREEN, E. L., JENKINS, S. I. & GRIFFIN, S. M. 2018. The Influence of Nicotinamide on Health and Disease in the Central Nervous System. *Int J Tryptophan Res,* 11**,** 1178646918776658.

FRIEBE, D., LOFFLER, D., SCHONBERG, M., BERNHARD, F., BUTTNER, P., LANDGRAF, K., KIESS, W. & KORNER, A. 2011. Impact of metabolic regulators on the expression of the obesity associated genes FTO and NAMPT in human preadipocytes and adipocytes. *PLoS One,* 6**,** e19526.

FRY, C. S., NAYEEM, S. Z., DILLON, E. L., SARKAR, P. S., TUMURBAATAR, B., URBAN, R. J., WRIGHT, T. J., SHEFFIELD-MOORE, M., TILTON, R. G. & CHOUDHARY, S. 2016. Glucocorticoids increase skeletal muscle NF-kappaB inducing kinase (NIK): links to muscle atrophy. *Physiol Rep,* 4.

FRYE, R. A. 1999. Characterization of five human cDNAs with homology to the yeast SIR2 gene: Sir2-like proteins (sirtuins) metabolize NAD and may have protein ADP-ribosyltransferase activity. *Biochem Biophys Res Commun,* 260**,** 273-9.

GABRIEL, S. E., JAAKKIMAINEN, L. & BOMBARDIER, C. 1991. Risk for serious gastrointestinal complications related to use of nonsteroidal anti-inflammatory drugs. A meta-analysis. *Ann Intern Med,* 115**,** 787-96.

GADDIPATI, R., SASIKALA, M., PADAKI, N., MUKHERJEE, R. M., SEKARAN, A., JAYARAJ-MANSARD, M., RABELLA, P., RAO-GUDURU, V. & REDDY-DUVVURU, N. 2010. Visceral adipose tissue visfatin in nonalcoholic fatty liver disease. *Ann Hepatol,* 9**,** 266-70.

GALLOWAY, C. A. & YOON, Y. 2012. Perspectives on: SGP symposium on mitochondrial physiology and medicine: what comes first, misshape or dysfunction? The view from metabolic excess. *J Gen Physiol,* 139**,** 455-63.

GAMBINERI, A., FORLANI, G., MUNARINI, A., TOMASSONI, F., COGNIGNI, G. E., CIAMPAGLIA, W., PAGOTTO, U., WALKER, B. R. & PASQUALI, R. 2009. Increased clearance of cortisol by 5beta-reductase in a subgroup of women with adrenal hyperandrogenism in polycystic ovary syndrome. *J Endocrinol Invest,* 32**,** 210-8.

GARCIA-EGUREN, G., SALA-VILA, A., GIRO, O., VEGA-BEYHART, A. & HANZU, F. A. 2020. Long-term hypercortisolism induces lipogenesis promoting palmitic acid accumulation and inflammation in visceral adipose tissue compared with HFD-induced obesity. *Am J Physiol Endocrinol Metab,* 318**,** E995-E1003.

GARIANI, K., MENZIES, K. J., RYU, D., WEGNER, C. J., WANG, X., ROPELLE, E. R., MOULLAN, N., ZHANG, H., PERINO, A., LEMOS, V., KIM, B., PARK, Y. K., PIERSIGILLI, A., PHAM, T. X., YANG, Y., KU, C. S., KOO, S. I., FOMITCHOVA, A., CANTO, C., SCHOONJANS, K., SAUVE, A. A., LEE, J. Y. & AUWERX, J. 2016. Eliciting the mitochondrial unfolded protein response by nicotinamide adenine dinucleotide repletion reverses fatty liver disease in mice. *Hepatology,* 63**,** 1190-204.

GASPARINI, S. J., SWARBRICK, M. M., KIM, S., THAI, L. J., HENNEICKE, H., CAVANAGH, L. L., TU, J., WEBER, M. C., ZHOU, H. & SEIBEL, M. J. 2019. Androgens sensitise mice to glucocorticoid-induced insulin resistance and fat accumulation. *Diabetologia,* 62**,** 1463-1477.

GASPARINI, S. J., WEBER, M. C., HENNEICKE, H., KIM, S., ZHOU, H. & SEIBEL, M. J. 2016. Continuous corticosterone delivery via the drinking water or pellet implantation: A comparative study in mice. *Steroids,* 116**,** 76-82.

GJERSTAD, J. K., LIGHTMAN, S. L. & SPIGA, F. 2018. Role of glucocorticoid negative feedback in the regulation of HPA axis pulsatility. *Stress,* 21**,** 403-416.

GOKULAKRISHNAN, G., CHANG, X., FLEISCHMANN, R. & FIOROTTO, M. L. 2017. Precocious glucocorticoid exposure reduces skeletal muscle satellite cells in the fetal rat. *J Endocrinol,* 232**,** 561-572.

GOODWIN, J. E. & GELLER, D. S. 2012. Glucocorticoid-induced hypertension. *Pediatr Nephrol,* 27**,** 1059-66.

GRAD, I. & PICARD, D. 2007. The glucocorticoid responses are shaped by molecular chaperones. *Mol Cell Endocrinol,* 275**,** 2-12.

GRAEFF, R. & LEE, H. C. 2002. A novel cycling assay for cellular cADP-ribose with nanomolar sensitivity. *Biochem J,* 361**,** 379-84.

GRAVHOLT, C. H., DALL, R., CHRISTIANSEN, J. S., MOLLER, N. & SCHMITZ, O. 2002. Preferential stimulation of abdominal subcutaneous lipolysis after prednisolone exposure in humans. *Obes Res,* 10**,** 774-81.

GRAY, N. E., LAM, L. N., YANG, K., ZHOU, A. Y., KOLIWAD, S. & WANG, J. C. 2012. Angiopoietin-like 4 (Angptl4) protein is a physiological mediator of intracellular lipolysis in murine adipocytes. *J Biol Chem,* 287**,** 8444-56.

GREMLICH, S., RODUIT, R. & THORENS, B. 1997. Dexamethasone induces posttranslational degradation of GLUT2 and inhibition of insulin secretion in isolated pancreatic beta cells. Comparison with the effects of fatty acids. *J Biol Chem,* 272**,** 3216-22.

GROENEWEG, F. L., KARST, H., DE KLOET, E. R. & JOELS, M. 2012. Mineralocorticoid and glucocorticoid receptors at the neuronal membrane, regulators of nongenomic corticosteroid signalling. *Mol Cell Endocrinol,* 350**,** 299-309.

GROSSMANN, C., SCHOLZ, T., ROCHEL, M., BUMKE-VOGT, C., OELKERS, W., PFEIFFER, A. F., DIEDERICH, S. & BAHR, V. 2004. Transactivation via the human glucocorticoid and mineralocorticoid receptor by therapeutically used steroids in CV-1 cells: a comparison of their glucocorticoid and mineralocorticoid properties. *Eur J Endocrinol,* 151**,** 397-406.

GROZIO, A., MILLS, K. F., YOSHINO, J., BRUZZONE, S., SOCIALI, G., TOKIZANE, K., LEI, H. C., CUNNINGHAM, R., SASAKI, Y., MIGAUD, M. E. & IMAI, S. I. 2019. Slc12a8 is a nicotinamide mononucleotide transporter. *Nat Metab,* 1**,** 47-57.

GUO, J., WANG, Z., WU, J., LIU, M., LI, M., SUN, Y., HUANG, W., LI, Y., ZHANG, Y., TANG, W., LI, X., ZHANG, C., HONG, F., LI, N., NIE, J. & YI, F. 2019. Endothelial SIRT6 Is Vital to Prevent Hypertension and Associated Cardiorenal Injury Through Targeting Nkx3.2-GATA5 Signaling. *Circ Res,* 124**,** 1448-1461.

GUO, Z., CHEN, Y. Z., XU, R. B. & FU, H. 1995. Binding characteristics of glucocorticoid receptor in synaptic plasma membrane from rat brain. *Funct Neurol,* 10**,** 183-94.

GUPTA, D. & MORLEY, J. E. 2014. Hypothalamic-pituitary-adrenal (HPA) axis and aging. *Compr Physiol,* 4**,** 1495-510.

HAIGIS, M. C. & SINCLAIR, D. A. 2010. Mammalian sirtuins: biological insights and disease relevance. *Annu Rev Pathol,* 5**,** 253-95.

HAKAMI, O. A., AHMED, S. & KARAVITAKI, N. 2021. Epidemiology and mortality of Cushing's syndrome. *Best Pract Res Clin Endocrinol Metab,* 35**,** 101521.

HALLER, J., MIKICS, E. & MAKARA, G. B. 2008. The effects of non-genomic glucocorticoid mechanisms on bodily functions and the central neural system. A critical evaluation of findings. *Front Neuroendocrinol,* 29**,** 273-91.

HAN, J. Z., LIN, W. & CHEN, Y. Z. 2005. Inhibition of ATP-induced calcium influx in HT4 cells by glucocorticoids: involvement of protein kinase A. *Acta Pharmacol Sin,* 26**,** 199-204.

HANNUN, Y. A. 1994. The sphingomyelin cycle and the second messenger function of ceramide. *J Biol Chem,* 269**,** 3125-8.

HARA, N., YAMADA, K., SHIBATA, T., OSAGO, H., HASHIMOTO, T. & TSUCHIYA, M. 2007. Elevation of cellular NAD levels by nicotinic acid and involvement of nicotinic acid phosphoribosyltransferase in human cells. *J Biol Chem,* 282**,** 24574-82.

HARA, N., YAMADA, K., TERASHIMA, M., OSAGO, H., SHIMOYAMA, M. & TSUCHIYA, M. 2003. Molecular identification of human glutamine- and ammonia-dependent NAD synthetases. Carbon-nitrogen hydrolase domain confers glutamine dependency. *J Biol Chem,* 278**,** 10914-21.

HARDY, R. S., ZHOU, H., SEIBEL, M. J. & COOPER, M. S. 2018. Glucocorticoids and Bone: Consequences of Endogenous and Exogenous Excess and Replacement Therapy. *Endocr Rev,* 39**,** 519-548.

HASMANN, M. & SCHEMAINDA, I. 2003. FK866, a highly specific noncompetitive inhibitor of nicotinamide phosphoribosyltransferase, represents a novel mechanism for induction of tumor cell apoptosis. *Cancer Res,* 63**,** 7436-42.

HASSELGREN, P. O. 1999. Glucocorticoids and muscle catabolism. *Curr Opin Clin Nutr Metab Care,* 2**,** 201-5.

HAYAT, F. & MIGAUD, M. E. 2020. Nicotinamide riboside-amino acid conjugates that are stable to purine nucleoside phosphorylase. *Org Biomol Chem,* 18**,** 2877-2885.

HAZLEHURST, J. M., OPRESCU, A. I., NIKOLAOU, N., DI GUIDA, R., GRINBERGS, A. E., DAVIES, N. P., FLINTHAM, R. B., ARMSTRONG, M. J., TAYLOR, A. E., HUGHES, B. A., YU, J., HODSON, L., DUNN, W. B. & TOMLINSON, J. W. 2016. Dual-5alpha-Reductase Inhibition Promotes Hepatic Lipid Accumulation in Man. *J Clin Endocrinol Metab,* 101**,** 103-13.

HEITZER, M. D., WOLF, I. M., SANCHEZ, E. R., WITCHEL, S. F. & DEFRANCO, D. B. 2007. Glucocorticoid receptor physiology. *Rev Endocr Metab Disord,* 8**,** 321-30.

HENRIKSEN, E. J., DIAMOND-STANIC, M. K. & MARCHIONNE, E. M. 2011. Oxidative stress and the etiology of insulin resistance and type 2 diabetes. *Free Radic Biol Med,* 51**,** 993-9.

HERMAN, T. F. & SANTOS, C. 2022. First Pass Effect. *StatPearls.* Treasure Island (FL).

HERRERA, N. A., DUCHATSCH, F., KAHLKE, A., AMARAL, S. L. & VASQUEZ-VIVAR, J. 2020a. In vivo vascular rarefaction and hypertension induced by dexamethasone are related to phosphatase PTP1B activation not endothelial metabolic changes. *Free Radic Biol Med,* 152**,** 689-696.

HERRERA, N. A., DUCHATSCH, F., KAHLKE, A., AMARAL, S. L. & VASQUEZ-VIVAR, J. 2020b. In vivo vascular rarefaction and hypertension induced by dexamethasone are related to phosphatase PTP1B activation not endothelial metabolic changes. *Free Radic Biol Med*.

HILLER-STURMHOFEL, S. & BARTKE, A. 1998. The endocrine system: an overview. *Alcohol Health Res World,* 22**,** 153-64.

HIRSCHEY, M. D., SHIMAZU, T., GOETZMAN, E., JING, E., SCHWER, B., LOMBARD, D. B., GRUETER, C. A., HARRIS, C., BIDDINGER, S., ILKAYEVA, O. R., STEVENS, R. D., LI, Y., SAHA, A. K., RUDERMAN, N. B., BAIN, J. R., NEWGARD, C. B., FARESE, R. V., JR., ALT, F. W., KAHN, C. R. & VERDIN, E. 2010. SIRT3 regulates mitochondrial fatty-acid oxidation by reversible enzyme deacetylation. *Nature,* 464**,** 121-5.

HO, K. K. Y. 2018. Diet-induced thermogenesis: fake friend or foe? *J Endocrinol,* 238**,** R185-R191.

HOLLAND, W. L., BROZINICK, J. T., WANG, L. P., HAWKINS, E. D., SARGENT, K. M., LIU, Y., NARRA, K., HOEHN, K. L., KNOTTS, T. A., SIESKY, A., NELSON, D. H., KARATHANASIS, S. K., FONTENOT, G. K., BIRNBAUM, M. J. & SUMMERS, S. A. 2007. Inhibition of ceramide synthesis ameliorates glucocorticoid-, saturated-fat-, and obesity-induced insulin resistance. *Cell Metab,* 5**,** 167-79.

HOLUBIEC, P., LEONCZYK, M., STASZEWSKI, F., LAZARCZYK, A., JAWOREK, A. K. & ROJAS-PELC, A. 2021. Pathophysiology and clinical management of pellagra - a review. *Folia Med Cracov,* 61**,** 125-137.

HORBER, F. F., MARSH, H. M. & HAYMOND, M. W. 1991. Differential effects of prednisone and growth hormone on fuel metabolism and insulin antagonism in humans. *Diabetes,* 40**,** 141-9.

HOUTKOOPER, R. H., CANTO, C., WANDERS, R. J. & AUWERX, J. 2010. The secret life of NAD+: an old metabolite controlling new metabolic signaling pathways. *Endocr Rev,* 31**,** 194-223.

HSIEH, S. K., LIN, H. Y., CHEN, C. J., JHUO, C. F., LIAO, K. Y., CHEN, W. Y. & TZEN, J. T. C. 2020. Promotion of myotube differentiation and attenuation of muscle atrophy in murine C2C12 myoblast cells treated with teaghrelin. *Chem Biol Interact,* 315**,** 108893.

HU, Z., WANG, H., LEE, I. H., DU, J. & MITCH, W. E. 2009. Endogenous glucocorticoids and impaired insulin signaling are both required to stimulate muscle wasting under pathophysiological conditions in mice. *J Clin Invest,* 119**,** 3059-69.

HUANG, R. X. & TAO, J. 2020. Nicotinamide mononucleotide attenuates glucocorticoidinduced osteogenic inhibition by regulating the SIRT1/PGC1alpha signaling pathway. *Mol Med Rep,* 22**,** 145-154.

ILNYTSKA, O. & ARGYROPOULOS, G. 2008. The role of the Agouti-Related Protein in energy balance regulation. *Cell Mol Life Sci,* 65**,** 2721-31.

IMAI, E., STROMSTEDT, P. E., QUINN, P. G., CARLSTEDT-DUKE, J., GUSTAFSSON, J. A. & GRANNER, D. K. 1990. Characterization of a complex glucocorticoid response unit in the phosphoenolpyruvate carboxykinase gene. *Mol Cell Biol,* 10**,** 4712-9.

IMAI, S., ARMSTRONG, C. M., KAEBERLEIN, M. & GUARENTE, L. 2000. Transcriptional silencing and longevity protein Sir2 is an NAD-dependent histone deacetylase. *Nature,* 403**,** 795-800.

IMAI, S. & GUARENTE, L. 2014. NAD+ and sirtuins in aging and disease. *Trends Cell Biol,* 24**,** 464-71.

IMAI, S. & YOSHINO, J. 2013. The importance of NAMPT/NAD/SIRT1 in the systemic regulation of metabolism and ageing. *Diabetes Obes Metab,* 15 Suppl 3**,** 26-33.

INDER, W. J., JANG, C., OBEYESEKERE, V. R. & ALFORD, F. P. 2010. Dexamethasone administration inhibits skeletal muscle expression of the androgen receptor and IGF-1--implications for steroid-induced myopathy. *Clin Endocrinol (Oxf),* 73**,** 126-32.

ISIDORI, A. M. & LENZI, A. 2007. Ectopic ACTH syndrome. *Arq Bras Endocrinol Metabol,* 51**,** 1217-25.

JAMES, E. R. 2007. The etiology of steroid cataract. *J Ocul Pharmacol Ther,* 23**,** 403-20.

JAVADOV, S., KOZLOV, A. V. & CAMARA, A. K. S. 2020. Mitochondria in Health and Diseases. *Cells,* 9.

JIANG, Y., BOTCHWAY, B. O. A., HU, Z. & FANG, M. 2019. Overexpression of SIRT1 Inhibits Corticosterone-Induced Autophagy. *Neuroscience,* 411**,** 11-22.

JOBIN, N., DE JONGE, L. & GARREL, D. R. 1996. Effects of RU 486 on energy expenditure and meal tolerance in normal men. *J Am Coll Nutr,* 15**,** 283-8.

JOELS, M., KARST, H., DERIJK, R. & DE KLOET, E. R. 2008. The coming out of the brain mineralocorticoid receptor. *Trends Neurosci,* 31**,** 1-7.

JU, H. Q., ZHUANG, Z. N., LI, H., TIAN, T., LU, Y. X., FAN, X. Q., ZHOU, H. J., MO, H. Y., SHENG, H., CHIAO, P. J. & XU, R. H. 2016. Regulation of the Nampt-mediated NAD salvage pathway and its therapeutic implications in pancreatic cancer. *Cancer Lett,* 379**,** 1-11.

KAIKAEW, K., STEENBERGEN, J., VAN DIJK, T. H., GREFHORST, A. & VISSER, J. A. 2019. Sex Difference in Corticosterone-Induced Insulin Resistance in Mice. *Endocrinology,* 160**,** 2367-2387.

KANG, B. N., JUDE, J. A., PANETTIERI, R. A., JR., WALSETH, T. F. & KANNAN, M. S. 2008. Glucocorticoid regulation of CD38 expression in human airway smooth muscle cells: role of dual specificity phosphatase 1. *Am J Physiol Lung Cell Mol Physiol,* 295**,** L186-93.

KARATSOREOS, I. N., BHAGAT, S. M., BOWLES, N. P., WEIL, Z. M., PFAFF, D. W. & MCEWEN, B. S. 2010. Endocrine and physiological changes in response to chronic corticosterone: a potential model of the metabolic syndrome in mouse. *Endocrinology,* 151**,** 2117-27.

KARST, H., BERGER, S., TURIAULT, M., TRONCHE, F., SCHUTZ, G. & JOELS, M. 2005. Mineralocorticoid receptors are indispensable for nongenomic modulation of hippocampal glutamate transmission by corticosterone. *Proc Natl Acad Sci U S A,* 102**,** 19204-7.

KATSUKI, R., SAKATA, S., NAKAO, R., OISHI, K. & NAKAMURA, Y. 2019. Lactobacillus curvatus CP2998 Prevents Dexamethasone-Induced Muscle Atrophy in C2C12 Myotubes. *J Nutr Sci Vitaminol (Tokyo),* 65**,** 455-458.

KAUPPINEN, T. M., GAN, L. & SWANSON, R. A. 2013. Poly(ADP-ribose) polymerase-1-induced NAD(+) depletion promotes nuclear factor-kappaB transcriptional activity by preventing p65 de-acetylation. *Biochim Biophys Acta,* 1833**,** 1985-91.

KENDRICK, A. A., CHOUDHURY, M., RAHMAN, S. M., MCCURDY, C. E., FRIEDERICH, M., VAN HOVE, J. L., WATSON, P. A., BIRDSEY, N., BAO, J., GIUS, D., SACK, M. N., JING, E., KAHN, C. R., FRIEDMAN, J. E. & JONSCHER, K. R. 2011. Fatty liver is associated with reduced SIRT3 activity and mitochondrial protein hyperacetylation. *Biochem J,* 433**,** 505-14.

KERBEY, A. L., RADCLIFFE, P. M. & RANDLE, P. J. 1977. Diabetes and the control of pyruvate dehydrogenase in rat heart mitochondria by concentration ratios of adenosine triphosphate/adenosine diphosphate, of reduced/oxidized nicotinamide-adenine dinucleotide and of acetyl-coenzyme A/coenzyme A. *Biochem J,* 164**,** 509-19.

KILFOIL, P. J., TIPPARAJU, S. M., BARSKI, O. A. & BHATNAGAR, A. 2013. Regulation of ion channels by pyridine nucleotides. *Circ Res,* 112**,** 721-41.

KIM, J. A., WEI, Y. & SOWERS, J. R. 2008. Role of mitochondrial dysfunction in insulin resistance. *Circ Res,* 102**,** 401-14.

KLAIDMAN, L. K., MUKHERJEE, S. K., HUTCHIN, T. P. & ADAMS, J. D. 1996. Nicotinamide as a precursor for NAD+ prevents apoptosis in the mouse brain induced by tertiary-butylhydroperoxide. *Neurosci Lett,* 206**,** 5-8.

KOLTHUR-SEETHARAM, U., DANTZER, F., MCBURNEY, M. W., DE MURCIA, G. & SASSONE-CORSI, P. 2006. Control of AIF-mediated cell death by the functional interplay of SIRT1 and PARP-1 in response to DNA damage. *Cell Cycle,* 5**,** 873-7.

KOSTYO, J. L. & REDMOND, A. F. 1966. Role of protein synthesis in the inhibitory action of adrenal steroid hormones on amino acid transport by muscle. *Endocrinology,* 79**,** 531-40.

KRALISCH, S., KLEIN, J., LOSSNER, U., BLUHER, M., PASCHKE, R., STUMVOLL, M. & FASSHAUER, M. 2005. Hormonal regulation of the novel adipocytokine visfatin in 3T3-L1 adipocytes. *J Endocrinol,* 185**,** R1-8.

KRIEGER, D. T., ALLEN, W., RIZZO, F. & KRIEGER, H. P. 1971. Characterization of the normal temporal pattern of plasma corticosteroid levels. *J Clin Endocrinol Metab,* 32**,** 266-84.

KROON, J., PEREIRA, A. M. & MEIJER, O. C. 2020. Glucocorticoid Sexual Dimorphism in Metabolism: Dissecting the Role of Sex Hormones. *Trends Endocrinol Metab,* 31**,** 357-367.

KUANG, J., CHEN, L., TANG, Q., ZHANG, J., LI, Y. & HE, J. 2018. The Role of Sirt6 in Obesity and Diabetes. *Front Physiol,* 9**,** 135.

KUMAR, R. & THOMPSON, E. B. 2005. Gene regulation by the glucocorticoid receptor: structure:function relationship. *J Steroid Biochem Mol Biol,* 94**,** 383-94.

KUO, T., MCQUEEN, A., CHEN, T. C. & WANG, J. C. 2015. Regulation of Glucose Homeostasis by Glucocorticoids. *Adv Exp Med Biol,* 872**,** 99-126.

KUPIS, W., PALYGA, J., TOMAL, E. & NIEWIADOMSKA, E. 2016. The role of sirtuins in cellular homeostasis. *J Physiol Biochem,* 72**,** 371-80.

LACROIX, A., FEELDERS, R. A., STRATAKIS, C. A. & NIEMAN, L. K. 2015. Cushing's syndrome. *Lancet,* 386**,** 913-27.

LAKSHMI, V., NATH, N. & MUNEYYIRCI-DELALE, O. 1993. Characterization of 11 beta-hydroxysteroid dehydrogenase of human placenta: evidence for the existence of two species of 11 beta-hydroxysteroid dehydrogenase. *J Steroid Biochem Mol Biol,* 45**,** 391-7.

LAMBERTS, S. W., HUIZENGA, A. T., DE LANGE, P., DE JONG, F. H. & KOPER, J. W. 1996. Clinical aspects of glucocorticoid sensitivity. *Steroids,* 61**,** 157-60.

LAMBILLOTTE, C., GILON, P. & HENQUIN, J. C. 1997. Direct glucocorticoid inhibition of insulin secretion. An in vitro study of dexamethasone effects in mouse islets. *J Clin Invest,* 99**,** 414-23.

LANDRY, J., SLAMA, J. T. & STERNGLANZ, R. 2000. Role of NAD(+) in the deacetylase activity of the SIR2-like proteins. *Biochem Biophys Res Commun,* 278**,** 685-90.

LANGE, A. J., ARGAUD, D., EL-MAGHRABI, M. R., PAN, W., MAITRA, S. R. & PILKIS, S. J. 1994. Isolation of a cDNA for the catalytic subunit of rat liver glucose-6-phosphatase: regulation of gene expression in FAO hepatoma cells by insulin, dexamethasone and cAMP. *Biochem Biophys Res Commun,* 201**,** 302-9.

LEE, D. & GOLDBERG, A. L. 2013. SIRT1 protein, by blocking the activities of transcription factors FoxO1 and FoxO3, inhibits muscle atrophy and promotes muscle growth. *J Biol Chem,* 288**,** 30515-30526.

LEE, H., KIM, M., PARK, Y. H. & PARK, J. B. 2018a. Dexamethasone downregulates SIRT1 and IL6 and upregulates EDN1 genes in stem cells derived from gingivae via the AGE/RAGE pathway. *Biotechnol Lett,* 40**,** 509-519.

LEE, R. A., HARRIS, C. A. & WANG, J. C. 2018b. Glucocorticoid Receptor and Adipocyte Biology. *Nucl Receptor Res,* 5.

LEMKE, U., KRONES-HERZIG, A., BERRIEL DIAZ, M., NARVEKAR, P., ZIEGLER, A., VEGIOPOULOS, A., CATO, A. C., BOHL, S., KLINGMULLER, U., SCREATON, R. A., MULLER-DECKER, K., KERSTEN, S. & HERZIG, S. 2008. The glucocorticoid receptor controls hepatic dyslipidemia through Hes1. *Cell Metab,* 8**,** 212-23.

LENZEN, S. & BAILEY, C. J. 1984. Thyroid hormones, gonadal and adrenocortical steroids and the function of the islets of Langerhans. *Endocr Rev,* 5**,** 411-34.

LETTERON, P., BRAHIMI-BOUROUINA, N., ROBIN, M. A., MOREAU, A., FELDMANN, G. & PESSAYRE, D. 1997. Glucocorticoids inhibit mitochondrial matrix acyl-CoA dehydrogenases and fatty acid beta-oxidation. *Am J Physiol,* 272**,** G1141-50.

LEVINE, D. C., KUO, H. Y., HONG, H. K., CEDERNAES, J., HEPLER, C., WRIGHT, A. G., SOMMARS, M. A., KOBAYASHI, Y., MARCHEVA, B., GAO, P., ILKAYEVA, O. R., OMURA, C., RAMSEY, K. M., NEWGARD, C. B., BARISH, G. D., PEEK, C. B., CHANDEL, N. S., MRKSICH, M. & BASS, J. 2021. NADH inhibition of SIRT1 links energy state to transcription during time-restricted feeding. *Nat Metab,* 3**,** 1621-1632.

LI, L., PAN, R., LI, R., NIEMANN, B., AURICH, A. C., CHEN, Y. & ROHRBACH, S. 2011. Mitochondrial biogenesis and peroxisome proliferator-activated receptor-gamma coactivator-1alpha (PGC-1alpha) deacetylation by physical activity: intact adipocytokine signaling is required. *Diabetes,* 60**,** 157-67.

LI, X. 2013. SIRT1 and energy metabolism. *Acta Biochim Biophys Sin (Shanghai),* 45**,** 51-60.

LIN, Q., ZUO, W., LIU, Y., WU, K. & LIU, Q. 2021. NAD(+) and cardiovascular diseases. *Clin Chim Acta,* 515**,** 104-110.

LINDHOLM, J., JUUL, S., JORGENSEN, J. O., ASTRUP, J., BJERRE, P., FELDT-RASMUSSEN, U., HAGEN, C., JORGENSEN, J., KOSTELJANETZ, M., KRISTENSEN, L., LAURBERG, P., SCHMIDT, K. & WEEKE, J. 2001. Incidence and late prognosis of cushing's syndrome: a population-based study. *J Clin Endocrinol Metab,* 86**,** 117-23.

LIU, B., PAGE, A. J., HUTCHISON, A. T., WITTERT, G. A. & HEILBRONN, L. K. 2019. Intermittent fasting increases energy expenditure and promotes adipose tissue browning in mice. *Nutrition,* 66**,** 38-43.

LIU, D., GHARAVI, R., PITTA, M., GLEICHMANN, M. & MATTSON, M. P. 2009. Nicotinamide prevents NAD+ depletion and protects neurons against excitotoxicity and cerebral ischemia: NAD+ consumption by SIRT1 may endanger energetically compromised neurons. *Neuromolecular Med,* 11**,** 28-42.

LIU, L., SU, X., QUINN, W. J., 3RD, HUI, S., KRUKENBERG, K., FREDERICK, D. W., REDPATH, P., ZHAN, L., CHELLAPPA, K., WHITE, E., MIGAUD, M., MITCHISON, T. J., BAUR, J. A. & RABINOWITZ, J. D. 2018. Quantitative Analysis of NAD Synthesis-Breakdown Fluxes. *Cell Metab,* 27**,** 1067-1080 e5.

LIU, L., WANG, C., NI, X. & SUN, J. 2007. A rapid inhibition of NMDA receptor current by corticosterone in cultured hippocampal neurons. *Neurosci Lett,* 420**,** 245-50.

LIU, Z., JAHN, L. A., LONG, W., FRYBURG, D. A., WEI, L. & BARRETT, E. J. 2001. Branched chain amino acids activate messenger ribonucleic acid translation regulatory proteins in human skeletal muscle, and glucocorticoids blunt this action. *J Clin Endocrinol Metab,* 86**,** 2136-43.

LONG, W., BARRETT, E. J., WEI, L. & LIU, Z. 2003. Adrenalectomy enhances the insulin sensitivity of muscle protein synthesis. *Am J Physiol Endocrinol Metab,* 284**,** E102-9.

LONSER, R. R., NIEMAN, L. & OLDFIELD, E. H. 2017. Cushing's disease: pathobiology, diagnosis, and management. *J Neurosurg,* 126**,** 404-417.

LUNDGREN, M., BUREN, J., RUGE, T., MYRNAS, T. & ERIKSSON, J. W. 2004. Glucocorticoids down-regulate glucose uptake capacity and insulin-signaling proteins in omental but not subcutaneous human adipocytes. *J Clin Endocrinol Metab,* 89**,** 2989-97.

LUONGO, T. S., ELLER, J. M., LU, M. J., NIERE, M., RAITH, F., PERRY, C., BORNSTEIN, M. R., OLIPHINT, P., WANG, L., MCREYNOLDS, M. R., MIGAUD, M. E., RABINOWITZ, J. D., JOHNSON, F. B., JOHNSSON, K., ZIEGLER, M., CAMBRONNE, X. A. & BAUR, J. A. 2020. SLC25A51 is a mammalian mitochondrial NAD(+) transporter. *Nature,* 588**,** 174-179.

MA, K., MALLIDIS, C., BHASIN, S., MAHABADI, V., ARTAZA, J., GONZALEZ-CADAVID, N., ARIAS, J. & SALEHIAN, B. 2003. Glucocorticoid-induced skeletal muscle atrophy is associated with upregulation of myostatin gene expression. *Am J Physiol Endocrinol Metab,* 285**,** E363-71.

MA, L., LEE, B. H., MAO, R., CAI, A., JIA, Y., CLIFTON, H., SCHAEFER, S., XU, L. & ZHENG, J. 2014. Nicotinic acid activates the capsaicin receptor TRPV1: Potential mechanism for cutaneous flushing. *Arterioscler Thromb Vasc Biol,* 34**,** 1272-80.

MAGOMEDOVA, L. & CUMMINS, C. L. 2016. Glucocorticoids and Metabolic Control. *Handb Exp Pharmacol,* 233**,** 73-93.

MALAVASI, F., DEAGLIO, S., FUNARO, A., FERRERO, E., HORENSTEIN, A. L., ORTOLAN, E., VAISITTI, T. & AYDIN, S. 2008. Evolution and function of the ADP ribosyl cyclase/CD38 gene family in physiology and pathology. *Physiol Rev,* 88**,** 841-86.

MANCHESTER, K. L. 2000. Arthur Harden: an unwitting pioneer of metabolic control analysis. *Trends Biochem Sci,* 25**,** 89-92.

MARCINKOWSKA, M., LEWANDOWSKI, K. C., LEWINSKI, A., BIENKIEWICZ, M., BASINSKA-LEWANDOWSKA, M., SALATA, I. & RANDEVA, H. S. 2007. Visfatin levels do not change after the oral glucose tolerance test and after a dexamethasone-induced increase in insulin resistance in humans. *Endokrynol Pol,* 58**,** 188-94.

MARTENS, C. R., DENMAN, B. A., MAZZO, M. R., ARMSTRONG, M. L., REISDORPH, N., MCQUEEN, M. B., CHONCHOL, M. & SEALS, D. R. 2018. Chronic nicotinamide riboside supplementation is well-tolerated and elevates NAD(+) in healthy middle-aged and older adults. *Nat Commun,* 9**,** 1286.

MASSUDI, H., GRANT, R., BRAIDY, N., GUEST, J., FARNSWORTH, B. & GUILLEMIN, G. J. 2012. Age-associated changes in oxidative stress and NAD+ metabolism in human tissue. *PLoS One,* 7**,** e42357.

MCMAHON, M., GERICH, J. & RIZZA, R. 1988. Effects of glucocorticoids on carbohydrate metabolism. *Diabetes Metab Rev,* 4**,** 17-30.

MENCONI, M., GONNELLA, P., PETKOVA, V., LECKER, S. & HASSELGREN, P. O. 2008. Dexamethasone and corticosterone induce similar, but not identical, muscle wasting responses in cultured L6 and C2C12 myotubes. *J Cell Biochem,* 105**,** 353-64.

MERICSKAY, M. 2016. Nicotinamide adenine dinucleotide homeostasis and signalling in heart disease: Pathophysiological implications and therapeutic potential. *Arch Cardiovasc Dis,* 109**,** 207-15.

MEYERHOF, O. & OESPER, P. 1947. The oxidative reaction of fermentation. *Fed Proc,* 6**,** 278.

MIGLIAVACCA, E., TAY, S. K. H., PATEL, H. P., SONNTAG, T., CIVILETTO, G., MCFARLANE, C., FORRESTER, T., BARTON, S. J., LEOW, M. K., ANTOUN, E., CHARPAGNE, A., SENG CHONG, Y., DESCOMBES, P., FENG, L., FRANCIS-EMMANUEL, P., GARRATT, E. S., GINER, M. P., GREEN, C. O., KARAZ, S., KOTHANDARAMAN, N., MARQUIS, J., METAIRON, S., MOCO, S., NELSON, G., NGO, S., PLEASANTS, T., RAYMOND, F., SAYER, A. A., MING SIM, C., SLATER-JEFFERIES, J., SYDDALL, H. E., FANG TAN, P., TITCOMBE, P., VAZ, C., WESTBURY, L. D., WONG, G., YONGHUI, W., COOPER, C., SHEPPARD, A., GODFREY, K. M., LILLYCROP, K. A., KARNANI, N. & FEIGE, J. N. 2019. Mitochondrial oxidative capacity and NAD(+) biosynthesis are reduced in human sarcopenia across ethnicities. *Nat Commun,* 10**,** 5808.

MILLER, R., WENTZEL, A. R. & RICHARDS, G. A. 2020. COVID-19: NAD(+) deficiency may predispose the aged, obese and type2 diabetics to mortality through its effect on SIRT1 activity. *Med Hypotheses,* 144**,** 110044.

MILLER, W. L. & AUCHUS, R. J. 2011. The molecular biology, biochemistry, and physiology of human steroidogenesis and its disorders. *Endocr Rev,* 32**,** 81-151.

MILLS, K. F., YOSHIDA, S., STEIN, L. R., GROZIO, A., KUBOTA, S., SASAKI, Y., REDPATH, P., MIGAUD, M. E., APTE, R. S., UCHIDA, K., YOSHINO, J. & IMAI, S. I. 2016. Long-Term Administration of Nicotinamide Mononucleotide Mitigates Age-Associated Physiological Decline in Mice. *Cell Metab,* 24**,** 795-806.

MIN, H. K., KAPOOR, A., FUCHS, M., MIRSHAHI, F., ZHOU, H., MAHER, J., KELLUM, J., WARNICK, R., CONTOS, M. J. & SANYAL, A. J. 2012. Increased hepatic synthesis and dysregulation of cholesterol metabolism is associated with the severity of nonalcoholic fatty liver disease. *Cell Metab,* 15**,** 665-74.

MINA, A. I., LECLAIR, R. A., LECLAIR, K. B., COHEN, D. E., LANTIER, L. & BANKS, A. S. 2018. CalR: A Web-Based Analysis Tool for Indirect Calorimetry Experiments. *Cell Metab,* 28**,** 656-666 e1.

MISHRA, S., COSENTINO, C., TAMTA, A. K., KHAN, D., SRINIVASAN, S., RAVI, V., ABBOTTO, E., ARATHI, B. P., KUMAR, S., JAIN, A., RAMAIAN, A. S., KIZKEKRA, S. M., RAJAGOPAL, R., RAO, S., KRISHNA, S., ASIRVATHAM-JEYARAJ, N., HAGGERTY, E. R., SILBERMAN, D. M., KURLAND, I. J., VEERANNA, R. P., JAYAVELU, T., BRUZZONE, S., MOSTOSLAVSKY, R. & SUNDARESAN, N. R. 2022. Sirtuin 6 inhibition protects against glucocorticoid-induced skeletal muscle atrophy by regulating IGF/PI3K/AKT signaling. *Nat Commun,* 13**,** 5415.

MISSAGHIAN, E., KEMPNA, P., DICK, B., HIRSCH, A., ALIKHANI-KOUPAEI, R., JEGOU, B., MULLIS, P. E., FREY, B. M. & FLUCK, C. E. 2009. Role of DNA methylation in the tissue-specific expression of the CYP17A1 gene for steroidogenesis in rodents. *J Endocrinol,* 202**,** 99-109.

MITCHELL, S. J., BERNIER, M., AON, M. A., CORTASSA, S., KIM, E. Y., FANG, E. F., PALACIOS, H. H., ALI, A., NAVAS-ENAMORADO, I., DI FRANCESCO, A., KAISER, T. A., WALTZ, T. B., ZHANG, N., ELLIS, J. L., ELLIOTT, P. J., FREDERICK, D. W., BOHR, V. A., SCHMIDT, M. S., BRENNER, C., SINCLAIR, D. A., SAUVE, A. A., BAUR, J. A. & DE CABO, R. 2018. Nicotinamide Improves Aspects of Healthspan, but Not Lifespan, in Mice. *Cell Metab,* 27**,** 667-676 e4.

MIZOGUCHI, K., IKEDA, R., SHOJI, H., TANAKA, Y., MARUYAMA, W. & TABIRA, T. 2009. Aging attenuates glucocorticoid negative feedback in rat brain. *Neuroscience,* 159**,** 259-70.

MOHAMED, J. S., HAJIRA, A., PARDO, P. S. & BORIEK, A. M. 2014. MicroRNA-149 inhibits PARP-2 and promotes mitochondrial biogenesis via SIRT-1/PGC-1alpha network in skeletal muscle. *Diabetes,* 63**,** 1546-59.

MORALES, J., LI, L., FATTAH, F. J., DONG, Y., BEY, E. A., PATEL, M., GAO, J. & BOOTHMAN, D. A. 2014. Review of poly (ADP-ribose) polymerase (PARP) mechanisms of action and rationale for targeting in cancer and other diseases. *Crit Rev Eukaryot Gene Expr,* 24**,** 15-28.

MORGAN, S. A., GATHERCOLE, L. L., SIMONET, C., HASSAN-SMITH, Z. K., BUJALSKA, I., GUEST, P., ABRAHAMS, L., SMITH, D. M., STEWART, P. M., LAVERY, G. G. & TOMLINSON, J. W. 2013. Regulation of lipid metabolism by glucocorticoids and 11beta-HSD1 in skeletal muscle. *Endocrinology,* 154**,** 2374-84.

MORGAN, S. A., HASSAN-SMITH, Z. K., DOIG, C. L., SHERLOCK, M., STEWART, P. M. & LAVERY, G. G. 2016a. Glucocorticoids and 11beta-HSD1 are major regulators of intramyocellular protein metabolism. *J Endocrinol,* 229**,** 277-86.

MORGAN, S. A., HASSAN-SMITH, Z. K. & LAVERY, G. G. 2016b. MECHANISMS IN ENDOCRINOLOGY: Tissue-specific activation of cortisol in Cushing's syndrome. *Eur J Endocrinol,* 175**,** R83-9.

MORGAN, S. A., MCCABE, E. L., GATHERCOLE, L. L., HASSAN-SMITH, Z. K., LARNER, D. P., BUJALSKA, I. J., STEWART, P. M., TOMLINSON, J. W. & LAVERY, G. G. 2014. 11beta-HSD1 is the major regulator of the tissue-specific effects of circulating glucocorticoid excess. *Proc Natl Acad Sci U S A,* 111**,** E2482-91.

MORGAN, S. A., SHERLOCK, M., GATHERCOLE, L. L., LAVERY, G. G., LENAGHAN, C., BUJALSKA, I. J., LABER, D., YU, A., CONVEY, G., MAYERS, R., HEGYI, K., SETHI, J. K., STEWART, P. M., SMITH, D. M. & TOMLINSON, J. W. 2009. 11beta-hydroxysteroid dehydrogenase type 1 regulates glucocorticoid-induced insulin resistance in skeletal muscle. *Diabetes,* 58**,** 2506-15.

MUKHERJEE, S., MO, J., PAOLELLA, L. M., PERRY, C. E., TOTH, J., HUGO, M. M., CHU, Q., TONG, Q., CHELLAPPA, K. & BAUR, J. A. 2021. SIRT3 is required for liver regeneration but not for the beneficial effect of nicotinamide riboside. *JCI Insight,* 6.

NAKAHATA, Y., SAHAR, S., ASTARITA, G., KALUZOVA, M. & SASSONE-CORSI, P. 2009. Circadian control of the NAD+ salvage pathway by CLOCK-SIRT1. *Science,* 324**,** 654-7.

NAKAMURA, K., KAGEYAMA, S., KE, B., FUJII, T., SOSA, R. A., REED, E. F., DATTA, N., ZARRINPAR, A., BUSUTTIL, R. W. & KUPIEC-WEGLINSKI, J. W. 2017. Sirtuin 1 attenuates inflammation and hepatocellular damage in liver transplant ischemia/Reperfusion: From mouse to human. *Liver Transpl,* 23**,** 1282-1293.

NEWTON, R. 2000. Molecular mechanisms of glucocorticoid action: what is important? *Thorax,* 55**,** 603-13.

NHS. 2021. *Cushing's syndrome* [Online]. Available: https://www.nhs.uk/conditions/cushings-syndrome/ [Accessed 15.08.22].

NICOLAIDES, N. C., KYRATZI, E., LAMPROKOSTOPOULOU, A., CHROUSOS, G. P. & CHARMANDARI, E. 2015. Stress, the stress system and the role of glucocorticoids. *Neuroimmunomodulation,* 22**,** 6-19.

NIEMAN, L. K., BILLER, B. M., FINDLING, J. W., MURAD, M. H., NEWELL-PRICE, J., SAVAGE, M. O., TABARIN, A. & ENDOCRINE, S. 2015. Treatment of Cushing's Syndrome: An Endocrine Society Clinical Practice Guideline. *J Clin Endocrinol Metab,* 100**,** 2807-31.

NIKIFOROV, A., DOLLE, C., NIERE, M. & ZIEGLER, M. 2011. Pathways and subcellular compartmentation of NAD biosynthesis in human cells: from entry of extracellular precursors to mitochondrial NAD generation. *J Biol Chem,* 286**,** 21767-78.

OKABE, K., YAKU, K., TOBE, K. & NAKAGAWA, T. 2019. Implications of altered NAD metabolism in metabolic disorders. *J Biomed Sci,* 26**,** 34.

OLIJSLAGERS, J. E., DE KLOET, E. R., ELGERSMA, Y., VAN WOERDEN, G. M., JOELS, M. & KARST, H. 2008. Rapid changes in hippocampal CA1 pyramidal cell function via pre- as well as postsynaptic membrane mineralocorticoid receptors. *Eur J Neurosci,* 27**,** 2542-50.

OPHERK, C., TRONCHE, F., KELLENDONK, C., KOHLMULLER, D., SCHULZE, A., SCHMID, W. & SCHUTZ, G. 2004. Inactivation of the glucocorticoid receptor in hepatocytes leads to fasting hypoglycemia and ameliorates hyperglycemia in streptozotocin-induced diabetes mellitus. *Mol Endocrinol,* 18**,** 1346-53.

OPPONG, E. & CATO, A. C. 2015. Effects of Glucocorticoids in the Immune System. *Adv Exp Med Biol,* 872**,** 217-33.

ORAY, M., ABU SAMRA, K., EBRAHIMIADIB, N., MEESE, H. & FOSTER, C. S. 2016. Long-term side effects of glucocorticoids. *Expert Opin Drug Saf,* 15**,** 457-65.

OTHONOS, N., POFI, R., ARVANITI, A., WHITE, S., BONAVENTURA, I., NIKOLAOU, N., MOOLLA, A., MARJOT, T., STIMSON, R. H., VAN BEEK, A. P., VAN FAASSEN, M., ISIDORI, A. M., BATEMAN, E., SADLER, R., KARPE, F., STEWART, P. M., WEBSTER, C., DUFFY, J., EASTELL, R., GOSSIEL, F., CORNFIELD, T., HODSON, L., JANE ESCOTT, K., WHITTAKER, A., KIRIK, U., COLEMAN, R. L., SCOTT, C. A. B., MILTON, J. E., AGBAJE, O., HOLMAN, R. R. & TOMLINSON, J. W. 2023. 11beta-HSD1 inhibition in men mitigates prednisolone-induced adverse effects in a proof-of-concept randomised double-blind placebo-controlled trial. *Nat Commun,* 14**,** 1025.

OU, X., LEE, M. R., HUANG, X., MESSINA-GRAHAM, S. & BROXMEYER, H. E. 2014. SIRT1 positively regulates autophagy and mitochondria function in embryonic stem cells under oxidative stress. *Stem Cells,* 32**,** 1183-94.

OVERMAN, R. A., YEH, J. Y. & DEAL, C. L. 2013. Prevalence of oral glucocorticoid usage in the United States: a general population perspective. *Arthritis Care Res (Hoboken),* 65**,** 294-8.

PAN, S., CUI, Y., FU, Z., ZHANG, L. & XING, H. 2019. MicroRNA-128 is involved in dexamethasone-induced lipid accumulation via repressing SIRT1 expression in cultured pig preadipocytes. *J Steroid Biochem Mol Biol,* 186**,** 185-195.

PASQUEREAU, S., TOTOSON, P., NEHME, Z., ABBAS, W., KUMAR, A., VERHOEVEN, F., PRATI, C., WENDLING, D., DEMOUGEOT, C. & HERBEIN, G. 2021. Impact of glucocorticoids on systemic sirtuin 1 expression and activity in rats with adjuvant-induced arthritis. *Epigenetics,* 16**,** 132-143.

PATEL, M. S., NEMERIA, N. S., FUREY, W. & JORDAN, F. 2014. The pyruvate dehydrogenase complexes: structure-based function and regulation. *J Biol Chem,* 289**,** 16615-23.

PATEL, R., PATEL, M., TSAI, R., LIN, V., BOOKOUT, A. L., ZHANG, Y., MAGOMEDOVA, L., LI, T., CHAN, J. F., BUDD, C., MANGELSDORF, D. J. & CUMMINS, C. L. 2011. LXRbeta is required for glucocorticoid-induced hyperglycemia and hepatosteatosis in mice. *J Clin Invest,* 121**,** 431-41.

PAYNE, A. H. & HALES, D. B. 2004. Overview of steroidogenic enzymes in the pathway from cholesterol to active steroid hormones. *Endocr Rev,* 25**,** 947-70.

PECKETT, A. J., WRIGHT, D. C. & RIDDELL, M. C. 2011. The effects of glucocorticoids on adipose tissue lipid metabolism. *Metabolism,* 60**,** 1500-10.

PECORI GIRALDI, F., MORO, M., CAVAGNINI, F. & STUDY GROUP ON THE HYPOTHALAMO-PITUITARY-ADRENAL AXIS OF THE ITALIAN SOCIETY OF, E. 2003. Gender-related differences in the presentation and course of Cushing's disease. *J Clin Endocrinol Metab,* 88**,** 1554-8.

PELUSO, A., DAMGAARD, M. V., MORI, M. A. S. & TREEBAK, J. T. 2021. Age-Dependent Decline of NAD(+)-Universal Truth or Confounded Consensus? *Nutrients,* 14.

PEROGAMVROS, I., RAY, D. W. & TRAINER, P. J. 2012. Regulation of cortisol bioavailability--effects on hormone measurement and action. *Nat Rev Endocrinol,* 8**,** 717-27.

PILKIS, S. J. & GRANNER, D. K. 1992. Molecular physiology of the regulation of hepatic gluconeogenesis and glycolysis. *Annu Rev Physiol,* 54**,** 885-909.

PILLAI, J. B., ISBATAN, A., IMAI, S. & GUPTA, M. P. 2005. Poly(ADP-ribose) polymerase-1-dependent cardiac myocyte cell death during heart failure is mediated by NAD+ depletion and reduced Sir2alpha deacetylase activity. *J Biol Chem,* 280**,** 43121-30.

PISSIOS, P. 2017. Nicotinamide N-Methyltransferase: More Than a Vitamin B3 Clearance Enzyme. *Trends Endocrinol Metab,* 28**,** 340-353.

PITTELLI, M., FORMENTINI, L., FARACO, G., LAPUCCI, A., RAPIZZI, E., CIALDAI, F., ROMANO, G., MONETI, G., MORONI, F. & CHIARUGI, A. 2010. Inhibition of nicotinamide phosphoribosyltransferase: cellular bioenergetics reveals a mitochondrial insensitive NAD pool. *J Biol Chem,* 285**,** 34106-14.

POGGIOLI, R., UETA, C. B., DRIGO, R. A., CASTILLO, M., FONSECA, T. L. & BIANCO, A. C. 2013. Dexamethasone reduces energy expenditure and increases susceptibility to diet-induced obesity in mice. *Obesity (Silver Spring),* 21**,** E415-20.

POLLAK, N., DOLLE, C. & ZIEGLER, M. 2007. The power to reduce: pyridine nucleotides--small molecules with a multitude of functions. *Biochem J,* 402**,** 205-18.

PRANGER, I. G., VAN RAALTE, D. H., BRANDS, M., MUSKIET, M. H. A., KEMA, I. P., SERLIE, M. J., DIAMANT, M., BAKKER, S. J. L. & MUSKIET, F. A. J. 2018. Influence of prednisolone on parameters of de novo lipogenesis and indices for stearoyl-CoA- and Delta6- desaturase activity in healthy males: A Post-hoc analysis of a randomized, placebo-controlled, double-blind trial. *Prostaglandins Leukot Essent Fatty Acids,* 132**,** 8-15.

PRATT, W. B. & TOFT, D. O. 1997. Steroid receptor interactions with heat shock protein and immunophilin chaperones. *Endocr Rev,* 18**,** 306-60.

PUIGSERVER, P. & SPIEGELMAN, B. M. 2003. Peroxisome proliferator-activated receptor-gamma coactivator 1 alpha (PGC-1 alpha): transcriptional coactivator and metabolic regulator. *Endocr Rev,* 24**,** 78-90.

QI, A. Q., QIU, J., XIAO, L. & CHEN, Y. Z. 2005. Rapid activation of JNK and p38 by glucocorticoids in primary cultured hippocampal cells. *J Neurosci Res,* 80**,** 510-7.

QUATTROCELLI, M., WINTZINGER, M., MIZ, K., LEVINE, D. C., PEEK, C. B., BASS, J. & MCNALLY, E. M. 2022. Muscle mitochondrial remodeling by intermittent glucocorticoid drugs requires an intact circadian clock and muscle PGC1alpha. *Sci Adv,* 8**,** eabm1189.

QUINLAN, C. L., GONCALVES, R. L., HEY-MOGENSEN, M., YADAVA, N., BUNIK, V. I. & BRAND, M. D. 2014. The 2-oxoacid dehydrogenase complexes in mitochondria can produce superoxide/hydrogen peroxide at much higher rates than complex I. *J Biol Chem,* 289**,** 8312-25.

QUINN, M. A. & CIDLOWSKI, J. A. 2016. Endogenous hepatic glucocorticoid receptor signaling coordinates sex-biased inflammatory gene expression. *FASEB J,* 30**,** 971-82.

RADHAKUTTY, A., MANGELSDORF, B. L., DRAKE, S. M., SAMOCHA-BONET, D., HEILBRONN, L. K., SMITH, M. D., THOMPSON, C. H. & BURT, M. G. 2016. Effects of prednisolone on energy and fat metabolism in patients with rheumatoid arthritis: tissue-specific insulin resistance with commonly used prednisolone doses. *Clin Endocrinol (Oxf),* 85**,** 741-747.

RAFACHO, A., GIOZZET, V. A., BOSCHERO, A. C. & BOSQUEIRO, J. R. 2008. Functional alterations in endocrine pancreas of rats with different degrees of dexamethasone-induced insulin resistance. *Pancreas,* 36**,** 284-93.

RAFF, H. & CARROLL, T. 2015. Cushing's syndrome: from physiological principles to diagnosis and clinical care. *J Physiol,* 593**,** 493-506.

RAFF, H., SHARMA, S. T. & NIEMAN, L. K. 2014. Physiological basis for the etiology, diagnosis, and treatment of adrenal disorders: Cushing's syndrome, adrenal insufficiency, and congenital adrenal hyperplasia. *Compr Physiol,* 4**,** 739-69.

RAHBANI, J. F., ROESLER, A., HUSSAIN, M. F., SAMBORSKA, B., DYKSTRA, C. B., TSAI, L., JEDRYCHOWSKI, M. P., VERGNES, L., REUE, K., SPIEGELMAN, B. M. & KAZAK, L. 2021. Creatine kinase B controls futile creatine cycling in thermogenic fat. *Nature,* 590**,** 480-485.

RAHIMI, L., RAJPAL, A. & ISMAIL-BEIGI, F. 2020. Glucocorticoid-Induced Fatty Liver Disease. *Diabetes Metab Syndr Obes,* 13**,** 1133-1145.

RAINVILLE, J. R., WEISS, G. L., EVANSON, N., HERMAN, J. P., VASUDEVAN, N. & TASKER, J. G. 2019. Membrane-initiated nuclear trafficking of the glucocorticoid receptor in hypothalamic neurons. *Steroids,* 142**,** 55-64.

RAMAGE, L. E., AKYOL, M., FLETCHER, A. M., FORSYTHE, J., NIXON, M., CARTER, R. N., VAN BEEK, E. J., MORTON, N. M., WALKER, B. R. & STIMSON, R. H. 2016. Glucocorticoids Acutely Increase Brown Adipose Tissue Activity in Humans, Revealing Species-Specific Differences in UCP-1 Regulation. *Cell Metab,* 24**,** 130-41.

RAMAMOORTHY, S. & CIDLOWSKI, J. A. 2016. Corticosteroids: Mechanisms of Action in Health and Disease. *Rheum Dis Clin North Am,* 42**,** 15-31, vii.

RANI, V., DEEP, G., SINGH, R. K., PALLE, K. & YADAV, U. C. 2016. Oxidative stress and metabolic disorders: Pathogenesis and therapeutic strategies. *Life Sci,* 148**,** 183-93.

RATAJCZAK, J., JOFFRAUD, M., TRAMMELL, S. A., RAS, R., CANELA, N., BOUTANT, M., KULKARNI, S. S., RODRIGUES, M., REDPATH, P., MIGAUD, M. E., AUWERX, J., YANES, O., BRENNER, C. & CANTO, C. 2016. NRK1 controls nicotinamide mononucleotide and nicotinamide riboside metabolism in mammalian cells. *Nat Commun,* 7**,** 13103.

REBUFFE-SCRIVE, M., KROTKIEWSKI, M., ELFVERSON, J. & BJORNTORP, P. 1988. Muscle and adipose tissue morphology and metabolism in Cushing's syndrome. *J Clin Endocrinol Metab,* 67**,** 1122-8.

REICH, E., TAMARY, A., SIONOV, R. V. & MELLOUL, D. 2012. Involvement of thioredoxin-interacting protein (TXNIP) in glucocorticoid-mediated beta cell death. *Diabetologia,* 55**,** 1048-57.

REMIE, C. M. E., ROUMANS, K. H. M., MOONEN, M. P. B., CONNELL, N. J., HAVEKES, B., MEVENKAMP, J., LINDEBOOM, L., DE WIT, V. H. W., VAN DE WEIJER, T., AARTS, S., LUTGENS, E., SCHOMAKERS, B. V., ELFRINK, H. L., ZAPATA-PEREZ, R., HOUTKOOPER, R. H., AUWERX, J., HOEKS, J., SCHRAUWEN-HINDERLING, V. B., PHIELIX, E. & SCHRAUWEN, P. 2020. Nicotinamide riboside supplementation alters body composition and skeletal muscle acetylcarnitine concentrations in healthy obese humans. *Am J Clin Nutr,* 112**,** 413-426.

RHEN, T. & CIDLOWSKI, J. A. 2005. Antiinflammatory action of glucocorticoids--new mechanisms for old drugs. *N Engl J Med,* 353**,** 1711-23.

RINDLER, P. M., CREWE, C. L., FERNANDES, J., KINTER, M. & SZWEDA, L. I. 2013. Redox regulation of insulin sensitivity due to enhanced fatty acid utilization in the mitochondria. *Am J Physiol Heart Circ Physiol,* 305**,** H634-43.

RITTER, H. D. & MUELLER, C. R. 2014. Expression microarray identifies the unliganded glucocorticoid receptor as a regulator of gene expression in mammary epithelial cells. *BMC Cancer,* 14**,** 275.

ROMA, L. P., SOUZA, K. L., CARNEIRO, E. M., BOSCHERO, A. C. & BOSQUEIRO, J. R. 2012. Pancreatic islets from dexamethasone-treated rats show alterations in global gene expression and mitochondrial pathways. *Gen Physiol Biophys,* 31**,** 65-76.

RONACHER, K., HADLEY, K., AVENANT, C., STUBSRUD, E., SIMONS, S. S., JR., LOUW, A. & HAPGOOD, J. P. 2009. Ligand-selective transactivation and transrepression via the glucocorticoid receptor: role of cofactor interaction. *Mol Cell Endocrinol,* 299**,** 219-31.

ROSE, A. J. & HERZIG, S. 2013. Metabolic control through glucocorticoid hormones: an update. *Mol Cell Endocrinol,* 380**,** 65-78.

ROSENBAUM, D. M., RASMUSSEN, S. G. & KOBILKA, B. K. 2009. The structure and function of G-protein-coupled receptors. *Nature,* 459**,** 356-63.

RUSSELL, D. W. & WILSON, J. D. 1994. Steroid 5 alpha-reductase: two genes/two enzymes. *Annu Rev Biochem,* 63**,** 25-61.

RUSVAI, E. & NARAY-FEJES-TOTH, A. 1993. A new isoform of 11 beta-hydroxysteroid dehydrogenase in aldosterone target cells. *J Biol Chem,* 268**,** 10717-20.

RUZZIN, J., WAGMAN, A. S. & JENSEN, J. 2005. Glucocorticoid-induced insulin resistance in skeletal muscles: defects in insulin signalling and the effects of a selective glycogen synthase kinase-3 inhibitor. *Diabetologia,* 48**,** 2119-30.

RYU, D., ZHANG, H., ROPELLE, E. R., SORRENTINO, V., MAZALA, D. A., MOUCHIROUD, L., MARSHALL, P. L., CAMPBELL, M. D., ALI, A. S., KNOWELS, G. M., BELLEMIN, S., IYER, S. R., WANG, X., GARIANI, K., SAUVE, A. A., CANTO, C., CONLEY, K. E., WALTER, L., LOVERING, R. M.,

CHIN, E. R., JASMIN, B. J., MARCINEK, D. J., MENZIES, K. J. & AUWERX, J. 2016. NAD+ repletion improves muscle function in muscular dystrophy and counters global PARylation. *Sci Transl Med,* 8**,** 361ra139.

SAKODA, H., OGIHARA, T., ANAI, M., FUNAKI, M., INUKAI, K., KATAGIRI, H., FUKUSHIMA, Y., ONISHI, Y., ONO, H., FUJISHIRO, M., KIKUCHI, M., OKA, Y. & ASANO, T. 2000. Dexamethasone-induced insulin resistance in 3T3-L1 adipocytes is due to inhibition of glucose transport rather than insulin signal transduction. *Diabetes,* 49**,** 1700-8.

SAPOLSKY, R. M., KREY, L. C. & MCEWEN, B. S. 1986. The neuroendocrinology of stress and aging: the glucocorticoid cascade hypothesis. *Endocr Rev,* 7**,** 284-301.

SATO, A. Y., PEACOCK, M. & BELLIDO, T. 2018. Glucocorticoid Excess in Bone and Muscle. *Clin Rev Bone Miner Metab,* 16**,** 33-47.

SAVORY, J. G., HSU, B., LAQUIAN, I. R., GIFFIN, W., REICH, T., HACHE, R. J. & LEFEBVRE, Y. A. 1999. Discrimination between NL1- and NL2-mediated nuclear localization of the glucocorticoid receptor. *Mol Cell Biol,* 19**,** 1025-37.

SAYERS, S. R., BEAVIL, R. L., FINE, N. H. F., HUANG, G. C., CHOUDHARY, P., PACHOLARZ, K. J., BARRAN, P. E., BUTTERWORTH, S., MILLS, C. E., CRUICKSHANK, J. K., SILVESTRE, M. P., POPPITT, S. D., MCGILL, A. T., LAVERY, G. G., HODSON, D. J. & CATON, P. W. 2020. Structure-functional changes in eNAMPT at high concentrations mediate mouse and human beta cell dysfunction in type 2 diabetes. *Diabetologia,* 63**,** 313-323.

SCHAKMAN, O., GILSON, H. & THISSEN, J. P. 2008. Mechanisms of glucocorticoid-induced myopathy. *J Endocrinol,* 197**,** 1-10.

SCHAKMAN, O., KALISTA, S., BARBE, C., LOUMAYE, A. & THISSEN, J. P. 2013. Glucocorticoid-induced skeletal muscle atrophy. *Int J Biochem Cell Biol,* 45**,** 2163-72.

SCHIAFFINO, S., DYAR, K. A., CICILIOT, S., BLAAUW, B. & SANDRI, M. 2013. Mechanisms regulating skeletal muscle growth and atrophy. *FEBS J,* 280**,** 4294-314.

SCHMITTGEN, T. D. & LIVAK, K. J. 2008. Analyzing real-time PCR data by the comparative C(T) method. *Nat Protoc,* 3**,** 1101-8.

SECKL, J. R. 2004. 11beta-hydroxysteroid dehydrogenases: changing glucocorticoid action. *Curr Opin Pharmacol,* 4**,** 597-602.

SEFTON, C., HARNO, E., DAVIES, A., SMALL, H., ALLEN, T. J., WRAY, J. R., LAWRENCE, C. B., COLL, A. P. & WHITE, A. 2016. Elevated Hypothalamic Glucocorticoid Levels Are Associated With Obesity and Hyperphagia in Male Mice. *Endocrinology,* 157**,** 4257-4265.

SEO, K., KI, S. H. & SHIN, S. M. 2014. Methylglyoxal induces mitochondrial dysfunction and cell death in liver. *Toxicol Res,* 30**,** 193-8.

SHAN, L., YU, X. C., LIU, Z., HU, Y., STURGIS, L. T., MIRANDA, M. L. & LIU, Q. 2009. The angiopoietin-like proteins ANGPTL3 and ANGPTL4 inhibit lipoprotein lipase activity through distinct mechanisms. *J Biol Chem,* 284**,** 1419-24.

SHATS, I., WILLIAMS, J. G., LIU, J., MAKAROV, M. V., WU, X., LIH, F. B., DETERDING, L. J., LIM, C., XU, X., RANDALL, T. A., LEE, E., LI, W., FAN, W., LI, J. L., SOKOLSKY, M., KABANOV, A. V., LI, L., MIGAUD, M. E., LOCASALE, J. W. & LI, X. 2020. Bacteria Boost Mammalian Host NAD Metabolism by Engaging the Deamidated Biosynthesis Pathway. *Cell Metab,* 31**,** 564-579 e7.

SHIMA, A., SHINOHARA, Y., DOI, K. & TERADA, H. 1994. Normal differentiation of rat brown adipocytes in primary culture judged by their expressions of uncoupling protein and the physiological isoform of glucose transporter. *Biochim Biophys Acta,* 1223**,** 1-8.

SHIN, Y. S., FINK, H., KHIROYA, R., IBEBUNJO, C. & MARTYN, J. 2000. Prednisolone-induced muscle dysfunction is caused more by atrophy than by altered acetylcholine receptor expression. *Anesth Analg,* 91**,** 322-8.

SHORT, K. R., NYGREN, J., BIGELOW, M. L. & NAIR, K. S. 2004. Effect of short-term prednisone use on blood flow, muscle protein metabolism, and function. *J Clin Endocrinol Metab,* 89**,** 6198-207.

SIMS, J. L., BERGER, S. J. & BERGER, N. A. 1983. Poly(ADP-ribose) Polymerase inhibitors preserve nicotinamide adenine dinucleotide and adenosine 5'-triphosphate pools in DNA-damaged cells: mechanism of stimulation of unscheduled DNA synthesis. *Biochemistry,* 22**,** 5188-94.

SINGH, C. K., CHHABRA, G., NDIAYE, M. A., GARCIA-PETERSON, L. M., MACK, N. J. & AHMAD, N. 2018. The Role of Sirtuins in Antioxidant and Redox Signaling. *Antioxid Redox Signal,* 28**,** 643-661.

SLAVIN, B. G., ONG, J. M. & KERN, P. A. 1994. Hormonal regulation of hormone-sensitive lipase activity and mRNA levels in isolated rat adipocytes. *J Lipid Res,* 35**,** 1535-41.

SPAANDERMAN, D. C. E., NIXON, M., BUURSTEDE, J. C., SIPS, H. C., SCHILPEROORT, M., KUIPERS, E. N., BACKER, E. A., KOOIJMAN, S., RENSEN, P. C. N., HOMER, N. Z. M., WALKER, B. R., MEIJER, O. C. & KROON, J. 2018. Androgens modulate glucocorticoid receptor activity in adipose tissue and liver. *J Endocrinol*.

SPIERS, J. G., CHEN, H. J., SERNIA, C. & LAVIDIS, N. A. 2014. Activation of the hypothalamic-pituitary-adrenal stress axis induces cellular oxidative stress. *Front Neurosci,* 8**,** 456.

STAHN, C., LOWENBERG, M., HOMMES, D. W. & BUTTGEREIT, F. 2007. Molecular mechanisms of glucocorticoid action and selective glucocorticoid receptor agonists. *Mol Cell Endocrinol,* 275**,** 71-8.

STEGER, D. J., GRANT, G. R., SCHUPP, M., TOMARU, T., LEFTEROVA, M. I., SCHUG, J., MANDUCHI, E., STOECKERT, C. J., JR. & LAZAR, M. A. 2010. Propagation of adipogenic signals through an epigenomic transition state. *Genes Dev,* 24**,** 1035-44.

STEIN, L. R. & IMAI, S. 2012. The dynamic regulation of NAD metabolism in mitochondria. *Trends Endocrinol Metab,* 23**,** 420-8.

STINCONE, A., PRIGIONE, A., CRAMER, T., WAMELINK, M. M., CAMPBELL, K., CHEUNG, E., OLIN-SANDOVAL, V., GRUNING, N. M., KRUGER, A., TAUQEER ALAM, M., KELLER, M. A., BREITENBACH, M., BRINDLE, K. M., RABINOWITZ, J. D. & RALSER, M. 2015. The return of metabolism: biochemistry and physiology of the pentose phosphate pathway. *Biol Rev Camb Philos Soc,* 90**,** 927-63.

STRACK, A. M., BRADBURY, M. J. & DALLMAN, M. F. 1995. Corticosterone decreases nonshivering thermogenesis and increases lipid storage in brown adipose tissue. *Am J Physiol,* 268**,** R183-91.

STUCK, A. E., MINDER, C. E. & FREY, F. J. 1989. Risk of infectious complications in patients taking glucocorticosteroids. *Rev Infect Dis,* 11**,** 954-63.

SUGDEN, M. C. & HOLNESS, M. J. 2003. Recent advances in mechanisms regulating glucose oxidation at the level of the pyruvate dehydrogenase complex by PDKs. *Am J Physiol Endocrinol Metab,* 284**,** E855-62.

SUN, K., WANG, X., FANG, N., XU, A., LIN, Y., ZHAO, X., NAZARALI, A. J. & JI, S. 2020. SIRT2 suppresses expression of inflammatory factors via Hsp90-glucocorticoid receptor signalling. *J Cell Mol Med,* 24**,** 7439-7450.

SUZUKI, S., IBEN, J. R., COON, S. L. & KINO, T. 2018. SIRT1 is a transcriptional enhancer of the glucocorticoid receptor acting independently to its deacetylase activity. *Mol Cell Endocrinol,* 461**,** 178-187.

TALAL, S., CEASE, A., FARINGTON, R., MEDINA, H. E., ROJAS, J. & HARRISON, J. 2021. High carbohydrate diet ingestion increases post-meal lipid synthesis and drives respiratory exchange ratios above 1. *J Exp Biol,* 224.

TALLIS, M., MORRA, R., BARKAUSKAITE, E. & AHEL, I. 2014. Poly(ADP-ribosyl)ation in regulation of chromatin structure and the DNA damage response. *Chromosoma,* 123**,** 79-90.

TAMURA, Y., KAWAO, N., YANO, M., OKADA, K., OKUMOTO, K., CHIBA, Y., MATSUO, O. & KAJI, H. 2015. Role of plasminogen activator inhibitor-1 in glucocorticoid-induced diabetes and osteopenia in mice. *Diabetes,* 64**,** 2194-206.

TAN, B., YOUNG, D. A., LU, Z. H., WANG, T., MEIER, T. I., SHEPARD, R. L., ROTH, K., ZHAI, Y., HUSS, K., KUO, M. S., GILLIG, J., PARTHASARATHY, S., BURKHOLDER, T. P., SMITH, M. C., GEEGANAGE, S. & ZHAO, G. 2013. Pharmacological inhibition of nicotinamide phosphoribosyltransferase (NAMPT), an enzyme essential for NAD+ biosynthesis, in human cancer cells: metabolic basis and potential clinical implications. *J Biol Chem,* 288**,** 3500-11.

TANG, V. M., YOUNG, A. H., TAN, H., BEASLEY, C. & WANG, J. F. 2013. Glucocorticoids increase protein carbonylation and mitochondrial dysfunction. *Horm Metab Res,* 45**,** 709-15.

TASKINEN, M. R., NIKKILA, E. A., PELKONEN, R. & SANE, T. 1983. Plasma lipoproteins, lipolytic enzymes, and very low density lipoprotein triglyceride turnover in Cushing's syndrome. *J Clin Endocrinol Metab,* 57**,** 619-26.

TATARANNI, P. A., LARSON, D. E., SNITKER, S., YOUNG, J. B., FLATT, J. P. & RAVUSSIN, E. 1996. Effects of glucocorticoids on energy metabolism and food intake in humans. *Am J Physiol,* 271**,** E317-25.

TCHEN, C. R., MARTINS, J. R., PAKTIAWAL, N., PERELLI, R., SAKLATVALA, J. & CLARK, A. R. 2010. Glucocorticoid regulation of mouse and human dual specificity phosphatase 1 (DUSP1) genes: unusual cis-acting elements and unexpected evolutionary divergence. *J Biol Chem,* 285**,** 2642-52.

TEMPEL, W., RABEH, W. M., BOGAN, K. L., BELENKY, P., WOJCIK, M., SEIDLE, H. F., NEDYALKOVA, L., YANG, T., SAUVE, A. A., PARK, H. W. & BRENNER, C. 2007. Nicotinamide riboside kinase structures reveal new pathways to NAD+. *PLoS Biol,* 5**,** e263.

THOLEN, S., PATEL, R., AGAS, A., KOVARY, K. M., RABIEE, A., NICHOLLS, H. T., BIELCZYK-MACZYNSKA, E., YANG, W., KRAEMER, F. B. & TERUEL, M. N. 2022. Flattening of circadian glucocorticoid oscillations drives acute hyperinsulinemia and adipocyte hypertrophy. *Cell Rep,* 39**,** 111018.

TIMMERMANS, S., VANDEWALLE, J. & LIBERT, C. 2022. Dimerization of the Glucocorticoid Receptor and Its Importance in (Patho)physiology: A Primer. *Cells,* 11.

TIRYAKIOGLU, O., UGURLU, S., YALIN, S., YIRMIBESCIK, S., CAGLAR, E., YETKIN, D. O. & KADIOGLU, P. 2010. Screening for Cushing's syndrome in obese patients. *Clinics (Sao Paulo),* 65**,** 9-13.

TISCHLER, M. E., FRIEDRICHS, D., COLL, K. & WILLIAMSON, J. R. 1977. Pyridine nucleotide distributions and enzyme mass action ratios in hepatocytes from fed and starved rats. *Arch Biochem Biophys,* 184**,** 222-36.

TOMLINSON, J. W., DRAPER, N., MACKIE, J., JOHNSON, A. P., HOLDER, G., WOOD, P. & STEWART, P. M. 2002. Absence of Cushingoid phenotype in a patient with Cushing's disease due to defective cortisone to cortisol conversion. *J Clin Endocrinol Metab,* 87**,** 57-62.

TOMLINSON, J. W. & STEWART, P. M. 2001. Cortisol metabolism and the role of 11beta-hydroxysteroid dehydrogenase. *Best Pract Res Clin Endocrinol Metab,* 15**,** 61-78.

TOMLINSON, J. W., WALKER, E. A., BUJALSKA, I. J., DRAPER, N., LAVERY, G. G., COOPER, M. S., HEWISON, M. & STEWART, P. M. 2004. 11beta-hydroxysteroid dehydrogenase type 1: a tissue-specific regulator of glucocorticoid response. *Endocr Rev,* 25**,** 831-66.

TONG, L. & DENU, J. M. 2010. Function and metabolism of sirtuin metabolite O-acetyl-ADP-ribose. *Biochim Biophys Acta,* 1804**,** 1617-25.

TRAMMELL, S. A., SCHMIDT, M. S., WEIDEMANN, B. J., REDPATH, P., JAKSCH, F., DELLINGER, R. W., LI, Z., ABEL, E. D., MIGAUD, M. E. & BRENNER, C. 2016a. Nicotinamide riboside is uniquely and orally bioavailable in mice and humans. *Nat Commun,* 7**,** 12948.

TRAMMELL, S. A., WEIDEMANN, B. J., CHADDA, A., YOREK, M. S., HOLMES, A., COPPEY, L. J., OBROSOV, A., KARDON, R. H., YOREK, M. A. & BRENNER, C. 2016b. Nicotinamide Riboside Opposes Type 2 Diabetes and Neuropathy in Mice. *Sci Rep,* 6**,** 26933.

TRAMMELL, S. A., YU, L., REDPATH, P., MIGAUD, M. E. & BRENNER, C. 2016c. Nicotinamide Riboside Is a Major NAD+ Precursor Vitamin in Cow Milk. *J Nutr,* 146**,** 957-63.

TRIPATHI, R. C., PARAPURAM, S. K., TRIPATHI, B. J., ZHONG, Y. & CHALAM, K. V. 1999. Corticosteroids and glaucoma risk. *Drugs Aging,* 15**,** 439-50.

UMMARINO, S., MOZZON, M., ZAMPORLINI, F., AMICI, A., MAZZOLA, F., ORSOMANDO, G., RUGGIERI, S. & RAFFAELLI, N. 2017. Simultaneous quantitation of nicotinamide riboside, nicotinamide mononucleotide and nicotinamide adenine dinucleotide in milk by a novel enzyme-coupled assay. *Food Chem,* 221**,** 161-168.

UTO, A., MIYASHITA, K., ENDO, S., SATO, M., RYUZAKI, M., KINOUCHI, K., MITSUISHI, M., MEGURO, S. & ITOH, H. 2021. Transient Dexamethasone Loading Induces Prolonged Hyperglycemia in Male Mice With Histone Acetylation in Dpp-4 Promoter. *Endocrinology,* 162.

VALASSI, E., SANTOS, A., YANEVA, M., TOTH, M., STRASBURGER, C. J., CHANSON, P., WASS, J. A., CHABRE, O., PFEIFER, M., FEELDERS, R. A., TSAGARAKIS, S., TRAINER, P. J., FRANZ, H., ZOPF, K., ZACHARIEVA, S., LAMBERTS, S. W., TABARIN, A., WEBB, S. M. & GROUP, E. S. 2011. The European Registry on Cushing's syndrome: 2-year experience. Baseline demographic and clinical characteristics. *Eur J Endocrinol,* 165**,** 383-92.

VAN BAAK, M. A. 1999. Physical activity and energy balance. *Public Health Nutr,* 2**,** 335-9.

VAN DER VEER, E., HO, C., O'NEIL, C., BARBOSA, N., SCOTT, R., CREGAN, S. P. & PICKERING, J. G. 2007. Extension of human cell lifespan by nicotinamide phosphoribosyltransferase. *J Biol Chem,* 282**,** 10841-5.

VANDESOMPELE, J., DE PRETER, K., PATTYN, F., POPPE, B., VAN ROY, N., DE PAEPE, A. & SPELEMAN, F. 2002. Accurate normalization of real-time quantitative RT-PCR data by geometric averaging of multiple internal control genes. *Genome Biol,* 3**,** RESEARCH0034.

VAZQUEZ, B. N., THACKRAY, J. K., SIMONET, N. G., KANE-GOLDSMITH, N., MARTINEZ-REDONDO, P., NGUYEN, T., BUNTING, S., VAQUERO, A., TISCHFIELD, J. A. & SERRANO, L. 2016. SIRT7 promotes genome integrity and modulates non-homologous end joining DNA repair. *EMBO J,* 35**,** 1488-503.

VOLPE, J. J. & MARASA, J. C. 1975. Hormonal regulation of fatty acid synthetase, acetyl-CoA carboxylase and fatty acid synthesis in mammalian adipose tissue and liver. *Biochim Biophys Acta,* 380**,** 454-72.

WALKER, J. J., SPIGA, F., GUPTA, R., ZHAO, Z., LIGHTMAN, S. L. & TERRY, J. R. 2015. Rapid intra-adrenal feedback regulation of glucocorticoid synthesis. *J R Soc Interface,* 12**,** 20140875.

WANG, J., MA, S. F., YUN, Q., LIU, W. J., GUO, M. N., ZHU, Y. Q., LIU, Z. Z., QIAN, J. J. & ZHANG, W. N. 2021. Ameliorative effect of SIRT1 in postpartum depression mediated by upregulation of the glucocorticoid receptor. *Neurosci Lett,* 761**,** 136112.

WANG, J. C., GRAY, N. E., KUO, T. & HARRIS, C. A. 2012. Regulation of triglyceride metabolism by glucocorticoid receptor. *Cell Biosci,* 2**,** 19.

WANG, X. J., XIAO, J. J., LIU, L., JIAO, H. C. & LIN, H. 2017. Excessive glucocorticoid-induced muscle MuRF1 overexpression is independent of Akt/FoXO1 pathway. *Biosci Rep,* 37.

WEBER, K., BRUCK, P., MIKES, Z., KUPPER, J. H., KLINGENSPOR, M. & WIESNER, R. J. 2002. Glucocorticoid hormone stimulates mitochondrial biogenesis specifically in skeletal muscle. *Endocrinology,* 143**,** 177-84.

WEBSTER, J. M., SAGMEISTER, M. S., FENTON, C. G., SEABRIGHT, A. P., LAI, Y. C., JONES, S. W., FILER, A., COOPER, M. S., LAVERY, G. G., RAZA, K., LANGEN, R. & HARDY, R. S. 2021. Global Deletion of 11beta-HSD1 Prevents Muscle Wasting Associated with Glucocorticoid Therapy in Polyarthritis. *Int J Mol Sci,* 22.

WEINSTEIN, S. P., PAQUIN, T., PRITSKER, A. & HABER, R. S. 1995. Glucocorticoid-induced insulin resistance: dexamethasone inhibits the activation of glucose transport in rat skeletal muscle by both insulin- and non-insulin-related stimuli. *Diabetes,* 44**,** 441-5.

WEINSTEIN, S. P., WILSON, C. M., PRITSKER, A. & CUSHMAN, S. W. 1998. Dexamethasone inhibits insulin-stimulated recruitment of GLUT4 to the cell surface in rat skeletal muscle. *Metabolism,* 47**,** 3-6.

WEITZMAN, E. D., FUKUSHIMA, D., NOGEIRE, C., ROFFWARG, H., GALLAGHER, T. F. & HELLMAN, L. 1971. Twenty-four hour pattern of the episodic secretion of cortisol in normal subjects. *J Clin Endocrinol Metab,* 33**,** 14-22.

WESTERBACKA, J., YKI-JARVINEN, H., VEHKAVAARA, S., HAKKINEN, A. M., ANDREW, R., WAKE, D. J., SECKL, J. R. & WALKER, B. R. 2003. Body fat distribution and cortisol metabolism in healthy men: enhanced 5beta-reductase and lower cortisol/cortisone metabolite ratios in men with fatty liver. *J Clin Endocrinol Metab,* 88**,** 4924-31.

WILKINSON, K. D. & WILLIAMS, C. H., JR. 1981. NADH inhibition and NAD activation of Escherichia coli lipoamide dehydrogenase catalyzing the NADH-lipoamide reaction. *J Biol Chem,* 256**,** 2307-14.

WOODS, C. P., HAZLEHURST, J. M. & TOMLINSON, J. W. 2015. Glucocorticoids and non-alcoholic fatty liver disease. *J Steroid Biochem Mol Biol,* 154**,** 94-103.

WU, J., JIN, Z., ZHENG, H. & YAN, L. J. 2016. Sources and implications of NADH/NAD(+) redox imbalance in diabetes and its complications. *Diabetes Metab Syndr Obes,* 9**,** 145-53.

XIAO, C. Y., CHEN, M., ZSENGELLER, Z., LI, H., KISS, L., KOLLAI, M. & SZABO, C. 2005. Poly(ADP-Ribose) polymerase promotes cardiac remodeling, contractile failure, and translocation of apoptosis-inducing factor in a murine experimental model of aortic banding and heart failure. *J Pharmacol Exp Ther,* 312**,** 891-8.

XIAO, L., FENG, C. & CHEN, Y. 2010. Glucocorticoid rapidly enhances NMDA-evoked neurotoxicity by attenuating the NR2A-containing NMDA receptor-mediated ERK1/2 activation. *Mol Endocrinol,* 24**,** 497-510.

XIAO, Q., XIONG, Z., YU, C., ZHOU, J., SHEN, Q., WANG, L., XIE, X. & FU, Z. 2019. Antidepressant activity of crocin-I is associated with amelioration of neuroinflammation and attenuates oxidative damage induced by corticosterone in mice. *Physiol Behav,* 212**,** 112699.

XIE, N., ZHANG, L., GAO, W., HUANG, C., HUBER, P. E., ZHOU, X., LI, C., SHEN, G. & ZOU, B. 2020a. NAD(+) metabolism: pathophysiologic mechanisms and therapeutic potential. *Signal Transduct Target Ther,* 5**,** 227.

XIE, X., SHEN, Q., YU, C., XIAO, Q., ZHOU, J., XIONG, Z., LI, Z. & FU, Z. 2020b. Depression-like behaviors are accompanied by disrupted mitochondrial energy metabolism in chronic corticosterone-induced mice. *J Steroid Biochem Mol Biol,* 200**,** 105607.

XU, F., GAO, Z., ZHANG, J., RIVERA, C. A., YIN, J., WENG, J. & YE, J. 2010. Lack of SIRT1 (Mammalian Sirtuin 1) activity leads to liver steatosis in the SIRT1+/- mice: a role of lipid mobilization and inflammation. *Endocrinology,* 151**,** 2504-14.

YAN, L. J., RAJASEKARAN, N. S., SATHYANARAYANAN, S. & BENJAMIN, I. J. 2005. Mouse HSF1 disruption perturbs redox state and increases mitochondrial oxidative stress in kidney. *Antioxid Redox Signal,* 7**,** 465-71.

YANG, H., YANG, T., BAUR, J. A., PEREZ, E., MATSUI, T., CARMONA, J. J., LAMMING, D. W., SOUZA-PINTO, N. C., BOHR, V. A., ROSENZWEIG, A., DE CABO, R., SAUVE, A. A. & SINCLAIR, D. A. 2007. Nutrient-sensitive mitochondrial NAD+ levels dictate cell survival. *Cell,* 130**,** 1095-107.

YANG, W., KANG, X., QIN, N., LI, F., JIN, X., MA, Z., QIAN, Z. & WU, S. 2017. Melatonin protects chondrocytes from impairment induced by glucocorticoids via NAD(+)-dependent SIRT1. *Steroids,* 126**,** 24-29.

YANG, Y. & SAUVE, A. A. 2016. NAD(+) metabolism: Bioenergetics, signaling and manipulation for therapy. *Biochim Biophys Acta,* 1864**,** 1787-1800.

YANG, Y., ZHANG, N., ZHANG, G. & SAUVE, A. A. 2020. NRH salvage and conversion to NAD(+) requires NRH kinase activity by adenosine kinase. *Nat Metab,* 2**,** 364-379.

YI, C. X., FOPPEN, E., ABPLANALP, W., GAO, Y., ALKEMADE, A., LA FLEUR, S. E., SERLIE, M. J., FLIERS, E., BUIJS, R. M., TSCHOP, M. H. & KALSBEEK, A. 2012. Glucocorticoid signaling in the arcuate nucleus modulates hepatic insulin sensitivity. *Diabetes,* 61**,** 339-45.

YOON, J. C., PUIGSERVER, P., CHEN, G., DONOVAN, J., WU, Z., RHEE, J., ADELMANT, G., STAFFORD, J., KAHN, C. R., GRANNER, D. K., NEWGARD, C. B. & SPIEGELMAN, B. M. 2001. Control of hepatic gluconeogenesis through the transcriptional coactivator PGC-1. *Nature,* 413**,** 131-8.

YOSHINO, J., BAUR, J. A. & IMAI, S. I. 2018. NAD(+) Intermediates: The Biology and Therapeutic Potential of NMN and NR. *Cell Metab,* 27**,** 513-528.

YOSHINO, J., MILLS, K. F., YOON, M. J. & IMAI, S. 2011. Nicotinamide mononucleotide, a key NAD(+) intermediate, treats the pathophysiology of diet- and age-induced diabetes in mice. *Cell Metab,* 14**,** 528-36.

YU, C. Y., MAYBA, O., LEE, J. V., TRAN, J., HARRIS, C., SPEED, T. P. & WANG, J. C. 2010. Genome-wide analysis of glucocorticoid receptor binding regions in adipocytes reveal gene network involved in triglyceride homeostasis. *PLoS One,* 5**,** e15188.

ZAPATA-PEREZ, R., TAMMARO, A., SCHOMAKERS, B. V., SCANTLEBERY, A. M. L., DENIS, S., ELFRINK, H. L., GIROUD-GERBETANT, J., CANTO, C., LOPEZ-LEONARDO, C., MCINTYRE, R. L., VAN WEEGHEL, M., SANCHEZ-FERRER, A. & HOUTKOOPER, R. H. 2021. Reduced nicotinamide mononucleotide is a new and potent NAD(+) precursor in mammalian cells and mice. *FASEB J,* 35**,** e21456.

ZHANG, H., RYU, D., WU, Y., GARIANI, K., WANG, X., LUAN, P., D'AMICO, D., ROPELLE, E. R., LUTOLF, M. P., AEBERSOLD, R., SCHOONJANS, K., MENZIES, K. J. & AUWERX, J. 2016. NAD(+) repletion improves mitochondrial and stem cell function and enhances life span in mice. *Science,* 352**,** 1436-43.

ZHOU, C. C., YANG, X., HUA, X., LIU, J., FAN, M. B., LI, G. Q., SONG, J., XU, T. Y., LI, Z. Y., GUAN, Y. F., WANG, P. & MIAO, C. Y. 2016. Hepatic NAD(+) deficiency as a therapeutic target for non-alcoholic fatty liver disease in ageing. *Br J Pharmacol,* 173**,** 2352-68.

ZHU, X. H., LU, M., LEE, B. Y., UGURBIL, K. & CHEN, W. 2015. In vivo NAD assay reveals the intracellular NAD contents and redox state in healthy human brain and their age dependences. *Proc Natl Acad Sci U S A,* 112**,** 2876-81.